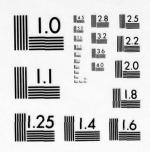
GENERAL DYNAMICS/POMONA CALIF POMONA DIV
TAGSEA PROGRAM. VOLUME III. SUPPORTIVE ANALYSES AND OUTPUTS.(U)
AUG 76

F/G
N00017-73-C-2244 AD-A036 973 F/G 17/9 N00017-73-C-2244 UNCLASSIFIED NL OF 4 ADA036973

OF 4 ADA036973



MICROCOPY RESOLUTION TEST CHART NATIONAL BUREAU OF STANDARDS-1963-A ADA 036973

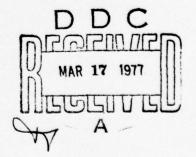
UNCLASSIFIED

TAGSEA PROGRAM FINAL REPORT VOLUME III SUPPORTIVE ANALYSES AND OUTPUTS

BR-9254-3

27 AUGUST 1976

Prime Contract No. N00017-73-C-2244





Approved for public release;
Distribution Unlimited

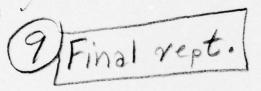


TAGSEA PROGRAM.

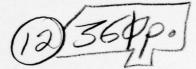
FINAL REPORT

SUPPORTIVE ANALYSES AND OUTPUTS

BR-9254-3



27 AUGUST 1976



Prepared For GENERAL DYNAMICS Pomona, California

Prime Contract No. N00017-73-C-2244

Prepared By RAYTHEON COMPANY MISSILE SYSTEMS DIVISION Bedford, Massachusetts

ACRESSION 105

HTIS White Station 12

BOC Buff Section 12

UNANHOUNGED 10231FIGATION 12

EV. B. SAN LIFERD ANALKSMATTE GOODS

BOL SAN LIFERD ANALKSMATTE GOODS

147 850

FOREWORD

This final report summarizes the work done by Raytheon Missile Systems Division for the TAGSEA Program under General Dynamics PO #304490-PB, prime contract no. N00017-73-C-2244. It is submitted in compliance with Data Item A015 and is organized into four volumes to ease handling and for the convenience of the readers.

Volume I, Clutter Models, reports the essence of the work and contains the models themselves which were the prime objective of the clutter portion of the TAGSEA program; it can be read on a stand-alone basis. Enough peripheral material is also included to provide a framework for a good understanding of the models. Volume II, Procedures and Output Forms, provides details and explanations on methodology including the form of the outputs and the structures of the clutter simulation effort. Volume III, Supportive Analyses and Outputs, provides analytical back-up and a more complete detailed view of the simulation software.

Volume IV, Standard Clutter Analysis Outputs, is a compilation in various forms of the mass of data analyzed during the program. Each volume has its own table of contents which serves to outline the specific material presented therein.

Raytheon wishes to acknowledge the valuable aid and support given by members of the team composed of personnel from NAVSEA, APL/JHU, Technology Service Corporation and General Dynamics.

Many helpful suggestions were made during a series of critiques and reviews which most assuredly contributed to a better resultant output. The assistance received ranged all the way from general support and overall guidance to specific supportive analyses, detailed unpublished comparative data, and suggestions of exact forms of clutter models and plots which would be most informative to the community at large.

iii

TABLE OF CONTENTS

				Page
APPENDIX A -	SUPPO	ORTIVE AN	: NALYSIS	
	1.1		of the Experiment	
		1.1.1	Objective of the Clutter Study	
		1.1.2	Data Requirements	
		1.1.3	Approach	
		1.1.4	Data Gathering	
		1.1.5	Performance	
	1.2	The Rada	ar Range Equation and Resolution	
		1.2.1	The Radar Range Equation for TAGSEA Power Received in a Range-Doppler Cell	
		1.2.2	Range-Doppler Surface Geometry	A-9
		1.2.3	Antenna Coordinate Transformation	A-18
		1.2.4	Transformation to Surface Coordinates	A-20
		1.2.5	Transformation in Terms of Transferred Data Form	A-22
		1.2.6	Radar Resolution Characteristics	A-23
	1.3	Statist	ics/Confidence	A-27
		1.3.1	Statistics of Meleer Noise	A-27
		1.3.2	Interpretation of the Results of Receiver Noise Analysis	A-30
		1.3.3	Conclusions on Statistics and Confidence of Receiver Noise	A-31
		1.3.4	Correction on the Average Noise Estimate Grouping	A-37
		1.3.5	Confidence Interval Analysis of Noise Mean	A-39
		1.3.6	Determination of Confidence Contours, $T_1(\gamma,p)$, $T_2(\gamma,p)$	A-46

			Page
	1.4	Equations for Computing Weighting Tables	A-47
	1.5	Conditional Probability Maps as Diagnostic Tools	.A-52
APPENDIX B -	OUTP	UTS-SPECIAL ANALYSIS	B-1
	1.1	Curve Matching of Histograms	B-1
		1.1.1 Curve Matching Weibull and Rayleigh Functions to Data	B-1
		1.1.2 Cubic Spline	B-19
	1.2	Histograms of the Mean	B-57
	1.3	Temporal Spectra and Autocorrelation Function of the Mean	B-70
	1.4	Variability of Selected Statistics	B-102
	1.5	Hit Map of Run 812 - Nantucket Light- Ship Target Validation	B-110
		1.5.1 Lightship Conditional Probability Maps	B-113
	1.6	Characteristics in the Neighborhood of Large Returns	B-134
		1.6.1 History of a Typical Large Sea Echo	B-134
	1.7	Unconditional vs. Conditional Probability Analysis	B-137
	1.8	Locally Normalized Histograms	B-139
		1.8.1 Histograms TOTAL N LOG Q	B-139
		1.8.2 Histograms TOTAL N WEIBULL	B-150
		1.8.3 Histograms TOTAL N Q=1-DIST	B-161
		1.8.4 Histograms TOTAL N PDF	B-172
		1.8.5 Histograms TOTAL N PDF TAIL	B-183
APPENDIX C -	ENVI	RONMENTAL CONDITIONS	.C-1
APPENDIX D -	DATA	ANALYSIS SOFTWARE	D-1
	1.1	Histogram and Mean Data Analysis Software	.D-1
		1.1.1 Histogram Program (TAGHIST)	D-1
		1.1.2 Probability Plots (PROBP)	D-5

			Page
	1.1.3	Statistics Plots and Processing (STATP)	.D-6
	1.1.4	Average Plots (MEANR)	D-7
1.2	Hit Sof	tware Flow Charts	.D-7
APPENDIX E - SIMU	LATION S	OFTWARE	.E-1
1.1	Simulat	ion Structure	E-1
1.2	Detaile	d Description	E-3
	1.2.1	Program Listing	E-3
	1.2.2	True Area Subroutine	E-9
	1.2.3	R ⁴ Subroutine	E-10
	1.2.4	Antenna Subroutine	E-11
	1.2.5	Mean Backscatter Subroutine	E-12
	1.2.6	Sin x/x Subroutine	E-13
	1.2.7	Gain Normalizing Subroutine	E-14
	1.2.8	Integer Array Subroutine	E-15
	1.2.9	Hit Subroutine	E-16
	1.2.10	Histogram Subroutine	E-17
	1.2.11	Range-Time Sort Subroutine	E-18
	1.2.12	Amplitude Generator Subroutine	.E-19
APPENDIX F - SIMU	LATION O	UTPUTS	.F-1

APPENDIX A SUPPORTIVE ANALYSIS

During the course of the TAGSEA program many analyses were done which were concerned with the technical conduct of the work rather than with analysis of the resultant data. Such analyses dealt with the requirements for various facets of the programs including the design of the experiments, application of the radar range equation, coordinate transformations, and weighting matrix determination which are presented in this appendix.

1.1 Design of the Experiment

This section discusses the considerations involved in designing the clutter-gathering experiment.

1.1.1 Objective of the Clutter Study

It was the primary objective of the clutter study effort to characterize sea clutter with emphasis on determining the distribution in space and time of the relatively rare large radar cross section returns. Such a characterization is valuable for use in future surface missile systems for specification of performance requirements, design of the missile seeker, as well as simulation and evaluation of candidate seekers. To achieve this objective it was desired to gather radar clutter data under a variety of conditions, to reduce and analyze the data, and to develop analytical and simulation models of clutter.

1.1.2 Data Requirements

Sea clutter has been shown to be representative of a non-stationary process. That is, statistics of the distribution function, such as the mean, vary with time more than can be attributed to chance alone. It has been suggested that the slowly varying nature of the distribution can be attributed to change in the shape of the coarse structure of ocean surface. A typical seeker looking down at the sea can resolve a patch on the surface of the ocean approximately 100 feet square. It is known that small patches exhibit time-varying distributions with decorrelation times varying over a couple of orders of magnitude, depending on conditions. On the other hand, larger patches can exhibit exponential cross section distributions and somewhat shorter decorrelation times. The nature of clutter statistics are needed for patches of sea 100 feet square viewed at grazing angles between 10° and 50°. The questions to be answered are:

- 1) How often does a large cross sections occur?
- 2) How long does it persist?
- 3) What is the nature of rapid fluctuation when the mean cross section is high?

The answers to these questions influence the final choice of parameters in clutter blanking and CFAR circuits of future seekers.

The amount of clutter data required to give answers is determined by the required false alarm probability. Some typical seeker parameters are used for this estimate as follows. If 1% of a 4 second search period is to be devoted (on the average) to dismissing false alarms, then the required false alarm probability per bin is approximately 10⁻⁶ for a 64 X 64 range-doppler matrix. Only two out of 64 doppler bins will be likely to cause false alarms, so a false alarm prob-

ability of 3 X 10^{-5} due to clutter would be reasonable. The distribution curve should be measured up to levels corresponding to this false alarm probability and would require that the level be exceeded about 16 times in order to estimate the level to a 1σ value of 0.1dB. This would require $16/3 \times 10^{+5} \stackrel{\sim}{=} 500,000$ decorrelation bins to be observed. The decorrelation time is expected to be less than 0.2 seconds, so 100,000 bin-seconds of information would be adequate for each condition.

1.1.3 Approach

Several data gathering flights were made, in which runs were performed under the 9 combinations of the following conditions:

Wind Direction: a) Upwind

b) Downwind

c) Crosswind

Grazing Angle: a) Low (11°-15°), Altitude 1100 ft

b) Medium (22°-32°), Altitude 2200 ft

c) High (34°-52°), Altitude 3300 ft

Each run lasted approximately five minutes and produced data in 16 contiguous 100 foot range gates using a side-looking horn as an antenna. (Contiguous gates were chosen to provide a map of a continuous patch of sea on each run, and to minimize the required receiver dynamic range). The output corresponding to each range gate was box-carred, filtered, and recorded on tape using frequency multiplexing.

1.1.4 Data Gathering

It was desirable to gather data quickly in order to reduce flight time. This was achieved by viewing as large a surface area as possible consistent with aircraft velocity and radar average power. It was also desirable to use a fixed

antenna thereby putting minimum demands on attitude-stability of the aircraft since the high sea state operations took place in rough weather. These considerations dictated the use of a horn with about 60° beamwidth and 10dB gain. The vertical beamwidth covered the 40° range of grazing angles allowing the horn to be mounted with a depression angle of 30°. The horizontal beamwidth permitted the aircraft to fly at a speed of as much as 300 knots (500 ft/sec) and still keep aliased spectra about 10dB below the desired spectrum in the region of interest.

The data gathering system parameters were as

follows:

a) Radar

Frequency X-Band Antenna Gain 11dB

Peak Power 1000W at the antenna

Pulse Width 0.2µsec PRF 19,320pps

Noise Figure 11dB at the antenna

No. of Range 16

gates

Range Gate 16 parallel analog channels, Output box-carred, filtered, and

offset in doppler one-quarter

of the PRF

Range Gate 4500 to 6100 feet settings

b) Recorder

No. of Channels 7

Speed 60 ips

Freq. Response 400Hz - 750KHz

Record Time/Reel 30 min.

Clutter Data 4 frequency-multiplexed FM recording channels on each of 4 tracks

c) Aircraft

Type

A3

Velocity required

250 knots (420 ft/sec)

1.1.5 Performance

As the detailed calculations presented in Subsection 1.2.1 will show, the received power in a range-doppler cell computes to be -110.4dBm and the noise power in a 5MHz bandwidth is -96dBm for an 1ldB noise figure. Thus, the clutter-to-noise ratio is -110.4-(-96) = -14.4dB per pulse per element. The integration gain is 128, or 2ldB. Therefore the integrated C/N per bin is 21-14.4 = 6.6dB at 4600 feet for $\sigma_{\rm O}$ = -27.5dB. This is adequate for establishing the mean value of σ with less than ldB error due to noise. A more exact determination of the statistical limits noise estimation appears in Section 1.3 of this appendix.

1.2 The Radar Range Equation and Resolution

1.2.1 The Radar Range Equation for TAGSEA Power Received in a Range-Doppler Cell

The basic equation for power received is:

$$P_{r} = \frac{P_{t} G_{t}}{4\pi R^{2}} \cdot \frac{\sigma}{4\pi R^{2}} \cdot A_{r}$$

where:

P₊ = Transmitted Power

G₊ = Transmit Antenna Gain

R = Range to Target or Clutter Point

σ = Radar Cross Section

A = Receive Antenna Aperture Area

Because a single X-Band horn is used, the gain on transmit and receive is identical and is related to aperture area by $G_r = 4\pi A_r/\lambda^2 = G_t$; where $\lambda = 0.1$ ft wavelength at X-Band.

Radar cross section σ is the product of reflectivity σ° and the area ΔA of a range-doppler cell; the size of which is determined by signal processing. Microwave losses L are about 2dB each way in the TAGSEA radar hardware. With these modifications the equation for power reduces to:

$$P_{r} = \frac{P_{t} (G/L)^{2} \lambda^{2} \sigma^{\circ} (\Delta A)}{(4\pi)^{3} R^{4}}$$
1.2-2

The Range-Doppler resolution cell size ΔA depends on geometry as well as signal processing and is closely approximated by the equation:

$$\Delta A = \frac{(\lambda/2V) R (\Delta R) (\Delta f_d)}{\sqrt{1 - (H/R)^2 - (\lambda f_d/2V)^2}}$$
1.2-3

derived in Subsection 1.2.2. Range resolution ΔR and doppler resolution Δf_d are fixed by signal processing. Altitude H, Range R and velocity V are a function of flight test conditions. Cell size increases slightly with altitude and doppler frequency; as indicated by the denominator terms in equation 1.2-3.

The antenna patter $G(\alpha,\beta)$ had to be related to flight test geometry in order to compute spectral shape. The expression for antenna gain (derived in Subsection 1.2.3) was modeled as being parabolic in decibels.

$$G_{dB}(\alpha, \beta) = G_0 - k_{az}(\alpha)^2 - k_{el}(\beta)^2$$
 1.2-4

where $G_0 = 9.8 dB$, $k_{az} = 0.00461 deg^{-2}$ and $k_{el} = 0.0047 deg^{-2}$. Angles (α, β) are in measures of degrees. Combining equations 1.2-2, 1.2-3 and 1.2-4 yields the result:

$$P_{r} = \frac{P_{t} G^{2}(\alpha, \beta) \lambda^{3} \sigma^{\circ}(\Delta R) (\Delta f_{d})}{(4\pi)^{3} R^{3}(2V) \sqrt{1 - (H/R)^{2} - (\lambda f_{d}/2V)^{2}} L^{2}}$$
1.2-5

Received clutter power in a range-doppler cell was computed in Table A-1 for a nominal set of geometric conditions: R = 4400 ft, $H \approx 2200$ ft, V = 420 fps and zero doppler. For this particular choice of parameters the depression angle is 30° and antenna gain is maximum; i.e., $\alpha = 0 = \beta$.

In Subsection 1.2.3 it is shown that the antenna steering coordinates (α,β) are functionally related to geometry by the vector relation:

$$\mathbf{U}_{\mathbf{A}} = \cos \psi \begin{bmatrix} \tan \alpha \\ 1 \\ \tan \beta \end{bmatrix} = \begin{bmatrix} 0 & \sin (\theta_{\mathbf{g}} - \theta_{\mathbf{d}}) \cos \gamma & 0 \\ \cos \xi & \cos (\theta_{\mathbf{g}} - \theta_{\mathbf{d}}) \cos \gamma + \sin \xi & \sin \gamma \\ -\sin \xi & \cos (\theta_{\mathbf{g}} - \theta_{\mathbf{d}}) \cos \gamma + \cos \xi & \sin \gamma \end{bmatrix} \quad 1.2-6$$

where:

 θ_g = azimuth angle of the range vector in the ground plane

 θ_d = aircraft drift angle

 γ = depression angle of the range vector

 ξ = depression angle (30°) of the antenna(X-Band horn)

$$\tan \psi = \sqrt{\tan^2 \alpha + \tan^2 \beta}$$

The coordinate rotation angles are measured with respect to a system determined by the velocity vector, altitude vector and zero doppler frequency. The depression angle is related to range and altitude by $\sin\gamma = H/R$ or $\cos\gamma = 1-(H/R)^2$. Azimuth in the ground plane is defined by $\sin\theta_g = (\lambda f_d/2V) \cos\gamma$ (see Subsection 1.2.2).

TABLE A-1
COMPUTATION OF POWER RECEIVED IN A RANGE-DOPPLER CELL

$P_{r} = \frac{P_{t} G^{2}(\alpha, \beta) \lambda^{3} \sigma^{\circ} (\Delta R) (\Delta f_{d})}{(4\pi)^{3} R^{3} (2V) \sqrt{1 - (H/R)^{2} - (\lambda f_{d}/2V)^{2}} L^{2}}$							
$H = 2200 \text{ ft}, R = 4400 \text{ ft}, \qquad \alpha = \beta = 0^{\circ}, f_{\bar{d}} = 0$							
Parameter							
P _t = 1000 watts 60dBm	60dBm						
$G^2(\alpha,\beta) = 2 \times 11dB @ \alpha=0=\beta$	22						
λ^3 , 30 log(0.1 ft) = -30dB ft ³		30.0					
$\sigma_{\rm O} = -27.5 \text{dB} @ 30^{\circ} \text{ depression, SS-3}$		27.5					
$\Delta R = 110 \text{ ft}$ +20.4dB ft	20.4						
$\Delta f_{d} = 10 \log(14KHz/128) = 20.4dB$	20.4						
$(4\pi)^3$ 30 log (4π) = 33dB		33					
R^3 30 log(4000) = 109.9dB ft ³		109.9					
(2V) 10 log(2X420) = 29.4dB ft/sec		29.4					
$\sqrt{1-(H/R)^2}$, 5 log(1-0.5 ²) = 0.624dB							
L^2 $L = 2dB$		4.0					
	123.4	233.8					
$P_r = 123.4 - 233.8 = -110.4 dBm$							

Equations 1.2-4, 1.2-5 and 1.2-6 were combined to plot the curves in Figures A-1 (SS-3) and A-2 (SS-5) for bounding conditions of range and altitude. These curves were normalized to zero decibels at zero doppler and replotted in Figure A-3. Because drift angle was set to zero the curves are symmetrical about zero doppler.

 $\mbox{Values of } \sigma_{\mbox{\scriptsize O}} \mbox{ used for plotting Figures A-1 and A-2 were taken from data provided by APL in Figure A-4.}$

1.2.2 Range-Doppler Surface Geometry

Consider the geometry in Figure A-5.

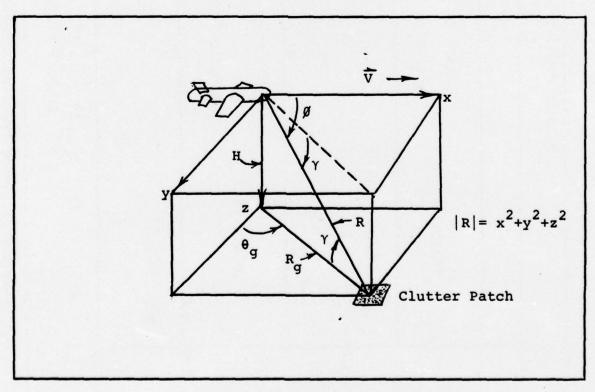


Figure A-5 Flight Test Geometry

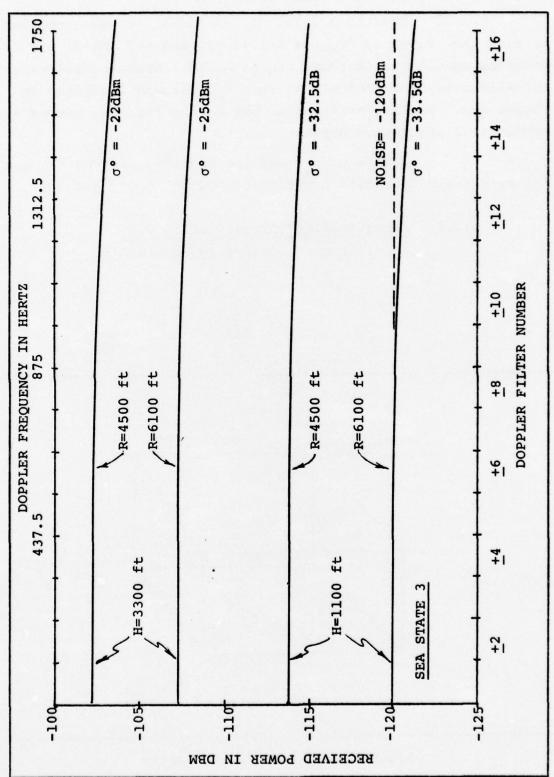
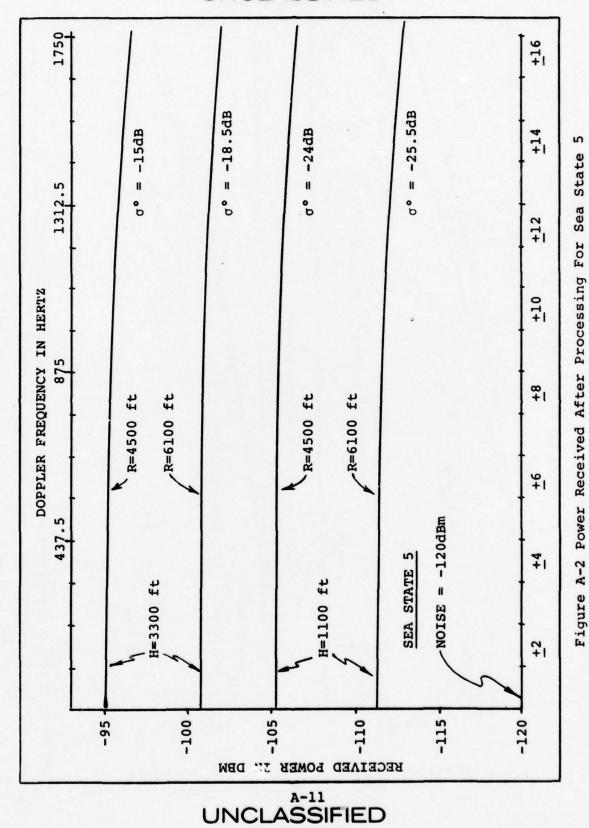


Figure A-1 Power Received After Processing for Sea State 3



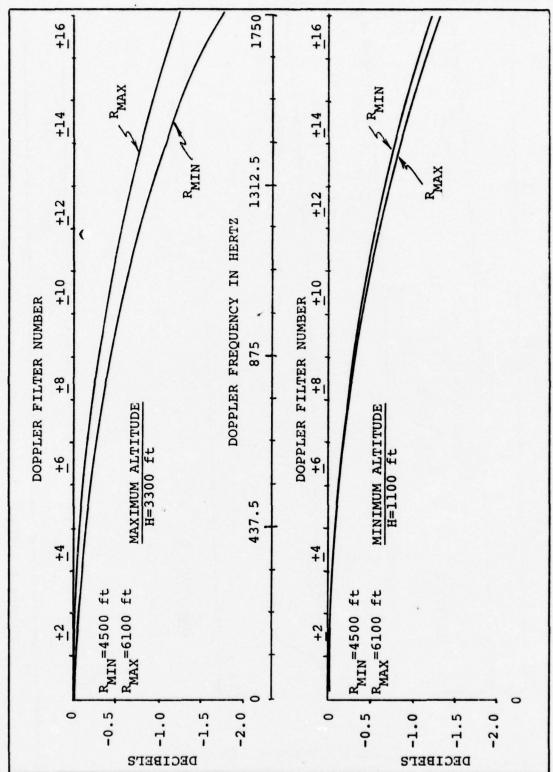


Figure A-3 Normalized Power Received as a Function of Doppler Frequency

unclassified

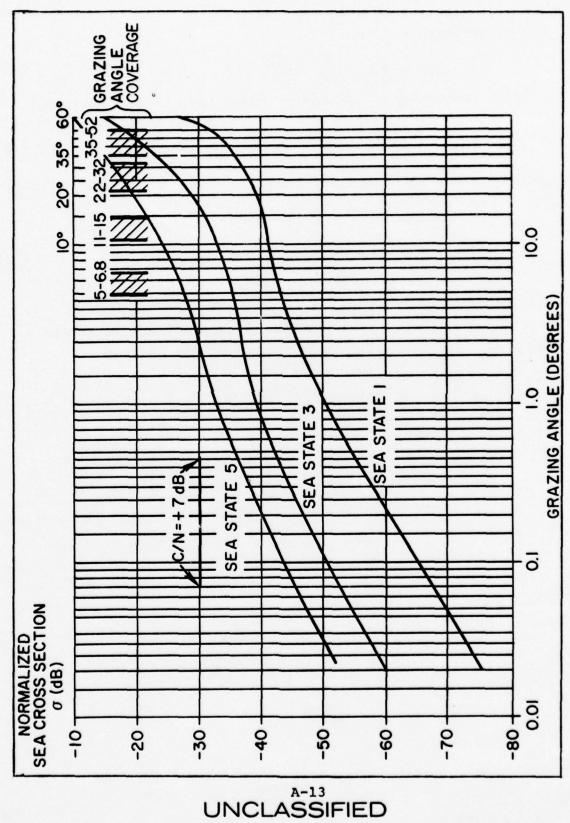


Figure A-4 Normalized Backscatter Coefficient

The range rate is given by:

$$R = V \cos \emptyset = \frac{V \cdot R}{|R|} = \frac{Vx}{R}$$

Doppler frequency is related to range rate by the equation.

$$f_{d} = \frac{2R}{\lambda} = \frac{2V}{\lambda} \cos \emptyset$$
 1.2-7

The above two equations can be combined to provide an expression for isodop contours

$$\frac{x}{R} = \frac{\lambda f_{d}}{2V} = \frac{x}{\sqrt{x^2 + y^2 + z^2}}$$
 1.2-8

The isodops intersect the clutter surface at altitude z = H. If a polar coordinate system on the clutter surface is chosen as indicated in Figure A-6 the isodop equation becomes

$$\frac{\lambda f_{d}}{2V} = \frac{R_{g} \sin \theta_{g}}{\sqrt{R_{g}^{2} + H^{2}}} = \sqrt{1 - (H/R)^{2}} \sin \theta_{g}$$
 1.2-9

The isodop equation was used to plot the ground maps in Figure A-6 as well as those in the body of the report.

The area of the clutter patch in Figure A-7 is

$$dA = (R_g d\theta_g) dR_g$$
 1.2-10

It is easily shown that

given by:

$$dR_g = d \left(\sqrt{R^2 - H^2} \right) = \frac{RdR}{\sqrt{R^2 - H^2}}$$
1.2-11

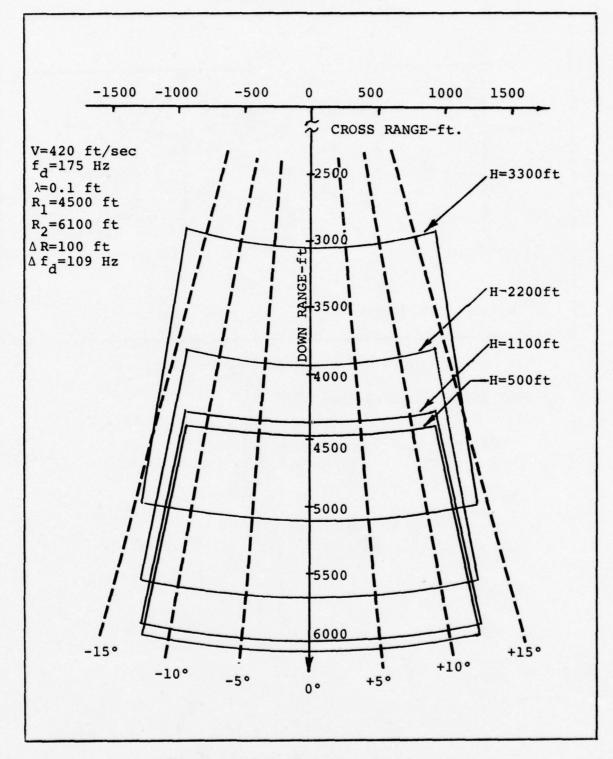


Figure A-6 Surface Map Overlays

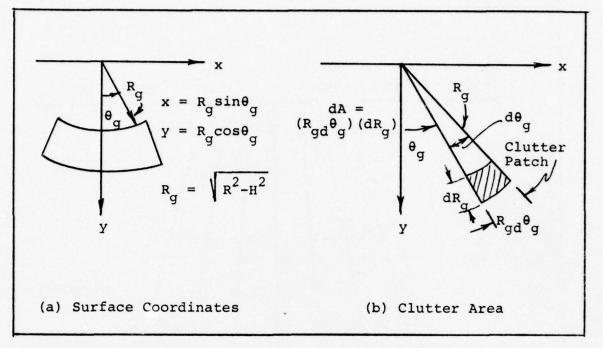


Figure A-7 Surface Plane Geometry

and from equation 1.2-9 that:

$$d\theta_{g} = d \left[\sin^{-1} \left(\frac{\lambda f_{d}/2V}{\sqrt{1 - (H/R)^{2}}} \right) \right] = 1.2-12$$

$$\frac{(\lambda/2V) df_{d}}{\sqrt{1 - (H/R)^{2} - (\lambda f_{d}/2V)^{2}}}$$

Substituting equations 1.2-11 and 1.2-12 into equation 1.2-10 provides the resultant expression for small areas as a function of range and doppler. Replacing differentials by deltas yields:

$$\Delta A = \frac{\lambda R (\Delta R) (\Delta f_d)}{2V \sqrt{1 - (H/R)^2 - (\lambda f_d/2V)^2}}$$
1.2-13

Coordinate rotations can be derived directly from Figure A-5. If a unit vector (0 1 0) along the range to a clutter point is to be rotated to the coordinate system of the velocity vector, the transformation is:

$$u = \frac{1}{|R|} = \begin{bmatrix} \cos\theta_g & \sin\theta_g & 0 \\ -\sin\theta_g & \cos\theta_g & 0 \\ 0 & 0 & 1 \end{bmatrix} \begin{bmatrix} 1 & 0 & 0 & 0 \\ 0 & \cos\gamma & -\sin\gamma & 0 \\ 0 & \sin\gamma & \cos\gamma & \end{bmatrix} \begin{bmatrix} 0 & 1 & 0 \\ 0 & \cos\gamma & -\sin\gamma & 0 \\ 0 & \sin\gamma & \cos\gamma & \end{bmatrix} \begin{bmatrix} 0 & 1 & 0 \\ 0 & \cos\gamma & -\sin\gamma & 0 \\ 0 & \sin\gamma & \cos\gamma & \end{bmatrix} = \begin{bmatrix} \cos\gamma & \sin\theta_g & \cos\gamma & \cos\theta_g & 0 \\ \cos\gamma & \cos\theta_g & \cos\gamma & \cos\theta_g & 0 \\ \sin\gamma & \sin\gamma & \sin\gamma & \sin\gamma & \cos\gamma & \end{bmatrix} \begin{bmatrix} \lambda f_d/2V & \lambda f_d/2V & \lambda f_d/2V \\ 0 & \sin\gamma & \cos\gamma & \cos\theta_g & \cos\gamma & \cos\gamma \end{bmatrix} \begin{bmatrix} 0 & \cos\gamma & -\sin\gamma & \cos\gamma & \cos\gamma \\ 0 & \sin\gamma & \cos\gamma & \cos\gamma & \cos\gamma & \cos\gamma \\ 0 & \sin\gamma & \cos\gamma & \cos\gamma & \cos\gamma & \cos\gamma \end{bmatrix} \begin{bmatrix} 0 & \cos\gamma & \cos\gamma & \cos\gamma & \cos\gamma \\ 0 & \sin\gamma & \cos\gamma & \cos\gamma & \cos\gamma & \cos\gamma \\ 0 & \sin\gamma & \cos\gamma & \cos\gamma & \cos\gamma & \cos\gamma \end{bmatrix} \begin{bmatrix} 0 & \cos\gamma & \cos\gamma & \cos\gamma & \cos\gamma \\ 0 & \sin\gamma & \cos\gamma & \cos\gamma & \cos\gamma & \cos\gamma \\ 0 & \sin\gamma & \cos\gamma & \cos\gamma & \cos\gamma & \cos\gamma & \cos\gamma \\ 0 & \sin\gamma & \cos\gamma & \cos\gamma & \cos\gamma & \cos\gamma \\ 0 & \sin\gamma & \cos\gamma & \cos\gamma & \cos\gamma & \cos\gamma \\ 0 & \sin\gamma & \cos\gamma & \cos\gamma & \cos\gamma & \cos\gamma \\ 0 & \cos\gamma & \cos\gamma & \cos\gamma & \cos\gamma & \cos\gamma \\ 0 & \cos\gamma & \cos\gamma & \cos\gamma & \cos\gamma & \cos\gamma \\ 0 & \cos\gamma & \cos\gamma & \cos\gamma & \cos\gamma & \cos\gamma \\ 0 & \cos\gamma & \cos\gamma & \cos\gamma & \cos\gamma & \cos\gamma \\ 0 & \cos\gamma & \cos\gamma & \cos\gamma & \cos\gamma & \cos\gamma \\ 0 & \cos\gamma & \cos\gamma & \cos\gamma & \cos\gamma \\ 0 & \cos\gamma & \cos\gamma & \cos\gamma & \cos\gamma \\ 0 & \cos\gamma & \cos\gamma & \cos\gamma & \cos\gamma \\ 0 & \cos\gamma & \cos\gamma & \cos\gamma & \cos\gamma \\ 0 & \cos\gamma & \cos\gamma & \cos\gamma & \cos\gamma \\ 0 & \cos\gamma & \cos\gamma & \cos\gamma & \cos\gamma \\ 0 & \cos\gamma & \cos\gamma & \cos\gamma & \cos\gamma \\ 0 & \cos\gamma & \cos\gamma & \cos\gamma & \cos\gamma \\ 0 & \cos\gamma & \cos\gamma \\ 0 & \cos\gamma & \cos\gamma & \cos\gamma \\ 0 &$$

where: $sin \gamma = H/R$

$$\cos \gamma = \sqrt{1 - (H/R)^2}$$

$$\sin\theta_g = \frac{(\lambda f_d/2V)}{\sqrt{1 - (H/R)^2}}$$
, $\cos\theta_g = \sqrt{1 - \frac{(\lambda f_d/2V)^2}{1 - (H/R)^2}}$

1.2.3 Antenna Coordinate Transformation

Equations for rotation of points in antenna space to a horizontal cartesian (x,y,z) coordinate systems based on x along the velocity, y along zero doppler and z along the vertical are derived from Figure A-8. The unit vector \mathbf{u}_{A} in antenna space is transformed to velocity space by the relation:

$$\begin{bmatrix} x \\ y \\ z \end{bmatrix} = \begin{bmatrix} \cos \theta_d & \sin \theta_d & 0 \\ -\sin \theta_d & \cos \theta_d & 0 \\ 0 & 1 \end{bmatrix} \begin{bmatrix} 1 & 0 & 0 \\ 0 & \cos \xi & -\sin \xi \\ 0 & \sin \xi & \cos \xi \end{bmatrix} \begin{bmatrix} \tan \alpha \\ 1 \\ \tan \beta \end{bmatrix} = 1.2-15$$

or, using the matrix notation, $u_v = [0_d]$ [5] u_A

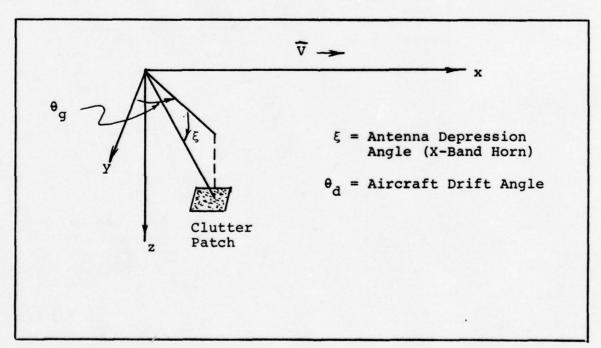


Figure A-8 Relationship Between Antenna Space and Velocity Space

The matrix relation for transforming the range vector into the velocity vector derived in Subsection 1.2.2 is given by:

$$\mathbf{u}_{\mathbf{V}} = [\theta_{\alpha}] [\dot{\gamma}] \mathbf{u}_{\mathbf{R}}$$
 1.2-17

where

$$u_p = [0 \ 1 \ 0]$$

The problem is to find an expression for the antenna vector $\mathbf{u}_{\mathbf{A}}$ in terms of the range vector. Thus, using matrix algebra and the previous two equations gives the result:

$$u_{A} = [\xi]^{-1} [\theta_{d}]^{-1} [\theta_{g}] [\gamma] u_{R}$$
 1.2-18

Because the θ_d matrix and θ_g matrix are of the same functional form it is easily shown that:

$$\begin{bmatrix} \Theta_{\mathbf{d}} \end{bmatrix}^{-1} \begin{bmatrix} \Theta_{\mathbf{g}} \end{bmatrix} = \begin{bmatrix} \Theta_{\mathbf{g}} - \Theta_{\mathbf{d}} \end{bmatrix}$$
 1.2-19

Therefore, equation 1.2-18 reduces to:

$$u_{A} = [\xi]^{-1} [\theta_{g} - \theta_{d}] [\gamma] u_{R}$$
 1.2-20

Expansion of equation 1.2-20 yields the final expression in antenna space:

$$\mathbf{u}_{\mathbf{A}} = \begin{bmatrix} 1 & 0 & 0 \\ 0 & \cos \xi & \sin \xi \\ 0 & -\sin \xi & \cos \xi \end{bmatrix} \begin{bmatrix} \cos(\theta_{\mathbf{g}} - \theta_{\mathbf{d}}) & \sin(\theta_{\mathbf{g}} - \theta_{\mathbf{d}}) & 0 \\ -\sin(\theta_{\mathbf{g}} - \theta_{\mathbf{d}}) & \cos(\theta_{\mathbf{g}} - \theta_{\mathbf{d}}) & 0 \\ 0 & 0 & 1 \end{bmatrix} \begin{bmatrix} 1 & 0 & 0 \\ 0 & \cos \gamma & -\sin \gamma \\ 0 & \sin \gamma & \cos \gamma \end{bmatrix} \begin{bmatrix} 0 \\ 1 \\ 0 \end{bmatrix}$$

The matrix products gives the result:

$$u_{A}^{=\cos\psi}\begin{bmatrix} \tan\alpha \\ 1 \\ \tan\beta \end{bmatrix} = \begin{bmatrix} 0 \\ \cos\xi \\ -\sin\xi \end{bmatrix} \begin{bmatrix} \sin(\theta_{g} - \theta_{d})\cos\gamma \\ \cos(\theta_{g} - \theta_{d})\cos\gamma + \sin\xi \\ \cos(\theta_{g} - \theta_{d})\cos\gamma + \cos\xi \end{bmatrix} \begin{bmatrix} 0 \\ \sin\gamma \\ \sin\gamma \end{bmatrix}$$
1.2-21

1.2.4 Transformation to Surface Coordinates

The clutter data was gathered by a monostatic radar mounted on a moving airplane. Consequently the coordinate system with the data was that of the aircraft. Radar returns were collected and sorted into bins by their range and doppler (range rate) from the moving aircraft.

Let us assume constant velocity and altitude for the aircraft. Now defining the following aircraft base and coordinates

Xa along the velocity vector (horizontal)

Ya horizontal and perpendicular towards the clutter collection side

Za altitude,

the range rate R to any stationary point from the moving platform is clearly

$$R = V \cos \alpha = \frac{V \cdot R}{|R|}$$

where $\cos \alpha$ is the half cone angle between range and aircraft velocity vector, see Figure A-9.

The following relationships are easily shown.

$$R^2 = X_a^2 + Y_a^2 + Z_a^2$$
 1.2-23

$$R = \frac{V X_a}{R}$$
 1.2-24

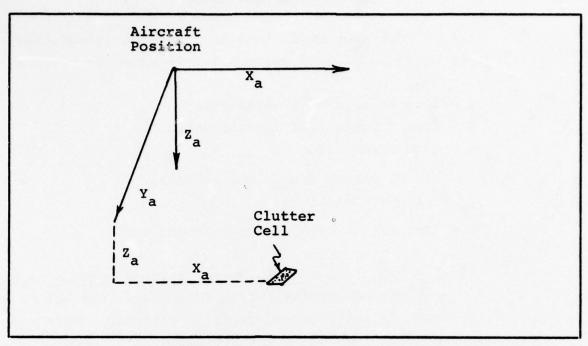


Figure A-9 Aircraft Relationship to a Surface Clutter Cell

. For any particular cell we have coordinates R, R and are presuming $\mathbf{Z}_{\mathbf{a}}$ known. Solving for the rectangular coordinates of the clutter with respect to the aircraft we have:

$$x_{a} = \frac{R R}{V}$$
 1.2-25

$$Y_a = \sqrt{R^2 - x_a^2 - z_a^2}$$
 1.2-26

If we now assume constant velocity V and a surface coordinate system centered under the aircraft at t=0; X, Y, Z at time t are given by:

$$X = X_a + Vt$$
 1.2-27

$$Y = Y_a$$
 1.2-28

$$Z = Z_a = altitude$$
 1.2-29

Our mapping of data into surface coordinates is given by equations 1.2-25 through 1.2-29 where we measure:

R = from range gate identification

R = from doppler cell identification

t = from frame index

We assume from pilot control:

Z_a = aircraft altitude

V = aircraft velocity (surface velocity)

Inputs available from flight plan and data logs are; V, aircraft velocity and Z, aircraft altitude. From the data tape the following inputs are available; A = power of return, I = range gate number, J = doppler cell number, K = frame number (number of FFT's since start of run).

The transformation is computed as follows:

$$R = R_0 + I(\Delta R)$$

$$R = R_O + J(\Delta R)$$

$$X' = R R/V$$

$$X = X' + VT$$

$$y = \sqrt{R^2 - x^2 - z^2}$$

ΔT is FFT frame time (data reduction parameter)

ΔR is range gate dimension (system parameter)

 $\Delta\,R$ is doppler cell size in velocity unit

Note that the doppler cell size can be defined

as:

$$\Delta R = \frac{\Delta F}{2f_0} \cdot c$$

Where:

 $\Delta F = frequency cell size$

f = range frequency

c = speed of light

1.2.6 Radar Resolution Characteristics

Radar range and doppler resolution characteristics are described in this section. Range resolution is primarily determined by transmitted pulsewidth and receiver video filters ahead of the sample and hold circuits. Doppler resolution is a function of the data reduction process and its associated Fast Fourier Transform (FFT) signal processing equipment.

The transmitted waveform envelope is closely approximated by a rectangular CW pulse with width T = 0.2usec time duration. The two-sided IF bandwidth of the receiver is 6.6 MHz with spectral characteristics determined by a two-pole Bessel filter. Time-bandwidth product for the filtered waveform is therefore BT = 6.6MHz X 0.2usec = 1.32. The effective pulsewidth has been computed as 1.2T = 0.24usec*.

^{*} L. W. Brooks, "Equivalent Pulsewidth of the TAGSEA Data Gathering System", Technology Service Corporation memo TSC-W2-65 B50711, dated 27 April 1976.

An ambiguity diagram for the transmitted pulse doppler waveform is sketched in Figure A-10. The PRF used for transmission of the pulse doppler waveform was 19.32KHz. Range ambiguities in the "bed of nails" are separated by 25,472 feet, or 4.19 nmi. Velocity ambiguities are separated by 974 feet/sec. The darkened area in Figure A-10 shows the range-velocity region mapped by the system. It is extended over 1600 feet in range and 176.4 ft/sec in velocity. The first range ambiguity is at 25.5KFT and the first velocity ambiguity is at 974 ft/sec. Therefore, the mapped region is clear from all ambiguities in range and velocity.

Figure A-11 shows an enlarged view of the ambiguity diagram in which both the waveform characteristics (after signal processing) and the mapped region are displayed in greater detail. Range resolution for an effective pulsewidth of 0.24usec is 118 feet. Velocity resolution calculations require an understanding of the data reduction process.

Briefly, pulse doppler echoes were applied to a sample and hold and boxcar integrator at a rate equal to the radar PRF (19.32 KHz). The integrated data was recorded on an analog tape for each range gate. Later, during data reduction playback, each range gate was played back and re-sampled at a reduced rate of 14 KHz. Continuous trains of 128 samples were processed without weighting by a Fast Fourier Transform (FFT) filter bank. Thirty-two out of the 128 filters output from the FFT were used for spectrum analysis. The spacing between doppler filters was 14KHz/128 = 109.375 Hz. Because the weighting was uniform, each FFT filter response was essentially a sin x/x function with doppler resolution equal to 0.886 of the filter spacing, or 96.57 Hz. Velocity resolution at X-band is given by

$$V_{RES} = \frac{\lambda}{2} f_{d(RES)} = \frac{0.1008}{2} \times 96.57 = 4.88 \text{ ft/sec.}$$

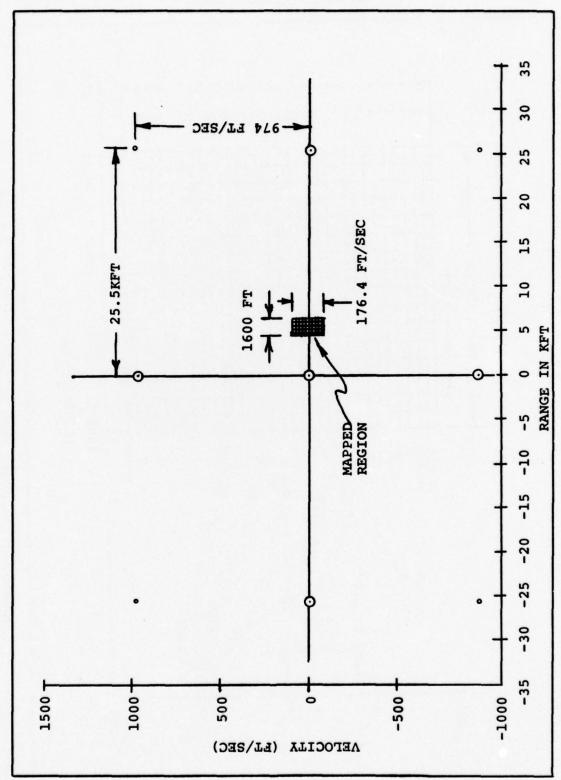


Figure A-10 Radar Ambiguity Diagram

UNCLAŜSIFIED

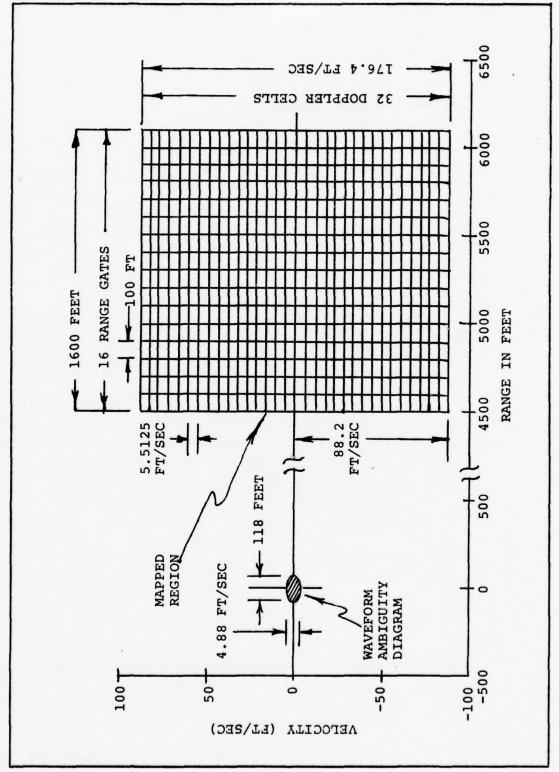


Figure A-11 Enlarged View of the Ambiguity Diagram

The range velocity waveform ambiguity diagram is compared to the mapped region in Figure A-11. Range resolution (118 ft) is slightly greater than the range gate spacing (100 ft). The velocity resolution (4.88 ft/sec) is slightly less than the spacing of velocity cells (5.5125 ft/sec). The mapped region spans 16 cells or 1600 feet in range and 32 cells or 176.4 ft/sec in velocity.

1.3 Statistics/Confidence

1.3.1 Statistics of Receiver Noise

This section is concerned with estimating the mean noise level of the TAGSEA radar system and obtaining confidence intervals for each estimate. At the end of each run a 10 to 15 second interval of a calibration signal was recorded and another interval of 10 to 15 seconds was noted with the transmitter off. This second period was an observation of the noise level of each range gate in the system during that run. The noise record, the calibration signal record, and the record of the setting of various meter readings were all kept as possible references for determining the gain of the receiver range gates. The received level was adjusted before each run so the average clutter power level fell between predetermined intervals.

The effect was to put the noise rather than the calibration signal more in the dynamic range of the clutter return in most range gates. This made the average noise power a more stable reference than the calibration signal and a more accurate measurement of the range gate gains; doing this allowed a better calculation of $\sigma_{\rm o}$.

In processing of the clutter data from analog to digital to form histograms, the signal strength was recorded only as a value between certain limits without regard to exactly where in that interval it fell. This "grouping" of the data has little effect on the uncertainty of the estimate of the average noise level for large noise levels. (See Figure A-12). For low noise levels the grouping has a more serious biasing effect in the estimate of the average noise level. The grouping of the data was performed by collecting the sample values into bins (or class intervals) depending upon their magnitude. There were 1024 class intervals and is a sample fell between levels 0 and 1 but was not equal to 1, it was counted as a value in bin 1. In an effort to maintain a constant average clutter return from range gate to range gate, the gains of the closer range gate filter were low enough in most runs to place most of the noise signal in bin 1. See Figure A-13. The question naturally arises as to the accuracy of any estimate of the average noise level for those range gates. Due to the grouping, the average power level can be anywhere between 0 and 1. fidence about the estimate of the mean of receiver noise is established using the concept of confidence intervals.

The most notable results coming from the use of confidence interval estimation is the relatively small error that is suffered for a high degree of confidence. If we have at least one value of noise power above class interval 1 we can make an estimate of its mean and feel confident that 99 out of 100 of these estimates will be in error by at most 1.6dB. This is a statement which can be made knowing only that we have at least one hit above bin one. Smaller errors naturally result from knowing exactly how many hits above class one there are.

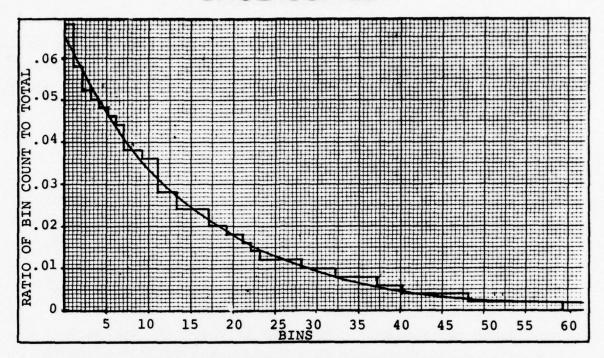


Figure A-12 Histogram of Noise with Mean About Bin 15

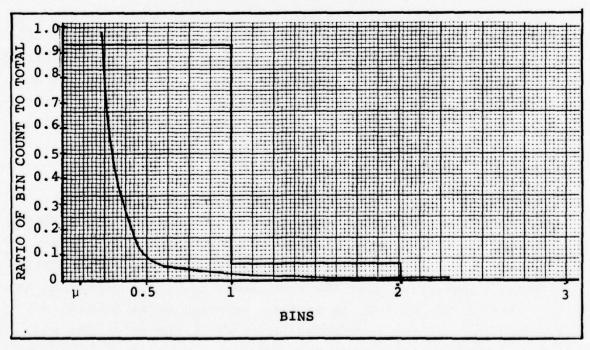


Figure A-13 Histogram of Noise with Histogram Mean About 0.5

The succeeding analysis is based on the assumption that the receiver power is exponentially distributed and hence determination of only one parameter, the mean of the noise power, will completely describe the distribution.

1.3.2 <u>Interpretation of the Results of Receiver</u> Noise Analysis

A complete understanding of how to interpret the results is needed before a summary of the analysis is given. The object is to make some inference about where a parameter of a one parameter distribution lies, in this case the mean of the distribution. We want to make such an inference with a certain degree of confidence, which will be measured by a "confidence coefficient". The mean of the noise during a particular noise histogram is a fixed quantity, not a random variable. This precludes inferences of the kind, "the probability of the mean being situated between two values is P, where P is a confidence coefficient". A statement of that type would make sense only if the mean were a random variable. However, it is also realized that from noise calibration to noise calibration the receiver gain may and does vary due to system variations and gain settings. The hope is to make an inference about the mean without having to hypothesize about its random and non-random nature. The concept of "confidence intervals" is one way to handle this problem.

Confidence intervals allow us to make the following statement: For a pre-assigned confidence coefficient γ (0<\gamma<1), we will count the number of occurances x_0 above interval 1 and using γ and x_0 determine lower and upper limits $(\underline{\mu}$ and $\overline{\mu})$ and claim that the true mean, μ_0 , lies between $\underline{\mu}$ and $\overline{\mu}$. Either the mean μ_0 is in that interval or it is not, but in the long run our inferences about where the mean lies will be in error by at most 100(1- γ) percent of the time.

If we choose γ close to 1, we will be in error a small percentage of the time. The price paid for a small error is that the confidence interval may then be large.

1.3.3 Conclusions on Statistics and Confidence of Receiver Noise

The results of the confidence interval estimation is best described by referring to Figure A-14 which tabulates what the confidence interval (μ , $\overline{\nu}$) is for specific hits above interval 1 and for various confidence levels. As expected, the figure does show that the lower the confidence level, the narrower the confidence interval is. For the values of γ in Figure A-14 the largest error would be committed if γ = 99% and the number of hits (m) equal 1. In this special case if the true mean, $\mu_{\rm O}$, were within the confidence interval .070 \leq $\mu_{\rm O}$ \leq .127, an estimate of 0.10139 for the mean is in error by at most 1.6dB. This is the maximum error at the 99% confidence level or less given one hit. The estimate, μ^* , of the mean is obtained by the equation

$$\mu^* = -\frac{1}{\ln(\overline{\Delta})}$$

where $\overline{\Delta}$ is the ratio of hits above interval 1 to total hits. If for each run we form the ratio $\overline{\Delta}$ and use the above equation to get an estimate μ^* of μ_O we note that at least 99 out of 100 of these estimates will be in error by at most 1.6dB assuming that we have at least one hit above interval 1.

Figures A-15, A-16 and A-17 give contours from which other confidence levels can be calculated for specific confidence coefficients. These figures are for γ = 0.99, 0.90, 0.6826 and hits less than or equal to 100.

ERROR OF 1* FROM 1(dB)	86.0	92.0	0.46	0.20	0.12	0.10	.73	.56	.31	.13	11.	.07	.54	.42	.18	60.	.05	.04
ERROR OF proceed to the proceed to the procedure of th	-1.6	-1.2	-0.53	-0.22	12	10	87	42	32	12	80	07	38	46	18	07	04	04
UPPER CONFIDENCE LIMIT	.127	.130	.147	.199	.348	.761	.120	.124	.142	.196	.344	.755	.115	.120	.138	.194	.342	.750
LOWER CONFIDENCE LIMIT	.070	.083	.117	.181	.329	.726	.083	.092	.123	.185	.332	.732	.093	860.	.127	.187	.335	.736
ESTIMATE v*	.10139	.10905	.13227	.19020	.3384	.7432	.10133	.10905	.13227	.19000	.3384	.7432	.10139	.10905	.13227	.19020	.3384	.7432
HITS ABOVE INTERVAL 1	1	7	10	100	1000	2000	1	7	10	100	1000	2000	1	7	10	100	1000	2000
CONFIDENCE LEVEL	866						806						68.268					

Figure A-14 Chart of Confidence Intervals with Likely Maximum Errors

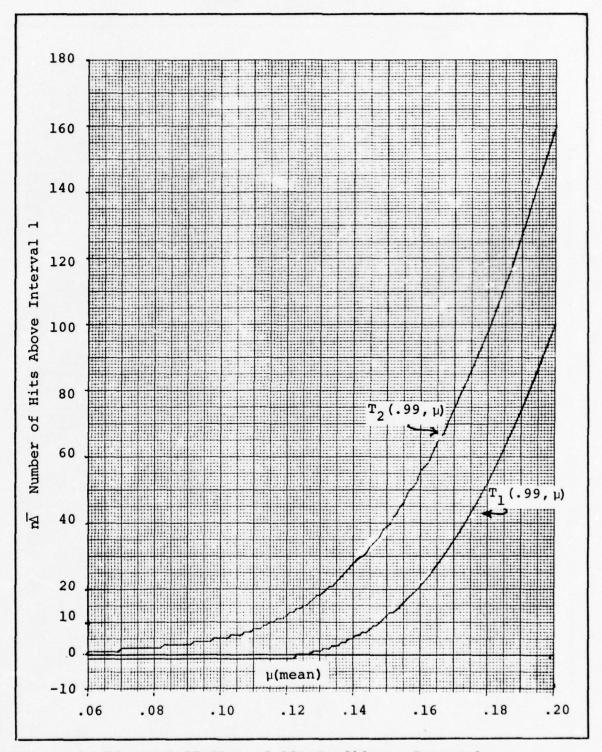


Figure A-15 Plot of 99% Confidence Intervals

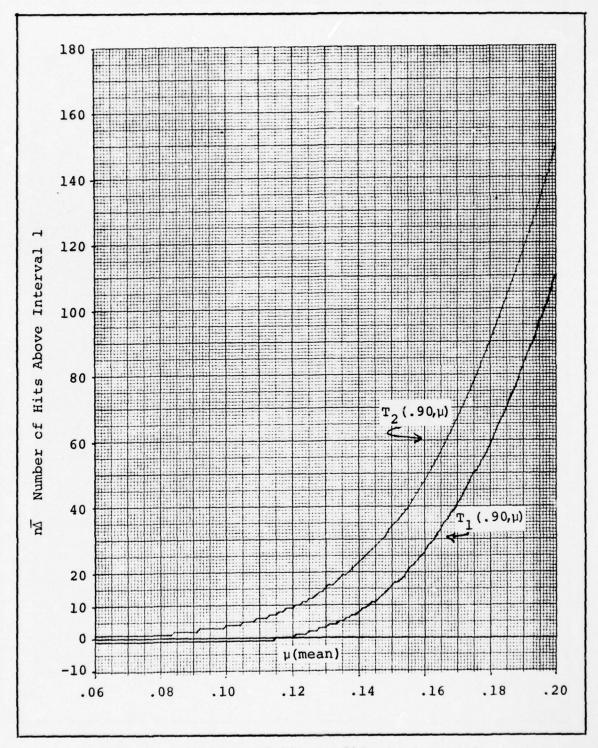


Figure A-16 Plot of 90% Confidence Interval

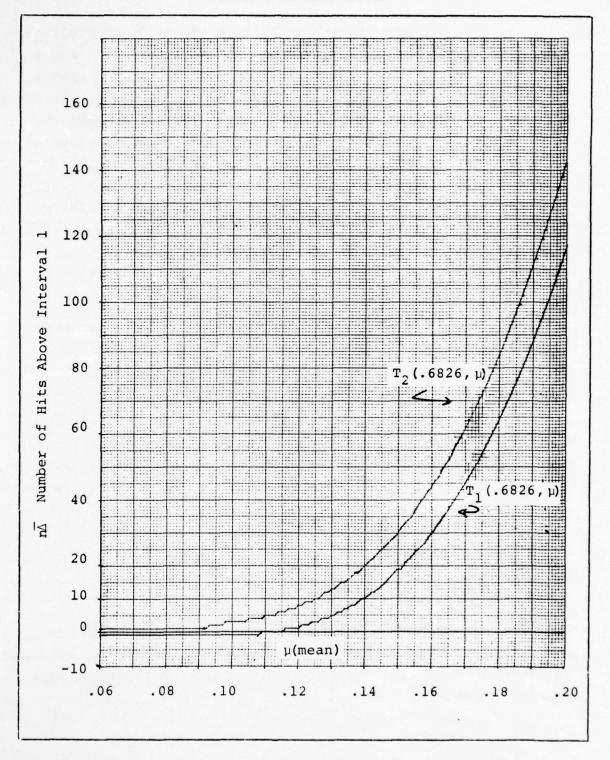


Figure A-17 Plot of 68.26% Confidence Interval

A-35

Using Figures A-15, A-16 and A-17, the following procedure is suggested to obtain confidence intervals. For a certain number of hits, \mathbf{x}_0 , in the range given in each figure, draw a horizontal line, Y, through the point $(0, \mathbf{x}_0)$ in the figure with the desired confidence coefficient. Where Y crosses the two contours \mathbf{T}_1 (γ, μ) and \mathbf{T}_2 (γ, μ), drop down to the horizontal axis and read μ and μ . For example, with 20 out of 19,200 values above class interval 1 and confidence at the 90% level go to FigureA-15. Draw a horizontal line Y through (0, 20) and from the intersection of Y and \mathbf{T}_2 (.90, μ) drop down to the μ axis and read 0.137 for μ . The upper confidence limit μ = 0.154 is obtained by dropping down from the intersection of Y with \mathbf{T}_1 (.90, μ).

If confidence intervals for hits greater than those given in Figure A-15, A-16 and A-17 are desired, the approximations given in Subsection 1.3.6 can be used. See equations 1.3-30 and 1.3-31.

For a large number of hits above interval 1, the error introduced in estimating the mean using the histogram mean is no longer large. As will be seen a relationship between the noise mean μ and the histogram mean $\hat{\mu}$ under certain assumptions is given by

$$\mu = \begin{cases} \frac{1}{\ln\left(\frac{2\stackrel{\sim}{\mu}+1}{2\stackrel{\sim}{\mu}-1}\right)} & \frac{1}{2} < \stackrel{\sim}{\mu} < \infty \\ 0 & \stackrel{\sim}{\mu} = \frac{1}{2} \end{cases}$$

$$1.3-2$$

The error in estimating μ using the above transformation for large number of hits above interval 1 can more easily be obtained by using the fact that the standard deviation $\frac{\sigma}{\hat{\lambda}}$ of the sample mean of the grouped data is

$$\frac{\sigma}{x} = \frac{1}{N} \frac{e^{-\frac{1}{\mu}}}{(1 - e^{-\frac{1}{\mu}})^2}$$
1.3-3

where N is the number of data points grouped and μ is the actual mean of the noise power.

1.3.4 Correction on the Average Noise Estimate Grouping

To determine estimates of the probability density function for clutter returns the data was grouped to form histograms. The noise signal was also grouped and the mean of the noise power was estimated using the sample mean of the noise histogram. The grouping was performed by collecting the data points into bins or class intervals according to the following scheme.

If x is a sample value such that $k-1 \le x \le k$ for $1 \le k \le 1023$ then x is counted as a value in bin k, but for x>1023 it is counted as a value in bin 1024. To form histograms the number of points in each bin is multiplied times a representative value of the data in that bin called the class mark. If the midpoint of each bin is chosen as the class mark then for bin k the class mark is $k-\frac{1}{2}$. A class mark of the left endpoint of each bin was used as a class mark for certain data reduction but the following equations are developed only for a class mark at the midpoint.

If we assume the data x is sampled from a stationary random process with a continuous distribution F(x) and probability density function f(x) then grouping the data implies we are no longer sampling the original random variable x but one, y, which is now discrete taking only values of

 $\frac{1}{2}$, $\frac{3}{2}$, $\frac{5}{2}$, ..., $1023\frac{1}{2}$. If we let the probability density function (pdf) of y be f(y) and assume y is not bounded by $1023\frac{1}{2}$ then

$$f(y) = p_k \text{ for } y = \frac{2k-1}{1}, k = 1,2,3,4...$$

where

$$p_k = \int_{k-1}^{k} f(x) dx$$
 $k = 1, 2, 3 \dots$ 1.2-4

If we take N independent sampled values of x, say x_1 , ..., x_n and group them, they give N independent sample values of y. Forming the sample mean, \overline{y} , of the grouped values gives an estimate of the mean $\widehat{\mu}$ of y and \overline{y} is a biased estimate of the mean, μ , of x. If we assume that the noise power, x, is exponentially distributed then the relationship between μ and $\widehat{\mu}$ is

$$\hat{\mu} = \sum_{k=1}^{\infty} \left(\frac{2k-1}{2} \right) p_k$$
 1.3-5

or

$$\hat{\mu} = \sum_{k=1}^{\infty} \left(\frac{2k-1}{2} \right) \int_{k-1}^{k} \frac{1}{\mu} e^{-\frac{x}{\mu}} dx$$
 1.3-6

This simplifies to

$$\hat{\mu} = \frac{1}{2} \frac{(1+e^{-\frac{1}{\mu}})}{(1-e^{-\frac{1}{\mu}})} \qquad \mu \neq 0 \qquad 1.3-7$$

and solving for µ gives

$$\mu = \begin{cases} \frac{1}{\ln\left(\frac{2\hat{\mu}+1}{2\hat{\mu}-1}\right)} & \frac{1}{2} < \hat{\mu} < \infty \\ 0 & \hat{\mu} = \frac{1}{2} \end{cases}$$

$$1.3-8$$

The standard deviation of the sample mean \overline{y} is easily seen to be

$$\sigma_{\overline{y}} = \sqrt{\frac{1}{N}} \frac{e^{-\frac{1}{\mu}}}{(1 - e^{-\frac{1}{\mu}})}$$
1.3-9

Where N is the number of samples.

To obtain confidence regarding the mean of receiver noise from noise histograms, the theory of interval estimation was employed. (1) To establish a "confidence interval" for the mean, some probalistic model of receiver noise is needed. The exponential model for noise power is known to be a good approximation and in the following analysis it is assumed that the noise voltage is Rayliegh distributed. This assumption implies that determination of only one parameter, the mean of the noise will completely describe the distribution. This one parameter distribution makes determination of confidence interval easier to handle and lends itself to fairly standard statistical analysis. (1)(2)(3)

If x is the random variable y describing noise power, then the pdf (probability density function) f(x) is

$$f(x) = \begin{cases} \frac{1}{\mu} & e^{-\frac{x}{\mu}} & x \ge 0 \\ 0 & x < 0 \end{cases}$$

⁽¹⁾ H. Cramer (1946), "Mathematical Methods of Statistics", Princeton University Press.

⁽²⁾ M. G. Kendell and A. Stuart, "The Advanced Theory of Statistics", Vol. II, 2nd Edn, Chapter 20, pp. 98 - 120.

⁽³⁾ Samuel S. Wilks, (1963), "Mathematical Statistics", John Wilkey & Sons, Inc.

where $\mu = E(x)$.

Considering only hits above interval one without recording where above one a hit falls, we obtain as the probability p of getting a hit

$$p = Pr\{x \ge 1\} = \int_{1}^{\infty} f_{x}(x')dx' = \frac{1}{\mu} \int_{1}^{\infty} e^{-\frac{x}{\mu}} dy'$$
 1.3-11

Evaluating the far left side of equation 1.3-11 gives

$$P = e^{-\frac{1}{\mu}}$$
 1.3-12a

Equation 1.3-12a is important since it relates to the mean, μ , of the exponential distribution to the probability p through an invertible function. The task of establishing confidence intervals for the parameter μ with a pre-assigned confidence level, γ , can be translated to one of estalishing confidence intervals for the parameter p with the same confidence level γ and then translating back by using equation 1.3-12a or equivalently

$$\mu = -\frac{1}{\ln(p)} \quad o
1.3-12b$$

Obtaining an efficient estimate of p requires only counting the number of hits above 1 in n independent samples x_1, x_2, \ldots, x_n and then dividing by n. Therefore given a value of x, let Δ (x) be the function.

$$\Delta(x) = \begin{cases} 1 & \text{if } x \ge 1 \\ 0 & \text{if } X \le 1 \end{cases}$$
 1.3-13

If x is a random variable with pdf given by equation 1.3-10, then Δ (x) is a random variable with pdf given by

$$f_{\Delta}(\Delta') = \begin{cases} p & \text{if } \Delta' = 1\\ 1-p & \text{if } \Delta' = 0\\ 0 & \text{if } \Delta \neq 0, 1 \end{cases}$$
1.3-14

where p is given by equation 1.3-11. The expected value and variance of $\boldsymbol{\Delta}$ are

$$E\{\Delta\} = p \cdot \text{and } \sigma_{\Delta}^2 = p(1-p)$$
 1.3-15

Let x_1, x_2, \ldots, x_n be n independent samples of receiver noise with each x having the same pdf as x (equation 1.3-10). Forming the sum S

$$S = \Delta(x_1) + \Delta(x_2) + ... + \Delta(x_n)$$

gives a random variable x which measures the number of hits above class interval 1. Dividing S by n gives the sample mean $\overline{\Delta}$ of the independent samples Δ (x₁), Δ (x₂), ..., Δ (x_n), i.e.,

$$\bar{\Delta} = \frac{1}{n} \sum_{k=1}^{n} \Delta(x_k)$$
1.3-16

For particular sample values $x_1, x_2, \ldots, x_n, \overline{\Delta}$ is the relative frequency of the number of hits above class interval 1 in n hits. The cdf (cumulative distribution function) of $\overline{\Delta}$ is just the binominal distribution given by

$$F(\overline{\Delta};p) = \sum_{k=0}^{\Delta n} {n \choose k} e^{k} (1-p)^{n-k}$$
1.3-17

with
$$E(\bar{h}) = p_0 \sigma_{\bar{h}}^2 = \frac{pq}{n}$$
 and $\binom{n}{k} = \frac{n}{k (n-k)}$

To apply the theory of confidence intervals to the parameter p, let γ , 0< γ <1, be the confidence coefficient and let α = $\frac{1-\gamma}{2}$. Let $T_1(\gamma,p)$ and $T_2(\gamma,p)$ be two integer valued functions of γ and p such that for a fixed γ and 0<p<1 we have the following inequalities using equation 1.3-17.

$$F(T_1/n;p) < \alpha \text{ and } F(T_1/n;p) \ge \alpha$$
 1.3-18

for T_1 (γ,p) and

$$1-F(T_2/n;p) < \alpha \text{ and } 1-F(T_2/n;p) \ge \alpha$$
 1.3-19 for $T_2(\gamma,p)$.

It can be shown that for the binominal distribution with parameter p functions T_1 , T_2 given by equations 1.3-18 and 1.3-19 do exist for every value of p. (3) Since $\overline{\Delta}$ is a discrete random variable, $T_1(\gamma,p)$, $T_2(\gamma,p)$ are step function with properties that

- a) $T_2(\gamma,p) > T_1(\gamma,p)$ for $0 , <math>0 < \gamma < 1$
- b) T₂, T₁ are non decreasing functions of p as illustrated in Figure A-18.

Note that for a fixed value of p, say p, we

have

$$P_{r} \left\{ T_{1} \ n\overline{\Delta} < T_{2}/P_{0} \right\} = \sum_{k=T_{1}+1}^{T_{2}-1} {n \choose k} (P_{0})^{k} (1-P_{0})^{n-R}$$
 1.3-20

⁽³⁾ ibid

Using equations 1.3-18 and 1.3-19 it is seen that

$$P_{r} \left\{ T_{1} < n \sqrt{1 - r_{2}} / P_{0} \right\} = 1 - F \left(T_{1} / n; P_{0} \right) - 1.3 - 21$$

$$[1 - F \left(T_{2} / n; P_{0} \right)]$$

or

$$P_{r}\left\{T_{1}<\sqrt{r_{0}} 1.3-22$$

Thus the probability of $\overline{\Delta}$ being in the 'tails' of the binominal distribution is less than 2α for a fixed p_0 .

i.e.,
$$P_r(n\overline{\Delta} \leq T_1) + P_r(n\overline{\Delta} \geq T_2) < 2\alpha$$
 1.3-23

The two contours T_1 , T_2 can now be used to generate confidence intervals for p with confidence coefficient γ .

For a particular sample mean $\overline{\Delta}$, let \underline{p} be the largest value of p such that

$$T_1(\gamma, p) \leq n\overline{\Delta}$$
 1.3-24

and let \overline{p} be the smallest value of p such that

$$T_2(\gamma,p) \geq m$$
 1.3-25

 \underline{p} and \overline{p} depend upon the sample mean and as such are random variables with property the $\underline{p} < \overline{p}$. (3)

p is called the lower confidence limit and \bar{p} is the upper confidence limit. The interval (p,\bar{p}) is called the 100 γ % confidence interval. This interval has the property that if p_0 is the true value of p, then the probability that the interval (p,\bar{p}) contains p_0 is greater than or equal to γ .

i.e.,
$$P_r \left\{ \underline{p} \leq \underline{p}_0 \leq \overline{p} \right\} \geq \gamma$$
 1.3-26

To see that equation 1.3-26 is valid, consider Figure A-18.

⁽³⁾ ibid

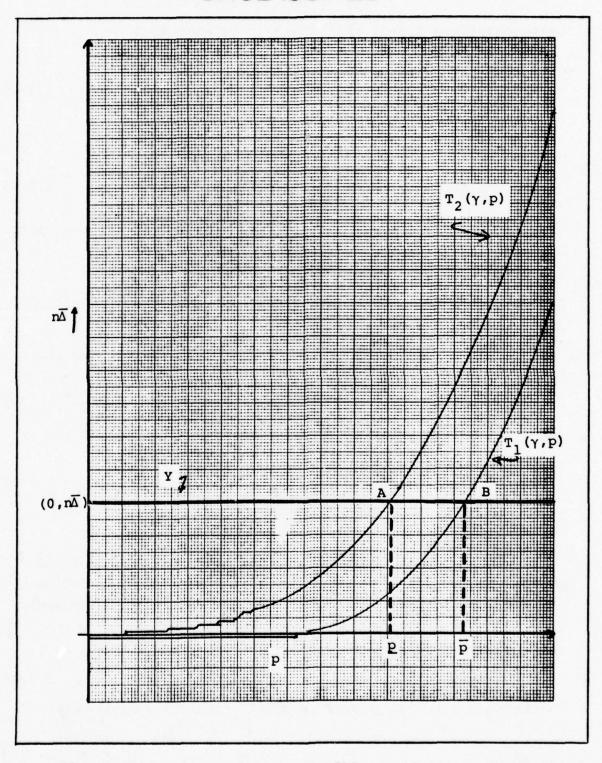


Figure A-18 Upper and Lower Confidence Limits

 T_2 and T_1 are the upper and lower 100 γ % confidence contours defined by equations 1.3-18 and 1.3-19. Let $\overline{\Delta}$ be the average number of "successful" hits in a random sample x_1 , ..., x_n and assume that p_0 is the true value of p. Then $n\overline{\Delta}$ is the number of hits above 1 in this sample and for $T_1(\gamma,p_0)< n\overline{\Delta}< T_2(\gamma,p_0)$ we have

$$P_r \left\{ T_1(\gamma, p_0) < n\overline{\Delta} < T_2(\gamma, p_0) / p_0 \right\} > \gamma$$

Using Figure A-18 it can be seen that $(\underline{p}, \overline{p})$ contains \underline{p}_0 if and only if

$$T_1(\gamma, p_0) \leq n\overline{\Delta} \leq T_2(\gamma, p_0)$$

We now have

$$P_{r}\left\{T_{1}(\gamma,p) \leq n\overline{\Delta} \leq T_{2}(\gamma,p)/p_{o}\right\} \geq \gamma \text{ if and only if}$$

$$P_r \left\{ \underline{p} \leq P_o \leq \overline{p} \right\} \geq \gamma$$
.

Which is what we set out to establish.

Because of equation 1.3-12, the confidence interval on p can be related to one on μ . Let

$$\mu = \frac{1}{\ln(\underline{p})}$$

1.3-27

$$\frac{1}{\mu} = \frac{1}{\ln{(\overline{p})}}$$

If μ_{O} is the actual mean and we let

$$p_0 = \exp(-\frac{1}{\mu_0})$$

then we have

$$P_{r}\left\{\underline{\mu} \leq \mu_{o} \leq \overline{\mu}\right\} = P_{r}\left\{\underline{p} \leq P_{o} \leq \overline{p}\right\} > \gamma \qquad 1.3-28$$

This gives confidence intervals on μ with confidence coefficient $\gamma_{\:\raisebox{1pt}{\text{\circle*{1.5}}}}$

1.3.6 Determination of Confidence Contours, $T_1(\gamma,p)$, $T_2(\gamma,p)$

It can be seen in Subsection 1.3.4 that from a sample x_1 , ..., x_n of receiver noise, computation of $n\overline{\Delta}$ gives the number of hits above interval 1. Using $\overline{\Delta}$, the values \underline{p} and \overline{p} or \underline{p} and \overline{p} can be calculated for a specific confidence coefficient γ . This procedure depends heavily upon having the functions $T_1(\gamma,p)$, $T_2(\gamma,p)$ for $0 . Calculation of <math>T_1$ and T_2 require solving equations 1.3-18 and 1.3-19. Figures A-13, A-16 and A-17 were obtained by a computer program evaluating equations 1.3-18 and 1.3-19 directly. Figure A-12 was partially obtained by using a normal approximation assuming n is large. As $n \to \infty$ and with p fixed, the binominal distribution equation 1.3-19 tends to the normal distribution with mean np and variance np(1-p).

i.e.,
$$\binom{n}{k} p^k (1-p)^{n-k} = \frac{1}{\sqrt{2\pi np(1-p)}} e^{-\frac{(x-np)^2}{2np(1-p)}}$$

Using this approximation \underline{p} and \overline{p} can be determined by the equation ⁽⁴⁾

$$\frac{\overline{p}}{p} = \frac{1}{n + \lambda^2 \alpha} \left[n\overline{\Delta} + \frac{1}{2} + \frac{\lambda^2 \alpha}{2} + \lambda_{\alpha} \sqrt{\frac{(n\overline{\Delta} + \frac{1}{2})(n - n\overline{\Delta} + \frac{1}{2})}{n} + \frac{\lambda^2 \alpha}{4}} \right]$$
1.3-30

⁽⁴⁾ A. Hald, "Statistical Theory with Engineering Applications", (Sixth printing 1965), John Wiley & Sons, Inc.

where λ_{α} is the solution to the equation,

$$\alpha = 2 \left[1 - \emptyset(\lambda_{\alpha})\right] = \frac{2}{2\pi} \int_{\lambda_{\alpha}}^{\infty} e^{-t^{2}/2} dt$$
 1.3-31

The normal approximation is a "good" approximation if np(1-p) is "large". (4) Error bounds can be obtained for this approximation and in the calculations of $\overline{\mu}$, $\underline{\mu}$ the error is less than 3×10^{-4} if $n\overline{\Delta} > 900$. (5)

1.4 Equations for Computing Weighting Tables

Weighting tables were used to compensate for variations in the data resulting from changes in range, doppler, and angles off antenna boresight. These are the theoretically known factors. The weighting was applied to the output of the FFT during data reduction. Hardware and other variabilities were considered separately during data analysis.

The weighting function as a multiplier is given by the expression:

$$MULT(N,R,A) = \frac{K \cdot R^4}{ANT(N,R,A) \cdot AREA(N,R,A) \cdot SINC(N) \cdot \sigma_O(A,R)}$$

where: N = doppler cell number

R = range

A = Altitude

K = Dynamic range scaling

ANT() = Antenna weighting

AREA() = Area of resolved patch on ground

⁽⁴⁾ A. Hald, "Statistical Theory with Engineering Applications", (Sixth printing 1965), John Wiley & Sons, Inc.

⁽⁵⁾ Harvard Computation Laboratory (1955), "Tables of the Cumulative Binomial Probability Distribution", Harvard University, introduction pp. XVIII

SINC() = Sample/Hold weighting

 $\sigma_{c}()$ = Grazing angle weighting

This expression comes directly from the radar range equation, and each of the components on the right hand side of the equation is described as follows:

a) R⁴ Factor

The computation of R⁴ is a simple function of the range gate number.

b) K Factor

This factor is chosen to optimize dynamic range in the succeeding computations.

c) SINC

The $\sin x/x$ frequency aperture generated by the S/H was obtained by simply evaluating the sine function at the appropriate frequencies.

d) Mean Radar Cross Section

The radar cross section was compensated as a function of grazing angle by taking data from the standard $\sigma_{\rm O}$ curves. This gives a fairly good approximation to the actual function and reduces the dynamic range required. To obtain an absolute measure of $\sigma_{\rm O}$ when desired, this compensation was reversed in the data analysis procedure.

e) ANT

The antenna pattern (ANT) equations used were those in Subsection 1.2.3 of this appendix. A function of the crab angle estimated from the data during data reduction was used for weighting. Using

the coordinate system of Figure A-19 the following definitions are applicable:

ANUM - doppler cell number starting from zero doppler

PRF - sampling rate (14900 Hz)

M - number of points in FFT (128)

V - aircraft velocity (420 F/S)

 λ - mean wavelength of transmitter output (0.1 FT)

G - antenna gain (11dB on axis)

P - transmitter power (60dBm)

RW - range dimension of equivalent rectangular resolution cell on sea

 angle of resolution cell off aircraft broadside in horizontal plane

R - range to approximate center of resolution cell

N - corrected mean value of receiver noise

The coordinates of the LOS in the antenna frame are given by:

 $R = V \cos \theta = C \cos \psi \cos \rho$

 $R = V \sin \alpha \cos \rho$

 $R = \frac{\lambda}{2} \frac{PRF}{M} (ANUM - 0.5)$

 $\alpha = \sin^{-1} \frac{PRF (ANUM-0.5)}{2VM \cos \rho}$

 $\tan \rho = \cos \alpha \tan \beta = \tan^{-1} \left(\frac{\tan \rho}{\cos \alpha} \right)$

 $\tan \emptyset = \tan^{-1} \left(\frac{\tan \rho}{\cos \alpha} \right)$

 $\emptyset = \tan^{-1} (\tan \alpha) (\cos \beta)$

 $\psi = \psi \text{ ANT-tan}^{-1} \left(\frac{\tan \rho}{\cos} \right)$

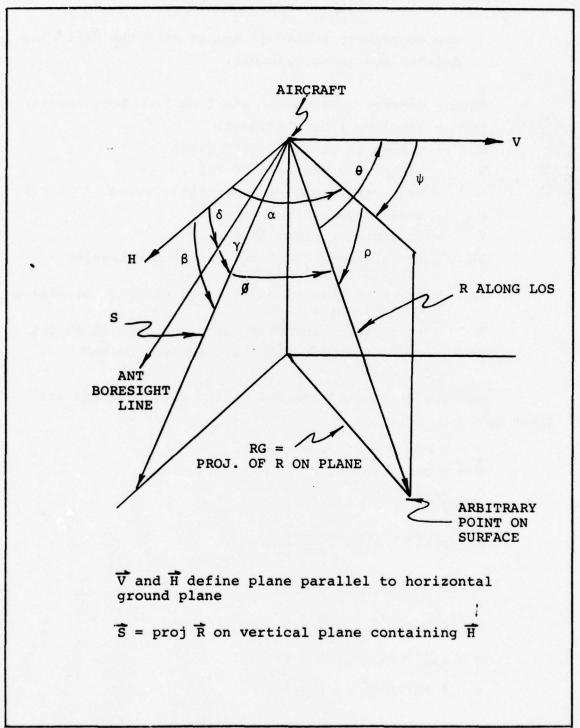
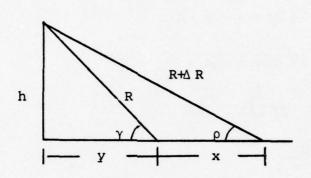


Figure A-19 Relative Position of Aircraft and Arbitrary Doppler Cell on the Surface

f) AREA

The area of each range-doppler cell was computed as explained below. The width of the doppler cell, i.e., the range dimension (x) is given in Figure A-20.



 ΔR = width of range gate

R = range to leading edge of range gate

$$y = R \cos x+y = (R+\Delta R)\cos \rho$$

$$= \sin^{-1}\left(\frac{h}{R}\right) \quad \rho = \sin^{-1}\left(\frac{h}{R+\Delta R}\right)$$

$$x = RW = (R+\Delta R)\cos\left(\sin^{-1}\left(\frac{h}{R+\Delta R}\right) - R\cos(\sin^{-1}\frac{h}{R}\right)$$

Figure A-20 Vertical Plan Containing the LOS to the Leading Edge of a Range Gate

Then the length of a doppler cell is

$$\dot{R} = V \cos \theta = V \cos \psi \cos \rho$$

$$\dot{R} = V \sin \alpha \cos \rho$$

$$f_{d} = \frac{2\dot{R}}{\lambda} = \frac{2V \cos \rho \sin \alpha}{\lambda}$$

$$\delta f_{d} = \frac{2\dot{V}}{\lambda} \cos \rho \cos \alpha d \alpha$$

$$d\alpha = \frac{\delta f_{d}}{2V \cos \rho \cos \alpha}$$

$$R_{G}d\alpha = \frac{\delta f_{d} \lambda R_{G}}{2V \cos \rho \cos \alpha}$$

$$R = \frac{R_G}{\cos \rho}$$

$$\delta f_d = \frac{PRF}{M}$$

$$D = \frac{\lambda (PRF) R}{2V M \cos \alpha} , \text{ and the area of a doppler cell is}$$

$$A = \frac{\lambda \times PRF \times R \times RW}{2 \times V \times N \times COS \alpha}$$

1.5 Conditional Probability Maps as Diagnostic Tools

Conditional probability maps were orginally intended to characterize the neighborhoods of large hits and were so used in the data analysis. These maps have also proved to be excellent detectors of anomalous behavior in runs. This property of conditional probability maps is illustrated below using run 1603 (flight 16 run 3) as an example.

The hit count versus time map of 1603 (Figure A-21) shows a sudden increase in hit level in range gate 2 at approximately 12.5 seconds. This unusually high level continues until 17.5 seconds.

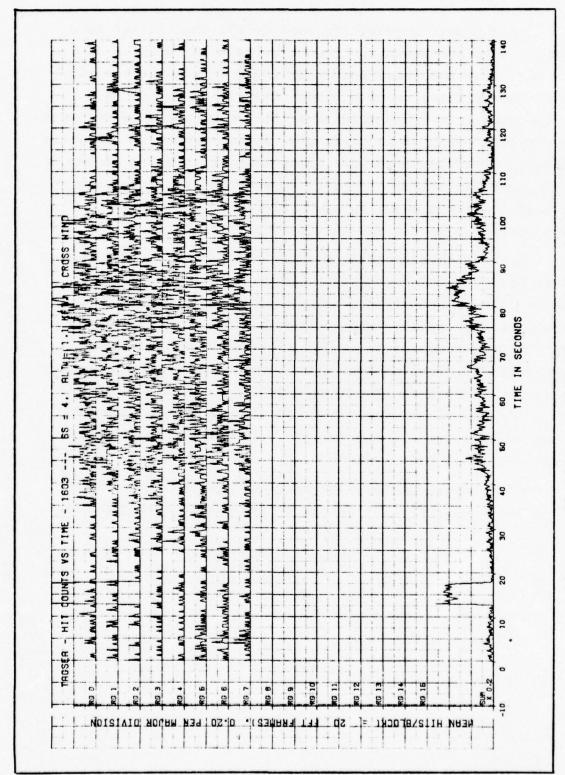


Figure A-21 Hits vs. Time Plots of Run 1603

Conditional probability maps of all the clutter data in flight 1603 are shown in Figures A-22, A-23, A-24, A-25 and A-26. That the phenomena is extended in time is readily seen in the relative range = 0 map (Figure A-23) and the relative doppler = 0 map (Figure A-24). From the time collapsed array (Figure A-25) it is clear that adjacent doppler cells are involved. From the normalization array (Figure A-26) it can be seen that the third range gate from the edge_of the maps contained the large majority of hits above T₁. This is of course confirmed by the hit time plot (Figure A-21).

Further investigation showed that erroneous responses were to be found in range gate 2 (probably due to computer problems in data reduction). Range gate 2 was deleted from the data to be processed and the resulting conditional probability maps (Figures A-27, A-28, A-29 and A-30) show the usual (vertical polarization) structure consisting of singular hits at the 0,0 point. The normalization array (Figure A-31) shows a biasing of the large hit towards one side of the map but not as severe as in Figure A-26. This is a direct result of deleting range gate 2 data.

Conditional probability maps have proven a valuable tool in locating sometimes subtle processing or data problems.

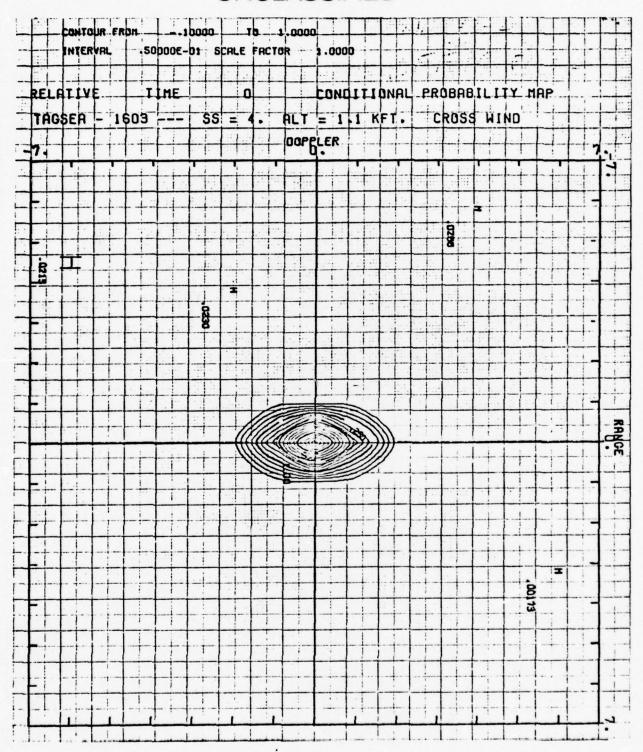


Figure A-22 Conditional Probability with Anomaly, Time=0

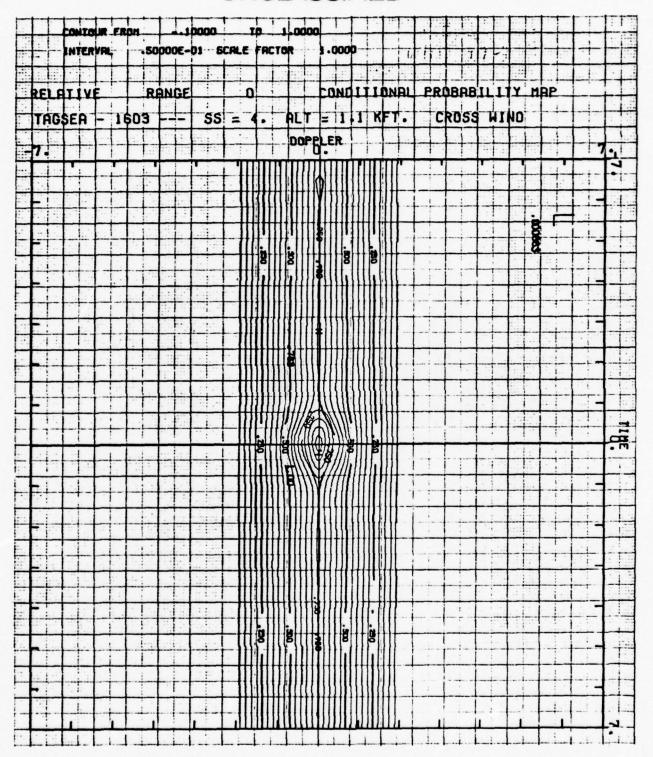


Figure A-23 Conditional Probability with Anomaly, Range=0

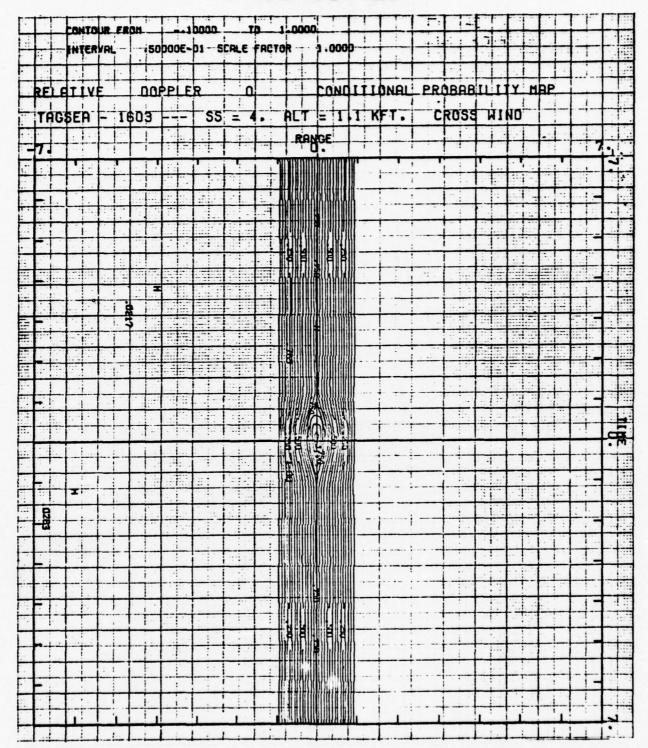


Figure A-24 Conditional Probability with Anomaly, Doppler=0

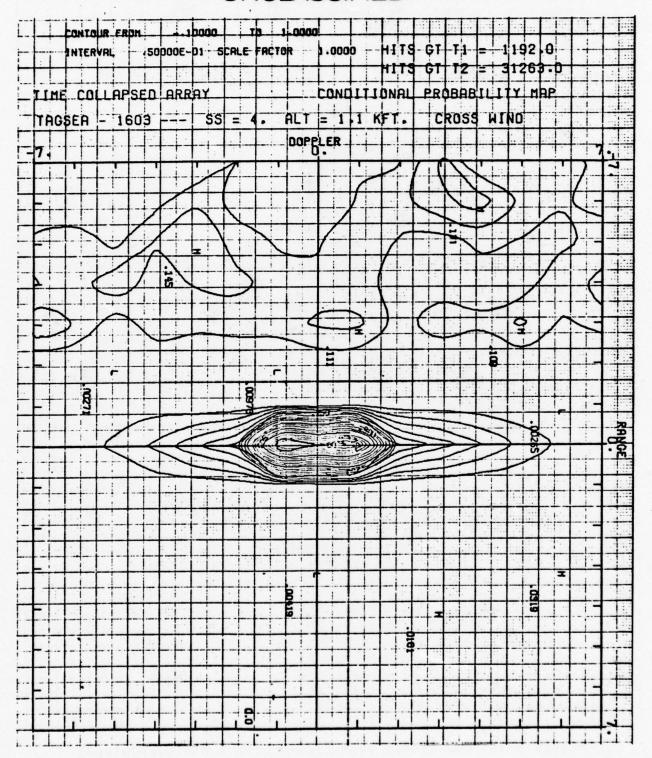


Figure A-25 Conditional Probability with Anomaly, Time Collapsed

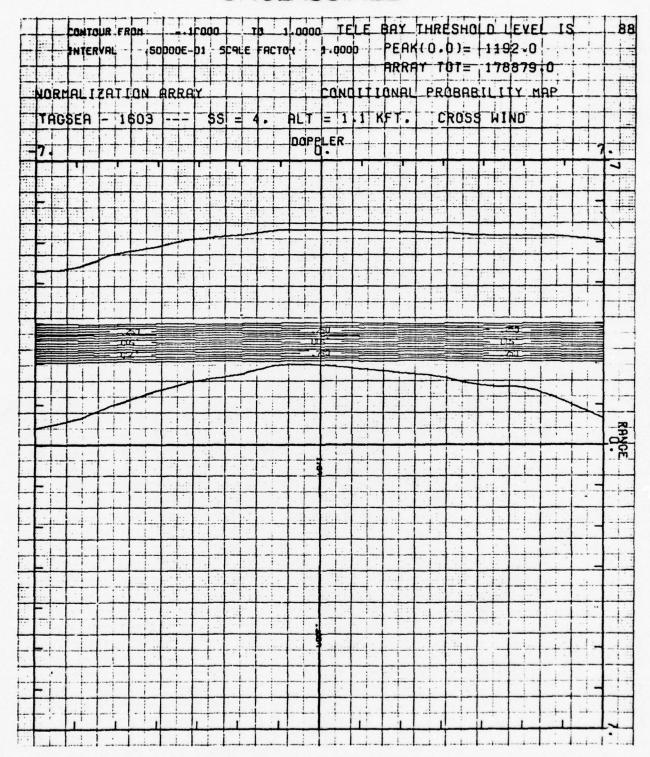


Figure A-26 Normalization Array with Anomaly

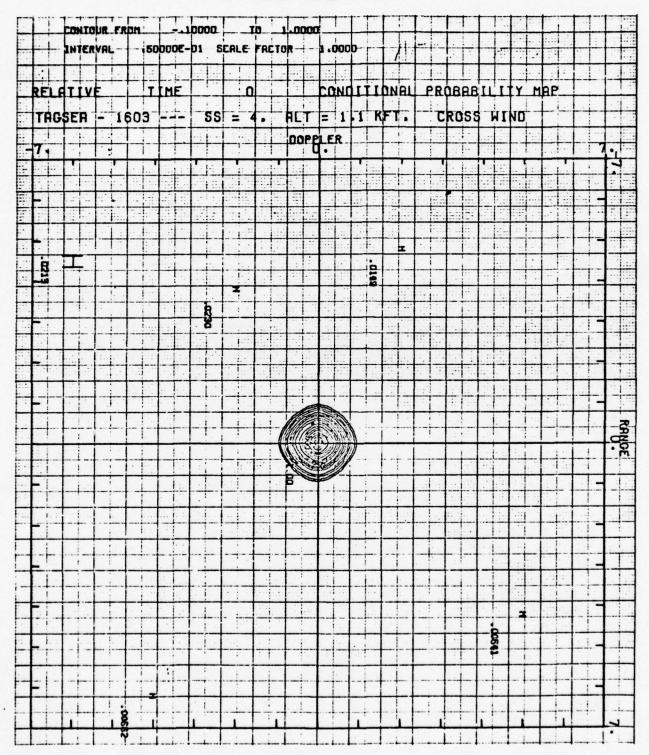


Figure A-27 Conditional Probability with Correction, Time=0

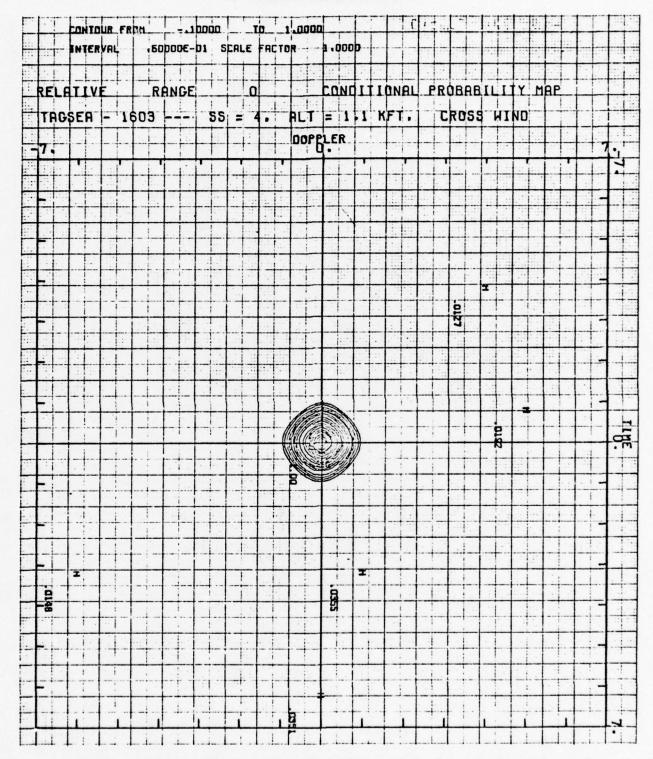


Figure A-28 Conditional Probability with Correction, Range=0

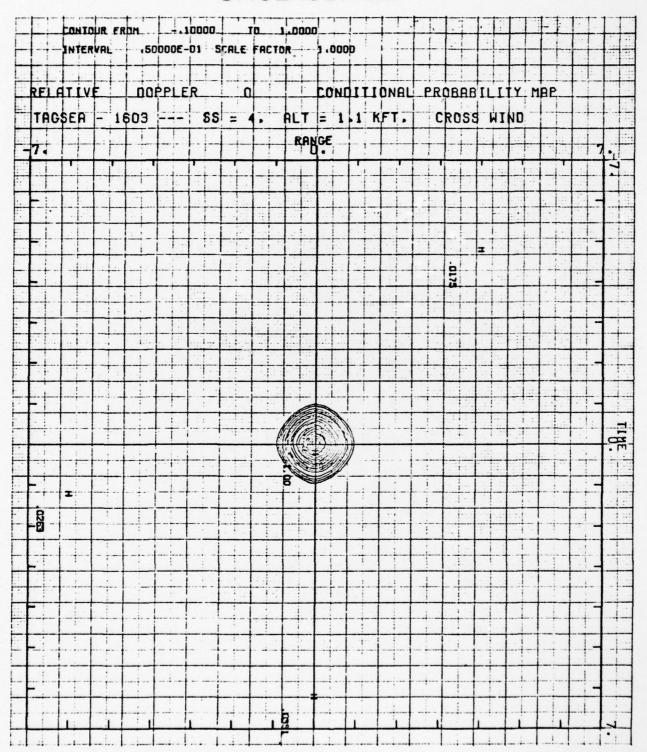


Figure A-29 Conditional Probability with Correction, Doppler=0

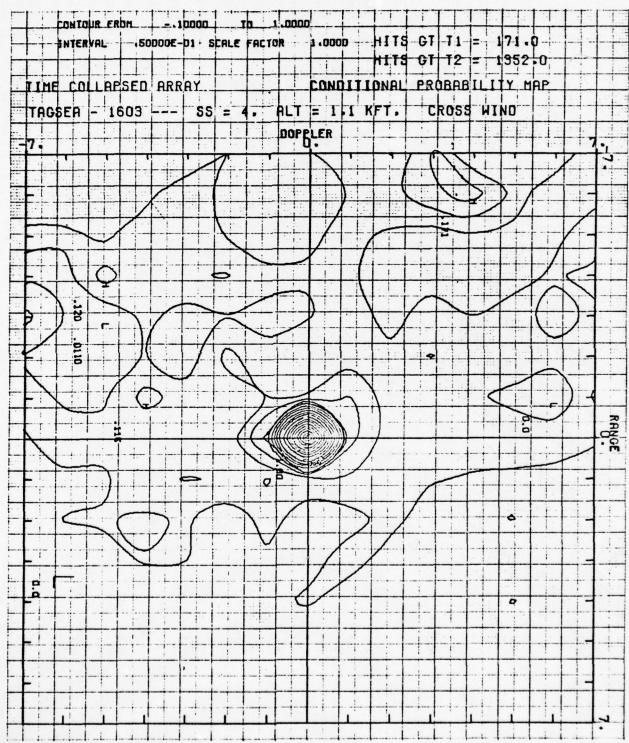


Figure A-30 Conditional Probability with Correction, Time Collapsed

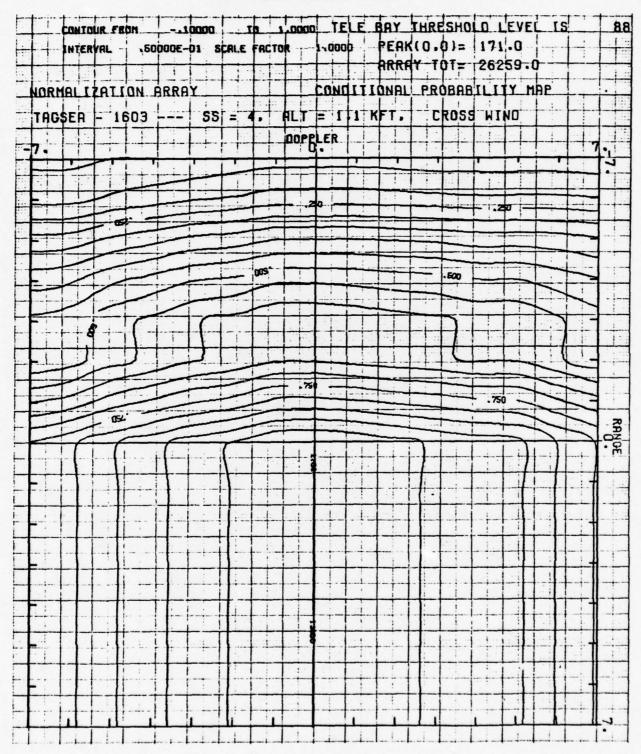


Figure A-31 Normalization Array with Correction

APPENDIX B OUTPUTS - SPECIAL ANALYSIS

This appendix gathers together the outputs of several special analyses. These are in addition to the standard histogram and other outputs which were done as a regular part of the data analysis. Included in this appendix are sections and subsections dealing with curve matching, histograms of the mean, variation of statistics, a special case of a ship in the field of view, behavior in the vicinity of a large hit and locally normalized histograms and associated plots.

1.1 Curve Matching of Histograms

This section is concerned with fitting the histograms of the sea clutter returns to some mathematically manageable function. The hope is to find an expression which has the property that the difference between it and the histogram is well within the sampling errors involved. When the histogram data was first observed there were attempts to characterize the data as coming from a time process whose mean was slowly varying and whose first oder distributions were Rayleigh or Weibull. These fits did not provide the best match since they did not track very well over the most useful part, the tails of the observed histograms. The need to find a curve, especially one which fit the tails, led to a match by cubic splines. Descriptions of the three types of curve matching follow.

1.1.1 Curve Matching Weibull and Rayleigh Functions to Data There are many theoretical models which are utilized as statistical models of clutter. The Weibull model which has the Rayleigh model as a special case (N=1) was chosen as a possible fit for the clutter data. A least squares fit of the

Weibull model to the data was performed and graphical results of these fits are given. The results of the fits show the Weibull model to be a fair-to-poor model expecially along the tails of the distributions. For the Rayleigh model a least squares fit was not performed but the mean at the exponential distribution was made equal to the sample mean of the data. For this model the fit was worse than for the more general Weibull.

The results of the fit for both models are shown only for mean adjusted data of flight 605 with vertical polarization, and flight 707 with horizontal polarization. Figures B-1 and B-2 are plots of both the data and the Weibull fitted for runs 605 and 707 respectively. Figures B-3 and B-4 are plots of the data and Weibull model with axes which make a Weibull distribution a straight line. The Weibull distribution is given by the equation

$$F(x) = \begin{cases} 1 - EXP - \left[\frac{x^{\eta}}{\alpha}\right] & 0 \le x < \infty & \eta, \alpha > 0 \\ 0 & x < 0 \end{cases}$$

This can be transformed into the equation

$$\ln \left[\frac{1}{\ln \left[\frac{1}{1 - F(x)} \right]} \right] = - \frac{\eta \ln(10)}{10} \cdot 10 \log_{10}(\frac{x}{10}) + \ln \frac{\alpha}{10^{\eta}}$$

which is a straight line if the coordinate axes are

$$ln[-ln[-(1-F(x))]]$$
 versus 10 $log_{10}(\frac{x}{10})$.

The least squres fit of a straight line to the data was performed in this coordinate system and values of η and x obtained are given in these graphs. The mean may be related to α and η by the expression

$$\overline{x} = \alpha^{\frac{1}{\eta}} \int (1 + \frac{1}{\eta})$$

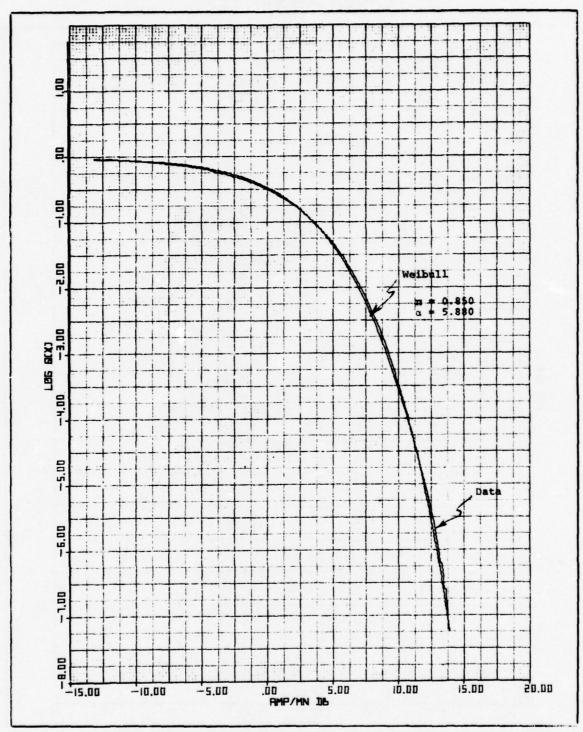


Figure B-1 Data Plot and Weibull Fit of Log Q From Flight 605

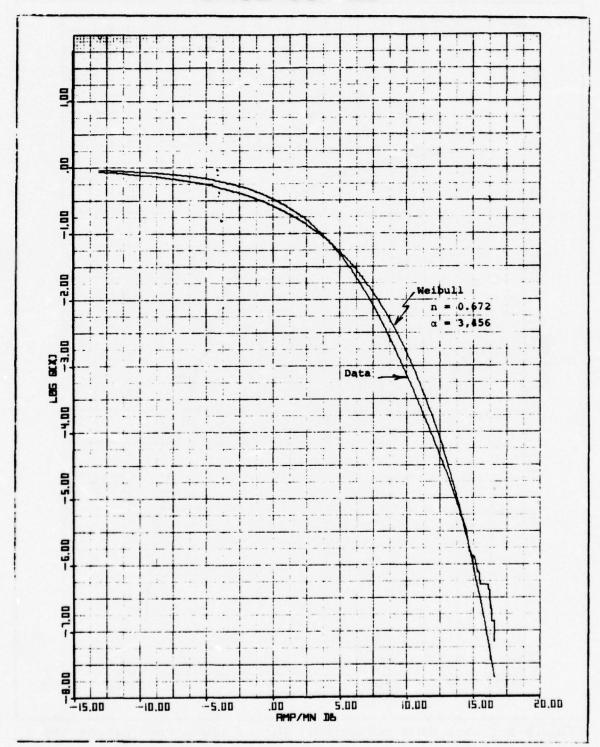


Figure B-2 Data Plot and Weibull Fit of Log Q From Flight 707

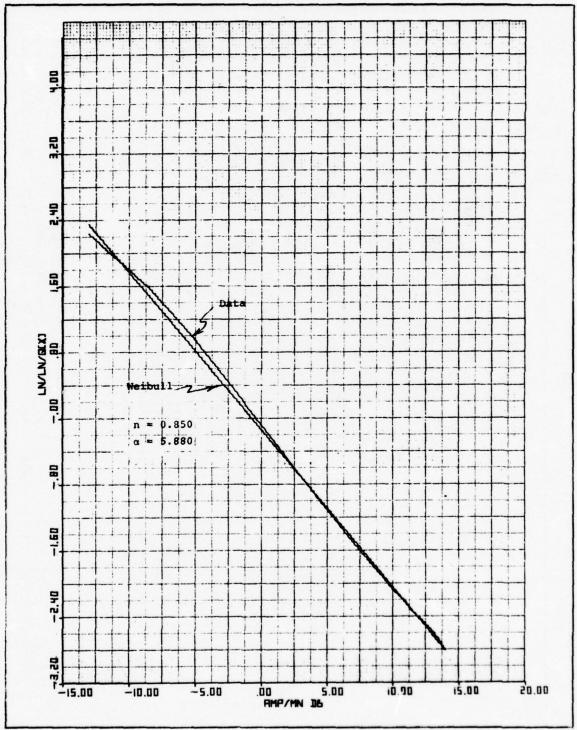


Figure B-3 Data Plot and Weibull Fit of Flight 605 in Weibull Coordinates

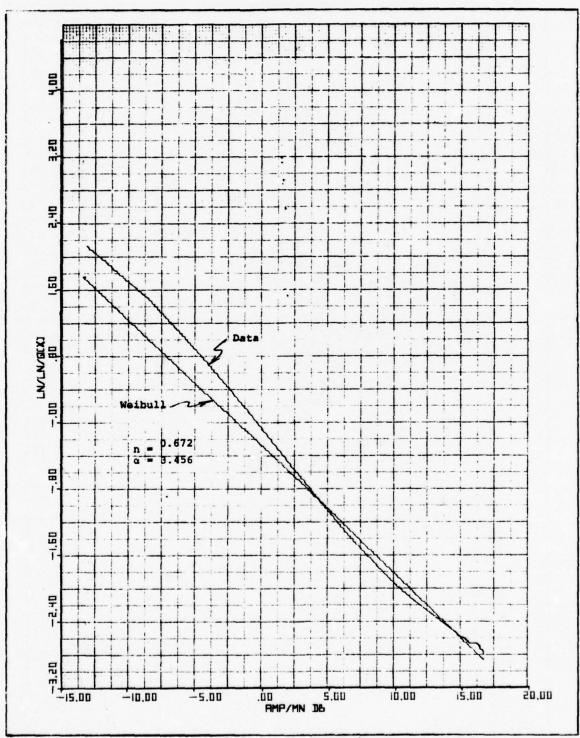


Figure B-4 Data Plot and Weibull Fit of Flight 707 in Weibull Coordinates

A measure of the goodness of fit is given by graphs B-5, B-6, B-7 and B-8.

For run 605 it can be seen that from the 10^{-1} to 10^{-6} points the model can differ from these points by as much as 0.25dB. For 707 this difference is high, about 0.75dB. However, if the ratio of the mean to the 10^{-3} point is considered, the error can be 2dB. As can be seen, the data from the vertical polarization, flight 605, is fitted better by the Weibull model than flight 707 with horizontal polarization. In either case, the Weibull is not an especially good fit when compared to the cubic spline fit of the next subsection.

The results for the Rayleigh fit are worse than those for the Weibull. One need only look at Figures B-9 and B-10 to see the poorer fit. The tails of the exponential distribution are much lower than the tails of the data. The errors in the match are given by Figures B-11 through B-14. Errors with respect to the matched mean are 1.8dB at the 10⁻⁶ point for run 605 and 3.8dB for run 707.

If, rather than attempting a Weibull least squares fit, we try only for a match at the mean and a close fit in the $Q = 10^{-3}$ through 10^{-6} region (but still use the Weibull plots) the problem becomes easier. The reason for doing this would be related to the usual radar CFAR use where the mean (or a point reasonably close) may be readily measured and false alarm thresholds can then be selected based on an extrapolation to the 10^{-3} or 10^{-6} point. Pragmatism rather than rigor is the guide and a fit in these terms to better than 1/2dB is quite acceptable. For this case, the fit for run 605 is already acceptable and run 707, an extreme case, almost satisfies the 1/2dB criterion. Figure B-15 is simply Figure B-4 with a new Weibull fit from the mean through +15dB (corresponding to Log Q = -6.0). This heuristic fit from the mean through the 10^{-6} point is within 0.75dB.

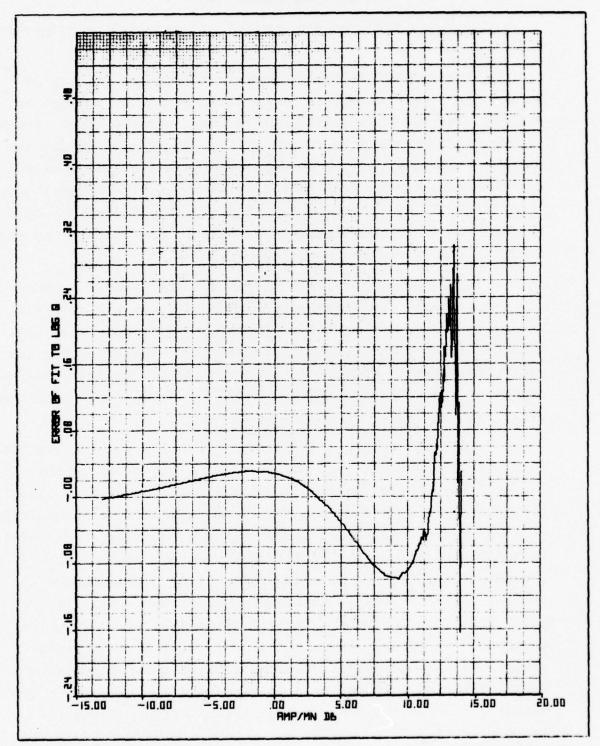


Figure B-5 Error of Weibull Fit to Log Q Data From Flight 605

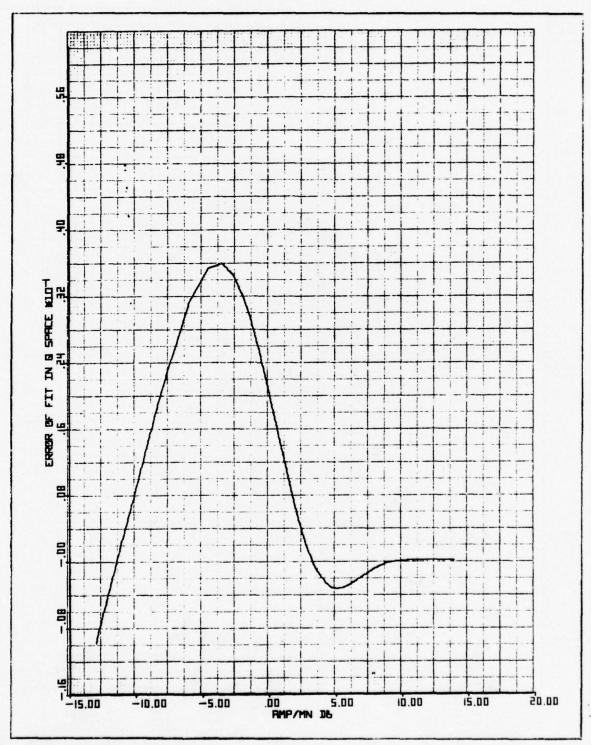


Figure B-6 Error of Weibull Fit to Q(x) Data From Flight 605

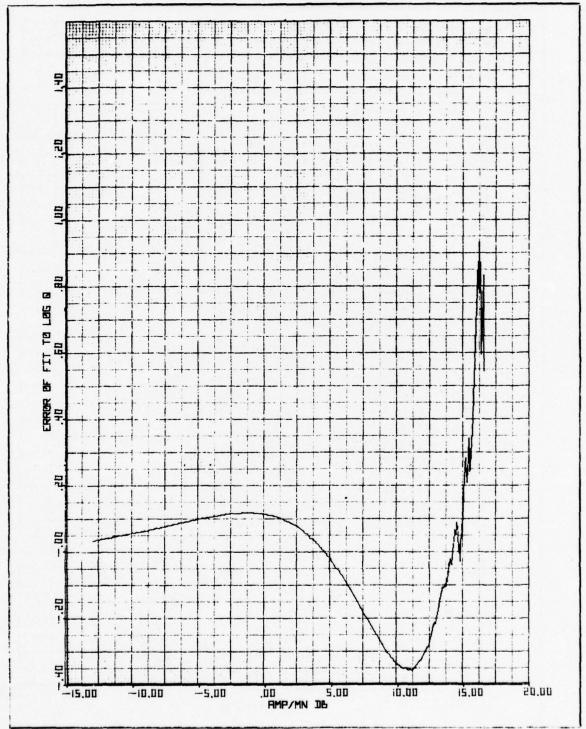


Figure B-7 Error of Weibull Fit to Log Q Data From Flight 707

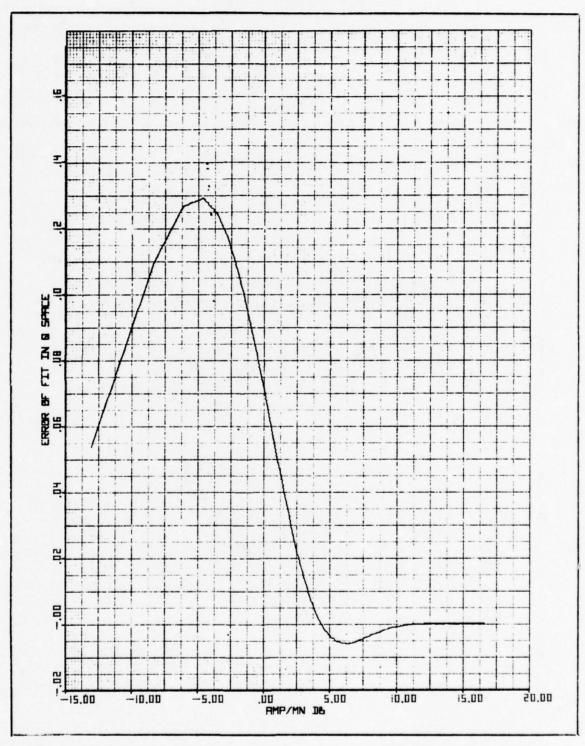


Figure B-8 Error of Weibull Fit to Q(x) Data From Flight 707

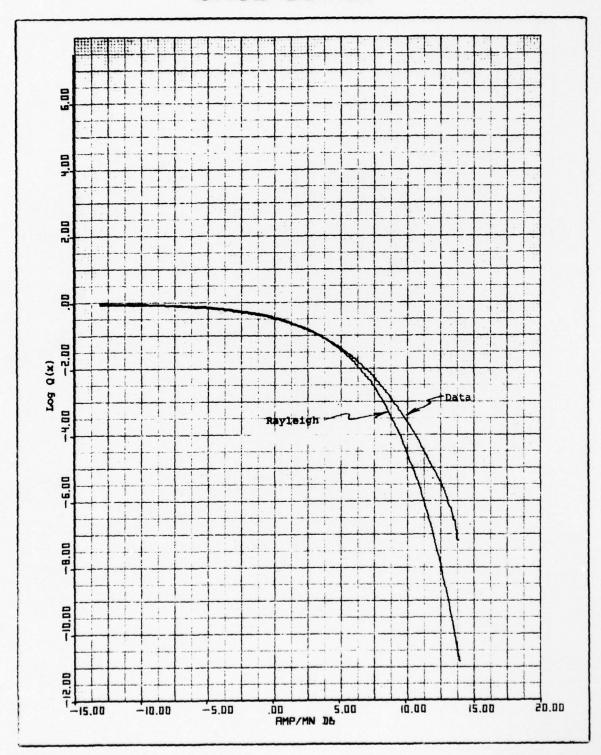


Figure B-9 Data Plot and Rayleigh Fit of Log Q From Flight 605

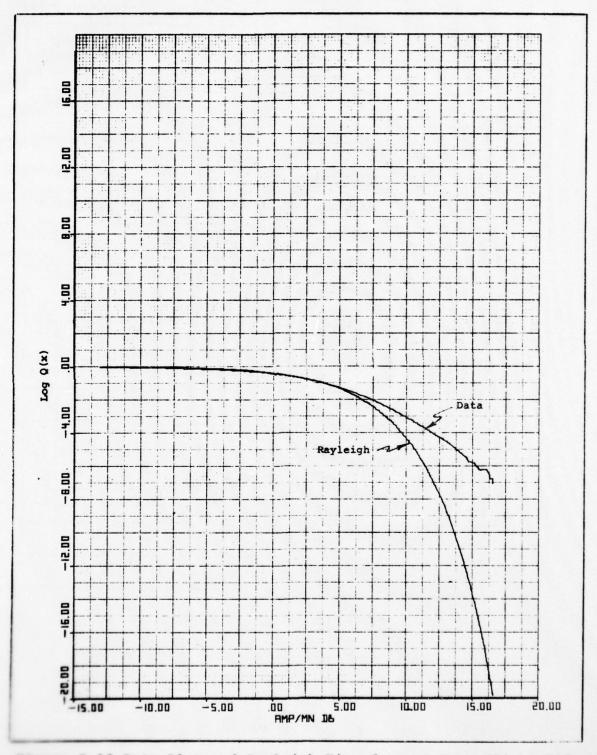


Figure B-10 Data Plot and Rayleigh Fit of Log Q From Flight 707

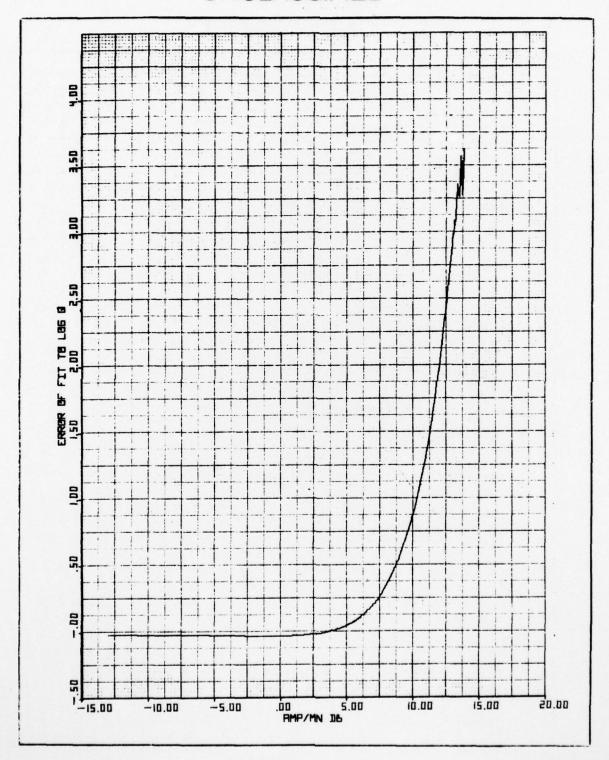


Figure B-11 Error of Rayleigh Fit to Log Q Data From Flight 605

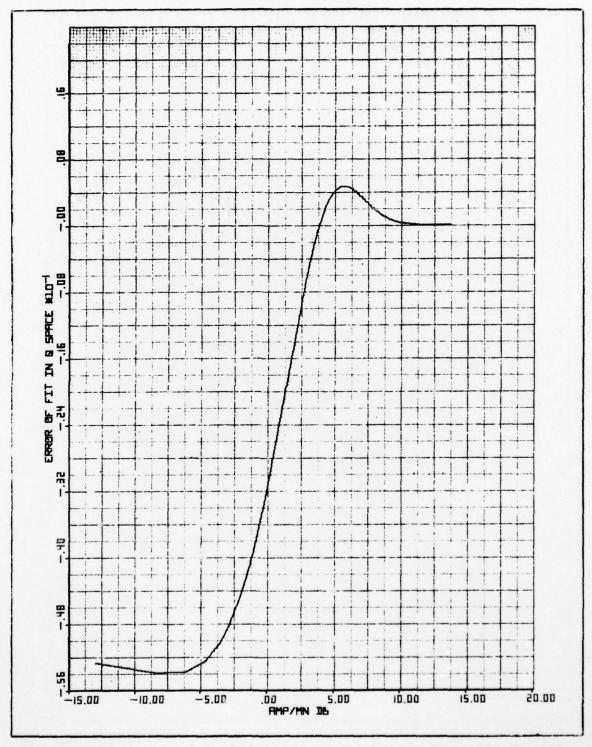


Figure B-12 Error of Rayleigh Fit to Q(x) Data From Flight 605

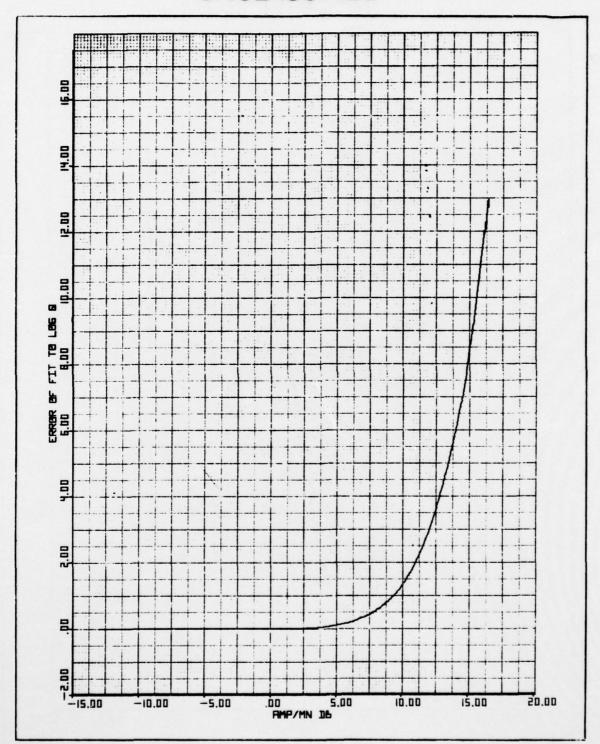


Figure B-13 Error of Rayleigh Fit to Log Q Data From Flight 707

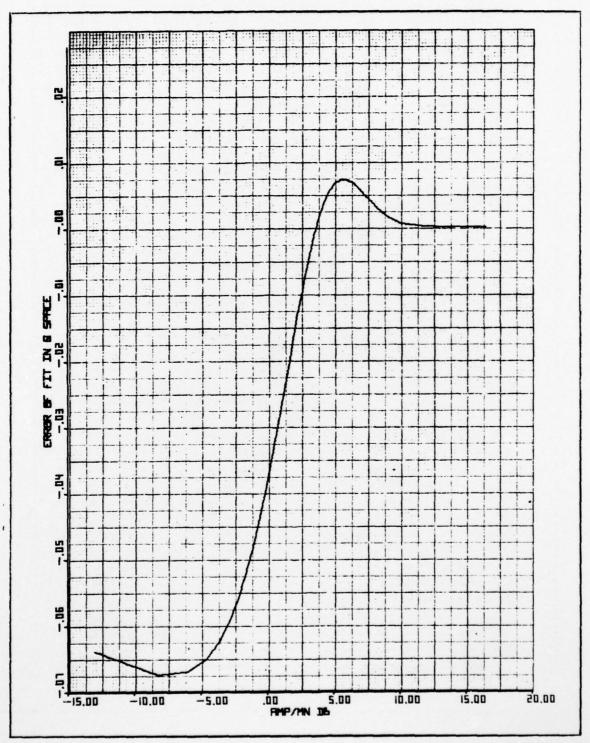


Figure B-14 Error of Rayleigh Fit to Q(x) Data From Flight 707

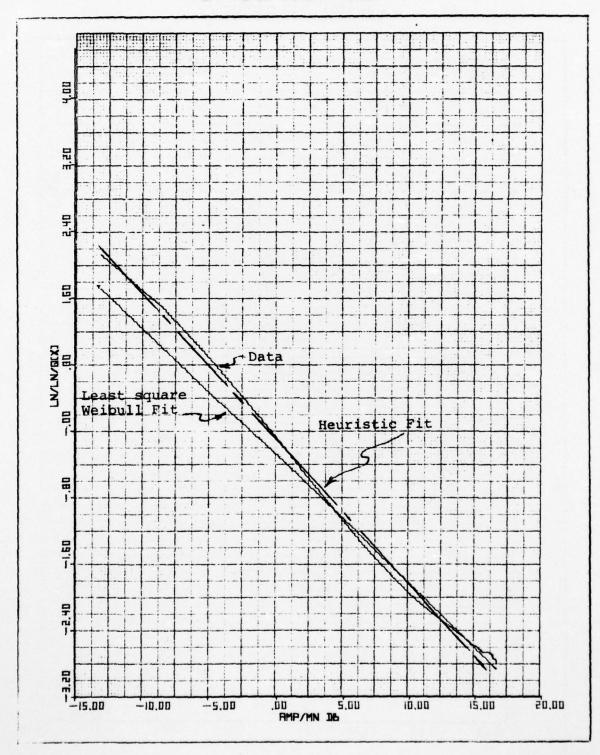


Figure B-15 Data Fit From Mean to +15dB

1.1.2 Cubic Spline

The cubic spline fit was made to the histogram of the data "x" expressed as a function H which is related to the histogram through the observed cumulative distribution. The function H is defined as $H(x) = \text{Log}_{10} \ Q(x)$ where Q(x) = 1-F(x) and F(X) is the cumulative distribution function of the observed variable x.

The function \log_{10} Q has the advantage that it explicitly gives the 10^{-k} points a_k , $k=1,2,3,\ldots$, and also gives a better description of the tails. The values a_k are identified by the equation

$$P_r (x > a_k) = \frac{1}{10^{-k}}$$
 $k = 0,1,2,...$

Using this definition of a_k we can easily see that

$$H(a_k) = \log_{10} Q(A_k) = \log_{10} [10^{-k}] = -k.$$
 $k = 0,1,2,...$

Thus a value of -5 for $\log_{10}Q(a)$ means that "a" is that number such that the probability of obtaining any value greater than it is $\frac{1}{10^5}$. The usefulness in having such points directly available is in easily observing important threshold levels especially those needed in determining false alarm rates.

a) Curve Matching to Cubic Spline

The spline function is defined in terms of a set of points called knots. If the m numbers $tk_1 < tk_2 < \ldots < tk_m$ are a set of knots then the spline S(t) is a polynominal of degree n between the knots with the condition that it have n-l continuous derivatives at the knots. Specifically for n=3 the spline S(t) is called a cubic spline and it is a piecewise cubic polynominal over the interval (tk_1, tk_m) which has the property that it is continuous and has continuous first and second derivatives. For knots $tl_1 < tk_2 < \ldots < tk_m$ the cubic spline S(t) is usually expressed as

$$S(t) = c_{i,3}^{2} D^{3} + c_{i,2}^{2} D^{2} + c_{i,1}^{2} D + y_{i}$$
with D = t - tk_i and tk_i \le t < tk_{i+1}.

Complete descriptions then of a cubic spline requires knowing the knot values and for each pair of consecutive knots the four coefficients in the cubic equation. The description of a cubic spline approximation to the data given in this report does not follow the usual convention. It was decided to use the format that if S(t) is cubuc spline approximation to H(x) where $t = \log_{10}{(x/10)}$ with four knots $tk_1 < tk_2 < tk_3 < tk_4$. Then for values $tk_1 \le t < tk_{1+1}$ $t = 1,2,3,\ldots$ so that $t = 1,2,3,\ldots$ so that $t = 1,2,3,\ldots$ so that $t = 1,2,3,\ldots$

$$S(t) = A_{i,1} t^{3} + A_{i,2} t^{2} + A_{i,3} t + A_{i,4}$$
where t = 10 log₁₀(x/10).

The above format of S(t) avoids the intermediate variable D and, for a complete description of a cubic spline with four knots, we need only a 3 X 4 matrix A defining the coefficient of the piecewise cubics and a matrix tk of knot values, i.e.,

$$A = \begin{bmatrix} A_{1,1} & A_{1,2} & A_{1,3} & A_{1,4} \\ A_{2,1} & A_{2,2} & A_{2,3} & A_{2,4} \\ A_{3,1} & A_{3,2} & A_{3,3} & A_{3,4} \end{bmatrix}$$

and $tk = (tk, tk_2, tk_3, tk_4)$. The matrix A and tk are given on the graph of the cubic spline approximation for each data set fitted.

For fixed knots the cubic spline approximation, S(t), to the data $H(x_i)$ $i=1,2,\ldots,N$ is made through a least square fit. The quantity, E, which is minimized is

$$E = \begin{bmatrix} \sum_{i=1}^{N} [H(x_i) - S(t_i)] W_i \end{bmatrix}^{\frac{1}{2}}$$
where $t_i = 10 \cdot \log_{10}(x_i/10)$ $i = 1, 2, ..., N$

$$W_i = \frac{t_2 - t_1}{t_N - t_1}$$

$$W_i = (t_{i+1} - t_{i-1})/t_N - t_1$$
 $i = 2, 3, ..., N-1$

$$W_N = (T_N - t_{N-1})/(t_N - t_1)$$

The key to the success of a spline approximation is the location of the knot values. A variable knot computer program was used to determine in an economical fashion the placement of the knots which gives the minimum least squares error. The computer program is a standard routine in the International Mathematical and Statistics Libraries (IMSL) called ICS VKU.

b) Summary of Cubic Spline Match

Cubic splines of various degrees were matched to the data and it was found that the use of four knots was sufficient to approximate down to the sample noise of the data. In this section we give only results on the fit by cubic splines with only four knots.

The chart on Table B-l gives the flights and runs that were fitted by splines. There was an attempt to fit a good cross section of the available data. Flight 707 and 1706 were the only flights with horizontal polarization fitted and flight 803 was a low grazing angle run. The data from flight 605 were processed two different ways, one as A type and once as N type. The process involved in forming the A type and N type

				A	171	AI TITUDE	1					-					
FLIGHT	FLIGHT FIGURE		YPE		(KFT)	35	,	SE	Q	51	AT	E	WIND	DIREC	SEA STATE WIND DIRECTION	POLARIZATION	ZATION
NUMBER	NUMBER	•	>	0.5	17	A N 0.5 1.1 2.2 3.3 1 2 3 4	3.3	-	N	n	7	5	UP	DOWN	CROSS	DOWN CROSS VERTICAL HORIZON-	HORIZON- TAL
909	B-16	×				×						×		×		×	
403	B-20		×		×					×					×	×	
909	B-24		×			×						×		×		×	
707	B-28		×				×					×	×				×
803	B-32		×	×							×				×	×	
1104	B-36		×			×		×					×			×	
1602	B-40		×		×						×			×		×	
1706	B-44		×			×					×				×		×

TABLE B-1 FLIGHT INFORMATION

UNCLASSIFIED

is described in detail in Volume II. The difference between them is that the N type was an attemp to remove the variations in mean clutter levels that were noticed during the runs. Cubic splines approximations were made to the two different processes of the data.

For each flight given in Table B-1 there corresponds four graphs. The four graphs for each flight are titled as follows:

- 1. Log Q
- 2. Cubic Spline Approximation to Log Q
- 3. Error of Fit of S(t) to Log Q
- 4. Error of Fit of 10^{S(t)} to 0

The first graph, Log Q, is the actual data which is being matched. The second graph, Cubic Spline Approximation to Log Q, is a graph of the cubic spline approximation. The final knot locations are identified by x's marked on this curve and matrices are given identifying the cubic spline that is plotted. In a) above a description is given on how to construct the cubic spline from the matrix A and tk which are given below each cubic spline curve.

The third graph, Error of Fit of S(t) to Log Q, is a plot of the difference D between Log Q(x), the data set, and S(t), $t = 10 \cdot \log_{10} \frac{X}{10}$ the cubic fit, i.e., D(t) = Log Q $(10^{1+} \frac{t}{10})$ - S(t). Along with the plot the least squares error of the cubic spline approximation is given. This graph gives us a measure of how well the cubic spline fits Log Q. One can see that in most cases the cubic spline fits out to the 10^{-4} point with an error of at most .02. Beyond the 10^{-4} point the error curve indicates that the spline is a fit down to what appears as sampling noise due to the smaller number of samples at these levels.

The fourth graph of a set, Error of Fit of $10^{S(t)}$ to Q is a measure of the fit of the spline surve in terms of Q. The quantity graphed, E(b), is given by the equation

$$E(t) = Q(10^{1+} \frac{t}{10}) - S(t)$$

where S(t) is the cubic spline fitted to Log Q. The horizontal axis of all graphs given are in terms of t $(\frac{x}{10})$ in dB) rather than in terms of x directly. The relation between t and the observed variable x is

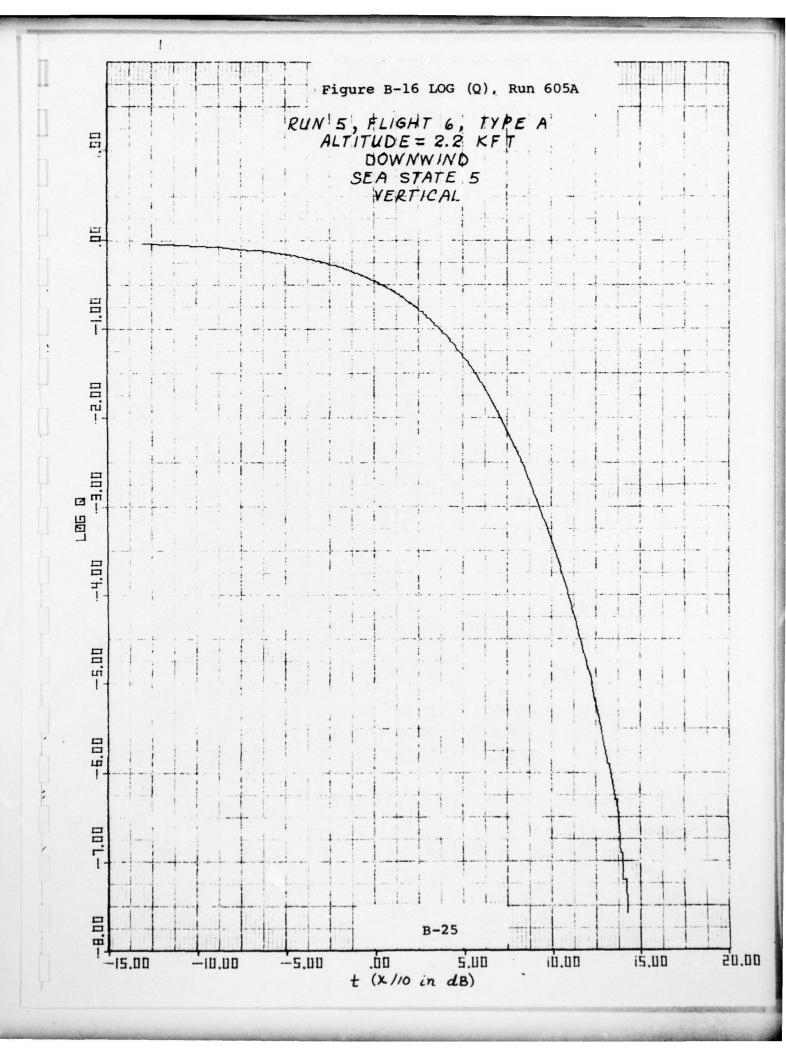
$$t = 10 [log_{10}(x/10)]$$

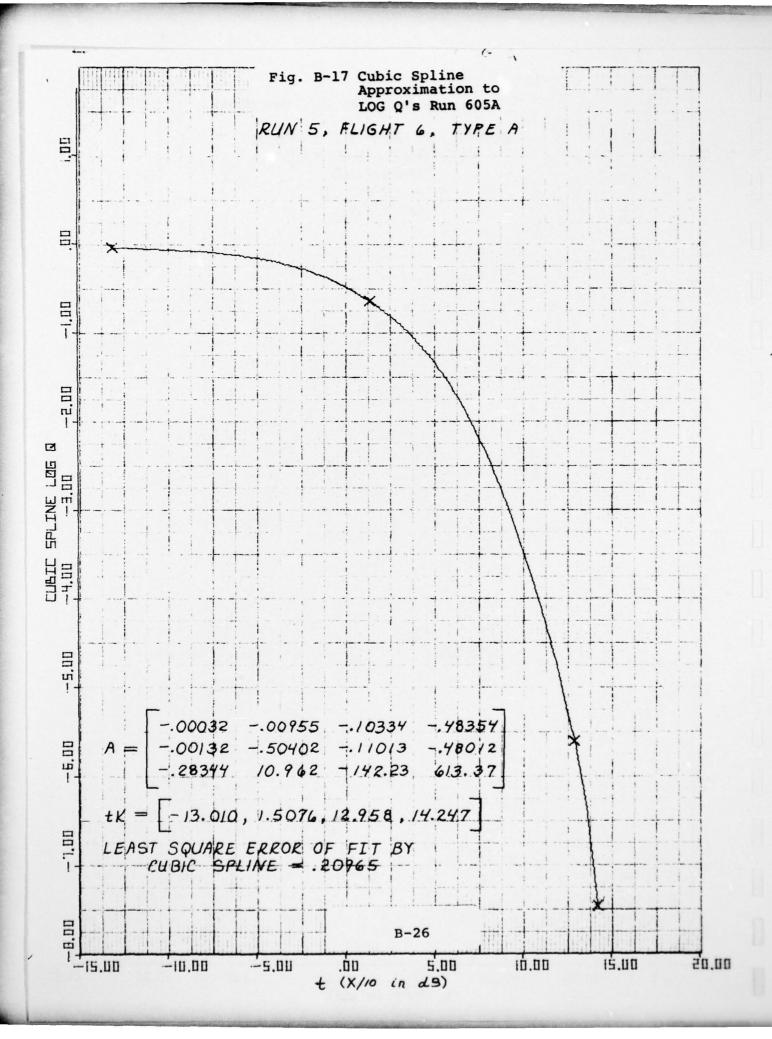
c) Graphical Results of Cubic Spline Approximation
The succeeding figures are the graphical results
of the spline curve fit. To aid in finding a particular graph
the cross-reference of Table B-2 may be used. This charts
tabulates the figure numbers for the type of graph and data set
desired.

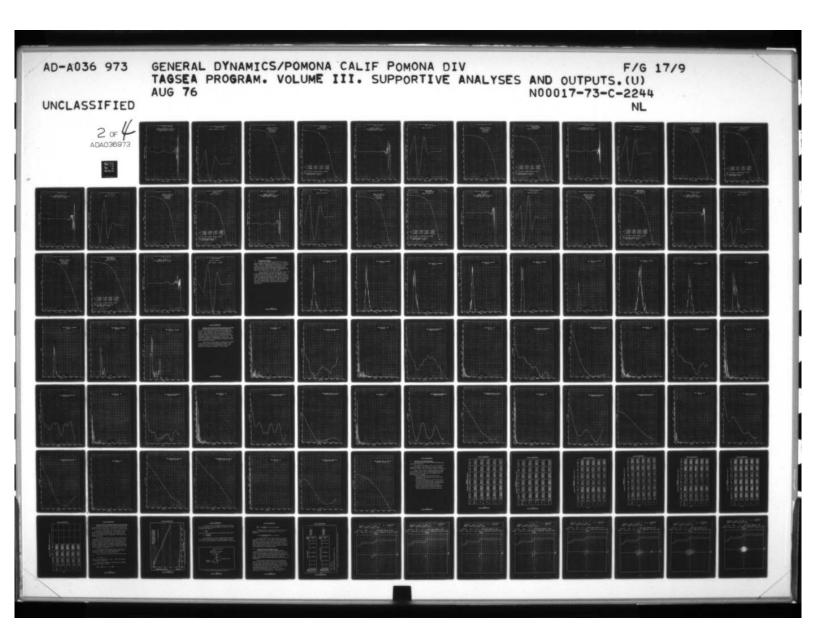
TABLE B-2 FIGURE NUMBER LOCATOR

Type Vo	605-A	403-N	605-N	707-N	803-N	1104-N	1602-N	1706-N
LOG Q	B-16	B-20	B-24	B-28	B-32	B-36	B-40	B-44
Cubic Spline Approx to LOG Q	в-17	B-21	B-25	B-29	B-33	в-37	B-41	B-45
Error of Fit S(t) to Log Q(x)	B-18	B-22	B-26	B-30	B-34	B-38	B-42	B-46
Error of Fit to 10 ^{S(t)} to Q(x)	B-19	B-23	B-27	B-31	B-35	B-39	B-43	B-47

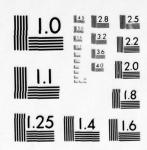
In summary, it may be simply stated that there is a maximum error between the cubic spline fit and the data of less than 0.1dB.



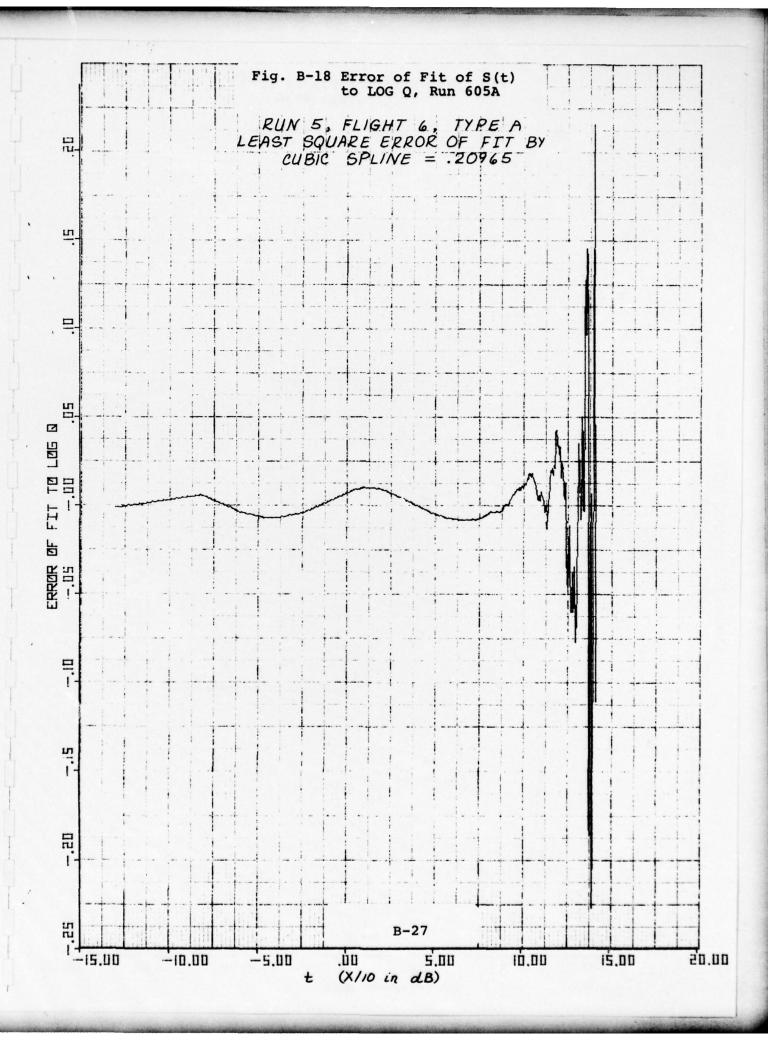


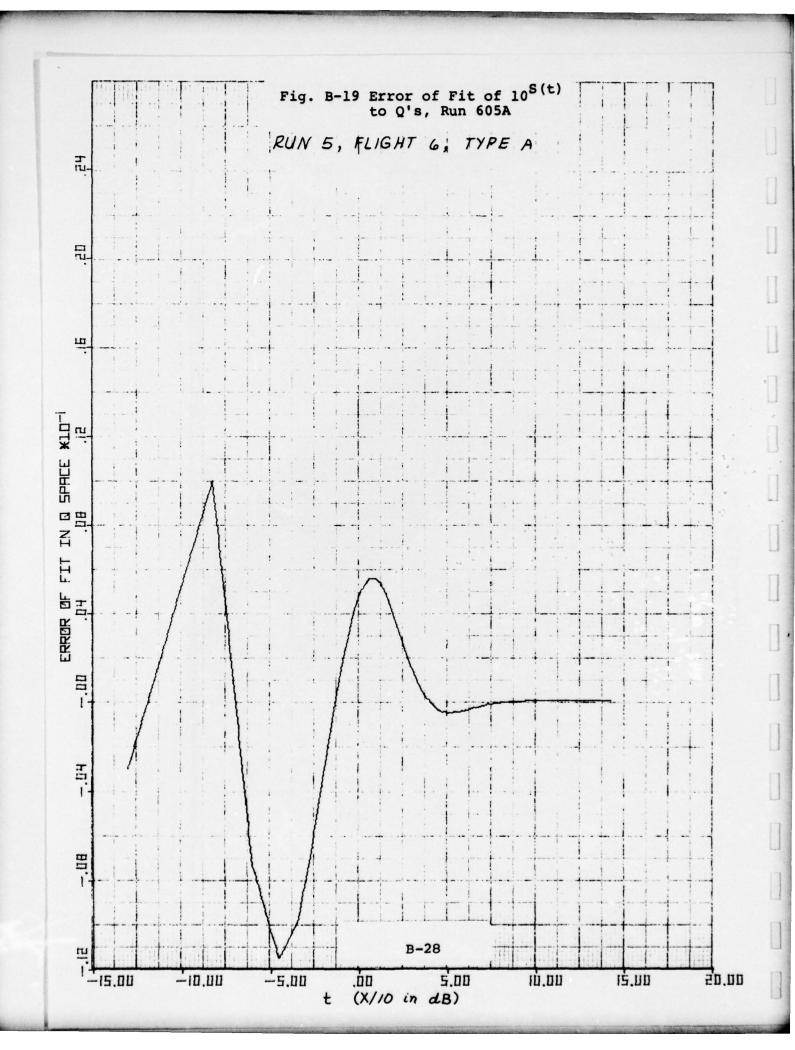


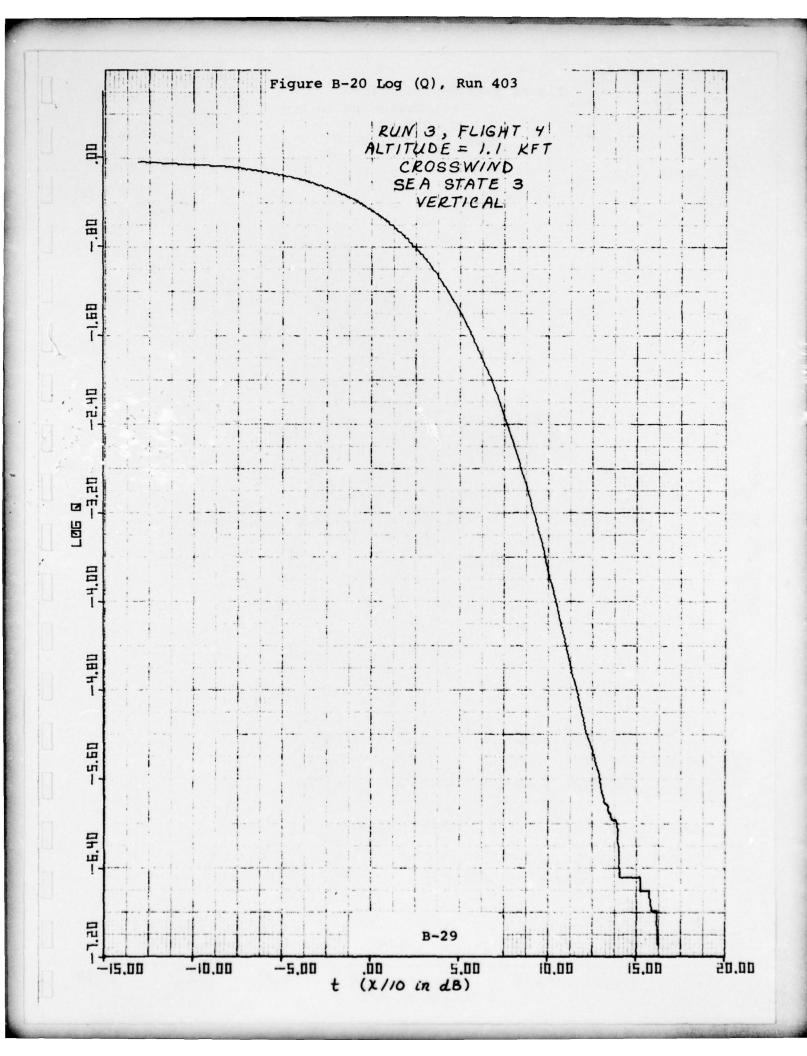
2 of 4 DA036973

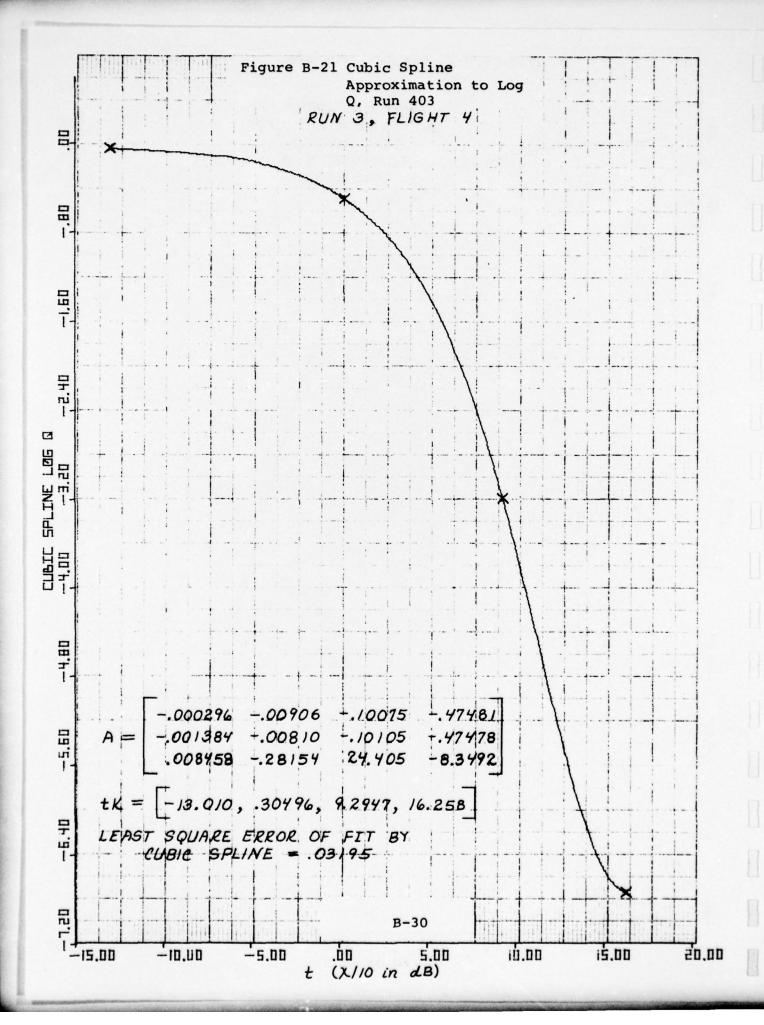


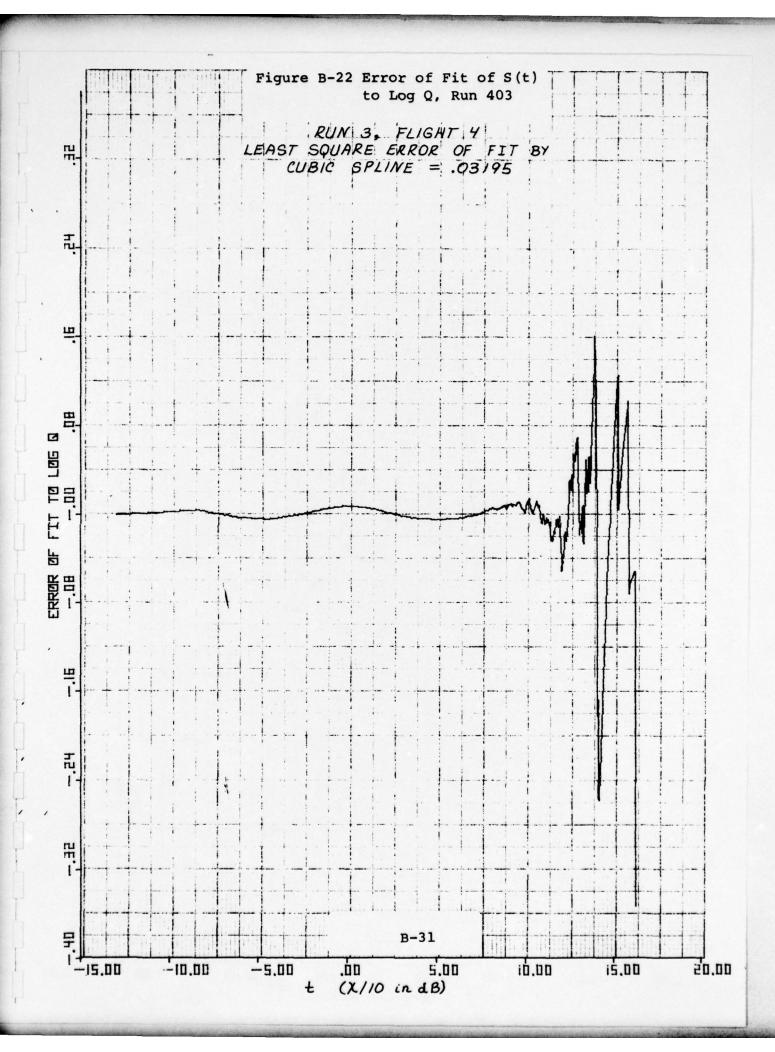
MICROCOPY RESOLUTION TEST CHART
NATIONAL BUREAU OF STANDARDS-1963-A

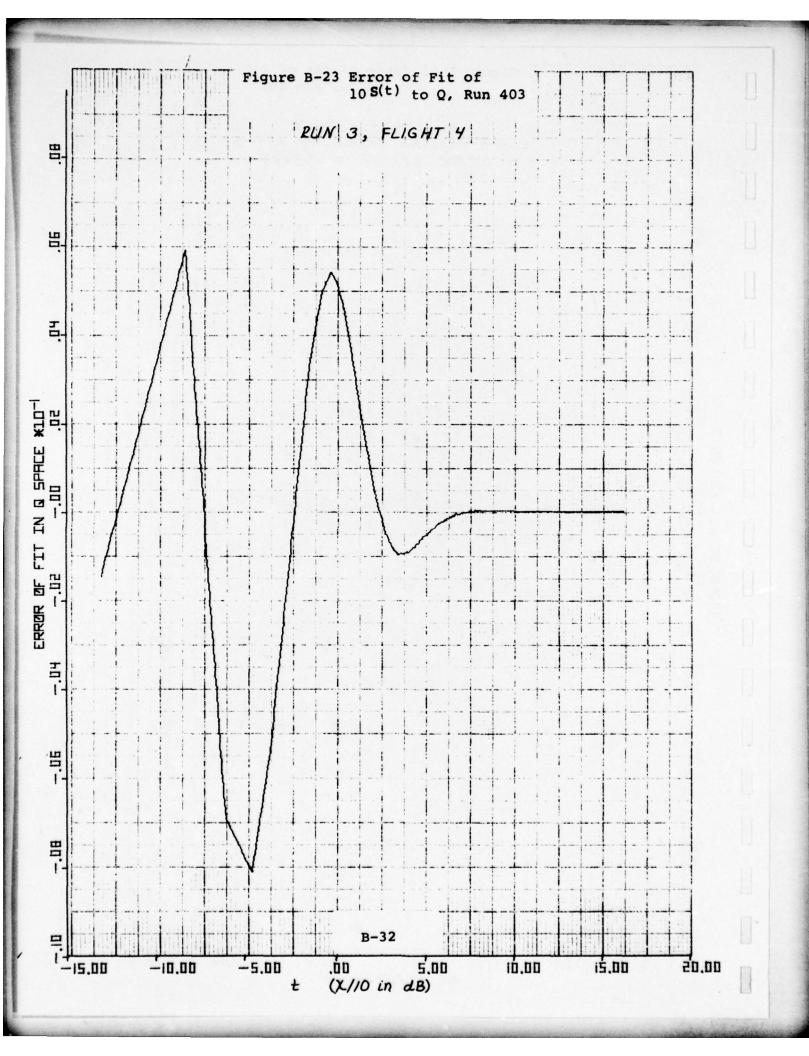


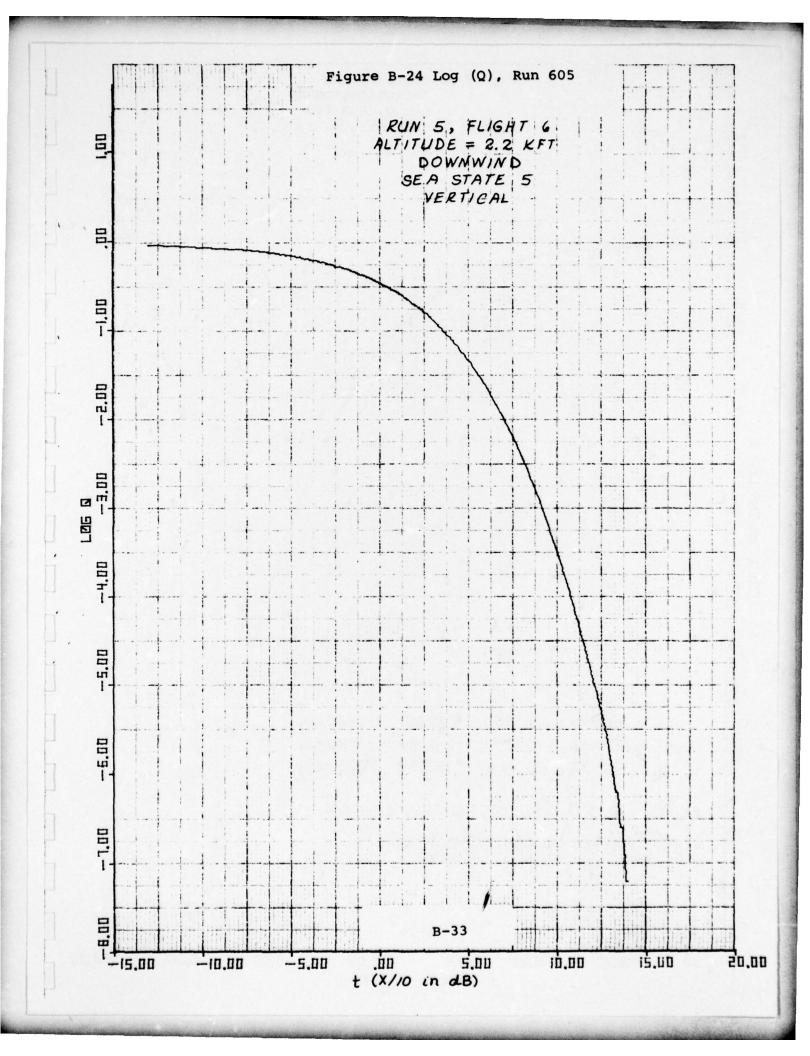


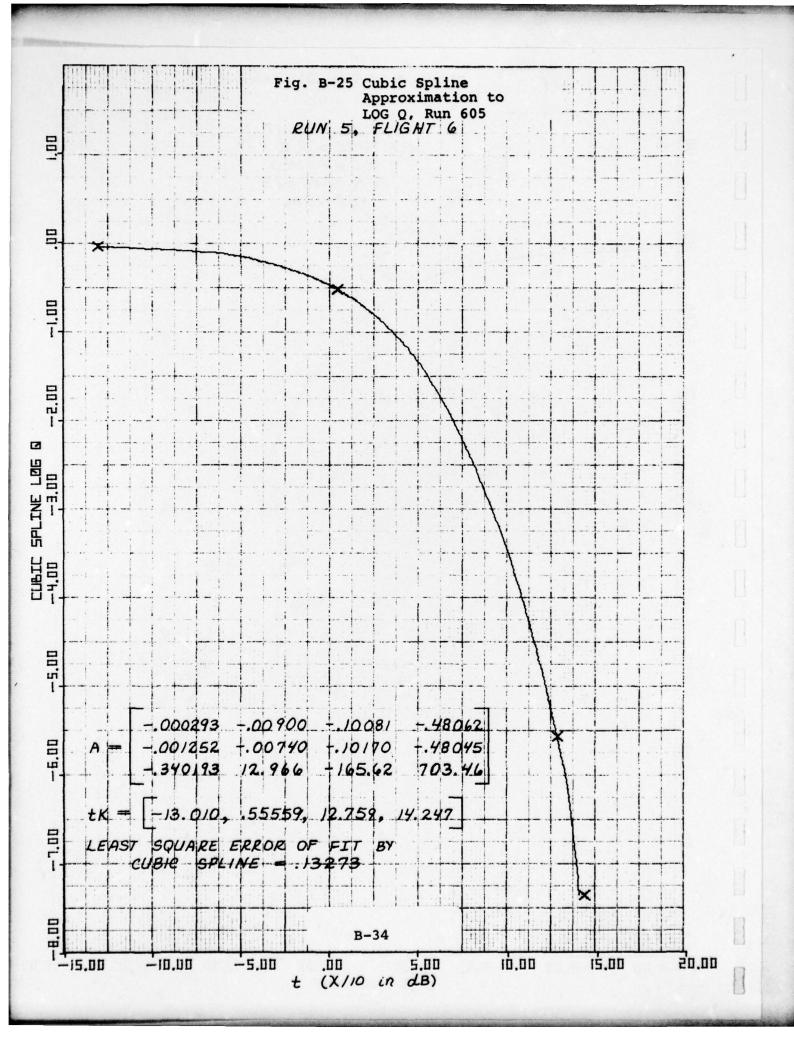


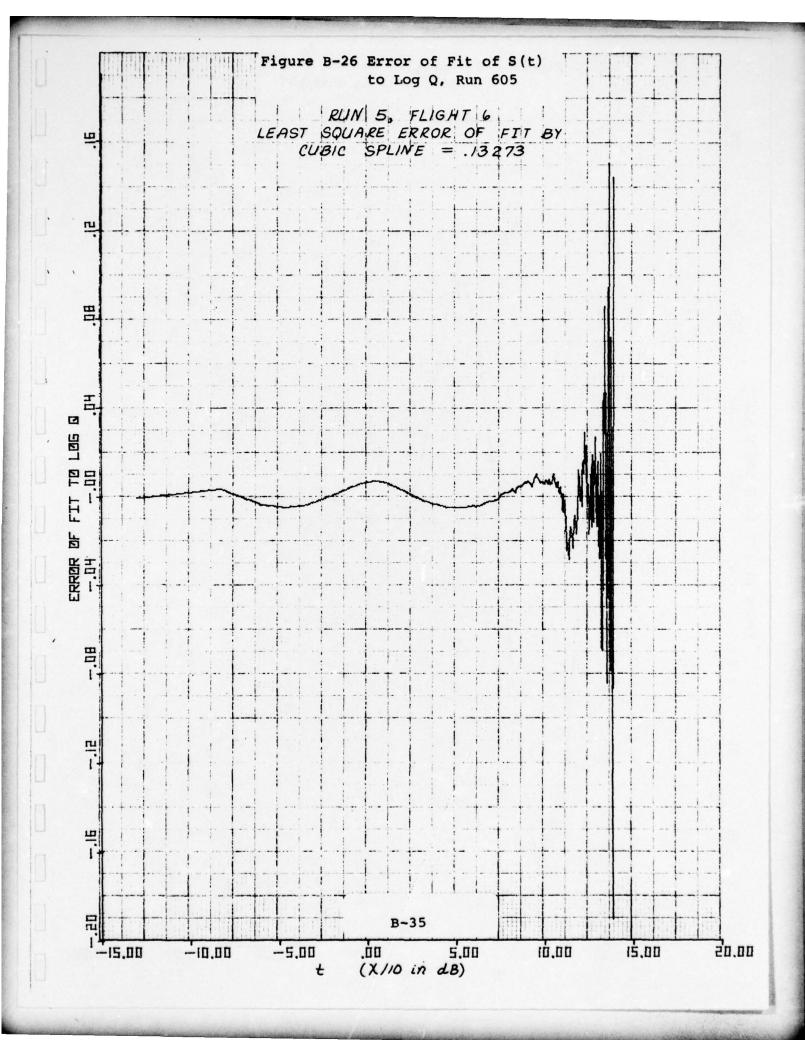


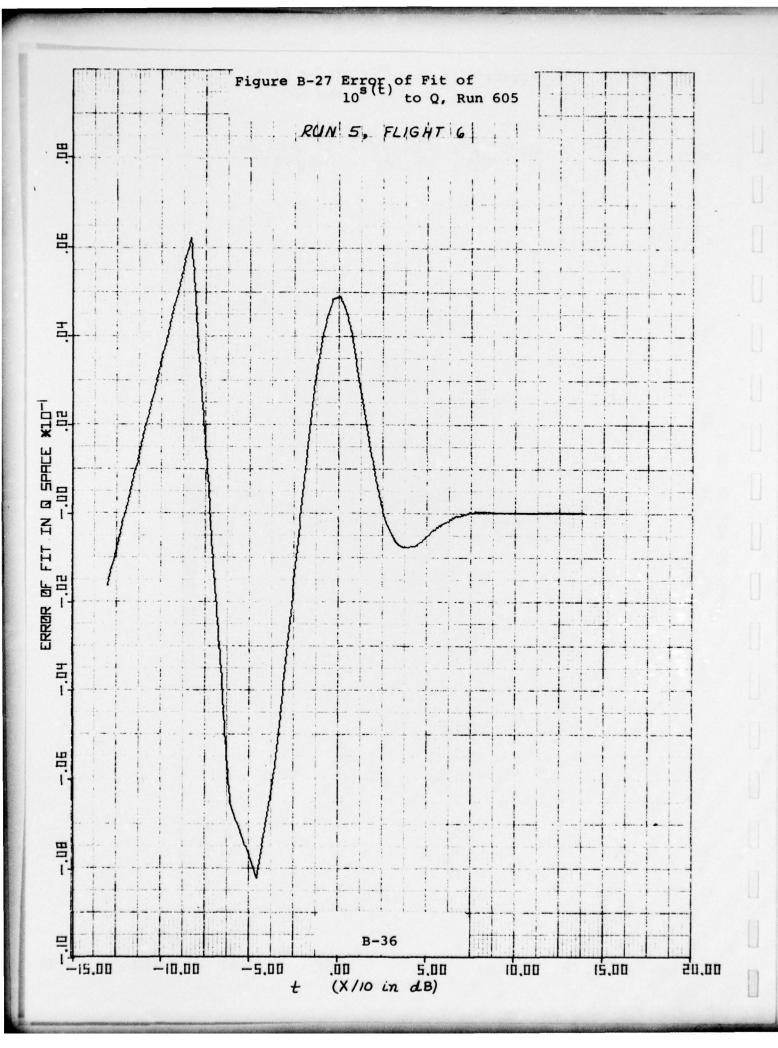


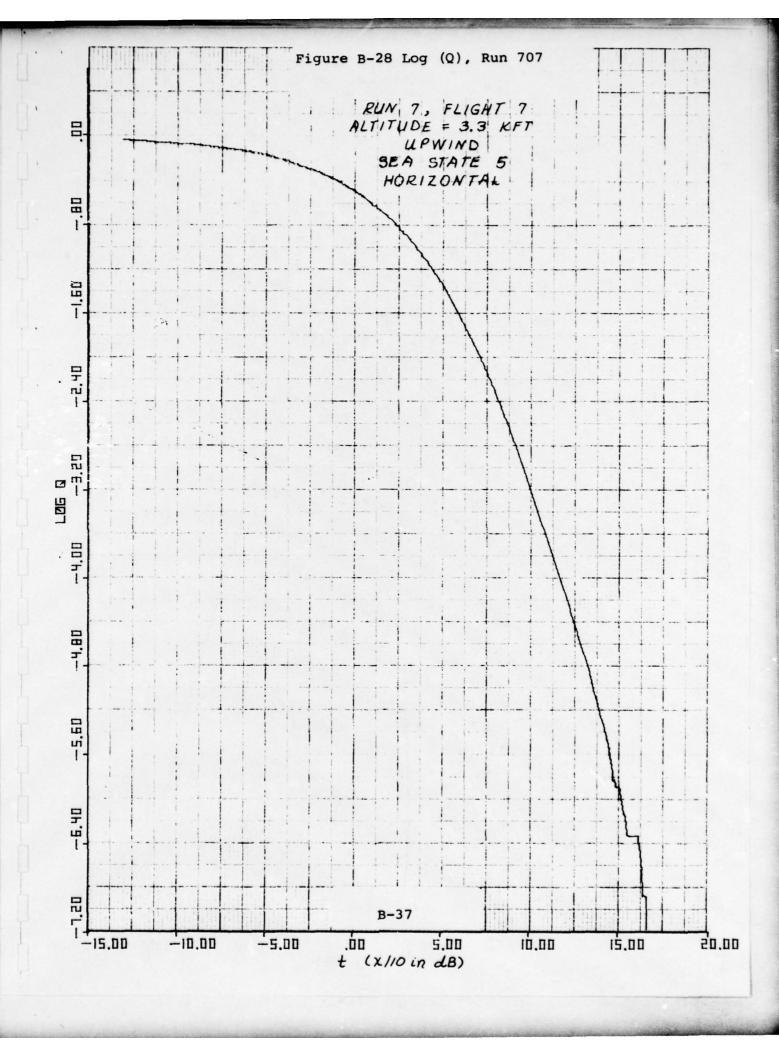


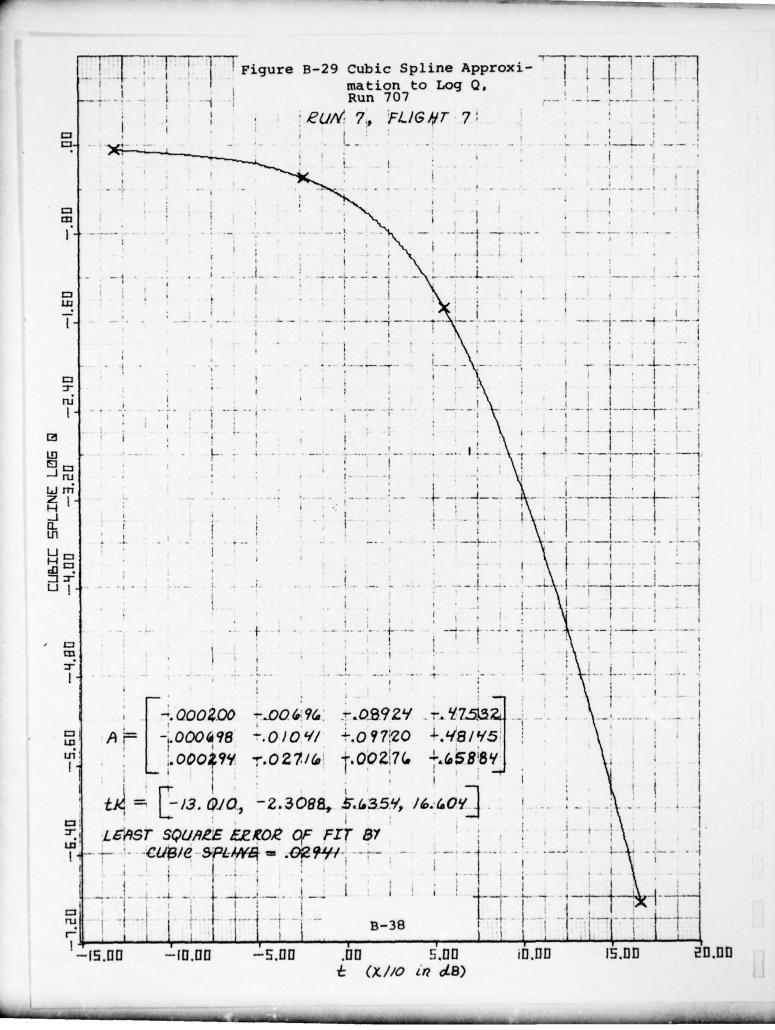


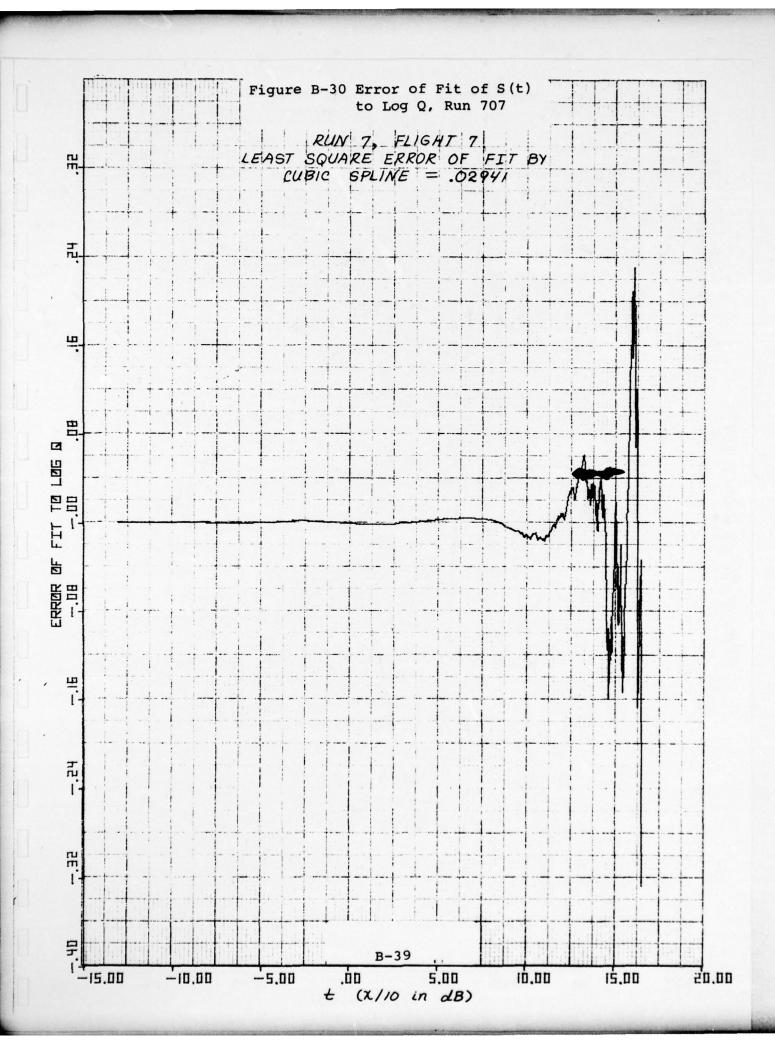


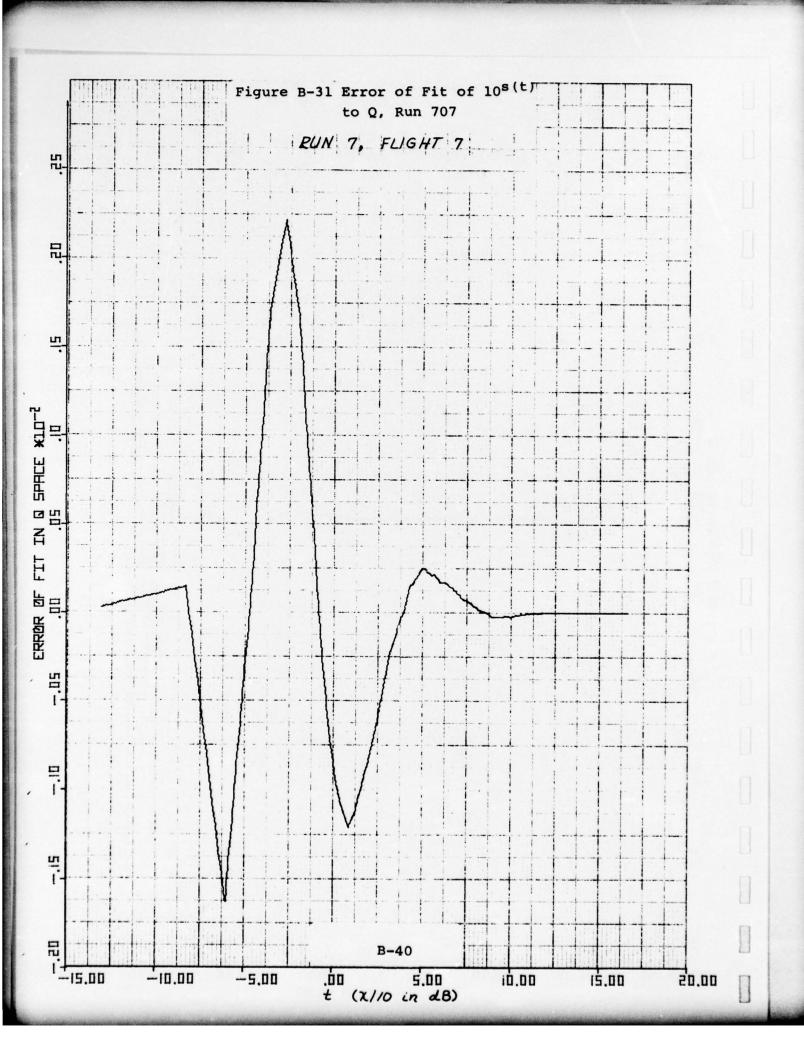


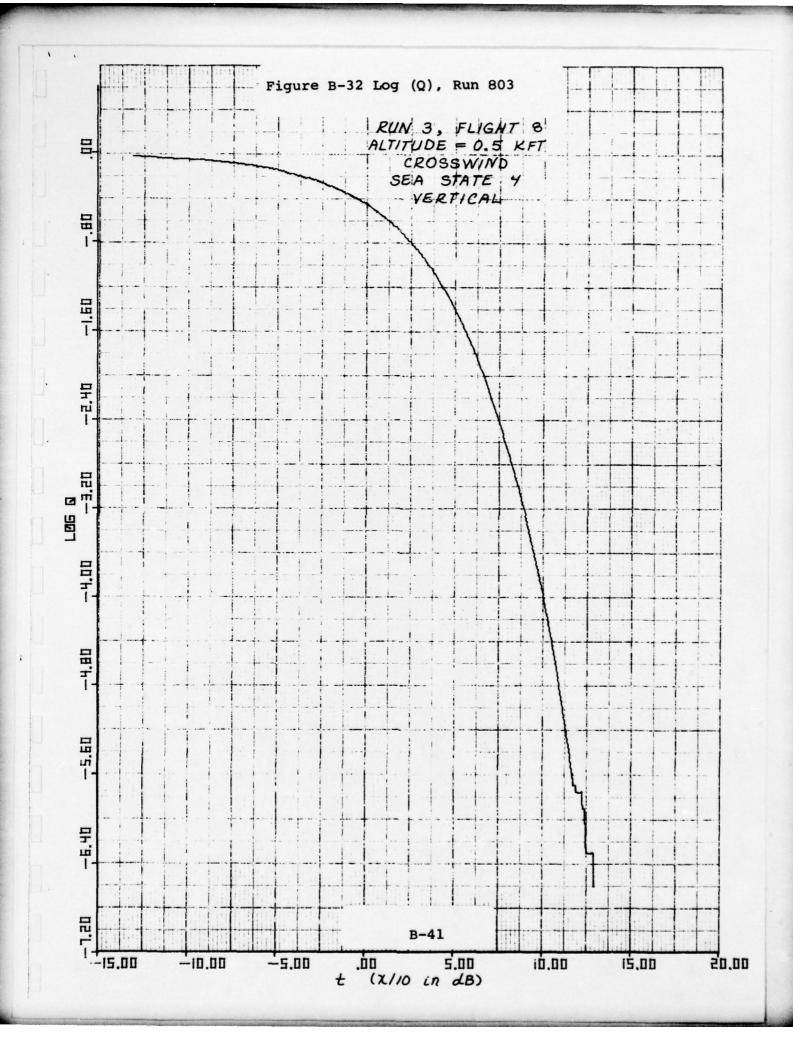


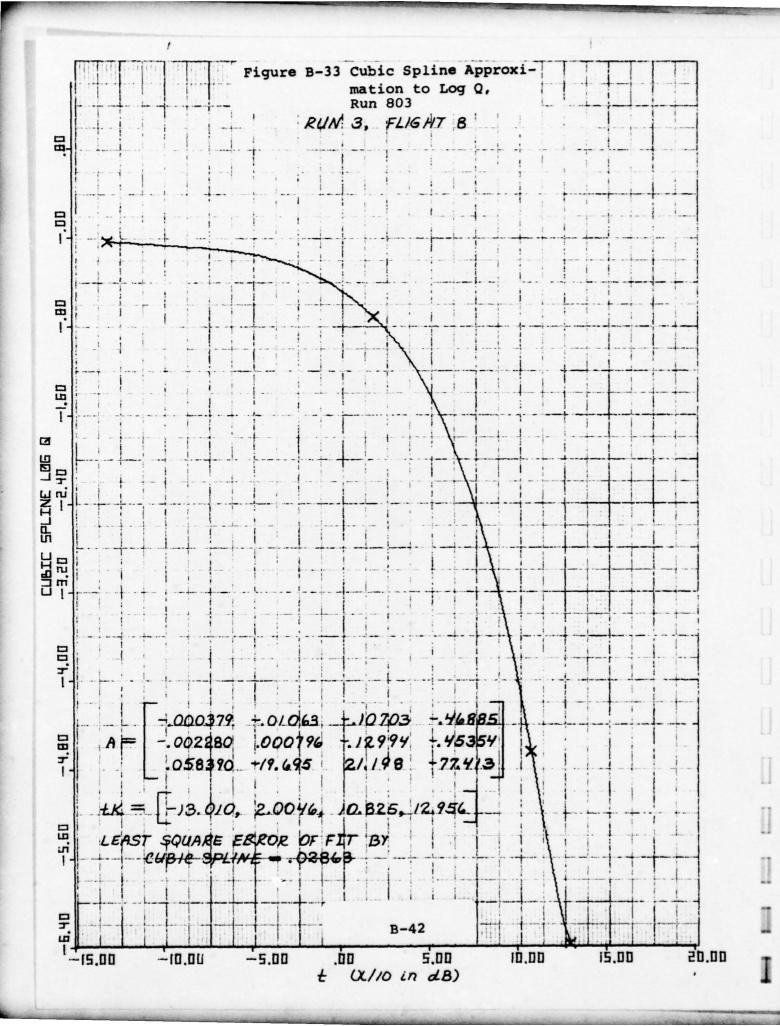


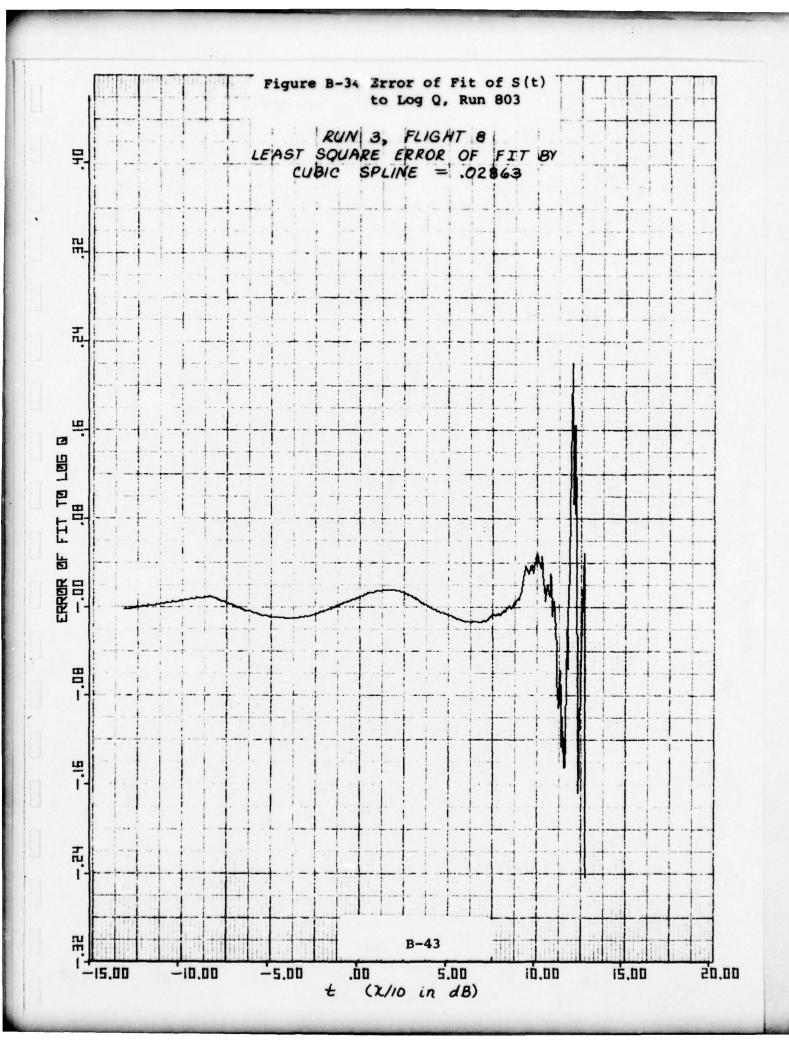


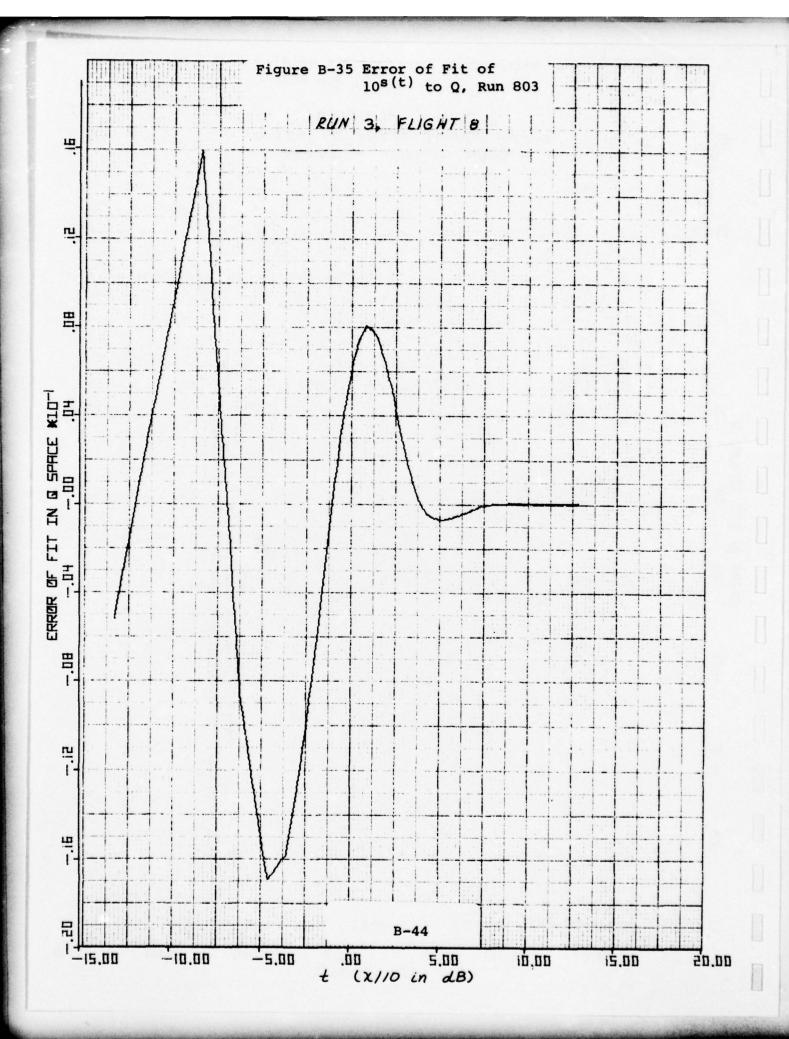


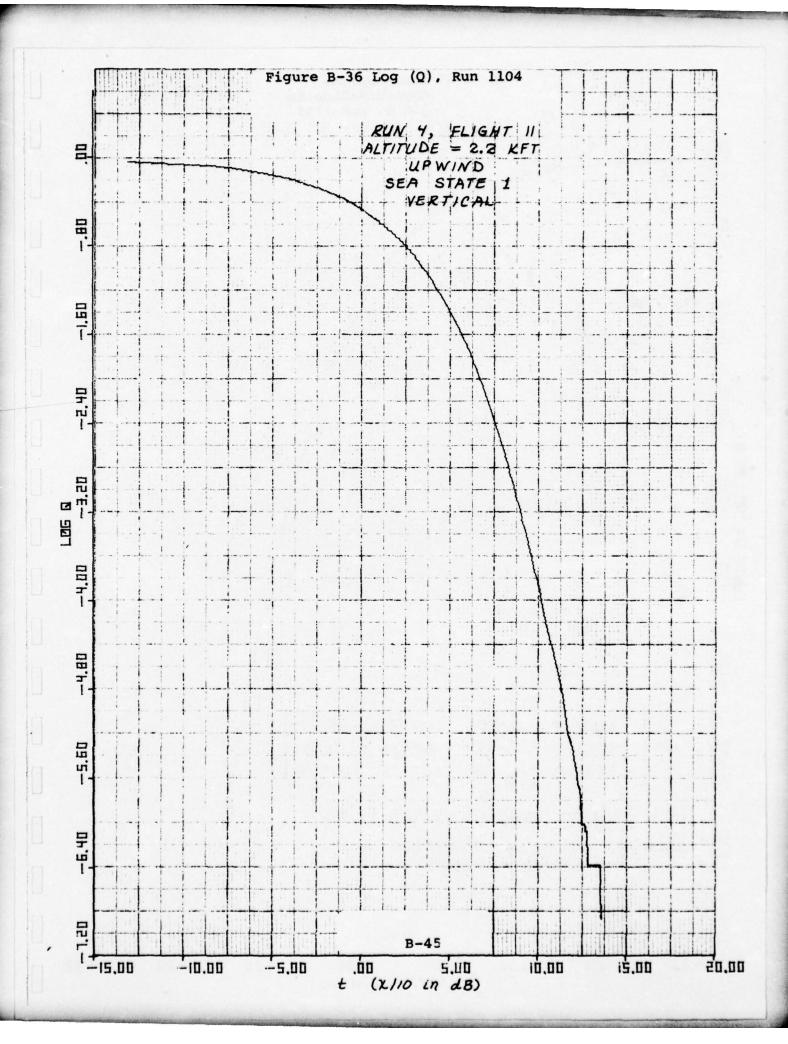


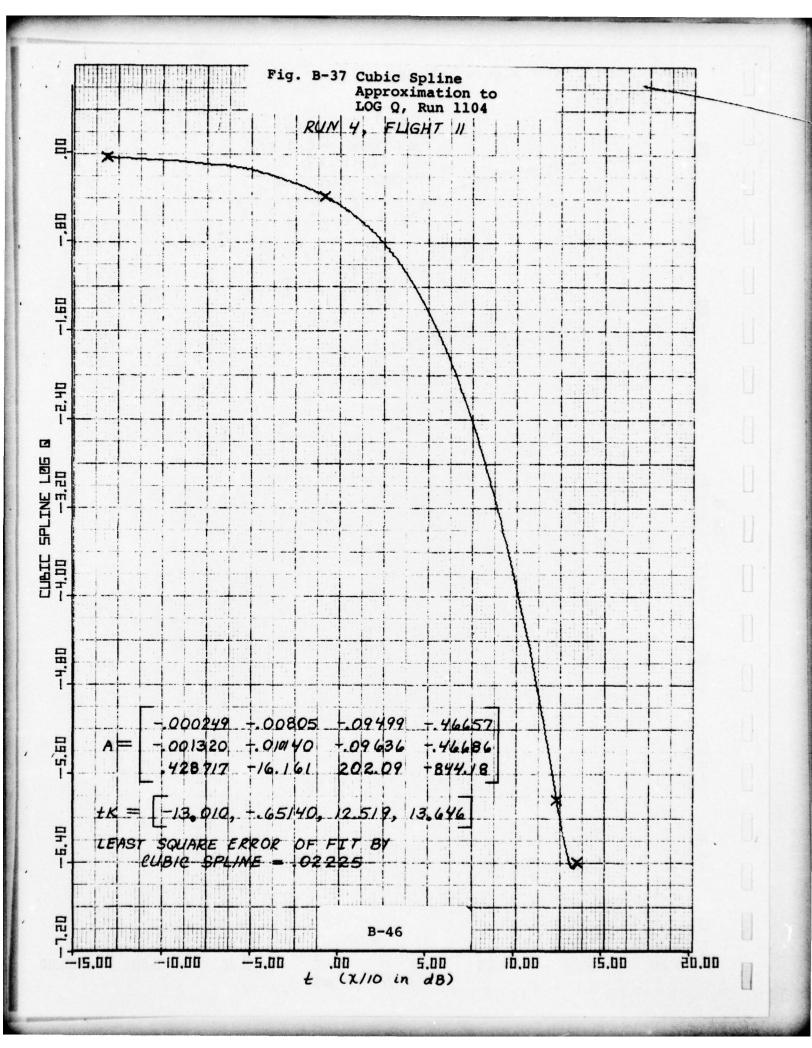


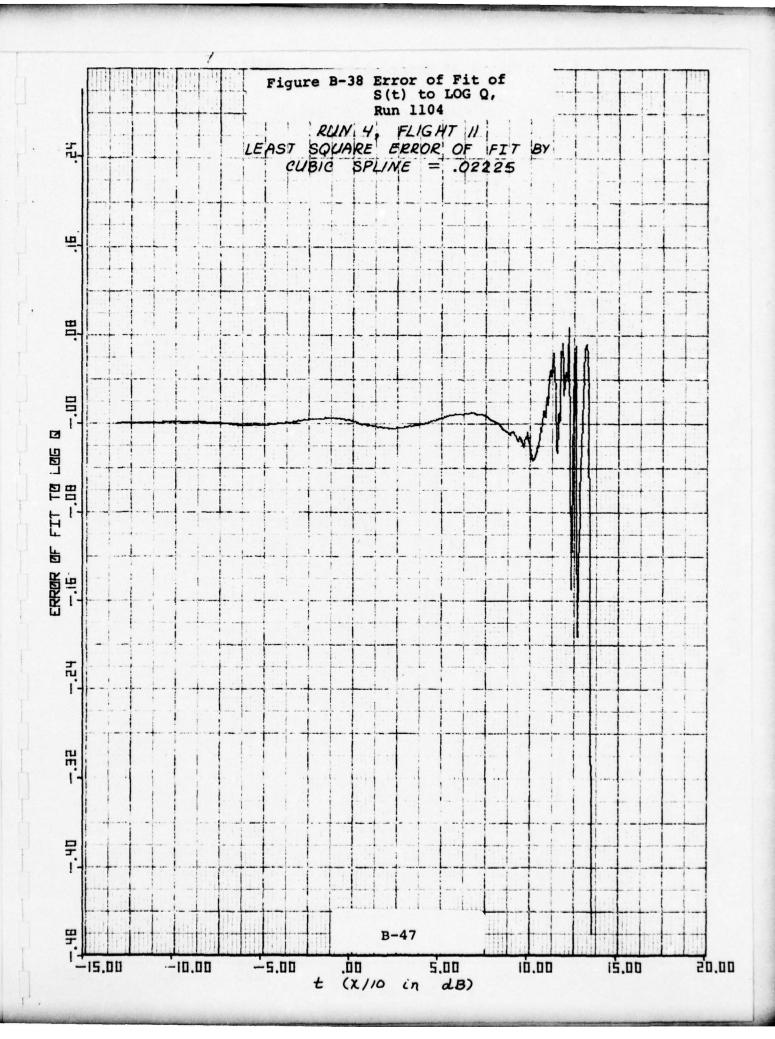


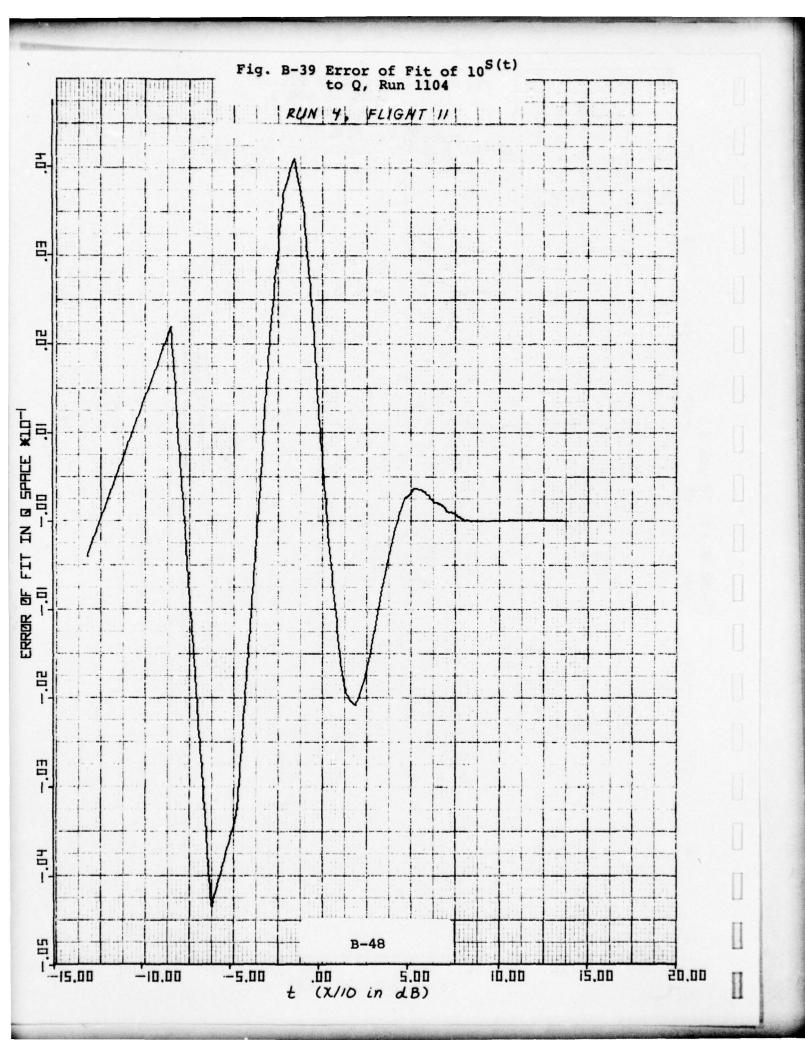


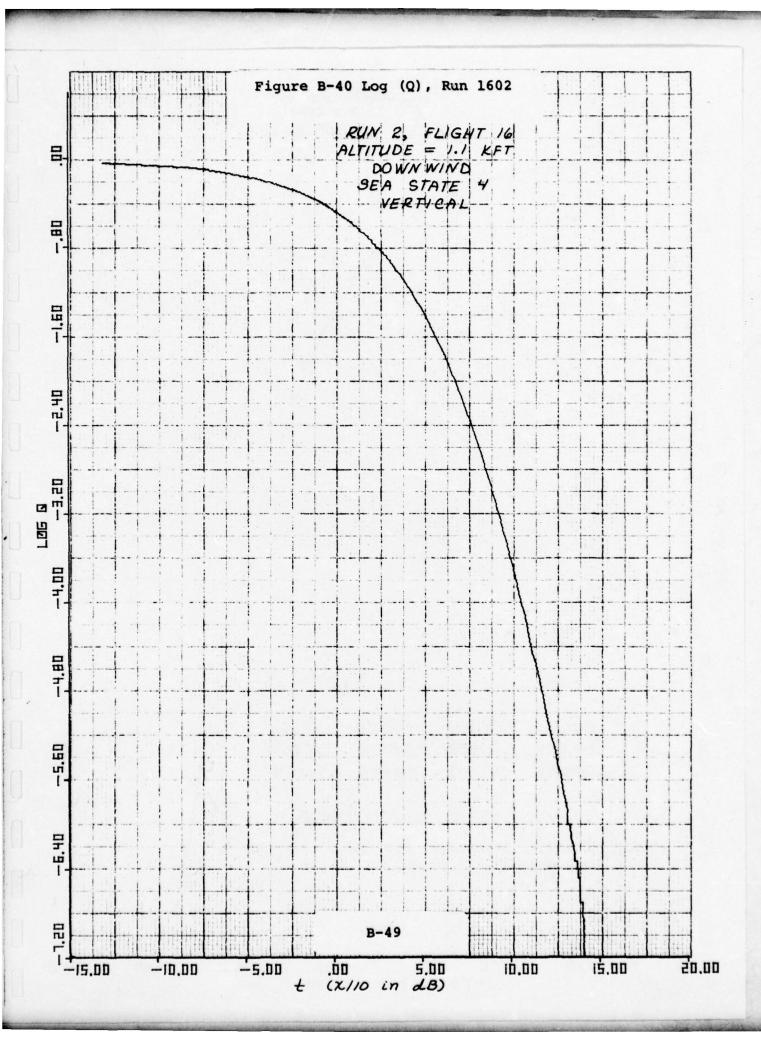


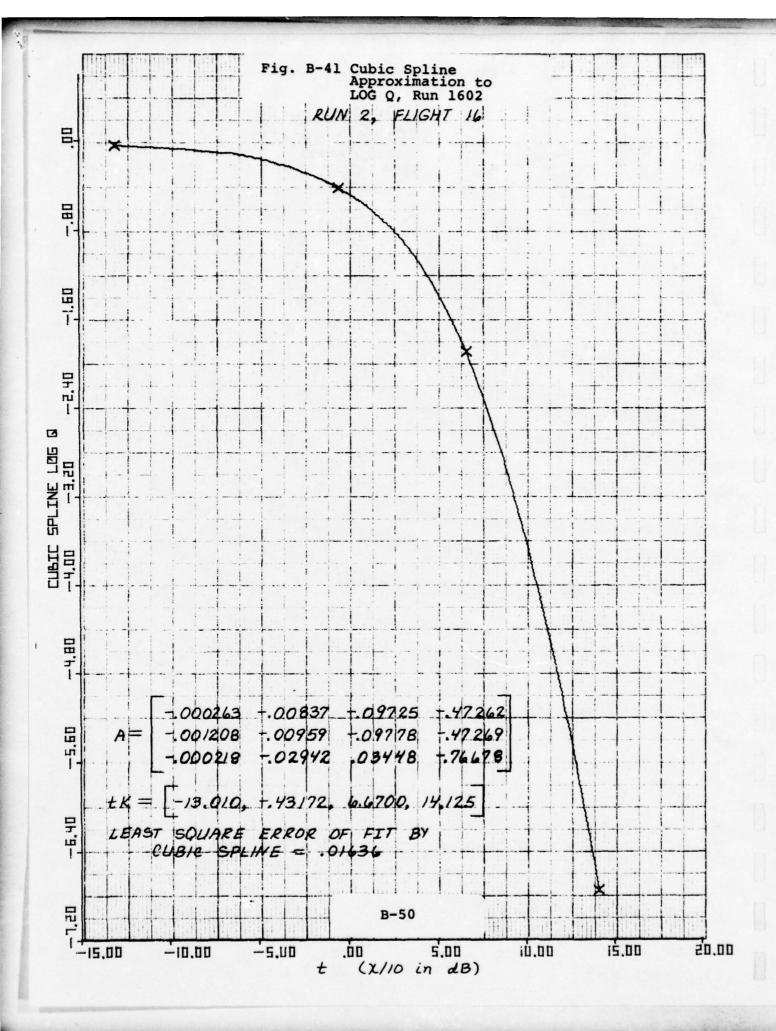


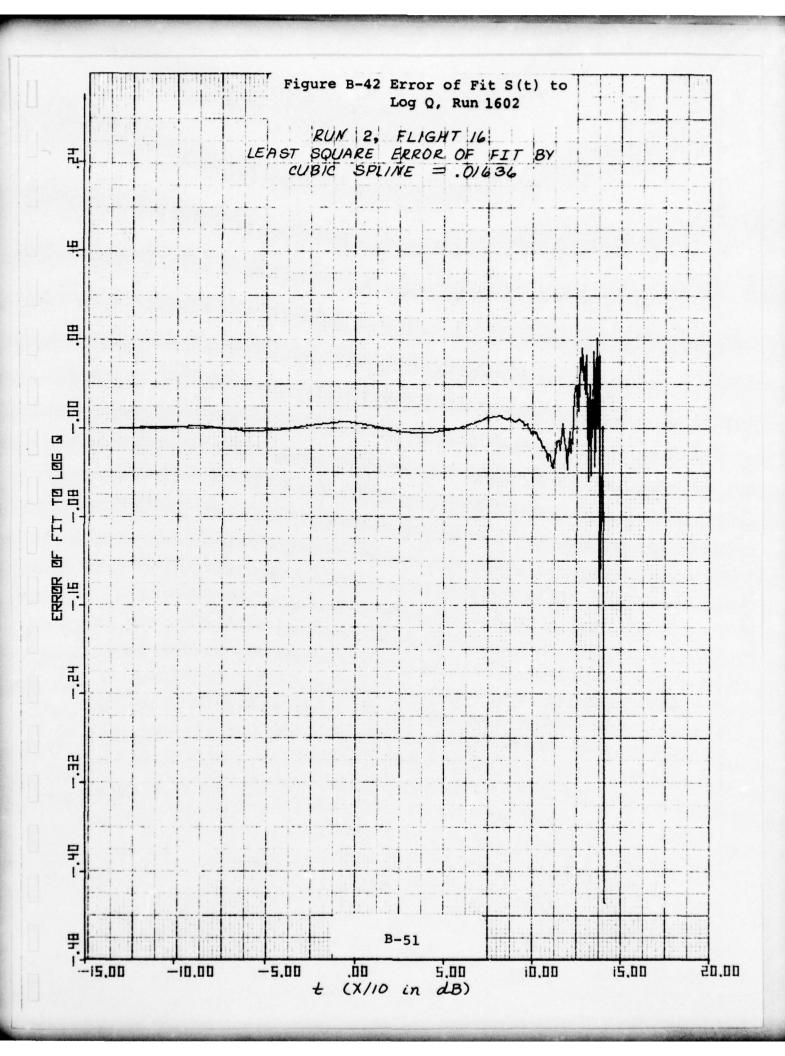


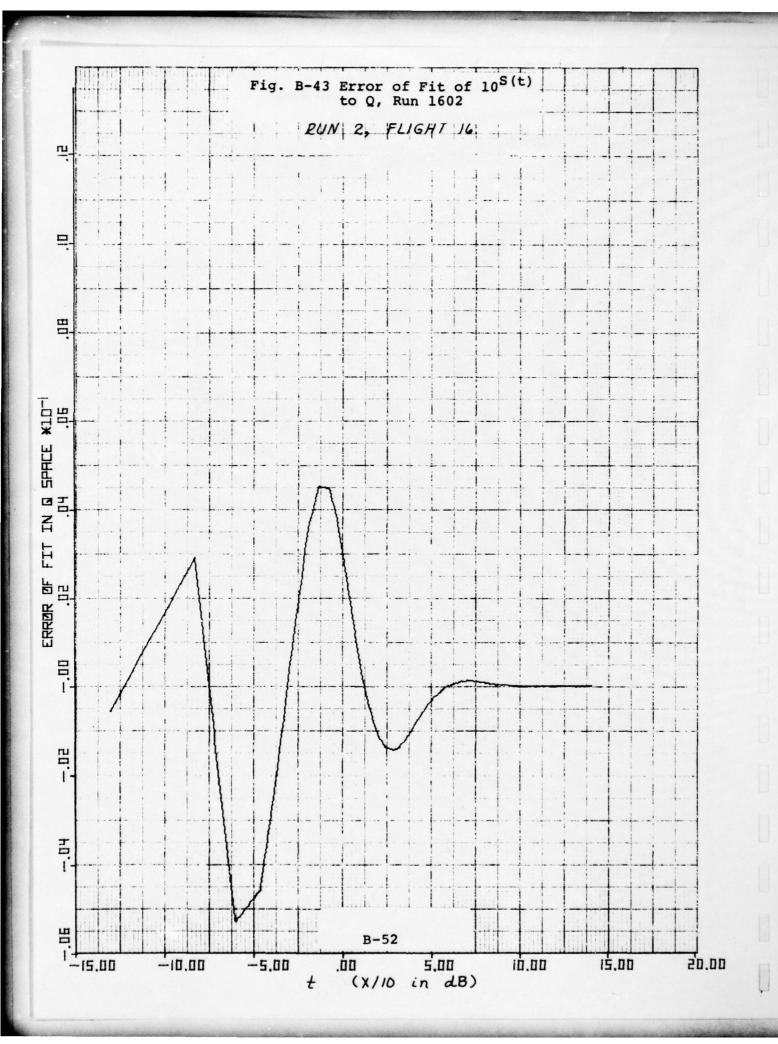


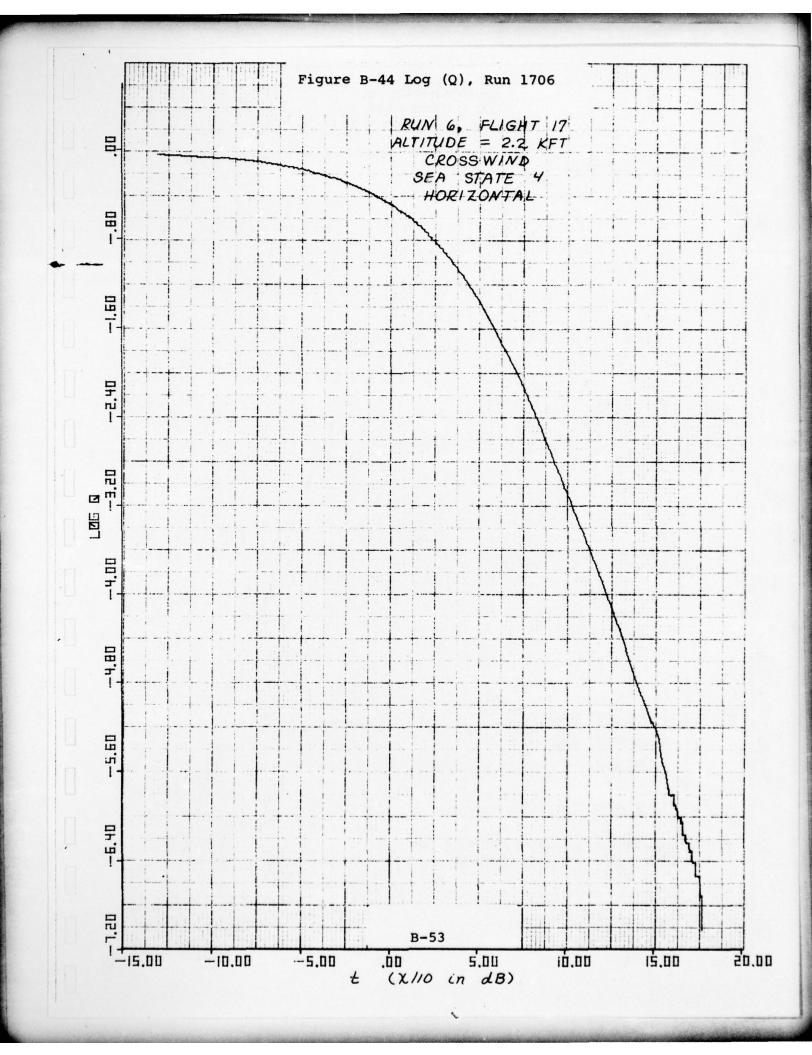


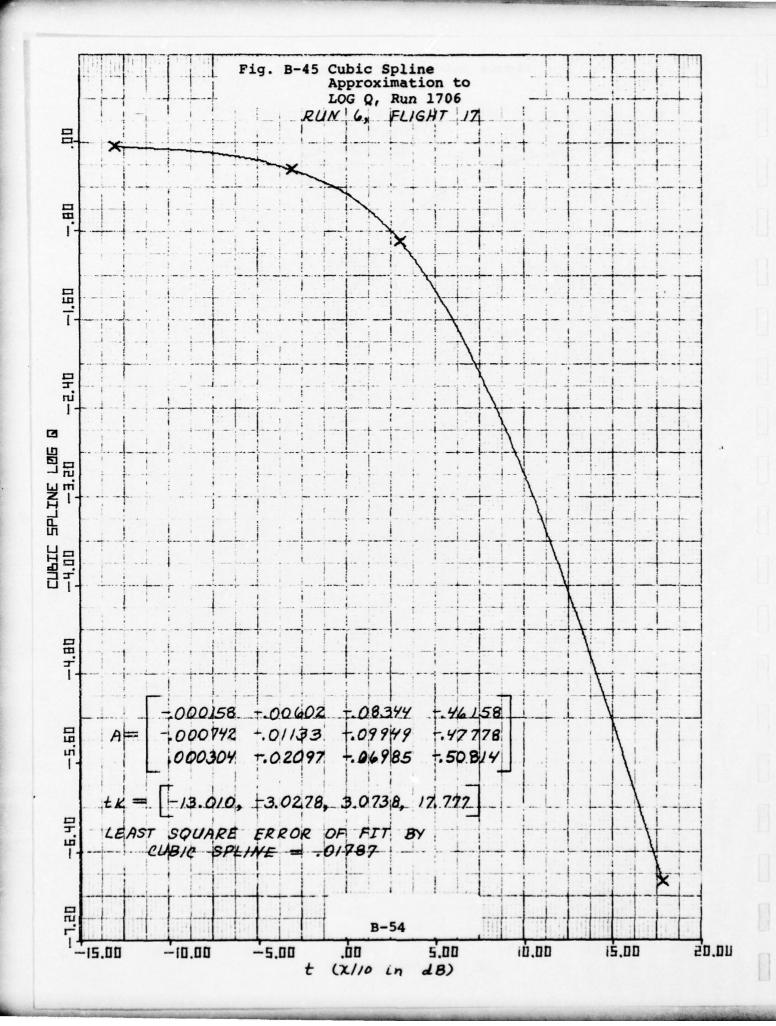


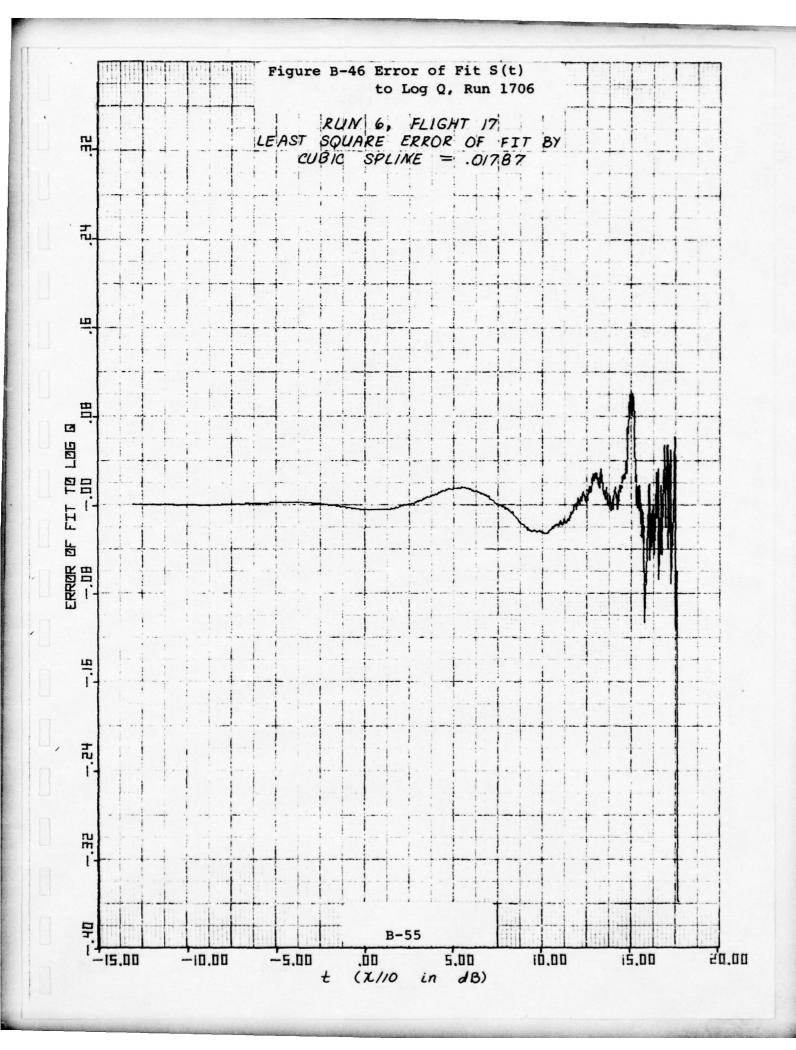


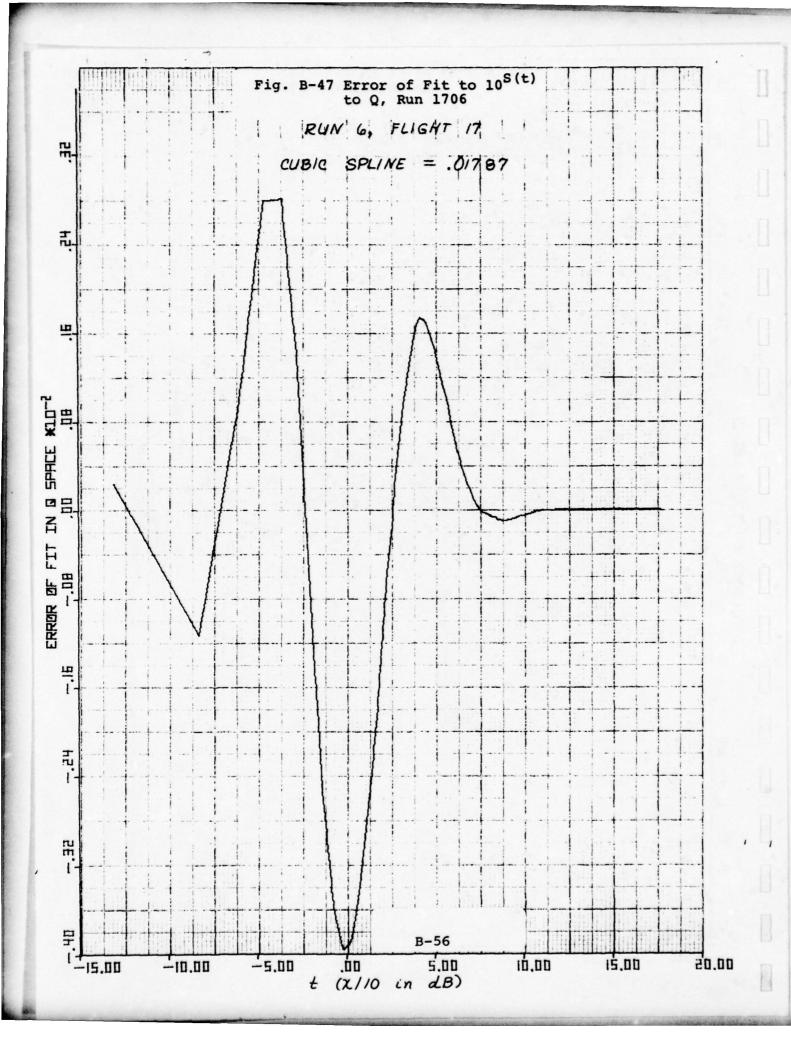










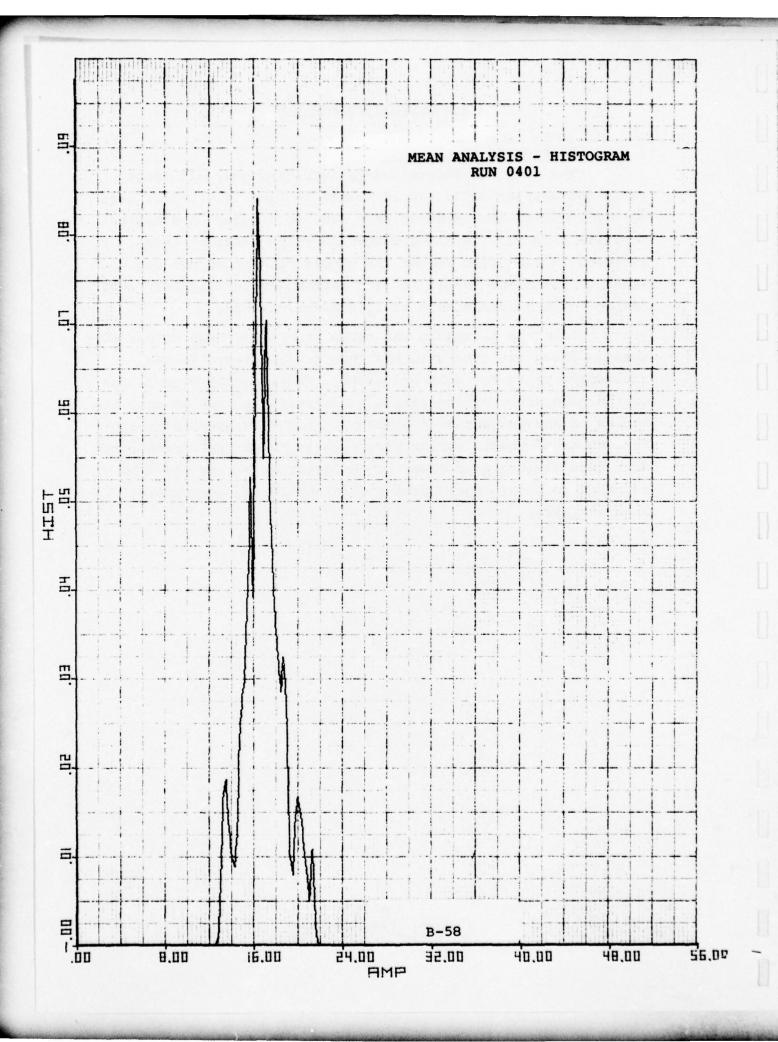


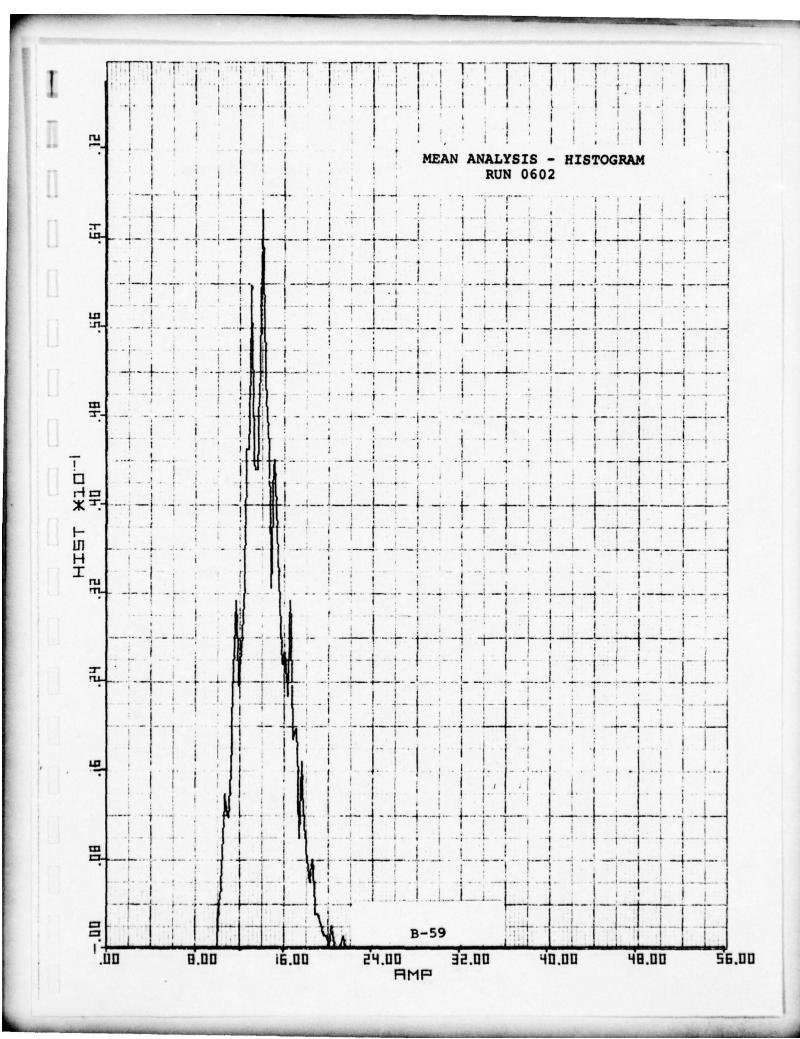
UNCLASSIFIED

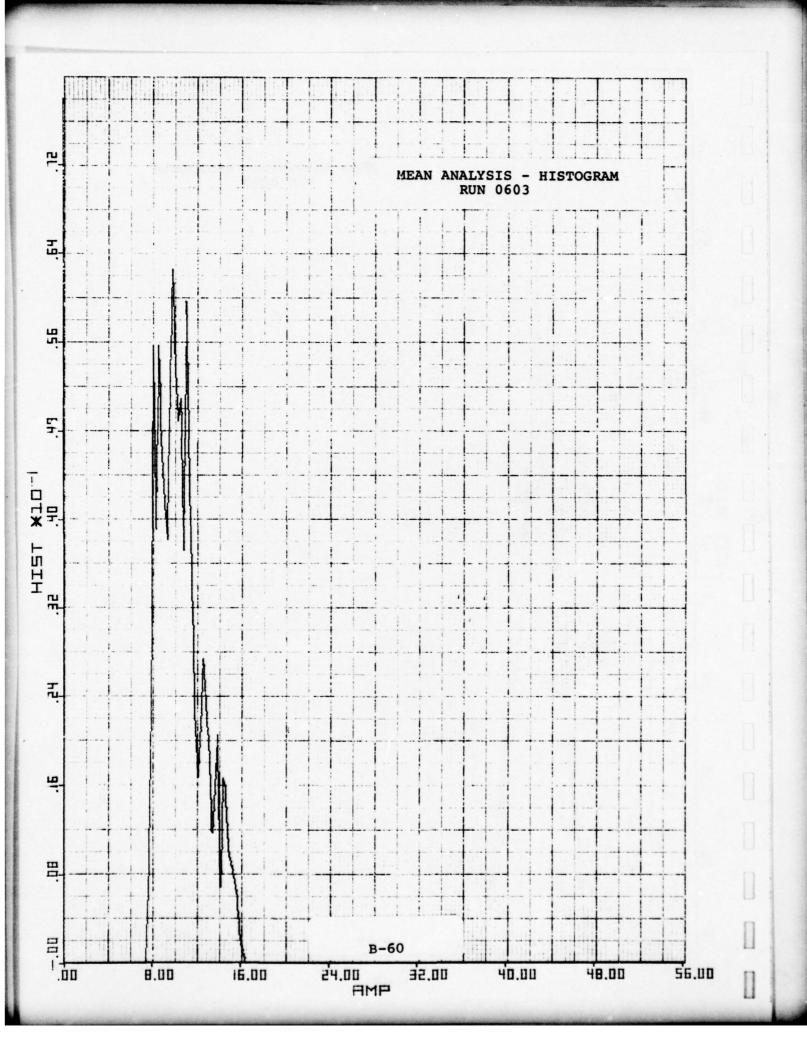
1.2 Histograms of the Mean

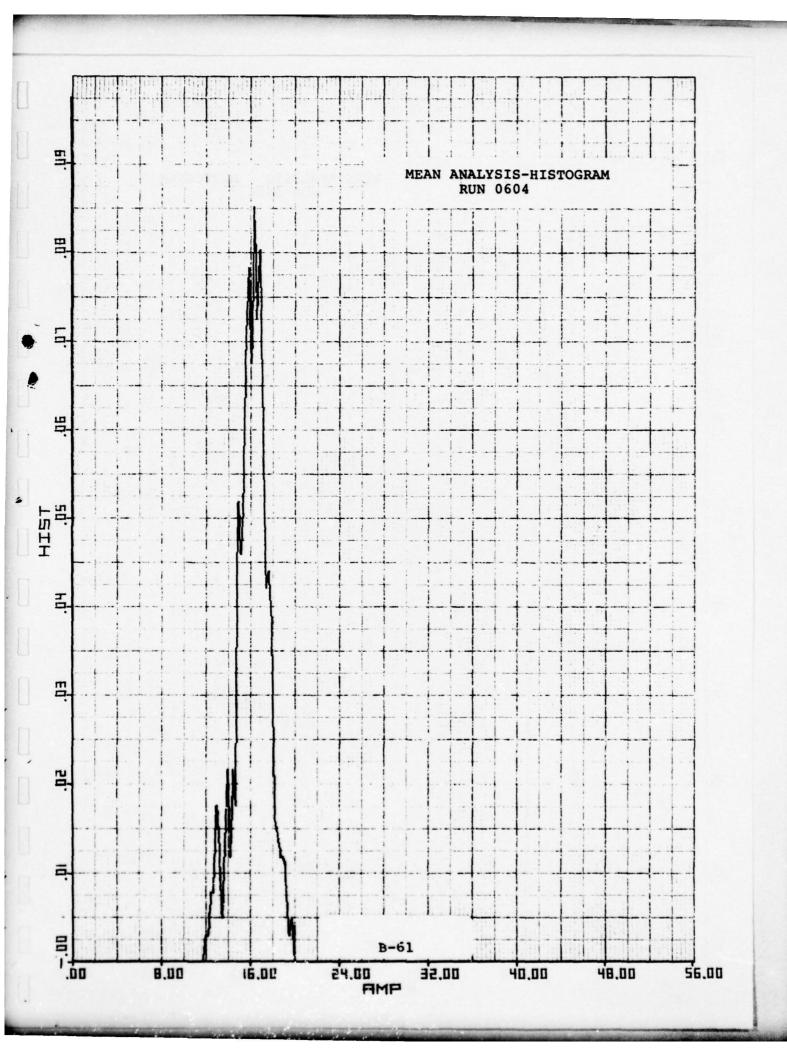
The mean was determined by averaging over all range gates and doppler cells and 10 frames in time (i.e., 5120 data points). There are approximately 3000 such means on a typical minute data run. Reduced number of range gates or time duration in some runs reduce the number of samples per run. These sample means result in data stream of approximately 3000 samples with a sample rate of 11.1 means/ second.

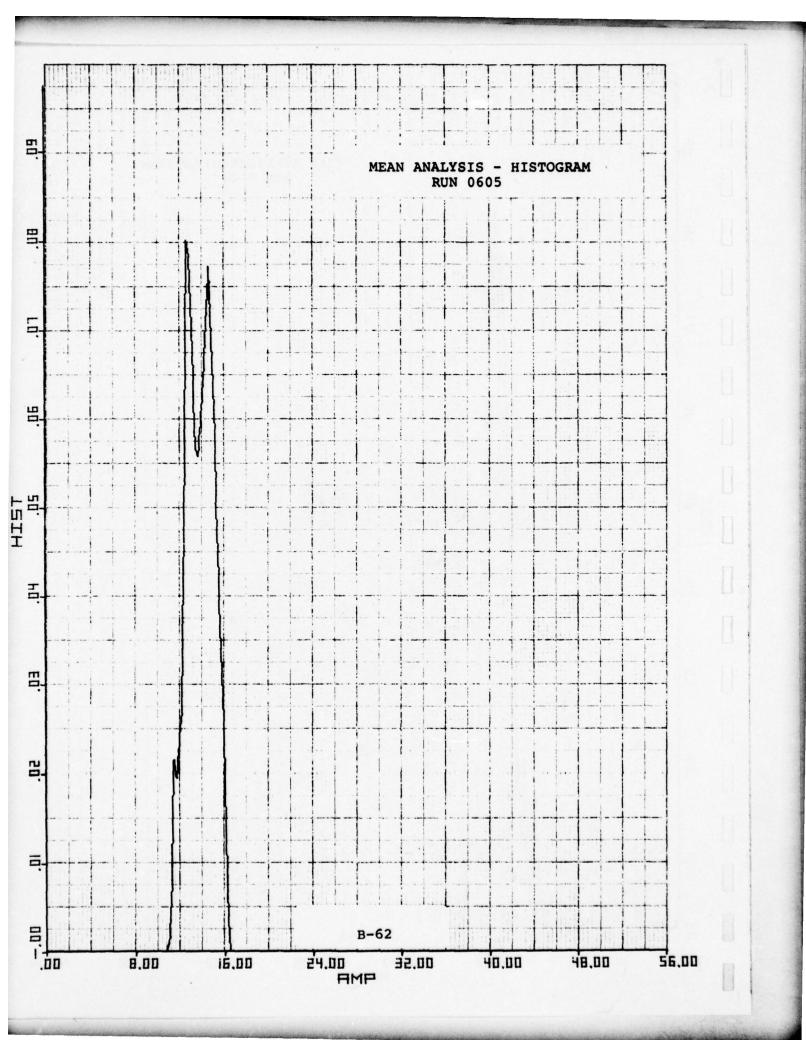
A simple histogram was found from these mean values over a run. These histograms in pdf form are displayed in the succeeding pages for selected cases. The temporal correlation of the mean (from autocorrelation analysis) is high so that the number of independent mean samples is low even for a 5 minute run. Some of the irregular structure in these histograms comes from this limited data base. Much longer data runs would be required to obtain data bases sufficient for more extensive mean analysis.

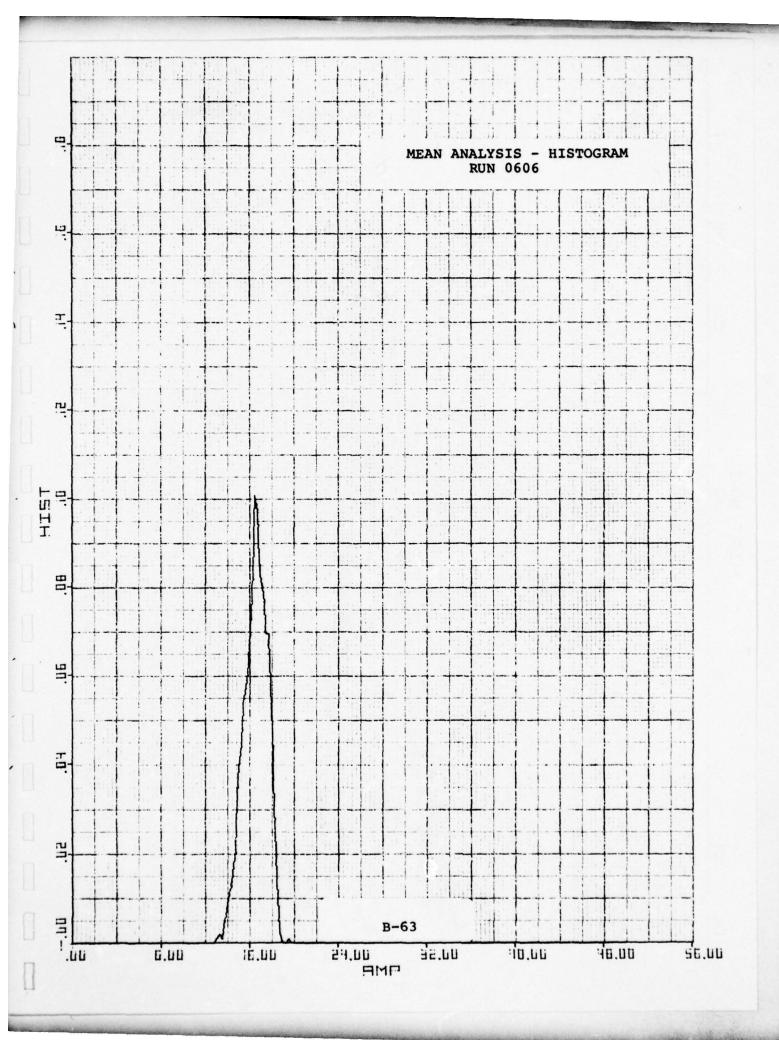


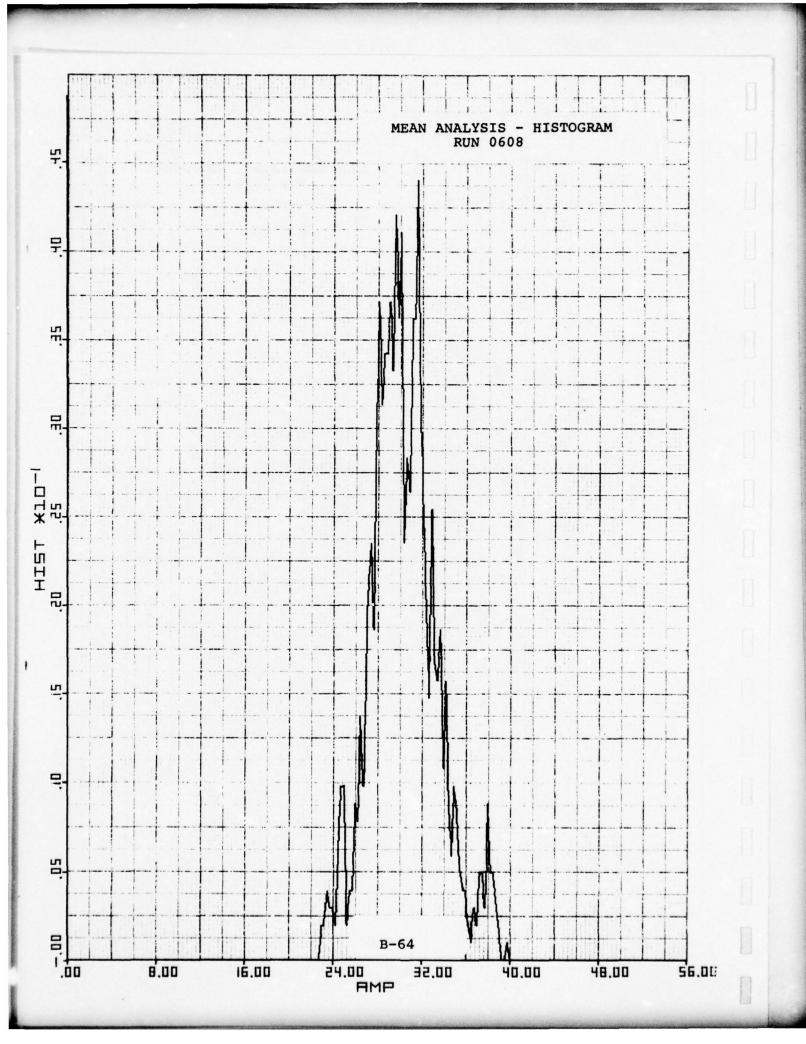


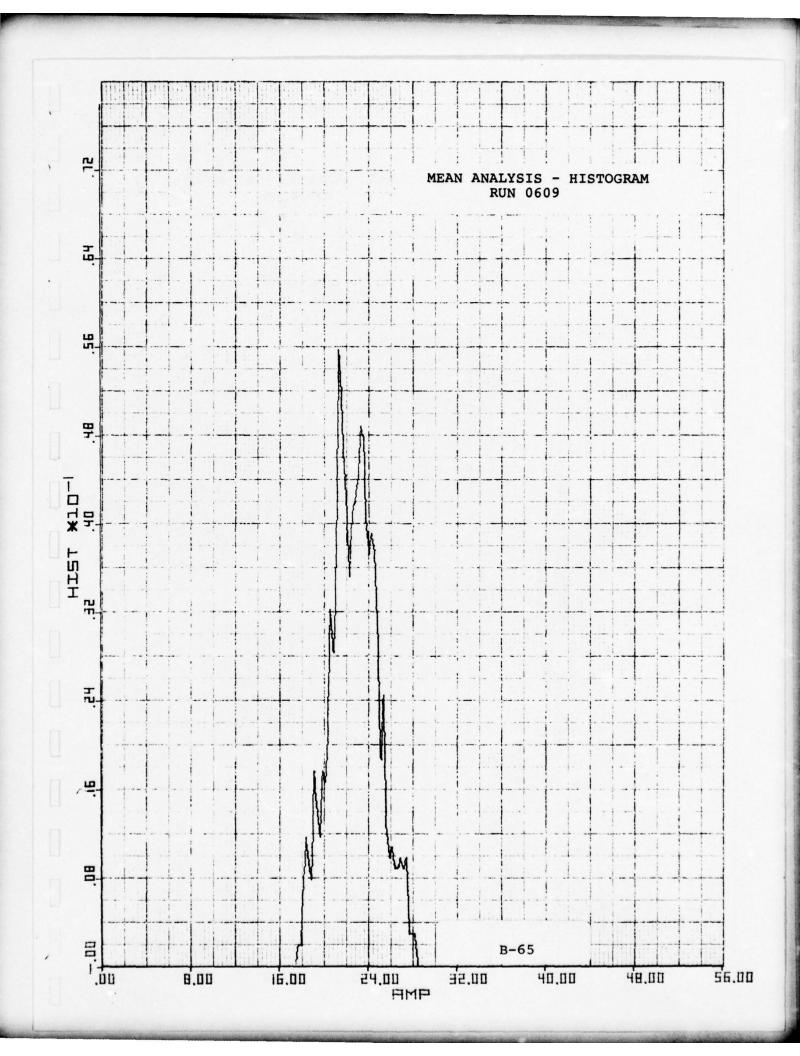


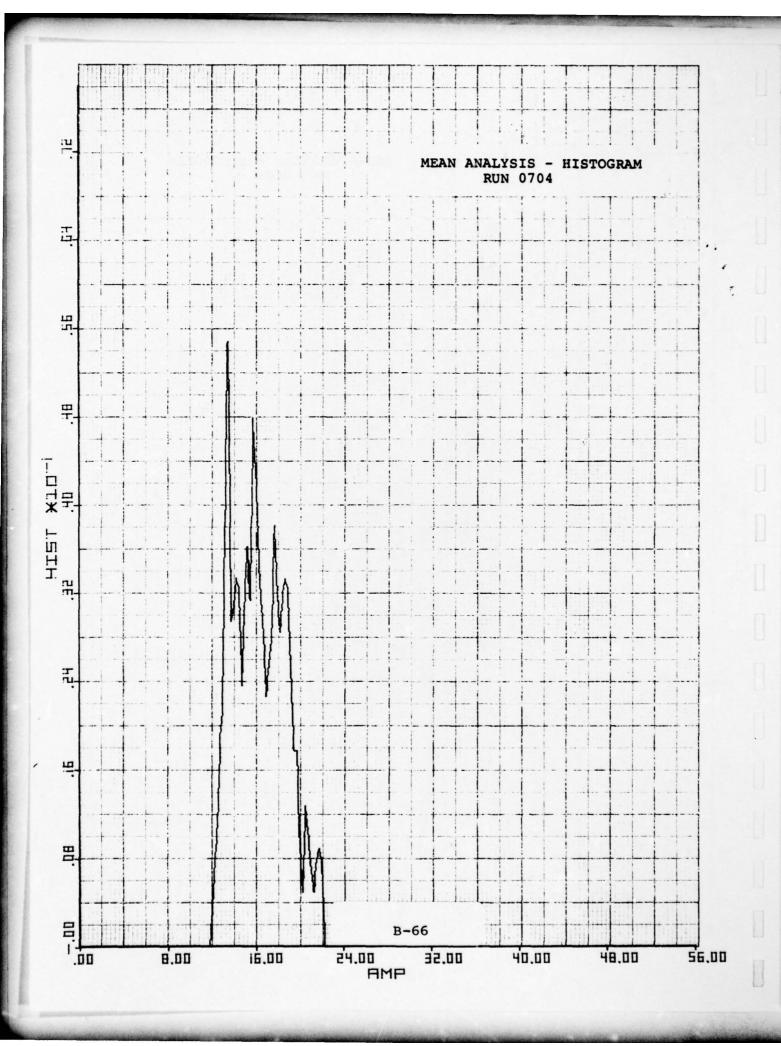


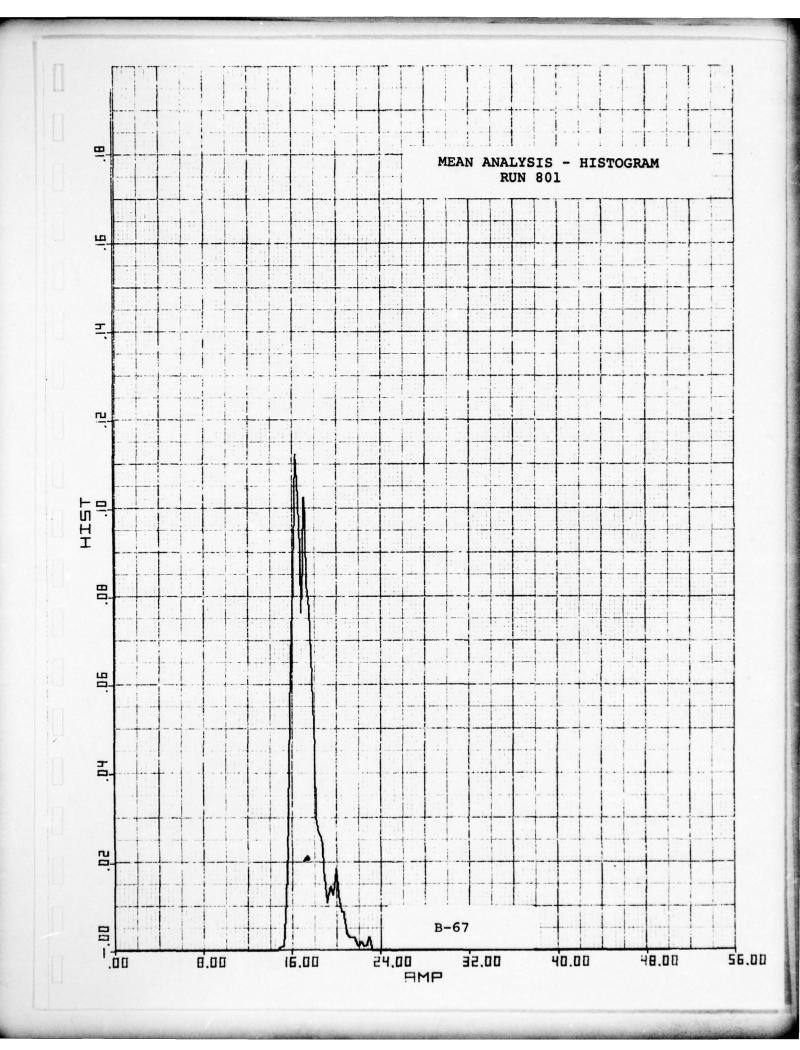


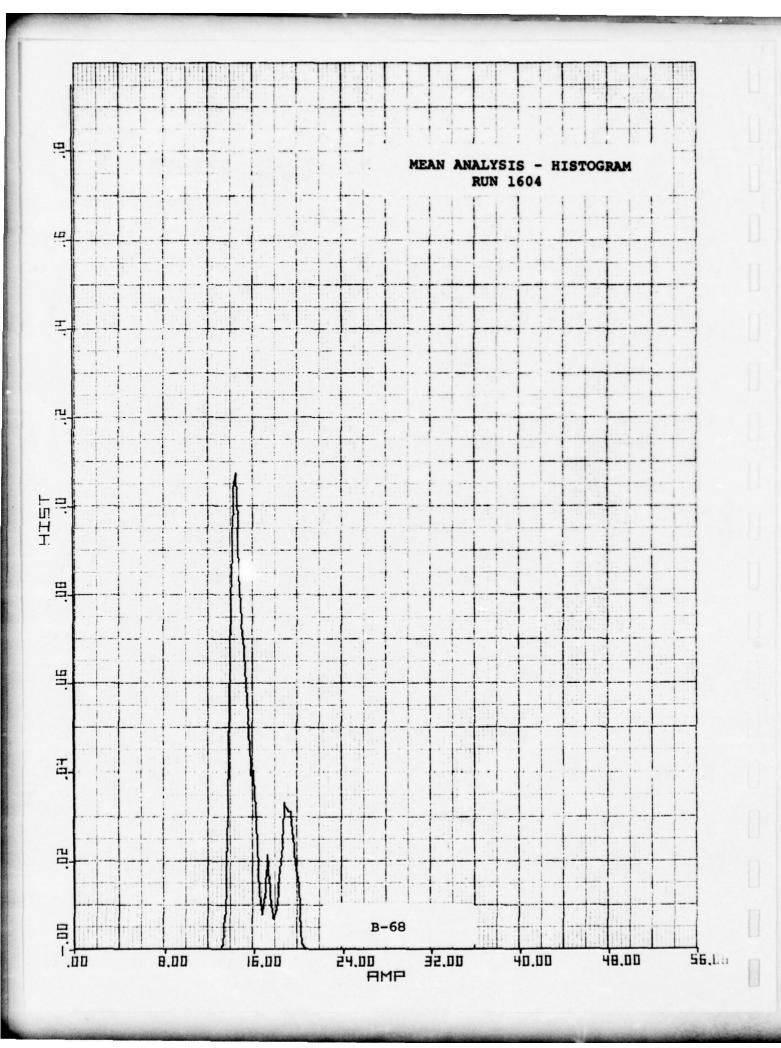


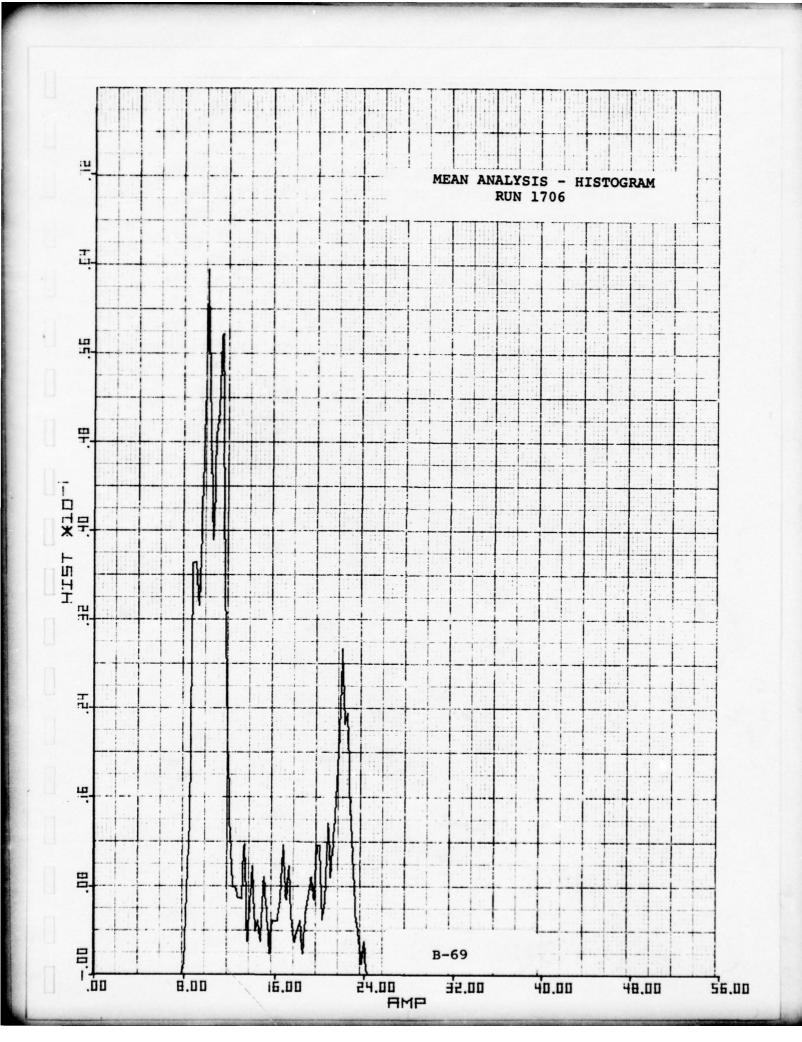








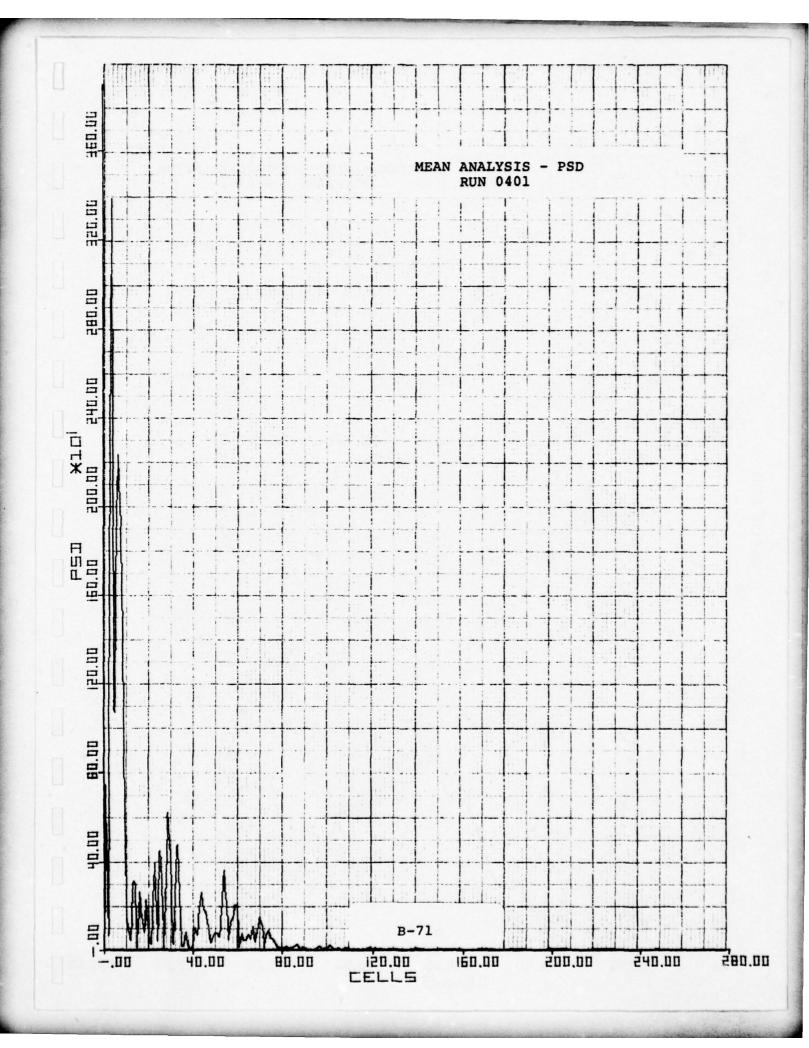


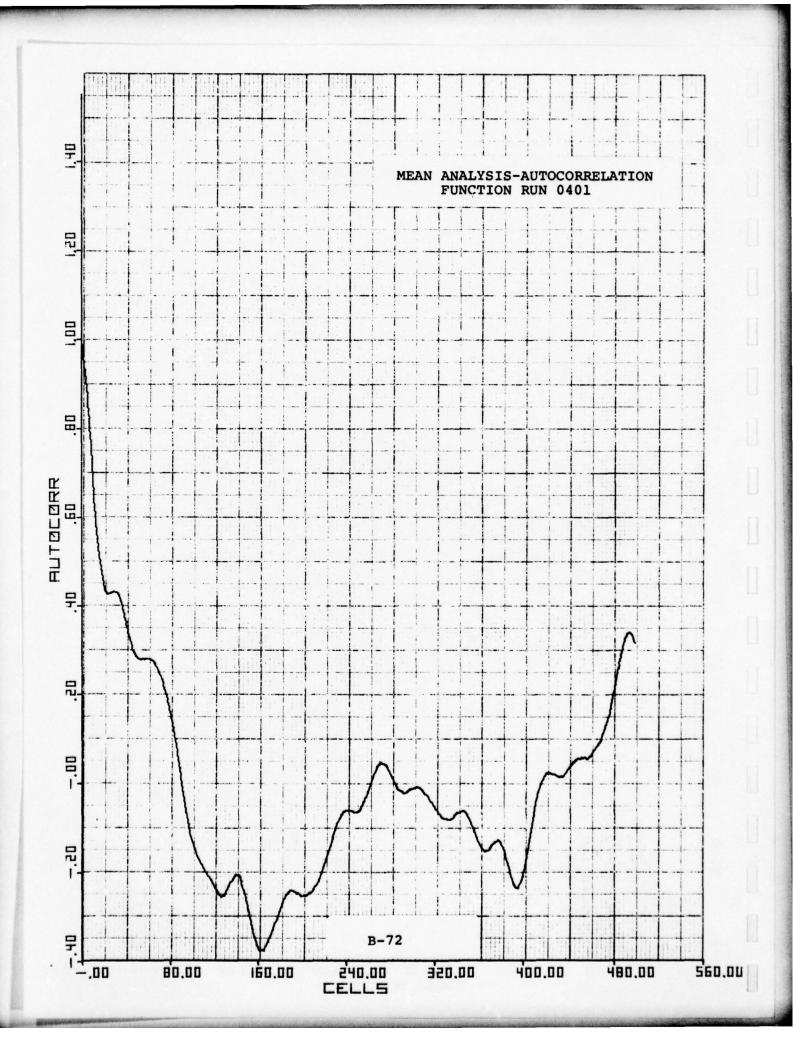


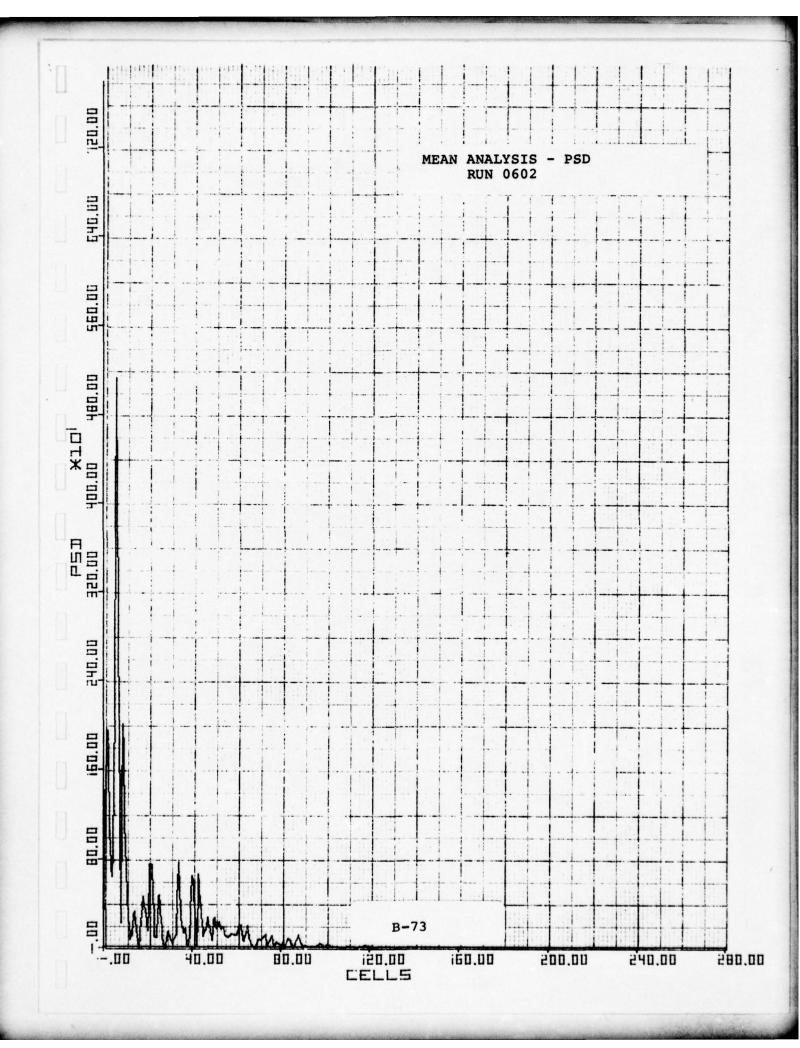
UNCLASSIFIED

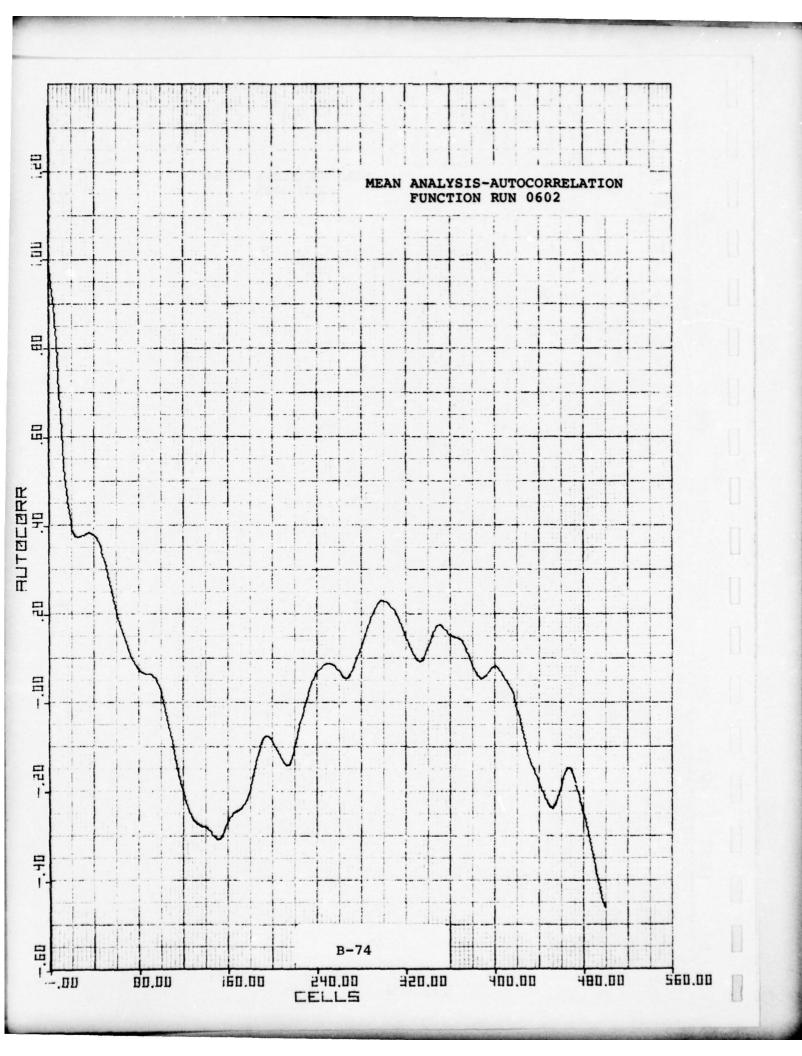
The data set for spectra and correlation Function of the Mean The data set for spectra and correlation analysis is the same as for histograms of the mean of the preceding subsection. A 1024 sample selection of the data was Fourier transformed to obtain a spectrum. Real and imaginary parts were squared and summed to obtain the PSD. The PSD was then Fourier transformed to obtain the autocorrelation function (ACF). This transform was aperiodic and compensated to obtain the ACF. The aperiodic compensation and higher sensitivity produced increased noise on the tails of the ACF.

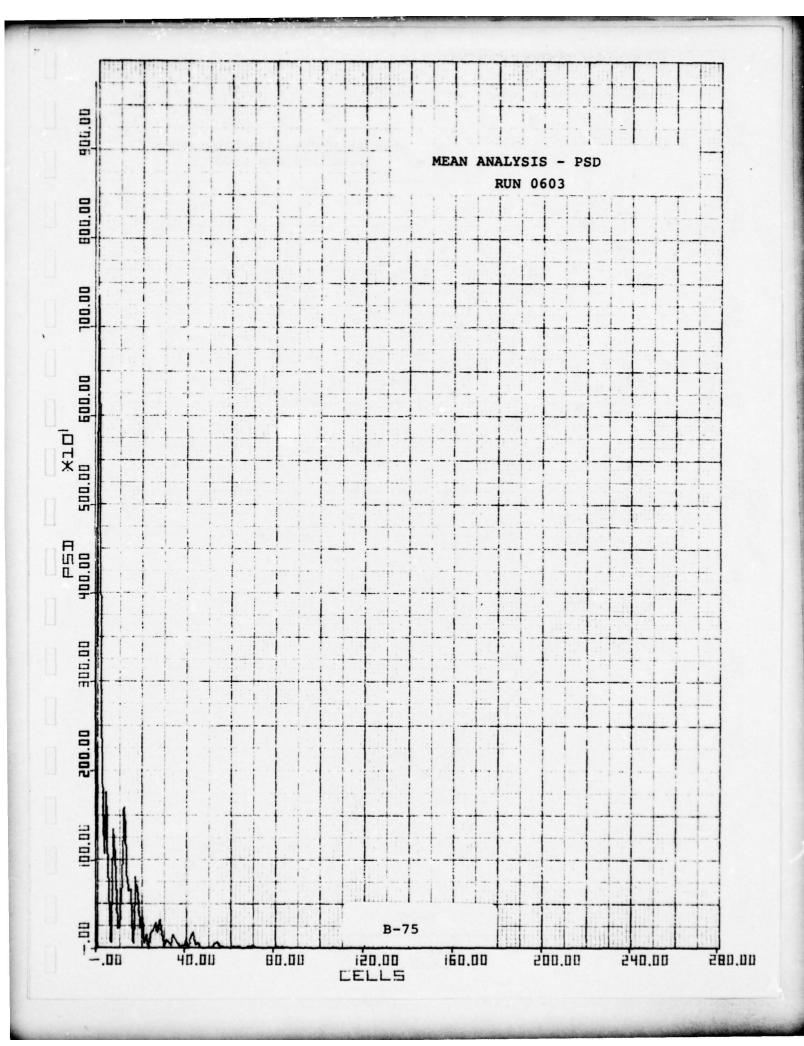
Again here the limited number of independent mean samples creates some of the long term oscillation in the ACF. This assessment has been born out by the simulation results (see Section 10 of Volume II and Appendix F of this volume).

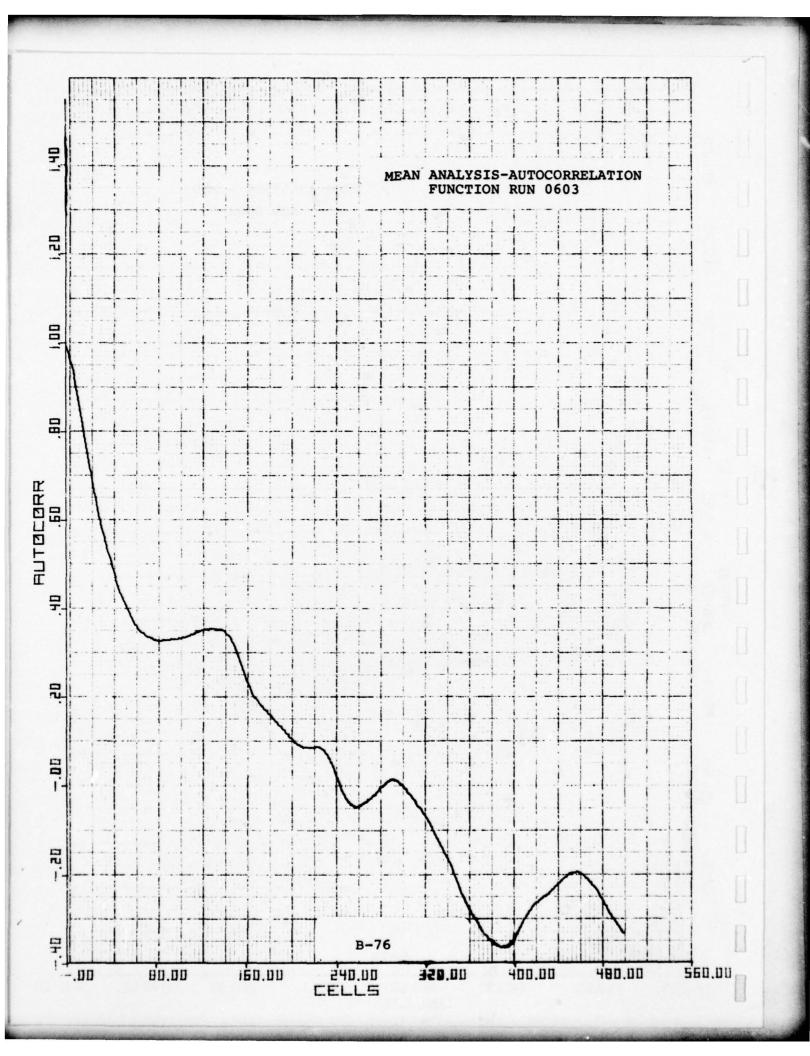


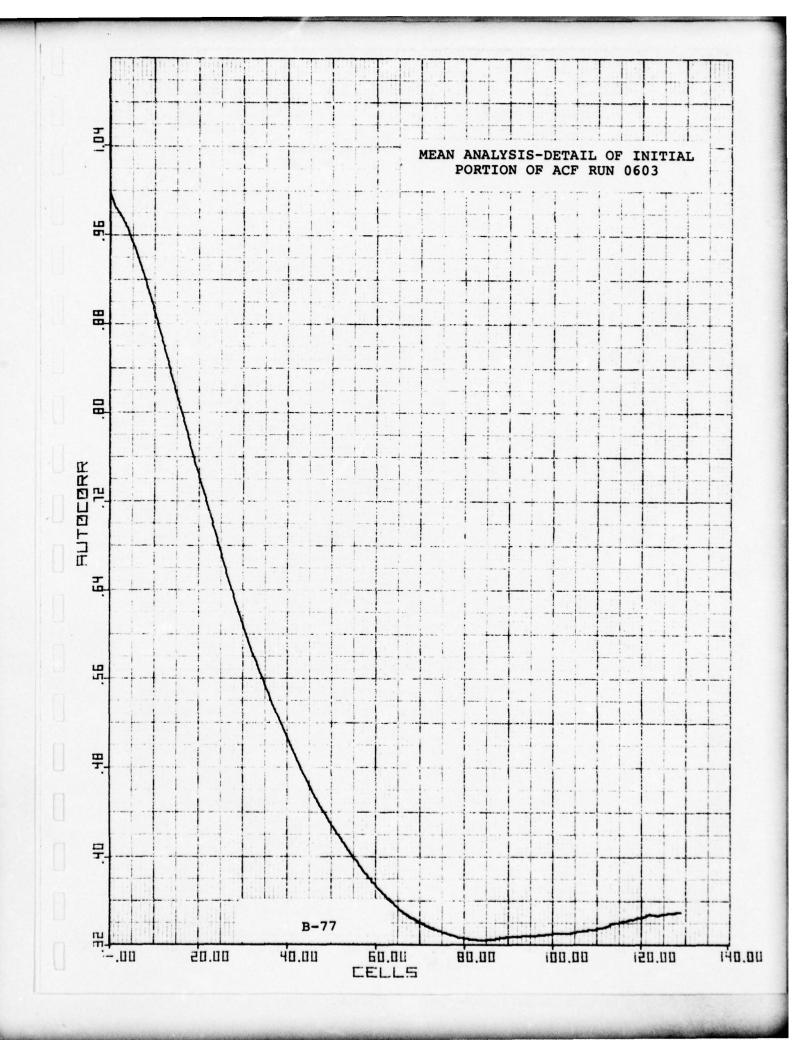


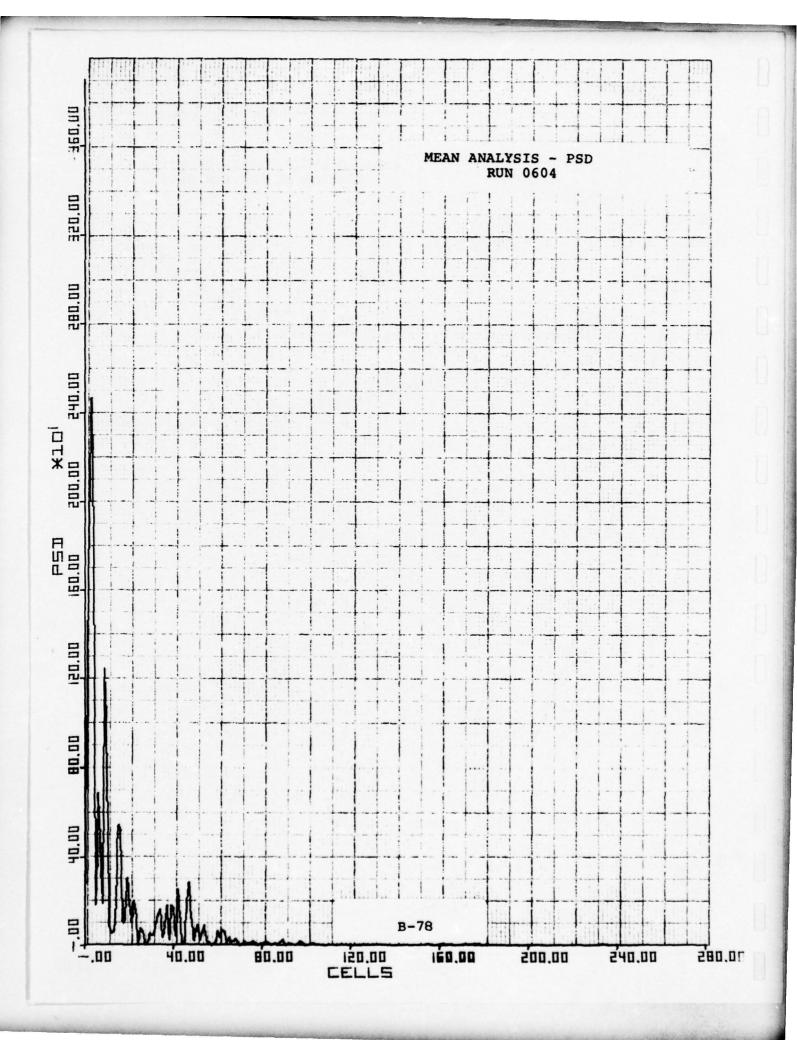


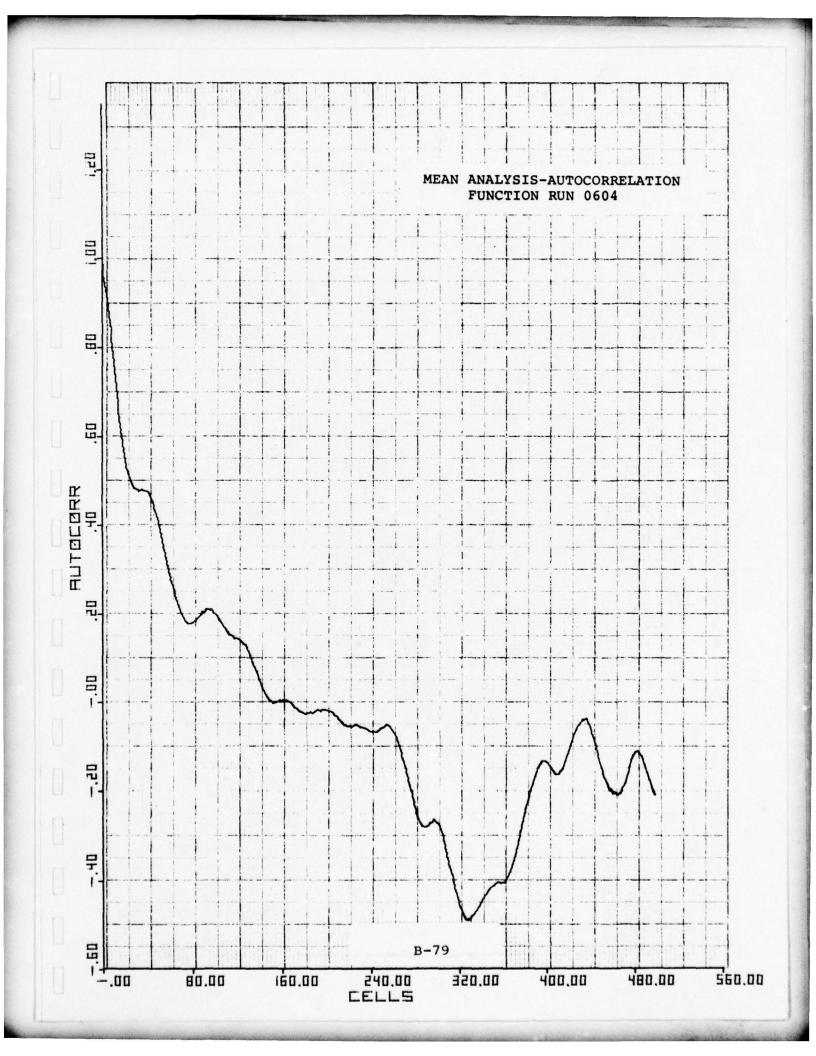


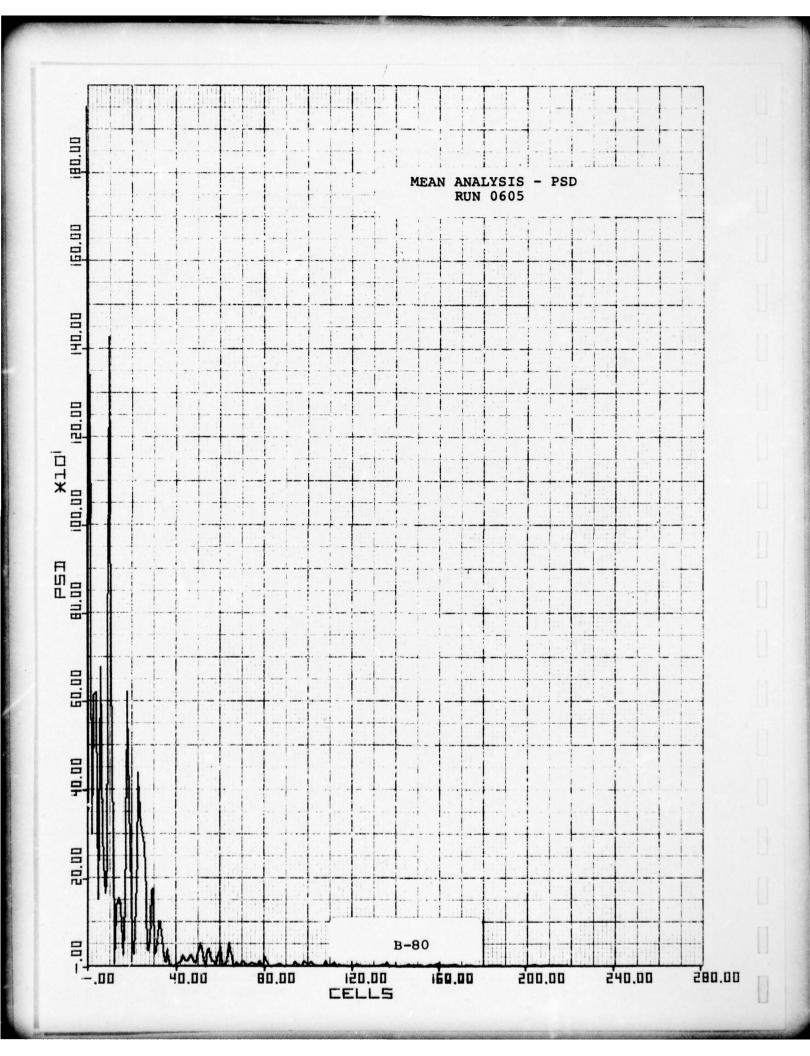


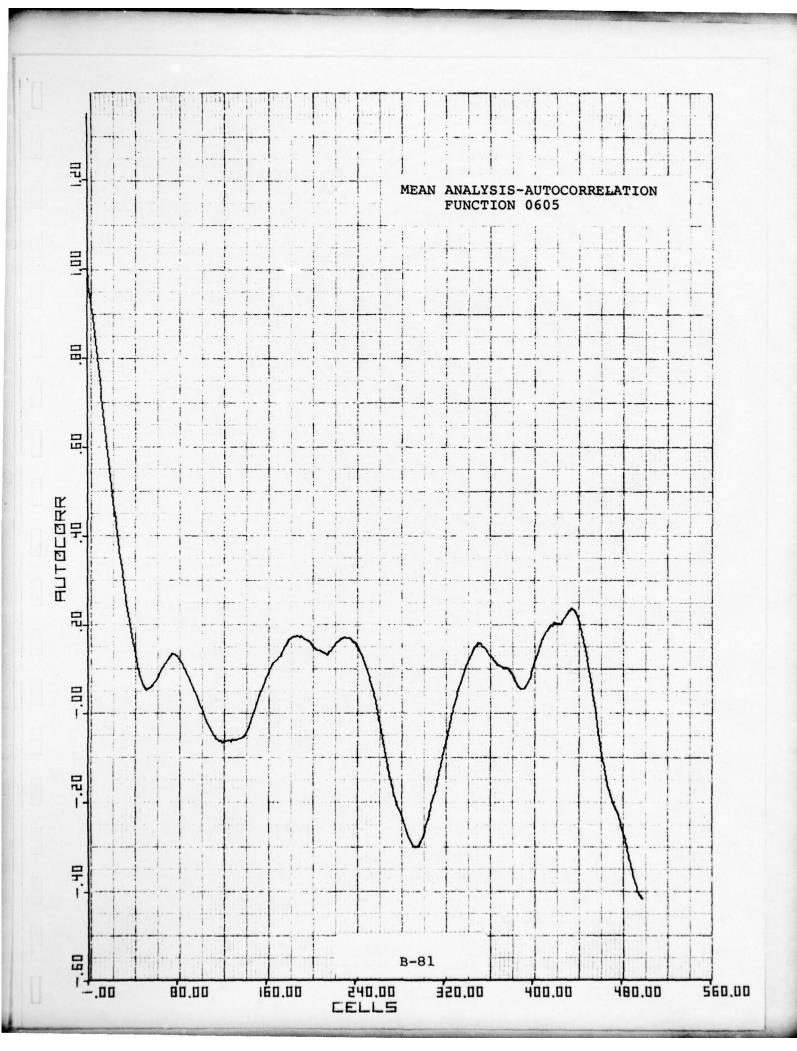


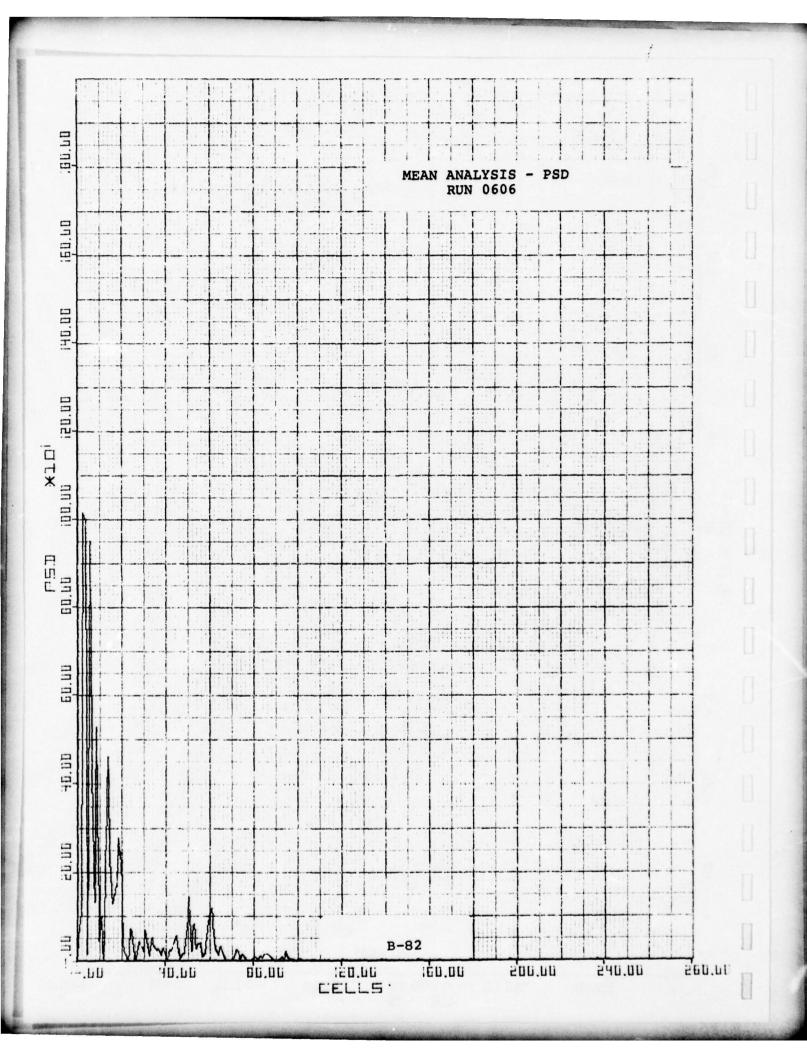


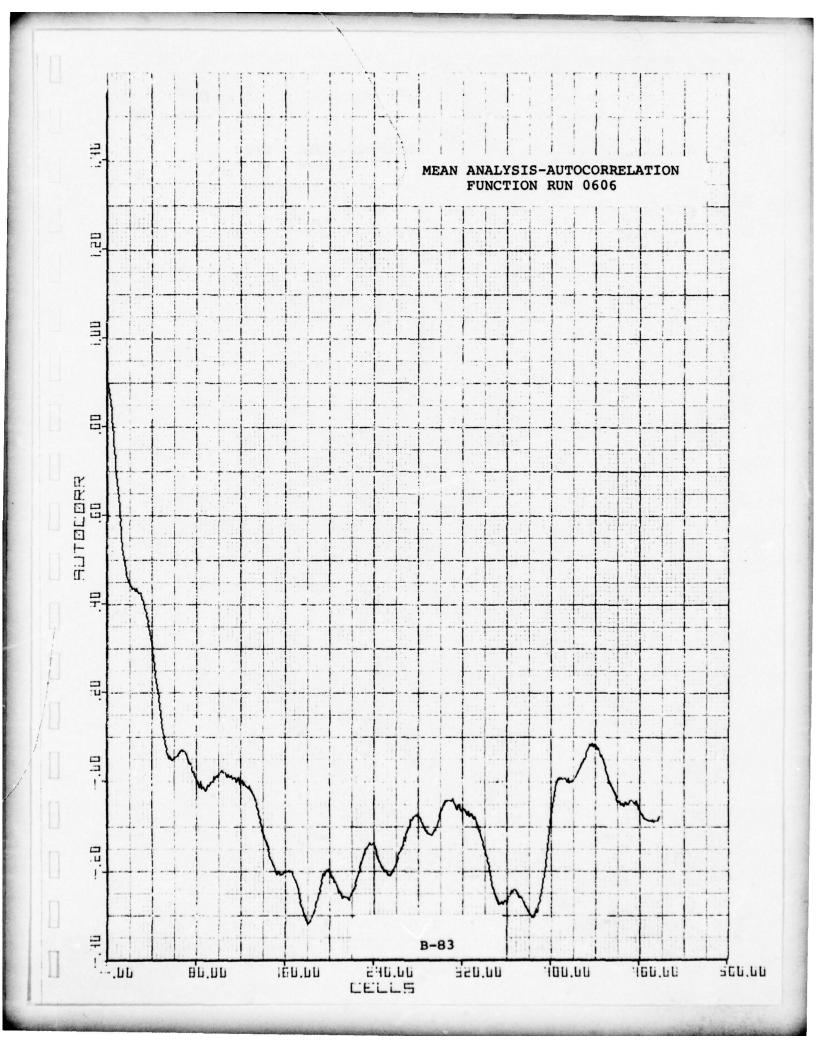


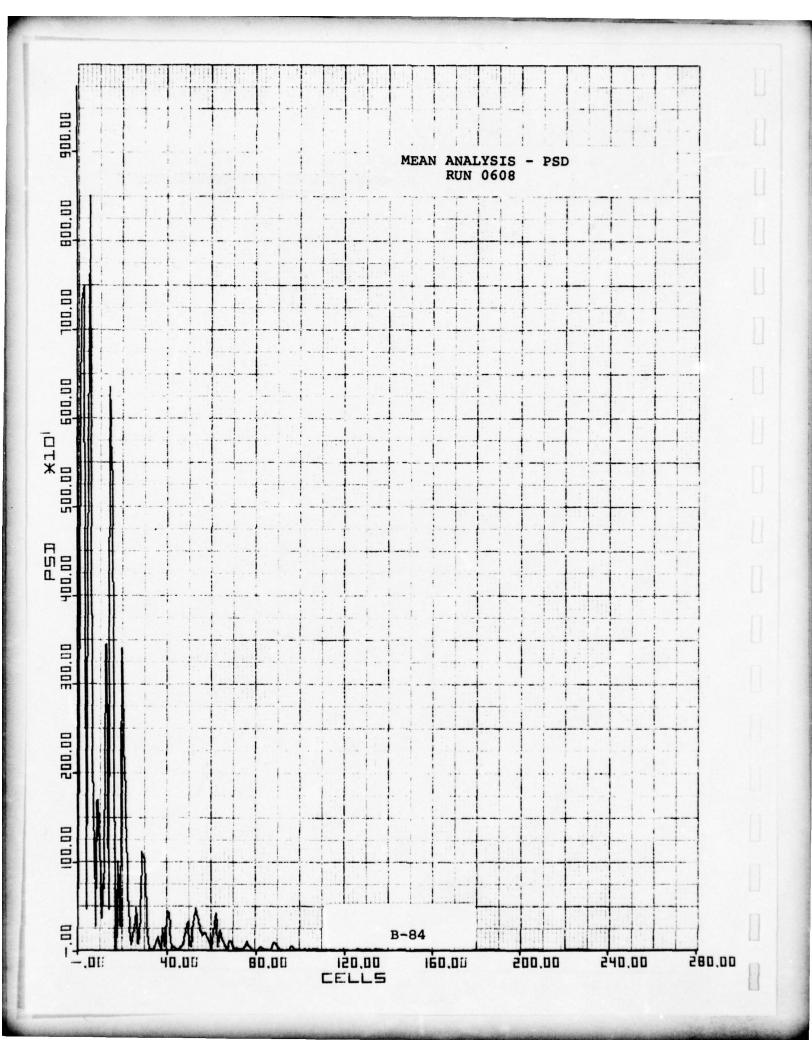


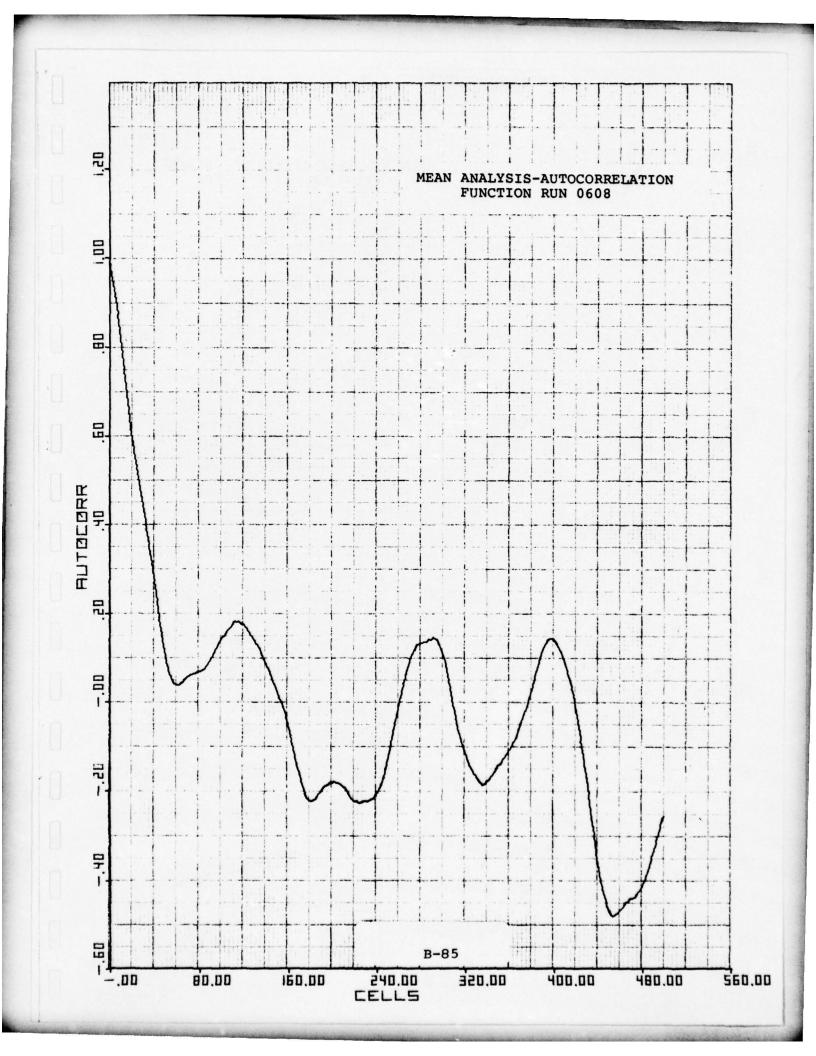


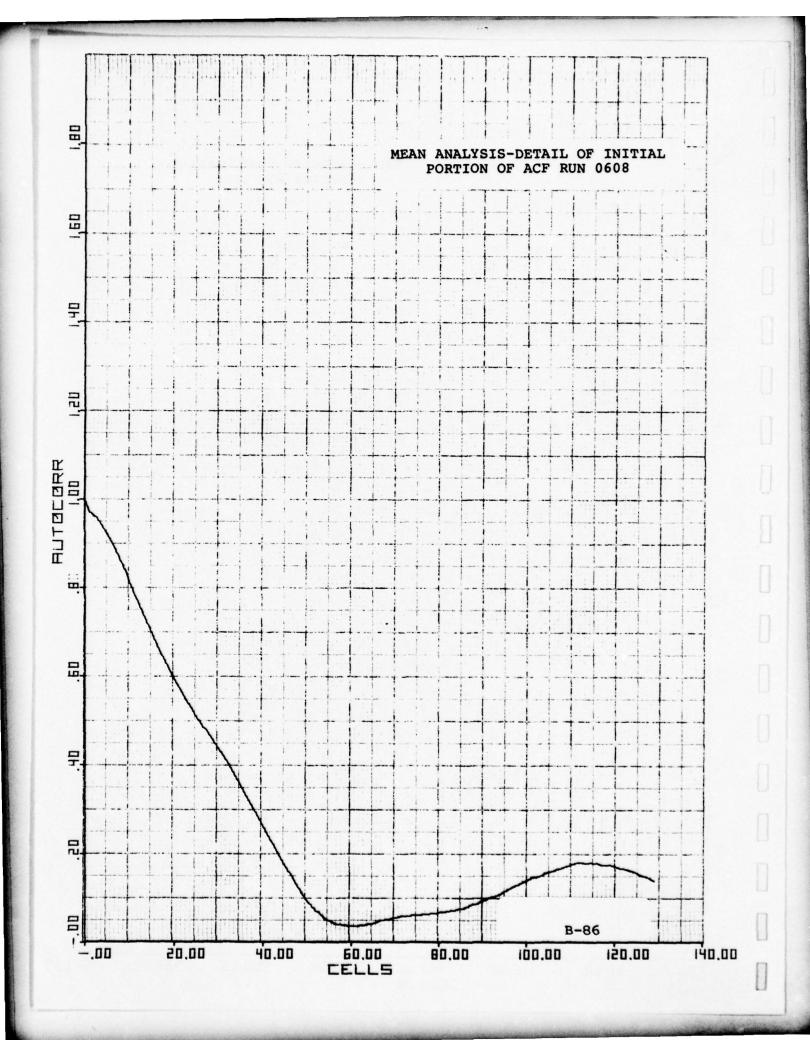


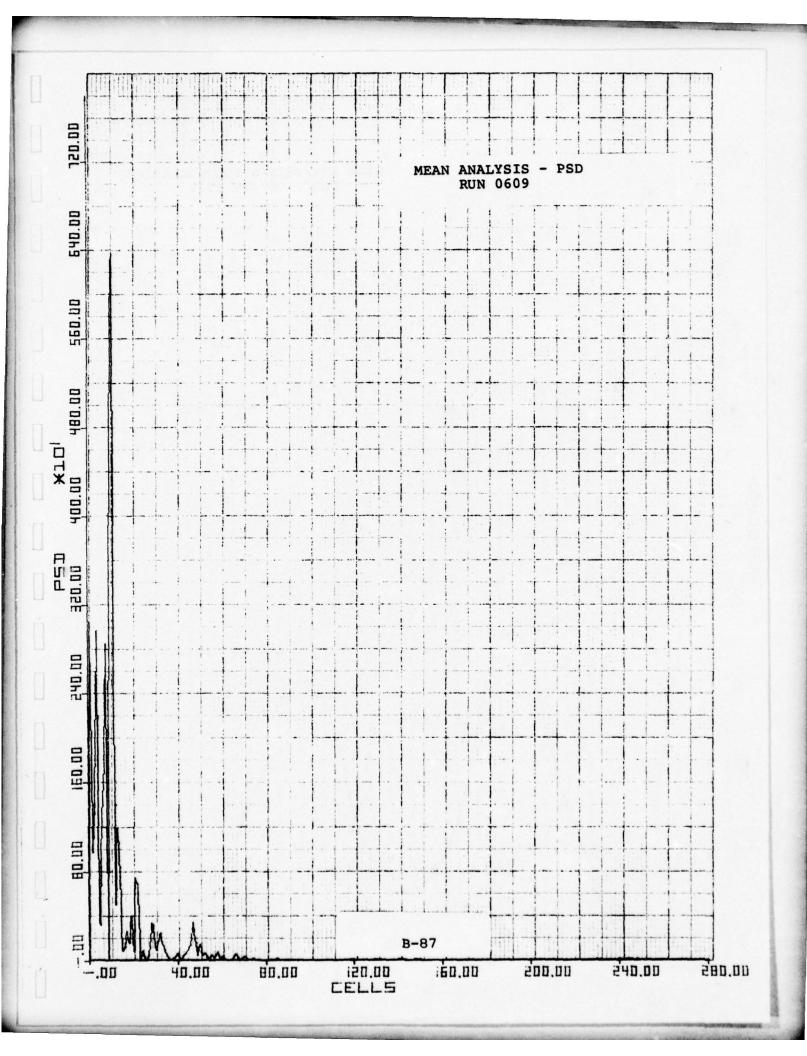


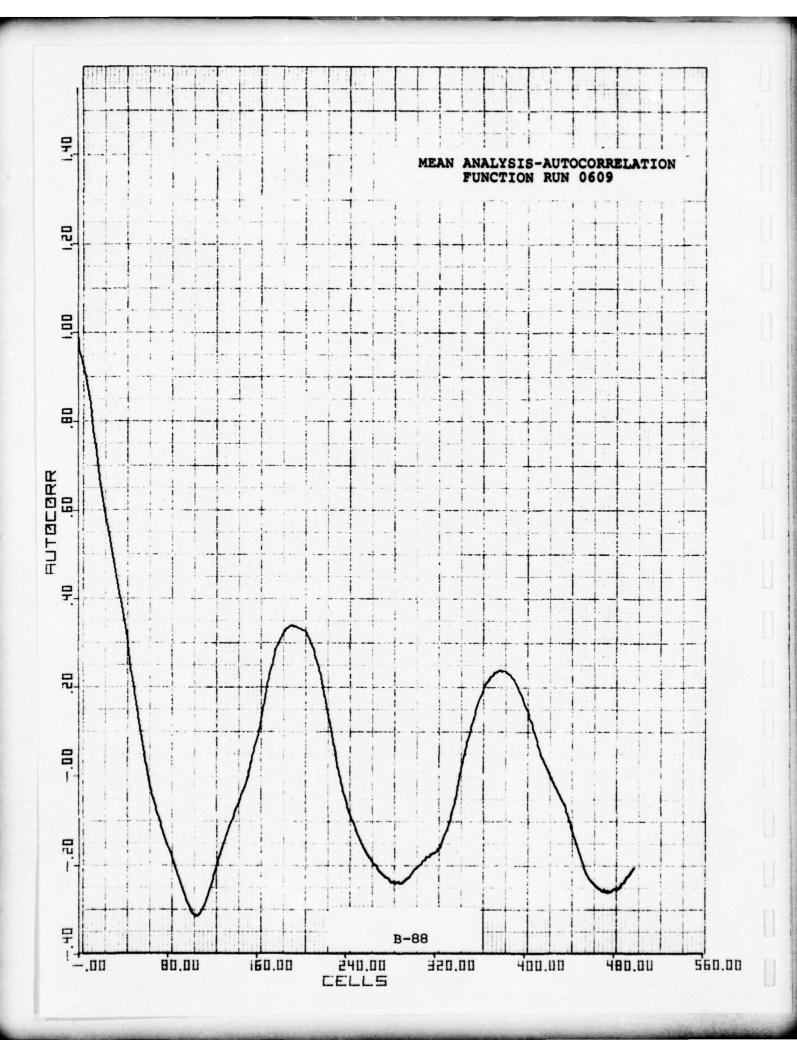


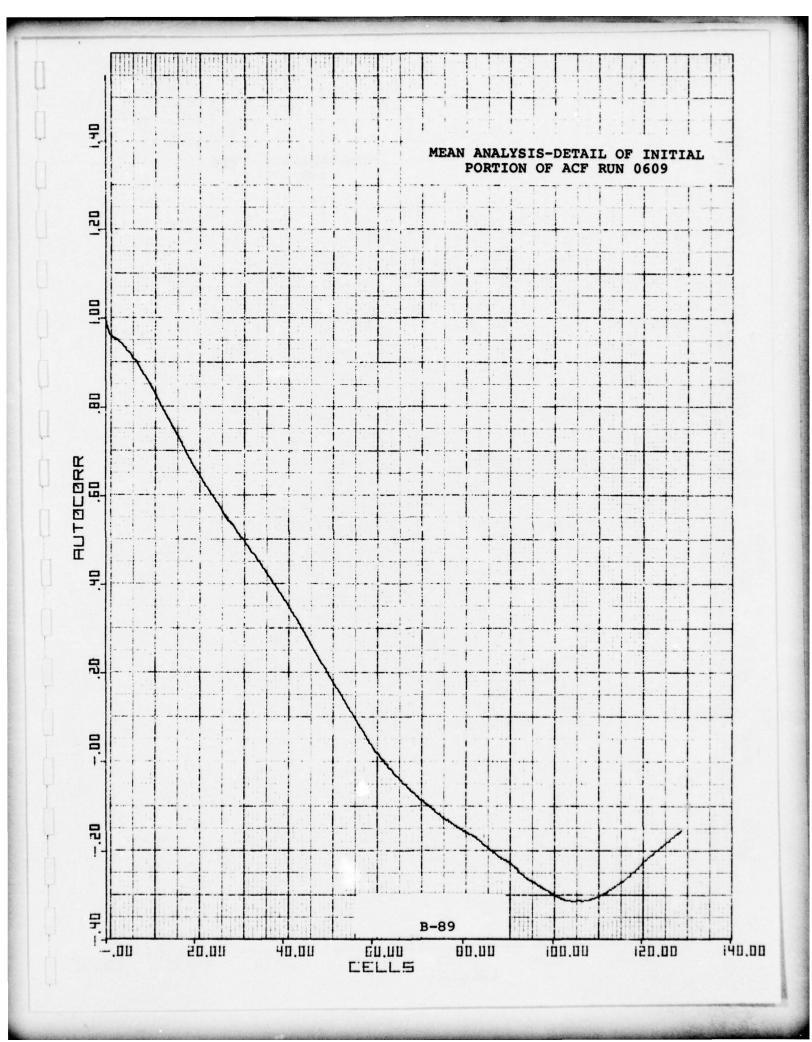


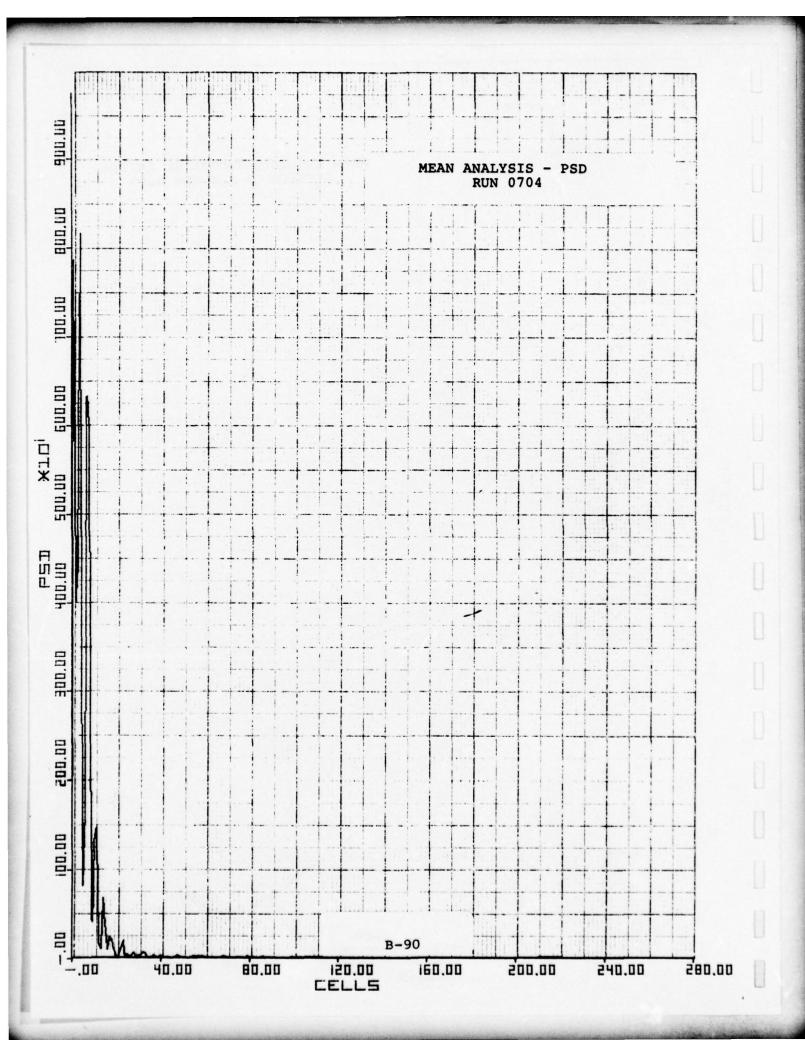


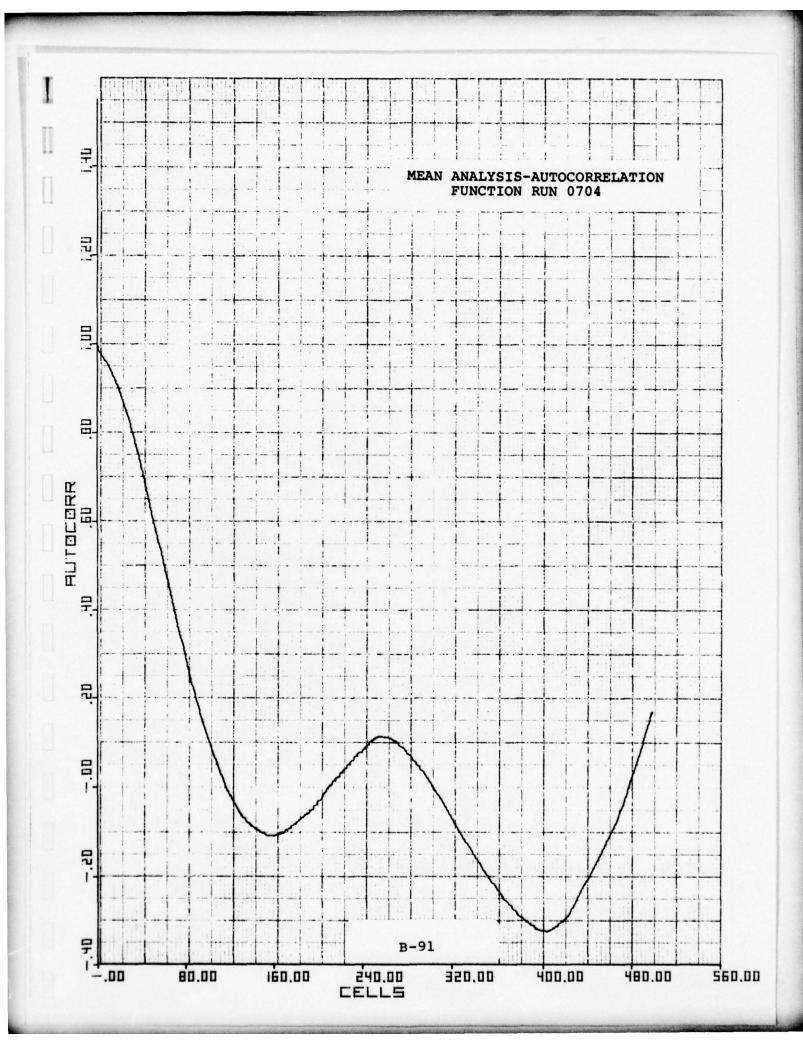


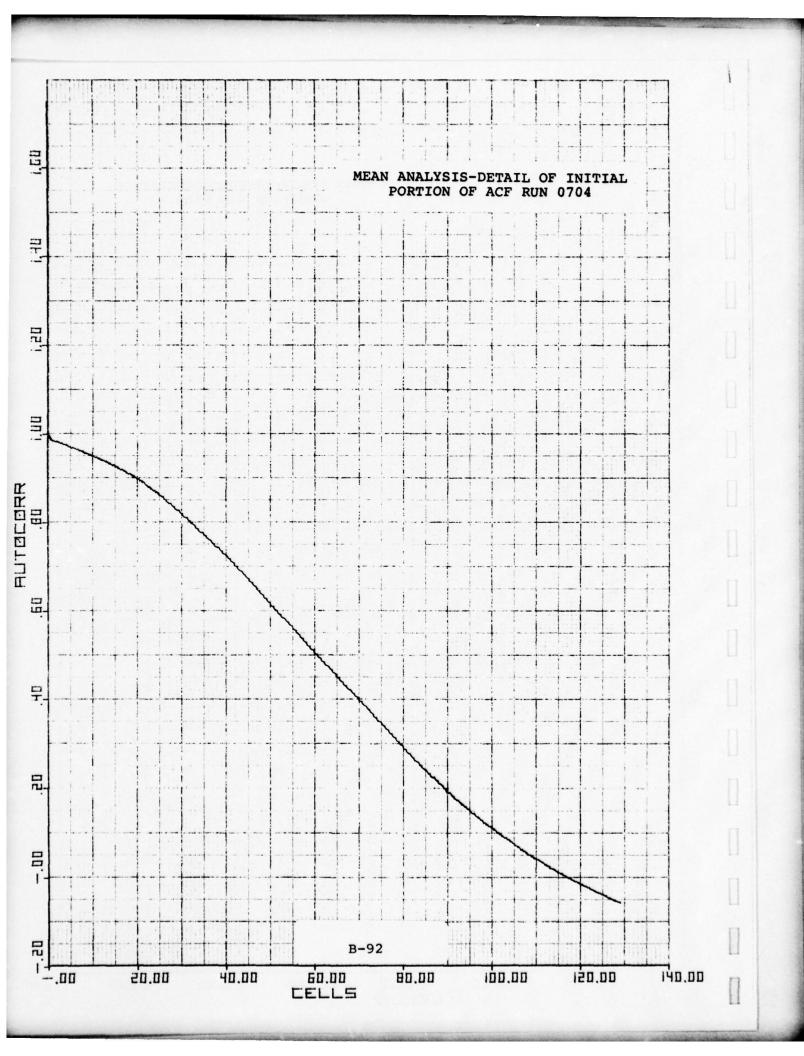


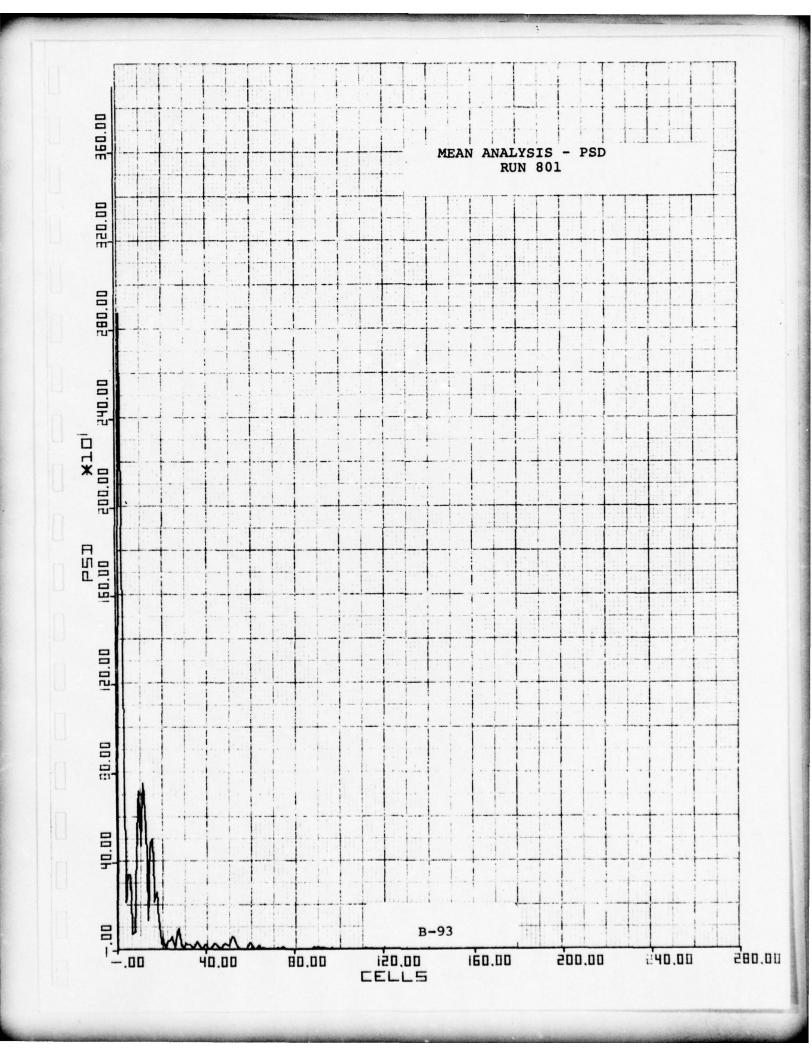


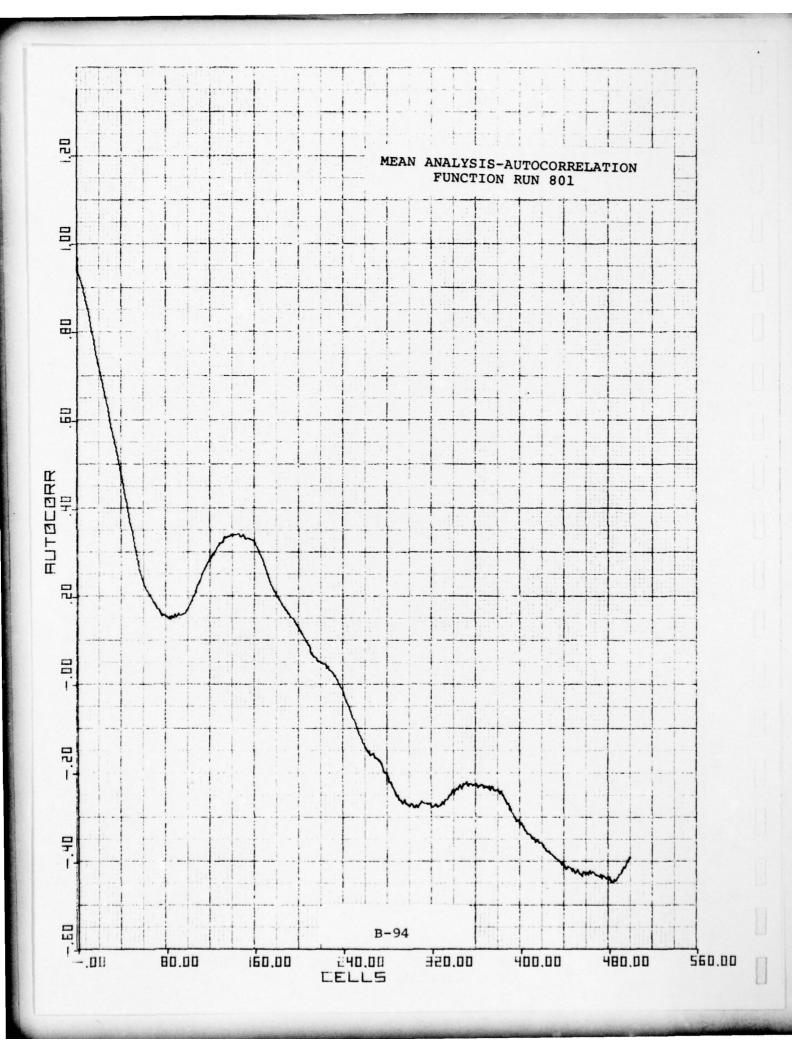


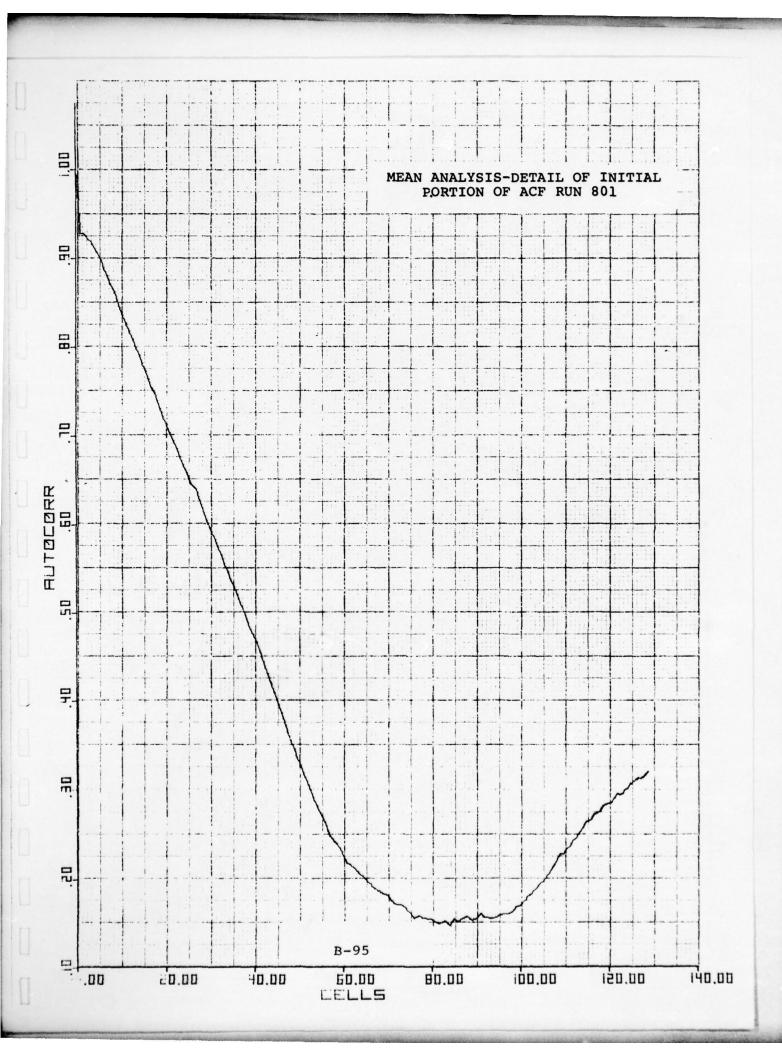


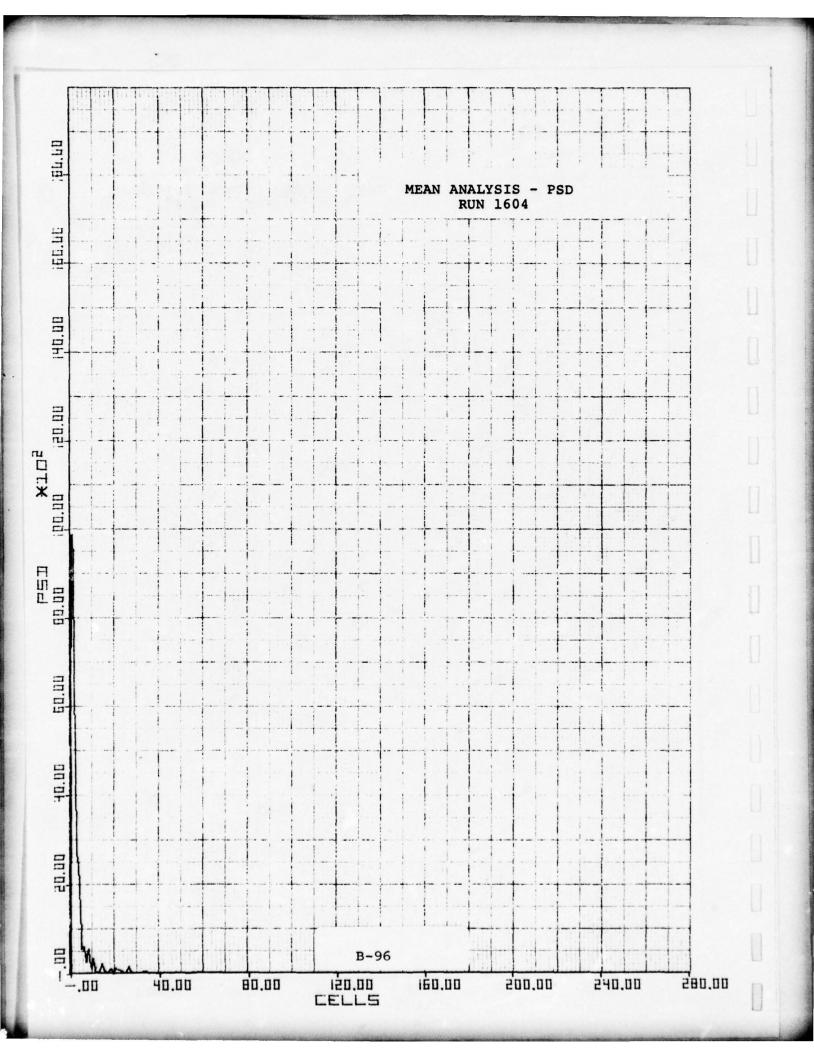


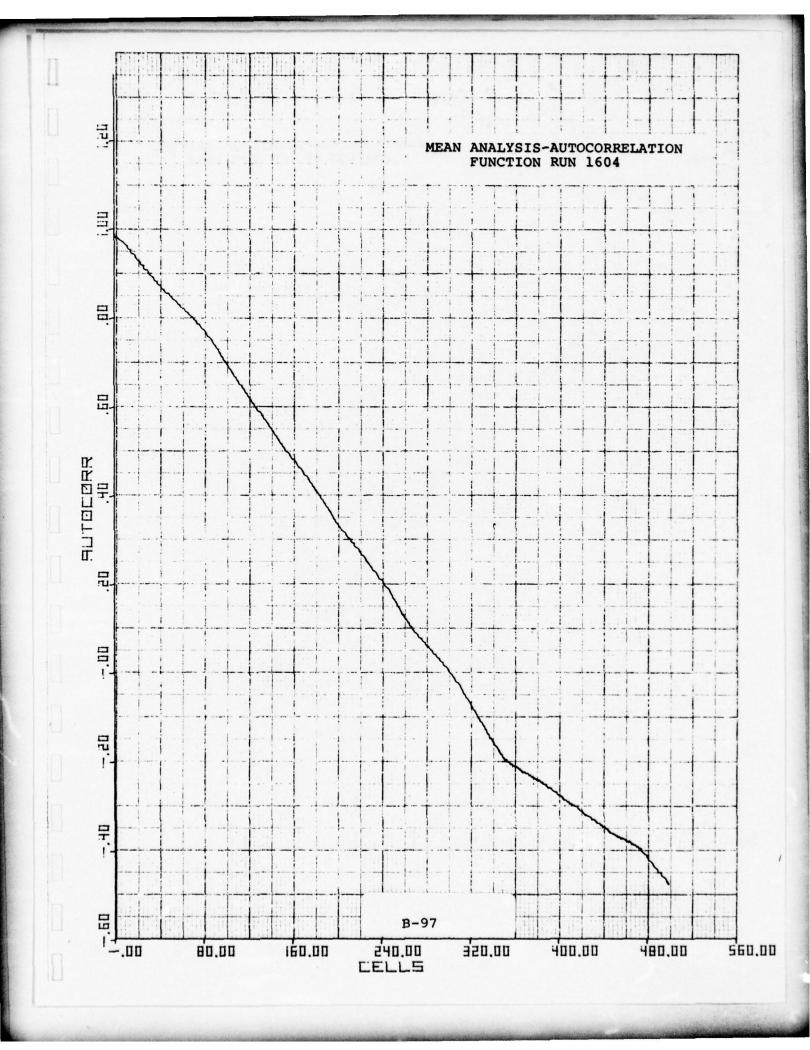


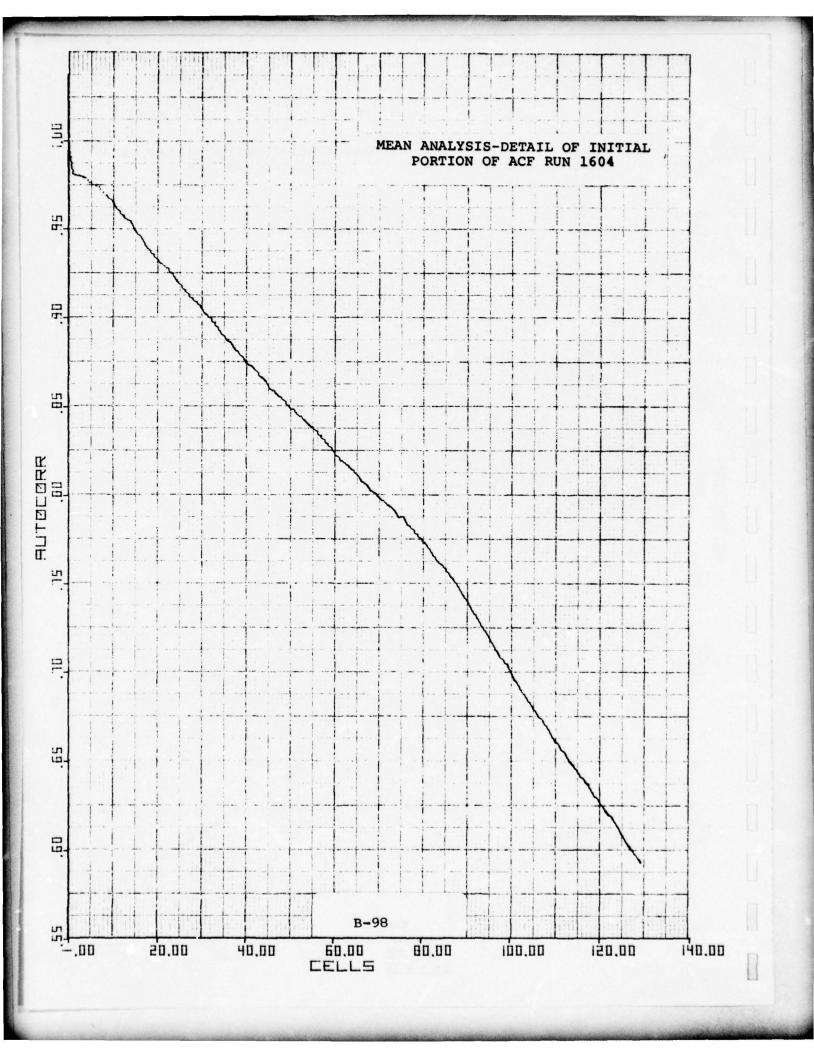


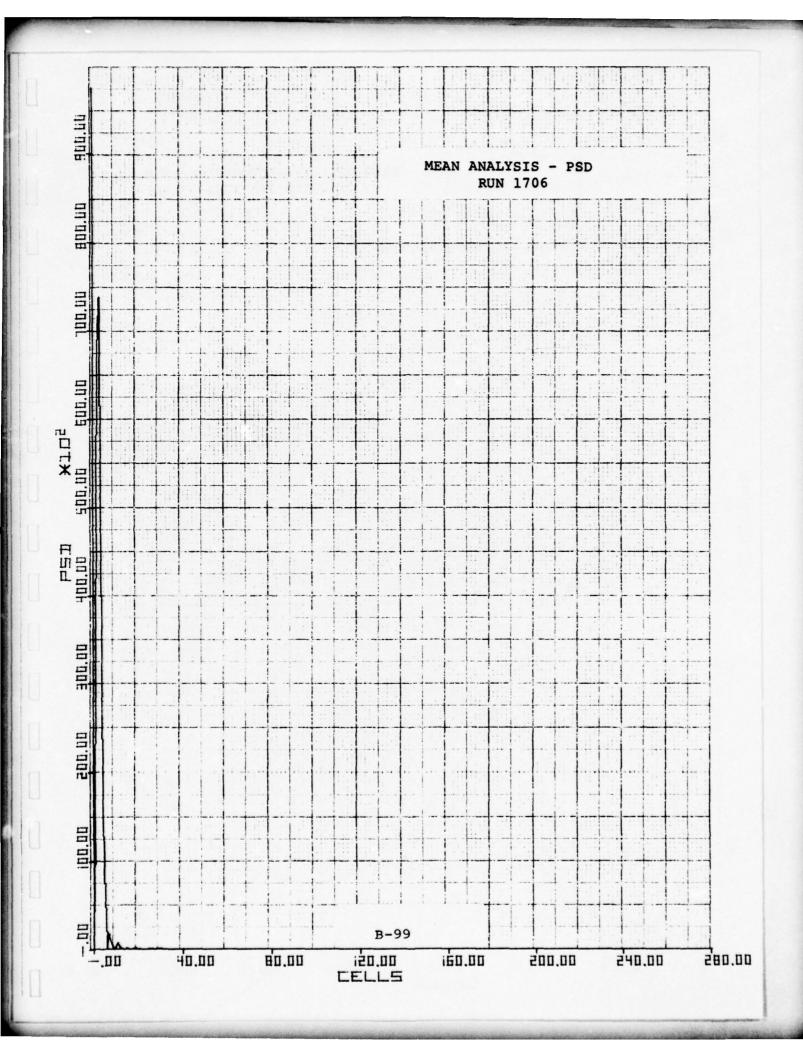


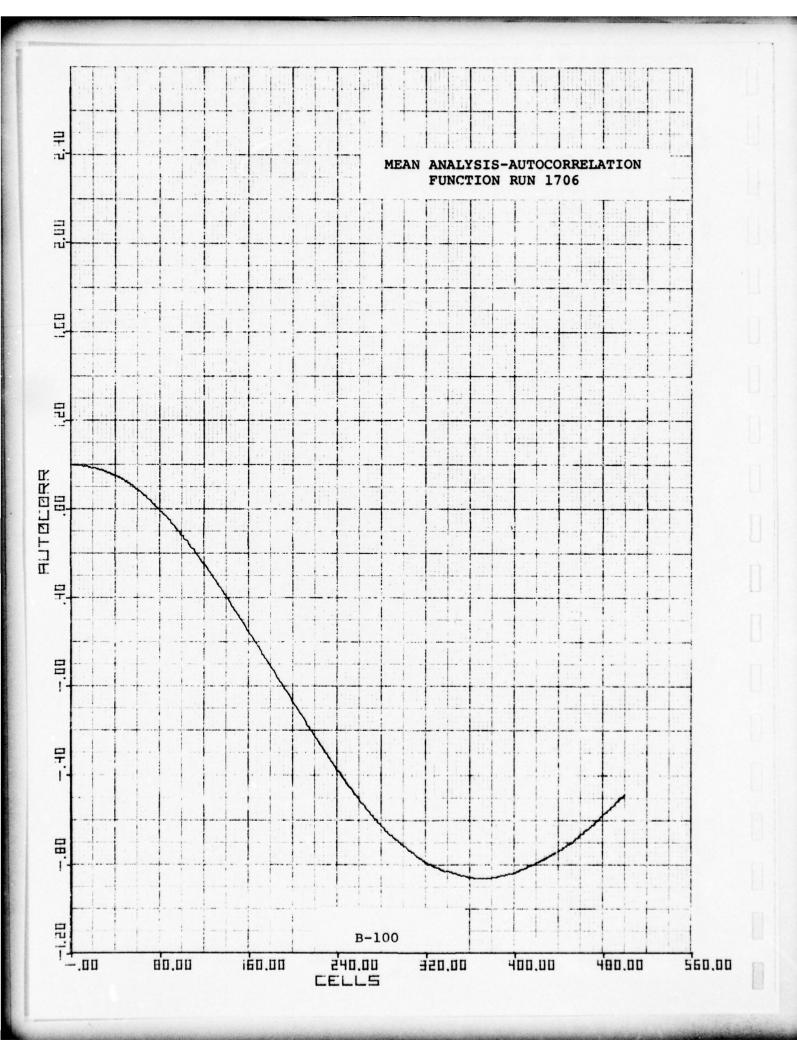


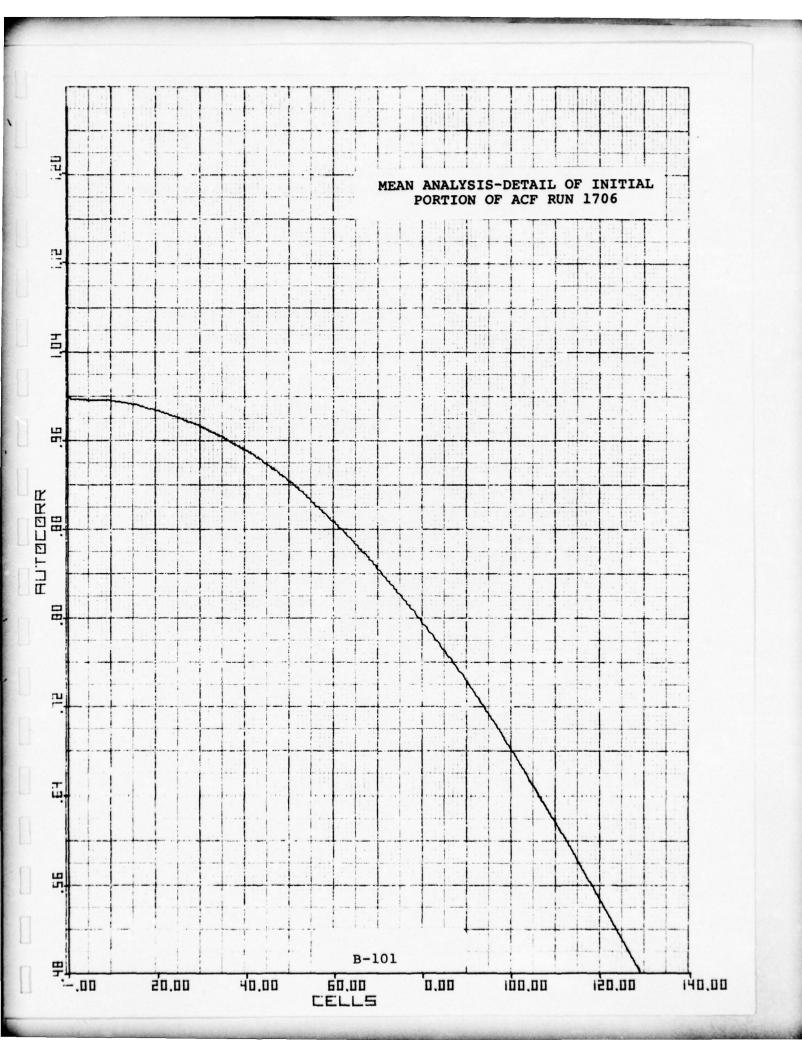












1.4 Variability of Selected Statistics

Selected statistics of mean normalized histograms were analyzed for variability.

The variance of the median, 10^{-1} , 10^{-2} , 10^{-3} and 10^{-4} points were computed. Both the mean value and the variance, organized by flight and run, are listed in Tables B-3 through B-9.

Before using this data in further analysis one should check hit maps, hits vs. time, the distribution function and scenarios to ensure that only valid and comparable data is being analyzed. For example:

- Horizontal polarization runs 7 and 17 show considerably more variability tham most vertical polarization runs.
- 2. The very high variability of the 10⁻⁴ point versus its value on 812 is worth noting. 812 was the run containing the light ship and as such describes its characteriztics rather than that of the sea.
- 3. Two run 403's are shown, 403(-1) has range gate 1 deleted. Range gate 1 is included in 403(All).
 Run 403 had data reduction errors in range gate 1.

UNCLASSIFIED

TABLE B-3
VARIABILITY OF SELECTED STATISTICS

		RUN 401	403 (-1)	402 (A11)	602	603	604
MEDIAN	M M2	.64581F+00 .41965E+00 .25789E-02	. 63095£ + 00 . 39893F + 00 . 83055E = 03	.65300F+00 .44625F+00	.62378E+00 .38959E+00	.62789F+0n .395n5F+0n .79659F-03	.64588F+0n .41749F+Un .33249F+Un
10_1	M M M	.22773F+01 .51936F+01 .74009E=0>	.22798F+01 .5198SE+01	.22481F+01 .5087FF+01	.22931E+01 .52589E+01 .73553F-03	.22744F+01 .51749F+01 .10314F-02	.52861F+01 .52269F+01 .52646F-03
10-2	M 2 0 2	.48380F+01 .23555E+02 .14945F+00	.49038F+01 .24082F+09 .34386F-01	.49661F+01 .2519AF+02 .5354AF+00	.5n544E+01 .25562F+02 .15306E=01	.48784F+01 .23816F+02 .16858F-01	. 48304401 . 833445401
10-3	M2 M2	.7636nE+01 .5987nE+02 .15623E+01	.78592E+01 .62158F+02 .39122E+00	.81019F+01 .70259F+02 .46190F+01	.82751F+01 .68657E+02 .17974E+00	.78034F+01 .61072F+02 .17954F+00	.74053F+01 .57943F+09
10-4	9 X Z	.11221F+02 +14559F+03 -19636E+02	.11585F+02 -13889E+03 -4684E+01	.12131F+02 .16993F+03	.12406E+02 .15530E+03	.11545F+0> *13621F+03 *29173F+01	-11010F+02 -12270F+03

TABLE B-4
VARIABILITY OF SELECTED STATISTICS (cont'd)

		RUN 605	909	607	809	609	701
MEDIAN	o w w	.61829F+0n .38289F+0n .61146F=03	.63000F+00 .39731E+00 .41033F-03	.42097E+00 .42097E+00	.41314F+00 .2438nF-03	.62810F+Un .39492F+Un .42578F=03	. 554 RAF+6n . 320 N4F+6n . 95440F-63
10_1	0 M M	.2293nF+01 .52589F+01	.2297nF+01 .5276RF*01 .58031E-03	.23020E+01 .52998E+01	.23142F+01 .53561F*01 .38436E*03	.23081F+01 .53277F+01 .52679F-03	.23006F+U1 .52940F+U1
10-2	o M S	.50634F+01 .25657F+02 .19593E-01	.50245F+01 .25262F+02 .16647E-01	.49313E+01 .24329E+02 .11150E-01	.50397F+01 .25407E+02 .14245E-01	.51134F+01 .26164F+02 .17694F-01	.60810F+01 .37192F+02 .2135AF+00
10-3	o M M	.82631F+01 .68471F+02 .19166F+06	.81726F+01 .6706E*02	•78703E•01 •62081E•02 •13862E•00	.81313F+01 .66272F*02 .15397E+0n	.83949F+01 .707]1F+02 .2367AF+00	.11942F+02 .14629F+03
10-4	922	.12323F+0> +1542nF+03 -23391F+01	.12119F.02 .14926E.03	•11551E•02 •13525E•03 •16256E•01	.12011£+02 .14630£+03 .20415£+01	.12614F+09 .16161F+03 .2474nF+01	.21111F+02 -47311F403 .27424E+02

UNCLASSIFIED

TABLE B-5
VARIABILITY OF SELECTED STATISTICS (Cont'd)

708	.60313E+00 .36439E+00 .62710E=03	.22947£+01 .52665£+01 .84448£-03	.53079£+01 .28216£*02 .41544£*01	.91766E+01 .85055E+02 .84520E+00	.14723E.02 .22856E ⁺ 03 .11792E ⁺ 02
707	.60738E+00 .37315E+00	.23195E+01 .59889E+01 .87642E-02	•53455E•01 •28941E•02 •36649E•00	.91453E+01 .84763E+02 .21265E+01	•14499E+02 •22255E+03 •12332E+02
705	.56997E+00 .37867E+00 .38122E-02	.22927E+01 .52595E+01 .29528E-02	.57860E+01 .33789E+02 .31151E+00	.11011E+02 .17623E+03 .49936E+01	.18986E+02 .39619E+03
704	.59348F+00 .35251E+00	.22913E+01 .52511E+01 .86891E-03	.55881E+01 .31356E+02 .12920E+00	.10254E+02 .1c725E+03 .21135E+01	.17212E+02 .31417F+03
703	.55207E+00 .30573E+00 .94119E=03	.22632E+01 .51242E+01 .22071E-02	.60922E+01 .37372E+02 .25755E+00	.12455E+02 .16124E+03 .61171E+01	.23064E+02 .58853E+03 .56602E+02
RUN 702	.55399F+Un .30948F+0n .25731F=02	.22413F+01 .50274F+01 .42201F-02	.60907F+01 .37671F+U2 .57418F+00	.13134F+02 .18613F+03 .13580F+02	.23972F+02 .64949F+03 .74842F+02
	M M Z	M M2 g2	M2 q2	M M2 o2	27 0 W W
	MEDIAN	10_1	10-2	10_3	10_4

STATISTICS (Cont'd)

OF SELECTED

VARIABILITY

TABLE B-6

.43000E+00 .22214E+02 .65551F+0A ·64037E-02 .55702F+02 .84677E+00 .48851F-03 .74064F+01 .11014F+02 .14624F+03 .24933F+02 .52070E+01 .47125F+01 .22818F+01 812 .10981F+02 .12214F+03 .41192F*00 .55822F+02 .15720E+01 .64139F+0n .52950F-03 .70069E-03 .22441F+02 .58000E-02 .10270E+0n .51607E*01 .22716F+01 .74648F+01 .47364E+01 810 .64470F+00 .41617E+00 .53193F-03 .47153E+01 . C2242E+02 -78838E-02 .5378E+01 .1 482F+UC .111UAF+03 .12038E+U1 .84580E-03 .51490F+01 .89923E-01 .22690E+01 805 .23458E+02 .58424F+02 .75997E+01 .94316F-03 .44339E+01 .91406F-01 •64803F+00 -12344F+03 .64028E+00 .41109E+00 -11297F-02 .51896F+U1 .1 982E+02 · < 8289£+01 • 22779E • 01 802 .23184F+02 .64624F+0n .41802F*0n .81123E-02 .10865F+02 .11934F+03 .37329E-03 .52113F-03 .48141F+01 .2285aF+01 ·52254F*01 .12833F+01 .57027F+02 .10212F+00 .75449F+U1 801 .15418E+02 .24888E+03 .34175E+00 .11068E-02 .51863E+01 .14295F-02 ·28853E+02 .96860F+02 .11173E+02 .58365E+00 .22770E+01 .53675E+01 .42778E-01 .94799F+01 .99124F+00 709 RUN 27 OW W SE D O WE SES SES M2M 10-2 10-3 10-1 10-4 MEDIAN

TABLE B-7
VARIABILITY OF SELECTED STATISTICS (Cont'd)

1601	.41814E+00 .30961E-03	. \$2428E+01 . \$7024E+03	.48404E+01 -23439E+02 -94984E-02	.75965E+01 .57818E+02 .11066E+00	.10978F.02 .12189E.03
1109	. 40006E+00 38324E-02	.22736E+01 .51719E+01 .27869E=02	.23300E+01 .68246E+07	.75572F+01 .57621E+02 .51022E+00	.10757E+02 .11825E+03
1108	.47147F+0n .47147F+0n .48550F-03	.59012F+01 .6756F-03	.27612F+U1 .22684F+U2 .15794F-U1	.74336F+01 .55436F+02 .17787F+05	.10721E+02 .11705E+03
1107	.65195E+00 .42540E+00 .3a704F=03	.52872E+01 .5237E+01 .26295F-03	.48607F+01 -23 E7E+02 -22 E12F-01	./s:87F+61 .55562F+02 .!4171E+00	.1 (135+02 .15341+04 .15755+03
1105	.47867E+00 .47867E+00 .59300E-03	.57749E+01 .51734F+01	.23534F+02 .33963E=01	.77578£.01 .60698£.02 .51505£-00	.11688F+02 .14460E+03
RUN 1104	.41878F+01 .41878F+01 .52057F-03	.51974F+01 .51974F+01 .85964F-03	.4766E+01 .2741E+02	.741935+61 .552315+62 .185185+00	. 1755er+02 . 1733fr+02
	0 Z Z	0 M M	0 Z Z	G M Z	0 Z Z
	MEDIAN	10_1	10-2	10-3	10-4

TABLE B-8
VARIABILITY OF SELECTED STATISTICS (Cont'd)

		RUN 1602	1603	1604	1605	1606	1607
MEDIAN	OZZ OZZ	.63327E+00 .40157E+00 .53613E-03	.65184F+00 .42528E+00 .35660E=03	.40183E.00 .40050E.00	.61014F+0ñ .38403F+0ñ .11765E-0ī	.64281E+00 .41359E+00 .38907E=03	.40938E+00 .40937E+00
10_1	M 2 0 2	-22794E+01 -51963E+01 -68514E-03	.528122.01 .520452.01 .599662.03	*22894E+01 *52422E*01 *10011E*02	.22011F+01 .49798F*01 .13511E+00	.22891E+01 .52406E+01	.23060g+0] .5318g+0] .46896g-03
10-2	0 M M M M M M M M M M M M M M M M M M M	.49215E+01 .24236E+02 .15046E-01	.47706E-01 .22768E-02 .90155E-02	.49190E+01 .24220E+02 .23356E=01	.56351F+01 .51418F+02 .19661F+02	.48704E+01 .23733E+02 .12330E=01	.49875E+01 .24892E+02 .16811E+91
10-3	0 Z Z	.79668E.01 .63678E.02 .20791E.00	.742592+01 .558482+02 .103562+00	.78358E+01 .61958E+02 .55522E+00	.84090F+01 .89684F+02 .18973E+02	.77524E+01 .60279E+02 .17887E+00	.79890E-01 .64029E-02
10-4	M M G M S	.11939E+02 .14531E+03 .27569E+01	.19696F+0> -11592F+03 .15049E+01	.11396E+02 .13480E+03 .49212E+01	.1175gE+0> .15689F+03 .18724F+0>	.11430E+02 .13318E+03 .25259E+01	.11732F+02 .13964E+03

UNCLASSIFIED

.29247£*02 .29188E=01 . 39533E+00 .16276E+03 .52470E+01 .52470E+01 .68302E-02 457972.00 .12553F+02 .82368g+01 1708 .36920E+00 52285F.01 .28913E+02 .2786AF+03 .19830F*02 .60703F+0n .95122F+02 .16089F+0> .22864F+01 .96498F+01 ·20032E*01 .53679F+01 .52833F+01 .22984E+01 .65265F+02 .8n667E+01 RUN 1609 .63617F+00 .40514E+00 .43145F-03 .24917F+02 .14661E-01 .12042E+02 ·14769E+03 .24855F+01 .49902E+01 0 ZZ M2 0 SES B MW NO O W W X 10-3 10-2 10-1 10-4 MEDIAN

OF SELECTED STATISTICS (Cont'd)

TABLE B-9

VARIABILITY

1.5 Hit Map of Run 812 - Nantucket Light Ship Target Validation Flight 812 was a special test in which a known target was present in the sea clutter data. The target was a light ship off the eastern coast of Massachusetts positioned off Nantucket Island.

A special Hit Map computer run was executed to validate the synthetic aperture mapping process. The threshold was set at 500 -- well above the clutter level so that target returns from the ship could be easily distinguished. The flight was run at 500 feet altitude.

Hits exceeding threshold for the target were dumped from a computer run. The results are plotted in Figure B-48. Range gate number, doppler filter number and FFT time frame for hits exceeding threshold were plotted to show the range-doppler time history. The target, initially observed in range gate 5 and at the highest doppler filter (51), passed through four range gates, and all 32 doppler filters at essentially a linear rate in about 770 FFT frames, or 7.04 seconds.

If the doppler rate is assumed linear, velocity of the aircraft with respect to the target may be estimated. This information is required for motion compensation.

Doppler frequency is related to velocity and look angle by

$$f_d = \frac{2V}{\lambda} \cos \theta$$

where λ is radar wavelength (0.1 feet). Flight test geometry is indicated in Figure B-49.

Doppler rate is computed by differentiation of doppler frequency with respect to time:

$$\frac{df_d}{dt} = \frac{2}{\lambda} \frac{dv}{dt} \cos \theta - V \sin \theta \frac{d\theta}{dt}.$$

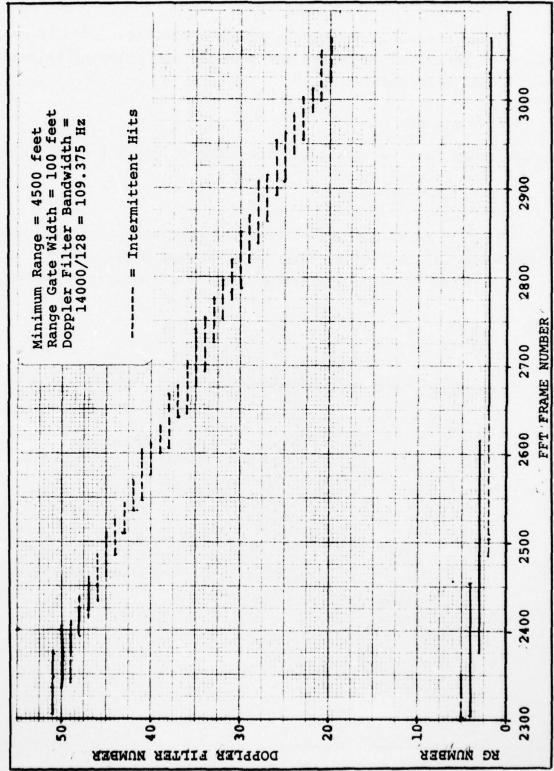


Figure B-48 TAGSEA 0812 Light Ship-Range Doppler Time History

UNCLASSIFIED

If aircraft velocity is constant the first term is small and will be neglected. From the geometry the velocity is related to angular rate $(d\theta/dt)$ by

$$V = R \frac{d\theta}{dt}$$
.

Solving the last two equations for velocity gives a simple result

$$V = \frac{-\lambda R (df_d/dt)}{2 \sin \theta}$$

From range-doppler history the doppler rate is estimated from number of doppler filters (32), doppler bandwidth (14000/ $128 = 109.375 \, Hz$) and observation time noted earlier (7.04 seconds).

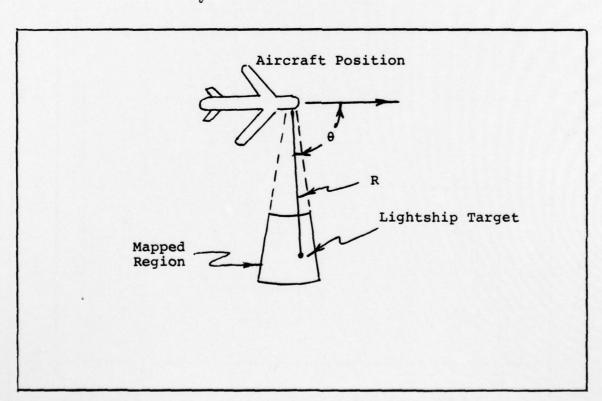


Figure B-49 Flight Test Geometry (Plan View)

$$\frac{df_d}{dt} = \frac{32 \times 109.375}{7.04} = -497.16 \text{ Hz/seconds.}$$

If nominal range (R = 4850 ft) and angle (θ = 90°) are assumed the velocity for the X-Band radar (λ = 0.1 ft) is computed as

$$V = \frac{-0.1 \times 4850 \times (-497.16)}{2 \sin (90^{\circ})} = 374 \text{ ft/sec.}$$

The velocity estimate was used to generate the hit map printouts in Figure B-50. In the upper map hits exceeding the threshold are plotted in each range gate vs. down-range distance. The lower map shows hits mapped into a cross-range vs. down-range coordinate system quantized to 100 foot cells. The range gate sum (when totaled) add up to 1215 hits exceeding threshold during observation of the Lightship Target.

1.5.1 Lightship Conditional Probability Maps

A complete set of conditional probability maps was generated for Flight 8 Run 12. Contour plots exist for all cuts in time, range and doppler through the conditional probability cube. A time collapsed array and normalization array were plotted as well. These plots validate the conditional probability mapping process against the range-doppler-time history plotted in Figure B-48.

The conditional probability time cuts in Figures B-51 through B-58 show the Lightship Target is extended from minus seven to zero FFT time frames (one FFT frame = 0.0091428571 sec). The range-doppler history indicates the target is well extended over several FFT time frames in each range-doppler cell. The conditional probability map cut at relative time = 0. (Figure B-58) shows doppler extent is a little greater than range extent for the Lightship Target. The result is in

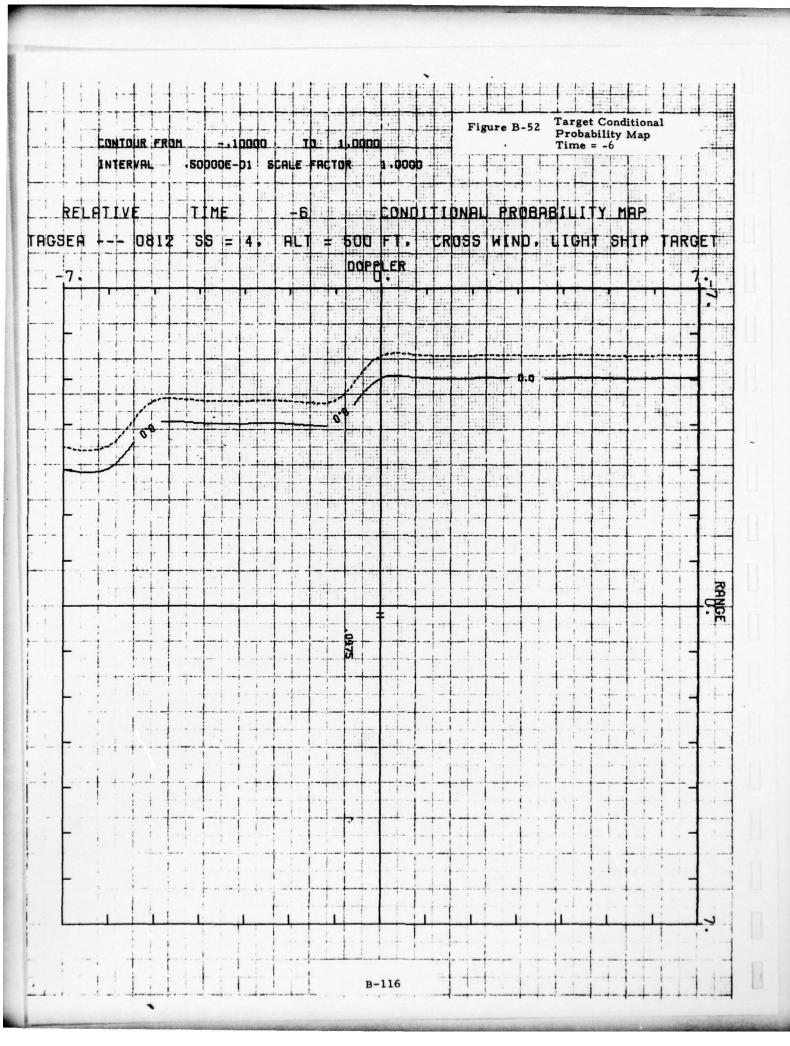
	Range Gate vs. Down-range (R-X Option)	Cross-Range vs. Down-Range (X-Y Option)
RANGE GATE SUM	0 0 0 0 0 0 0 0 0 0 0 0 0 0 0 0 0 0 0	RANGE GATE GATE SUM 0 0 0 0 0 0 0 0 0 0 0 0 0 0 0 0 0 0 0
٠	00000000	0000000
ın	000444000	w 0000000
-	0000 117 117 0000	PERT PERT 0 0 0 0 0 0 0 0 0
NUMBER 3	0001884	100's 3 3 3 2 2 2 3 3 3 2 2 2 9 9 9 9 9 9 9 9
RANGE GATE NUMBER 2 3	0000 74 76 76 76 76 76 76 76 76 76 76 76 76 76	REL. CROSS RANGE, 100's OF FERT 2 3 0 0 0 0 0 0 11 13 15 302 7 188 302 7 0 0 0 0 0 0 0 0 0 0 0 0 0 0 0 0 0 0 0
н	00000000	11 00 00 00 00 00 00 00 00 00 00 00 00 0
۰	00000000	00000000
DOWN RANGE (FEET)	8300.00 8500.00 8500.00 8700.00 8700.00 8900.00	DOWN RANGE (FEET) 8300.00 8400.00 8500.00 8600.00 8800.00 9000.00

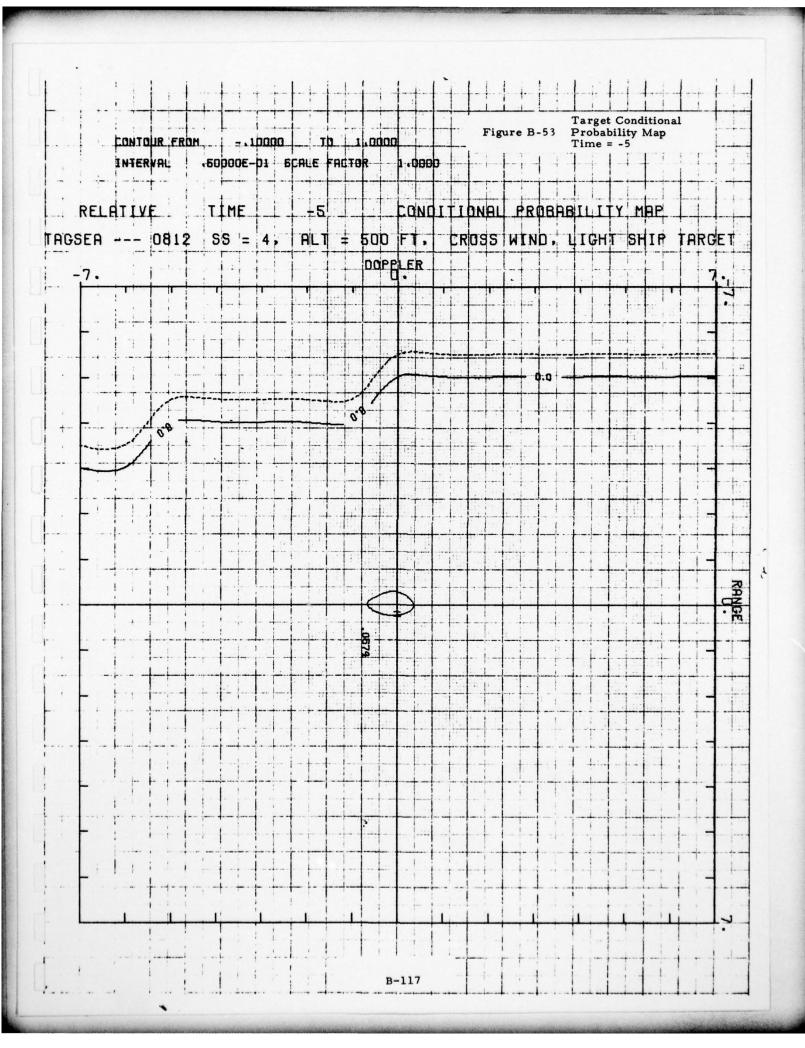
		Cross-Range vs.	Down-Dange	Series in the control of the control	(x-x obtion)					
	0	0	0	29	604	563	19	•	•	
	0	0	0	•	0	0	0	0	•	
	0	٥	0	0	•	0	0	0	•	
	0	0	0	-	6	26	7	•	•	
	0	0	0	13	229	302	15	0	•	
7	0	0	0	11	300	188	٣	•	0	
7 .	٥٫	0	0	•	99	17	0	•	0	
•	0	0	0	0	0	0	0	0	0	

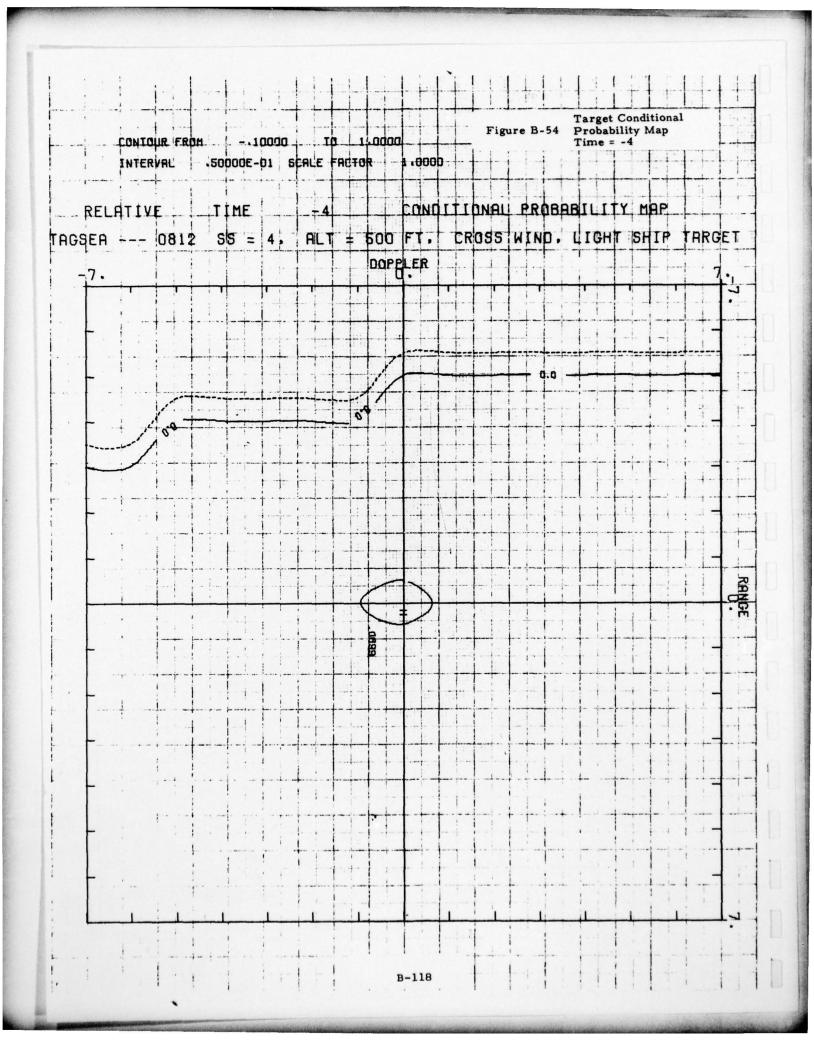
Numbers are hits above threshold (T = 500) V = 347 ft/sec $R_{MIN} = 4500$ ft

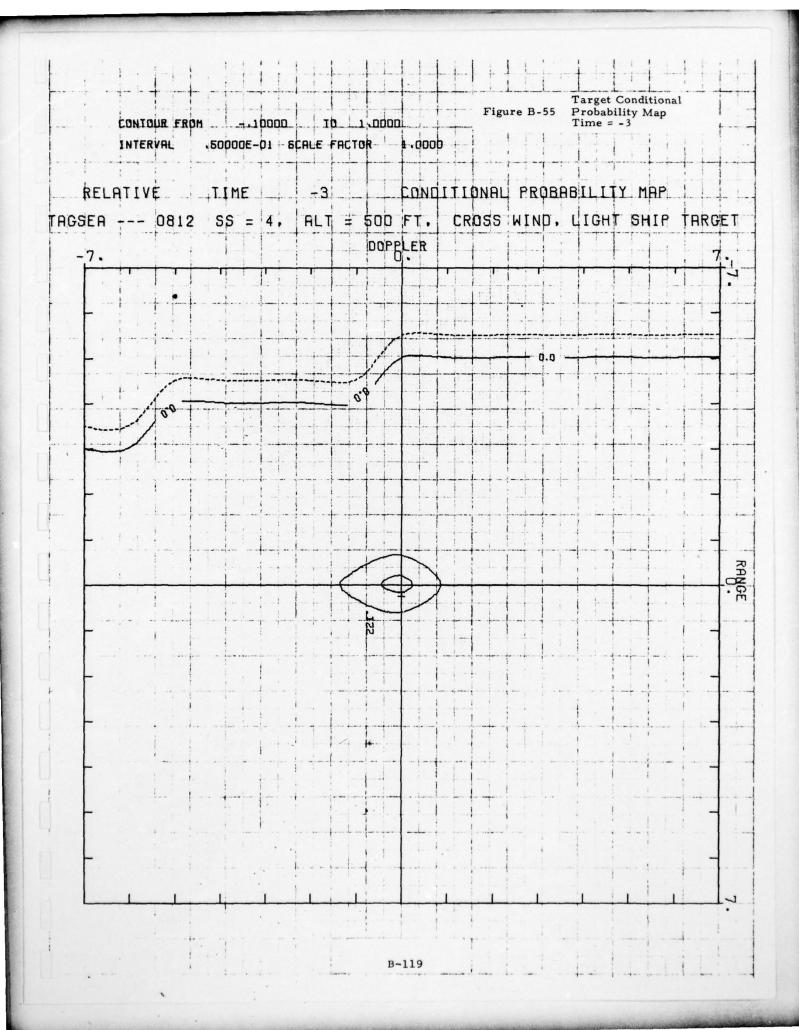
Figure B-50 Hit Maps for Flight 0812 Nantucket Lightship Target

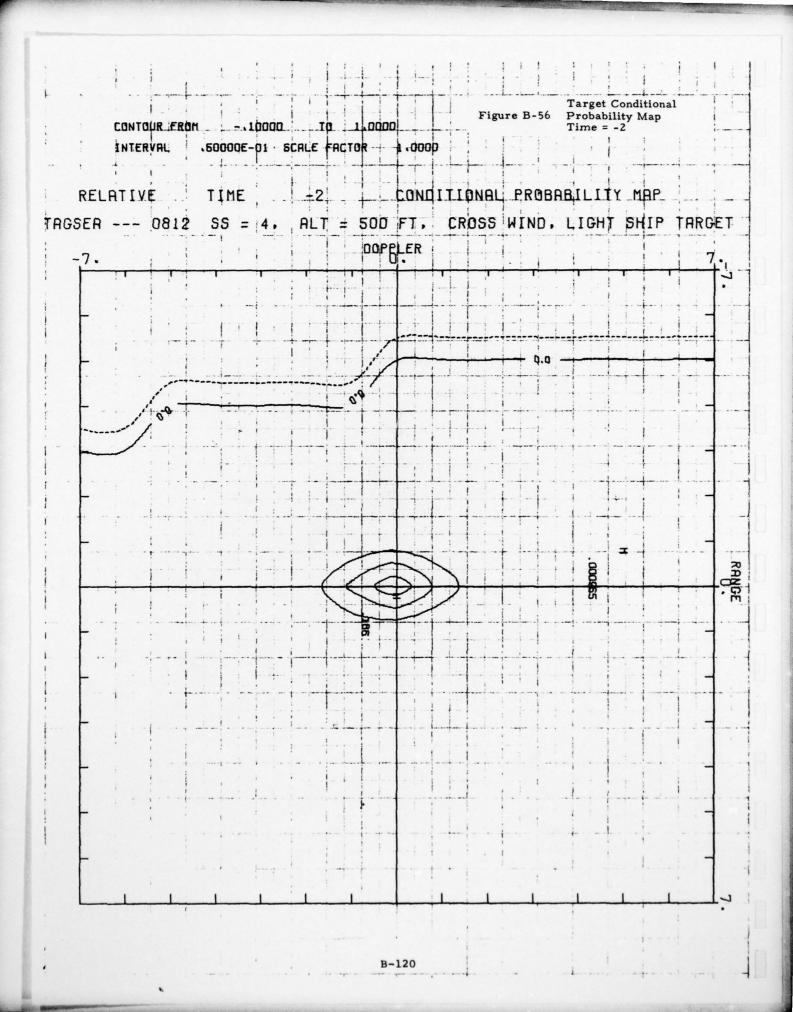
Target Conditional
Figure B-51 Probability Map
Time = -7 =.10000. SOPONE-PI SCALE FACTOR INTERVAL 1.0000 CONDITIONAL PROBABILITY MAP RELATIVE TIME TAGSER --- 0812 SS = 4. ALT = 500 FT. CROSS WIND, LIGHT SHIP TARGET DOPPLER B-115

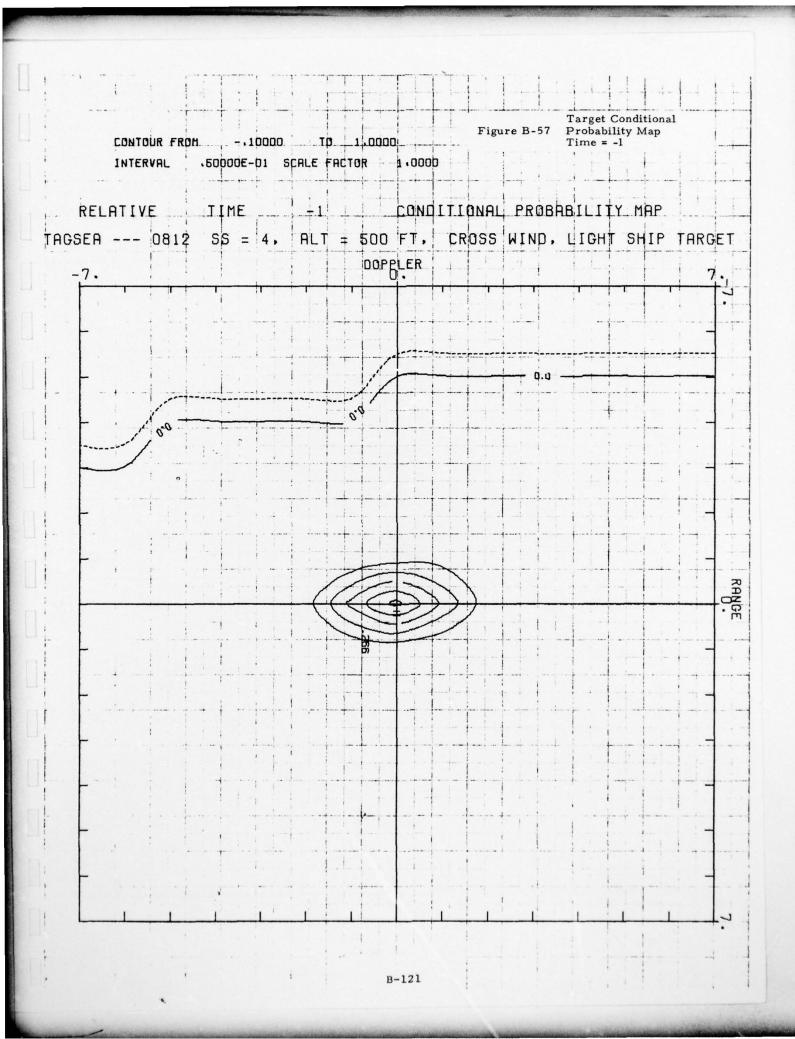


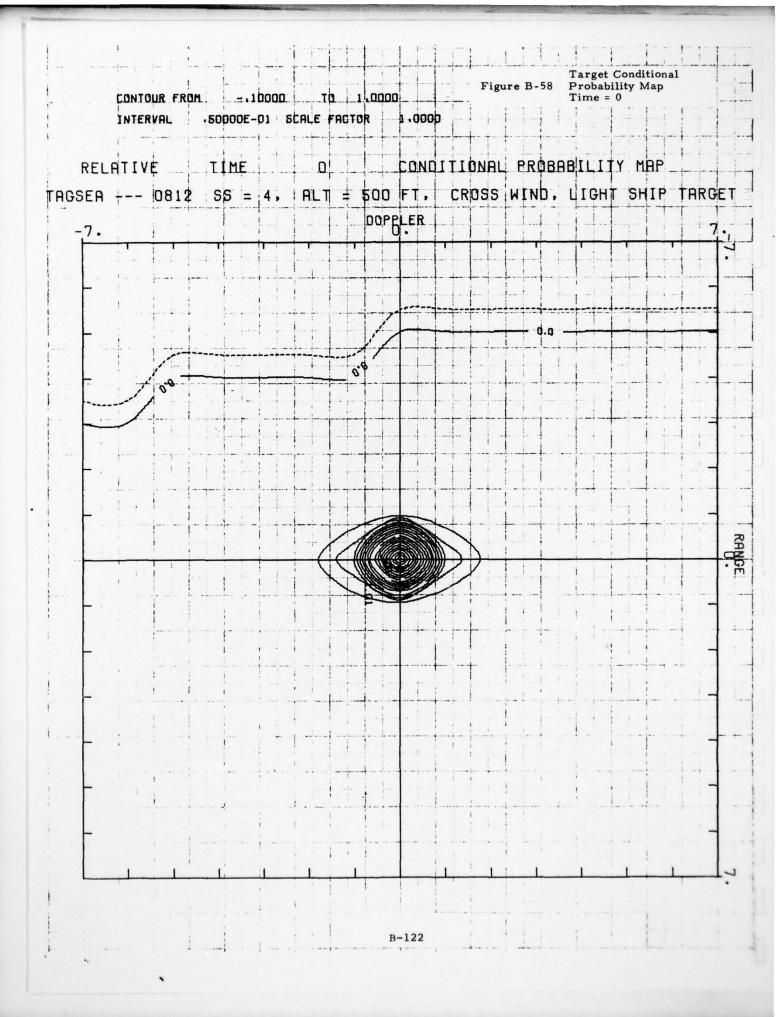












GENERAL DYNAMICS/POMONA CALIF POMONA DIV
TAGSEA PROGRAM. VOLUME III. SUPPORTIVE ANALYSES AND OUTPUTS. (U)
N00017-73-C-2244 AD-A036 973 F/G 17/9 UNCLASSIFIED NL 3 OF 4-



agreement with range-doppler history; in particular, hits exceed threshold in either one or two range gates and one to three doppler cells at any poly in time.

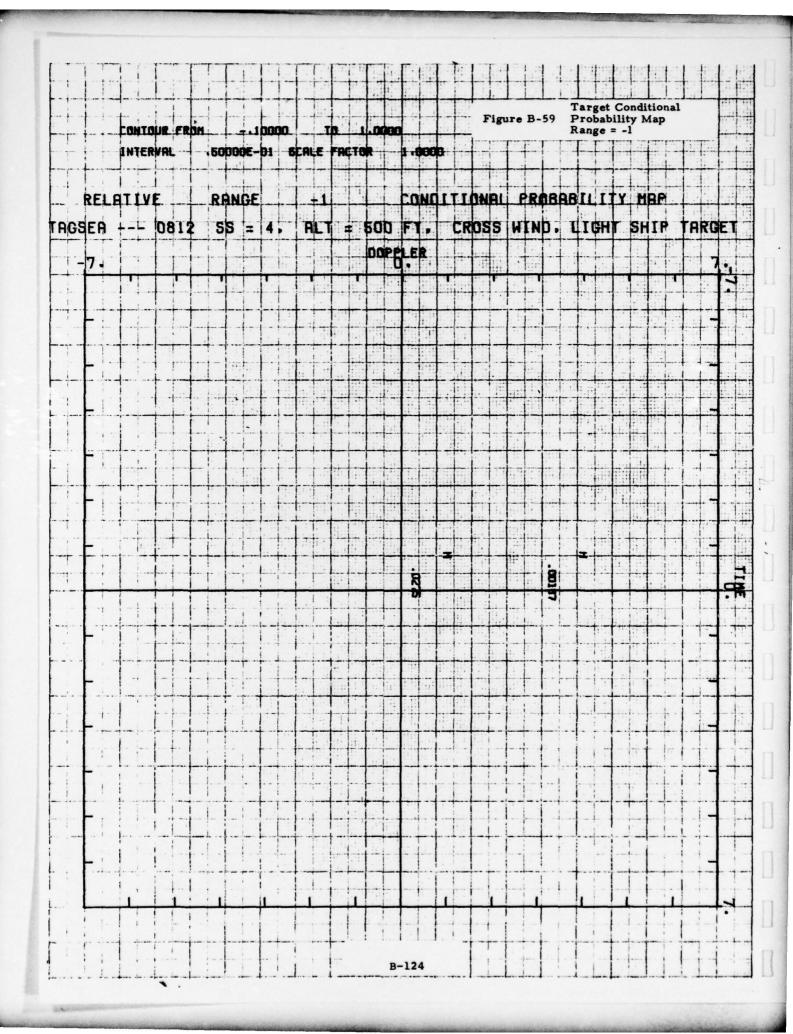
Figures B-59 to B-62 display conditional probability contour plots for relative range -1, 0, +1, +2. All other range cuts were void of data and have therefore been deleted. Very few points are indicated outside of the relative range = 0 cut; in fact, the number of hits was not enough to cause the first contour level to be exceeded. Cuts in doppler containing information are shown in Figures B-63 through B-65. Cuts at relative dopplers farther removed from the +1 points from relative doppler equal zero had very few hits. Only the three cuts shown had tiny probability contours (>0.05) which could be plotted.

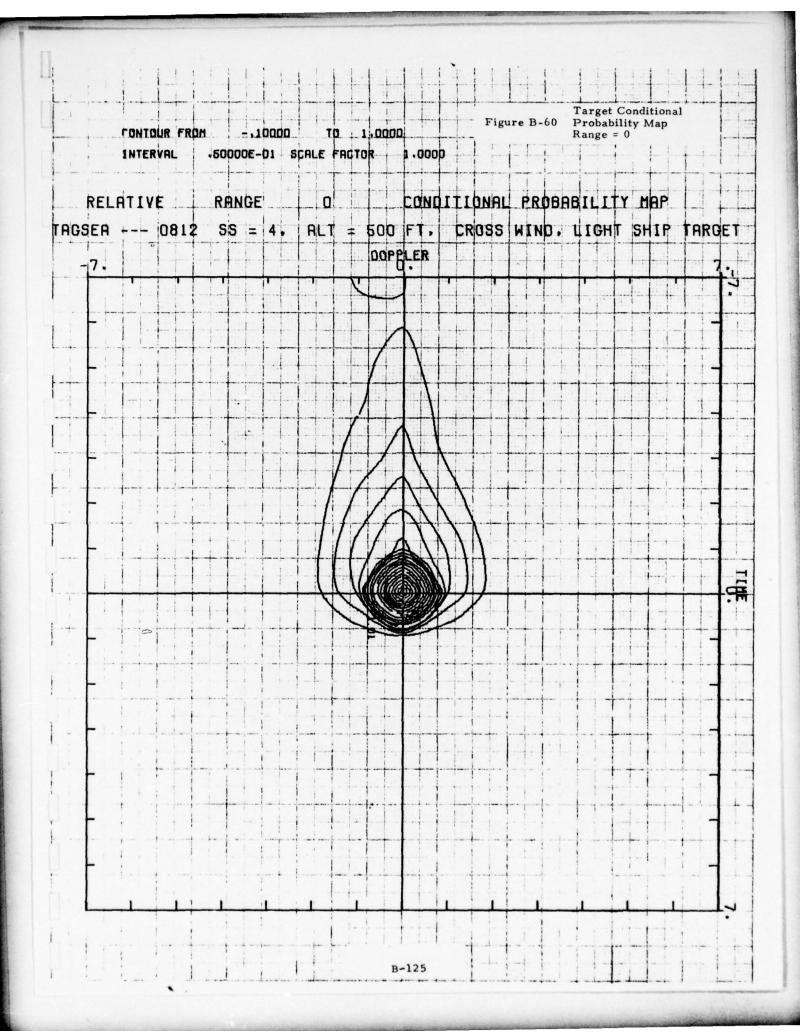
The time collapsed array in Figure B-66 shows the target is extended more in doppler than range. The range extent is never greater than two range gates. Total doppler extent is about three cells.

1.5.2 <u>Lightship Histograms</u>

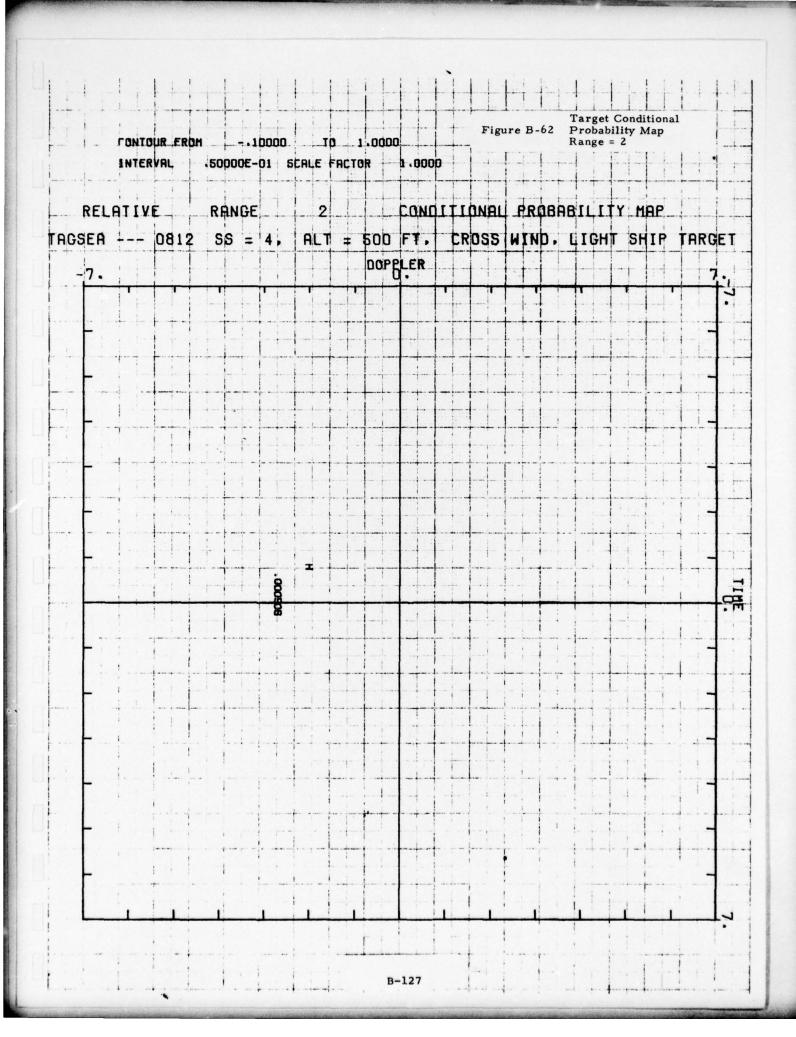
Absolute statistics data are plotted in Figures 6-67 and B-68. The first plot shows absolute amplitude in decibels plotted against range gate number. Results indicate saturation in range gates 2 - 5, in agreement with the range-doppler time history in Figure B-48. Saturation occured during an extended time period (4 histogram frames = 2400 FFT frames) in Figure B-48. The amplitude peak in histogram record frame five correlates well with time the lightship was known to be present. Frames 4 and 5 show the peak which corresponds to 2400 to 3000 FFT frames in Figure B-48.

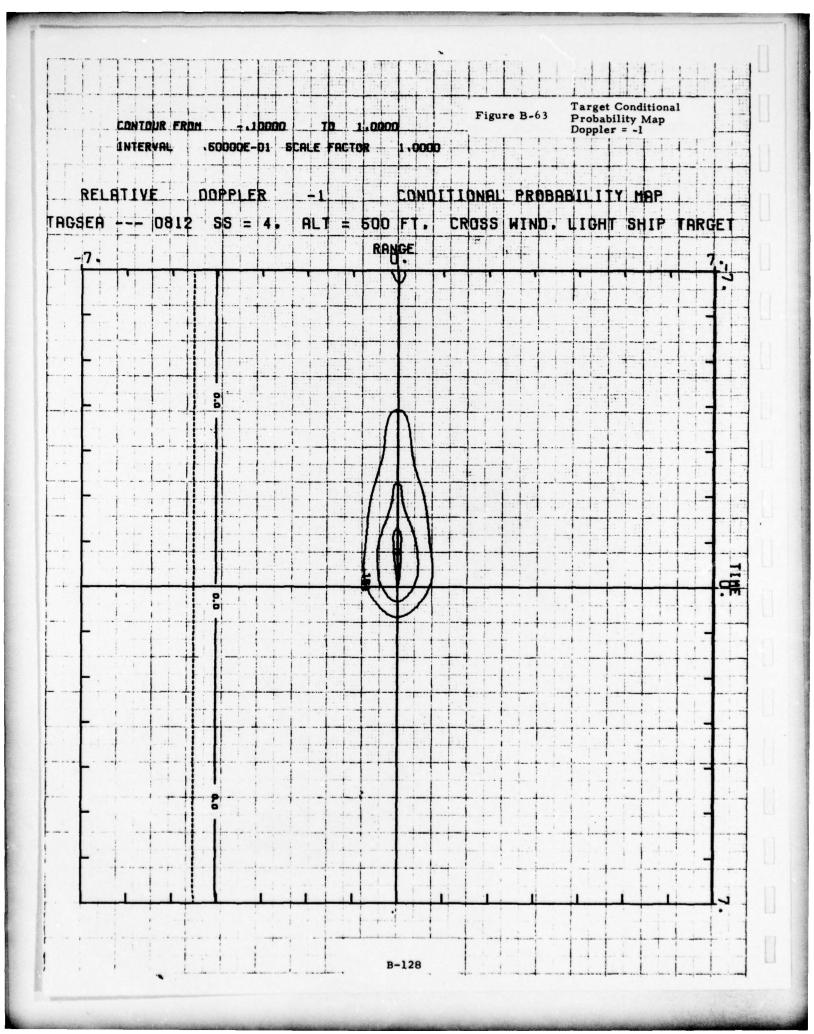
B-123 UNCLASSIFIED

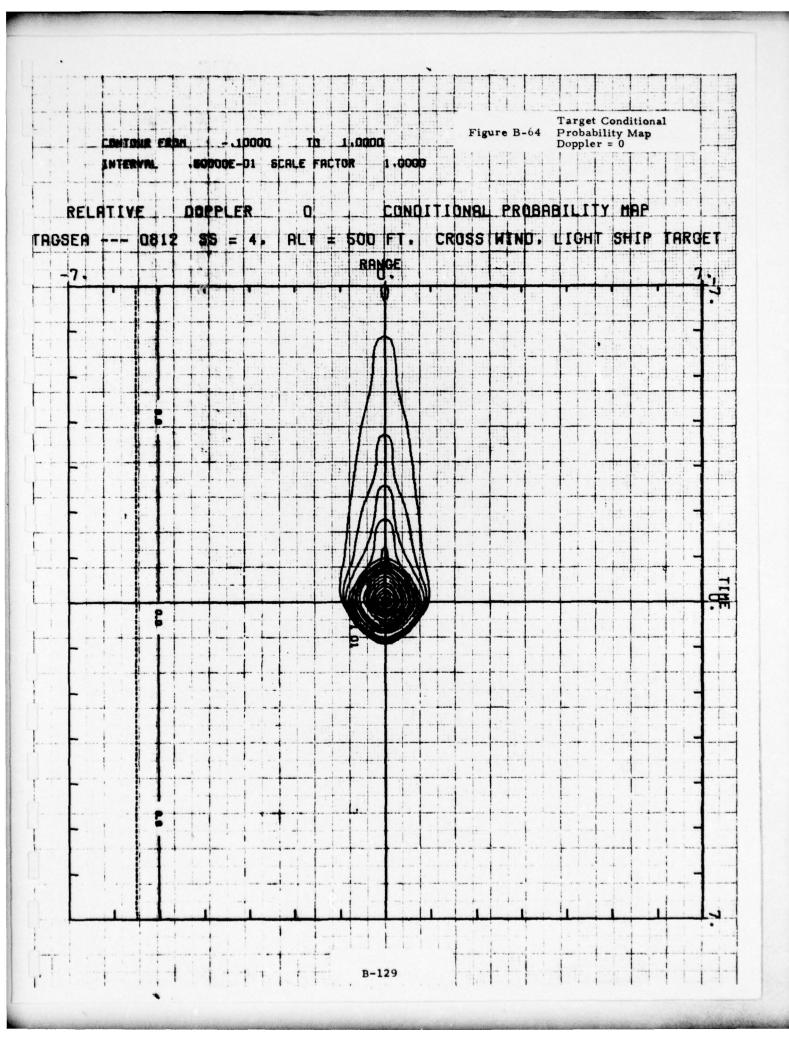


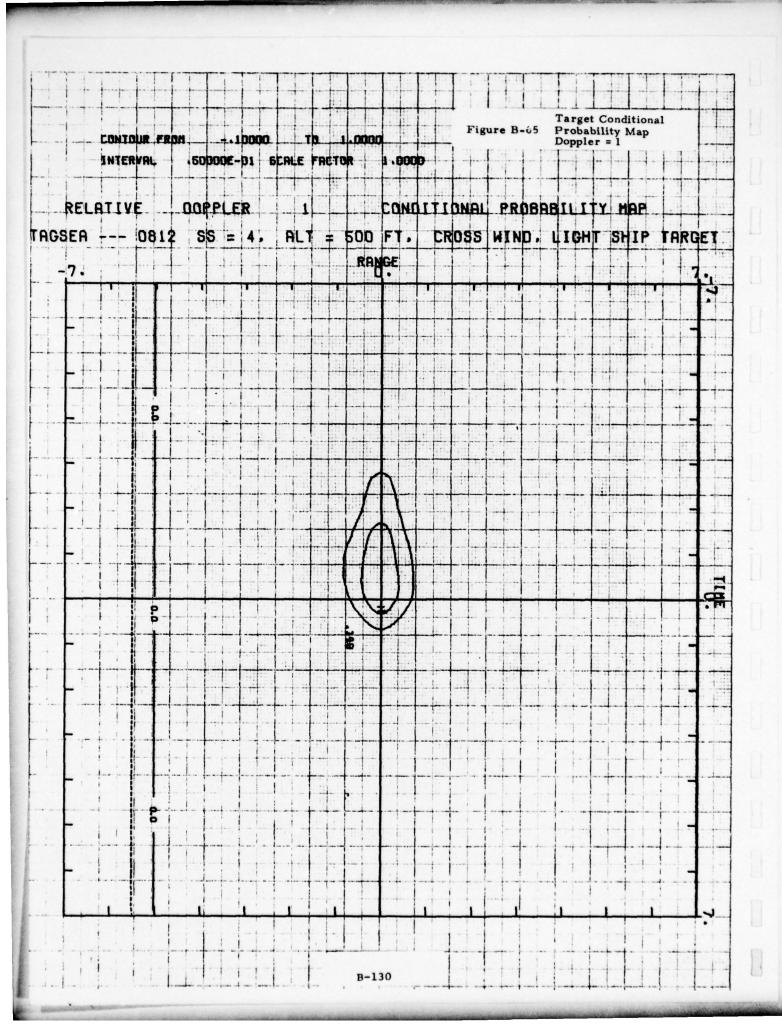


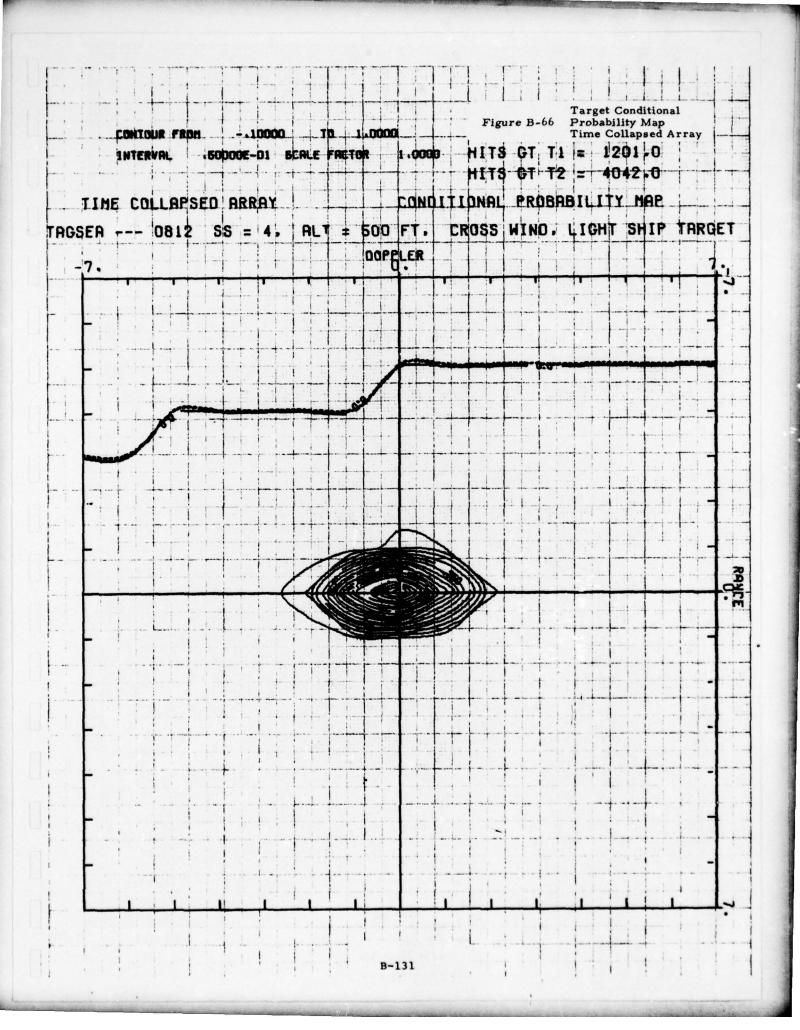
				Target Conditional	
CONTOUR FROM	10000	TD 1,0000	Figur	Target Conditional re B-61 Probability Map Range = 1	
INTERVAL	50000E-01 5	CALE FACTOR	1.0000		
RELATIVE	RANGE		CONDITIONS	PROBBBILITY MAP	
	SS = 4.				TARGET
		DOPE			THICK I
-7.	1 1			+++++++	++1:4-
-					4
F					
			+HHH		114
<u> </u>					1-1-1-
					1.18
					1.55
		i i i			+++
			+		
, -	44444				
	+			++++	
	1	1 1	4 1	1 1 1 1	7

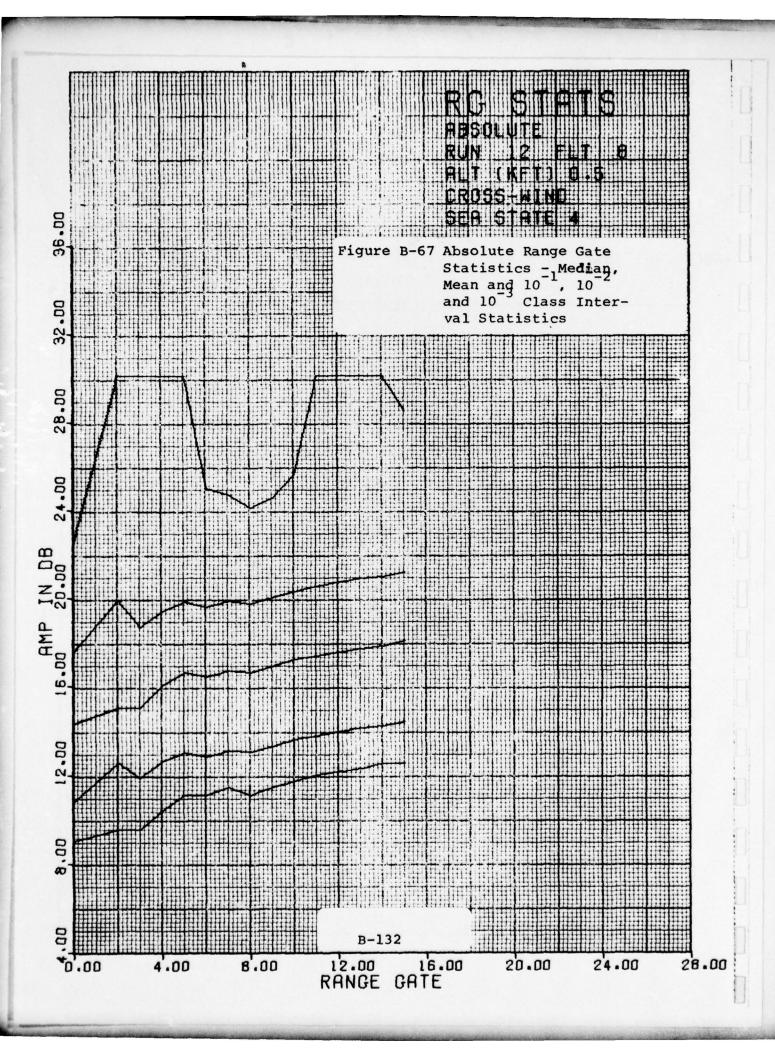


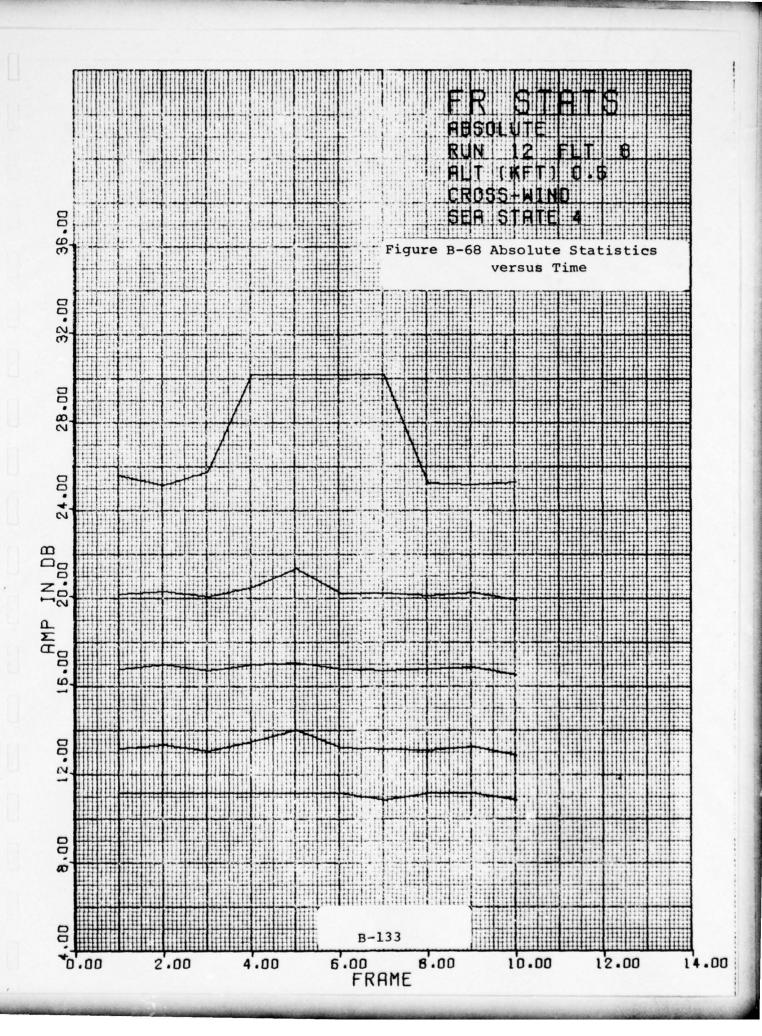












- 1.6 Characteristics in the Neighborhood of Large Returns
- Conditional probability maps presented elsewhere in this report give an overall picture of large hits and present information on returns in their immediate space-time vicinity.
 This section gives another view of the same phenomena.
 - 1.6.1 History of a Typical Large Sea Echo

The nature of a large echo when horizontal polarization is used is shown in Figure B-69. A bar graph of power versus time has been plotted for each doppler filter. Bars were used since the output was a series of values occurring as every FFT was completed. Only those values above the threshold (8m²) in range gate 3 are plotted. The patch of sea started ringing filter 34 first. Then, as the aircraft flew past the patch, the doppler shift was reduced as a consequence, causing the echo to pass through several filters in succession. (In the diagram an increasing doppler filter number corresponds to a decreasing doppler frequency.)

It can be seen that the output of each filter is fluctuating, rather than constant, and that during the time shown the probability of crossing the threshold is quite high compared with the rest of the hit map. In fact there are no returns above the threshold which are not on the main diagonal. This suggests that this series of large echoes come from a relatively stationary part of the sea where the mean cross-section was temporarily high and lasted for approximately 1.5 sec. The patch extended over three doppler cells at its maximum, implying an extent of one or two hundred feet.

More than one large response may be seen in some of the doppler filters (e.g. 39). This causes the conditional probability map to extend in time, causing the pattern seen in Figure B-70.

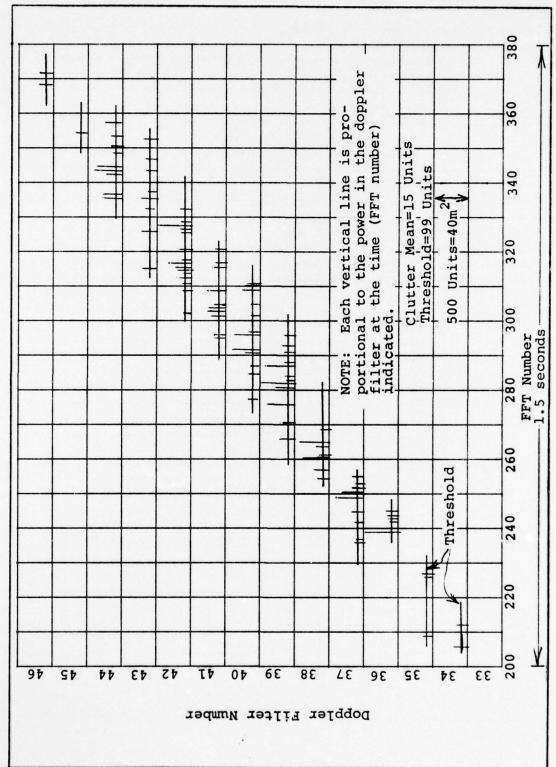


Figure B-69 History of a Typical Large Sea Echo

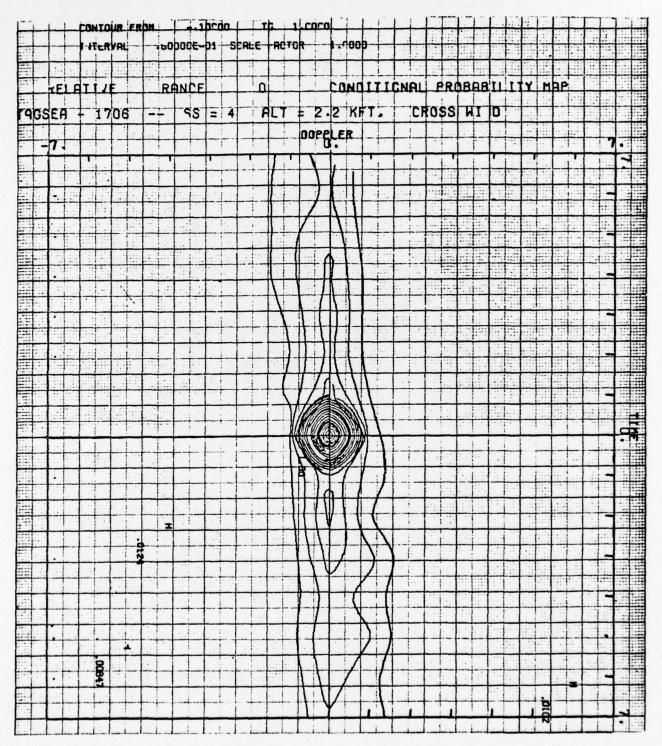


Figure B-70 Conditional Probability Map for R = 0

1.7 Unconditional vs. Conditional Probability Analysis
Detailed computer analysis performed on conditional
probability cubes indicates conditional probability of getting
a hit in the vicinity of a large hit is greater than unconditional
probability. This property is illustrated in the bar graph in
Figure B-71. This result is not unexpected - large clutter
returns generally occur in clumps and large returns have associated
relatively large returns in the immediate space-time vicinity.

Unconditional probability was computed from the ratio of total hits exceeding threshold (from the Hit Map printout) to total number of hits possible for the run (Histo records X 600 FFT frames/record X number of doppler filters X number of range gates).

Conditional probability was computed from the ratio of total hits to total trials within the conditional probability cube. The central cell in the cube was excluded from the calculation.

Conditional probability exceeded unconditional probability in all cases except 0801. The simulation results are included in the results at the bottom of the Figure B-71.

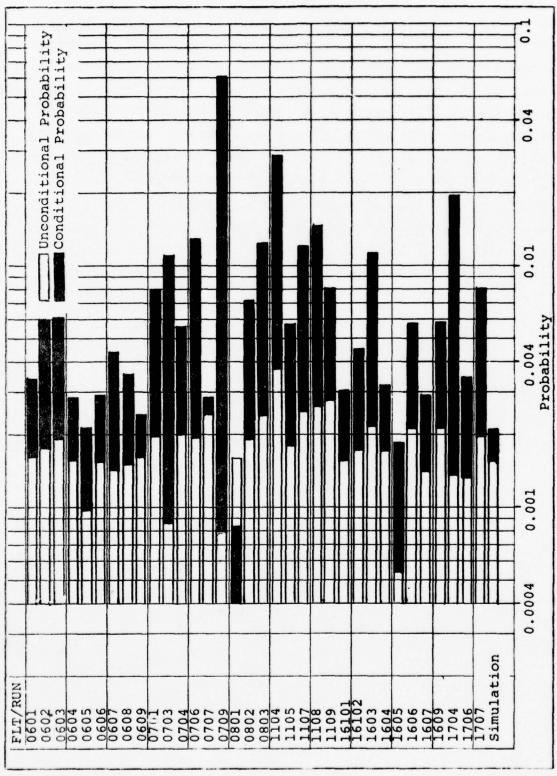


Figure B-71 Conditional and Unconditional Probability of Exceeding Threshold

UNCLASSIFIED

1.8 Locally Normalized Histograms

The histograms in this section are designated TOTAL N. They differ from the histograms in Volume IV in that they are locally normalized. Each clutter histogram transferred from data reduction is normalized by its mean before combining to obtain a total histogram.

N Histograms were obtained for both typical runs and for the runs with extreme tails in the A histograms.

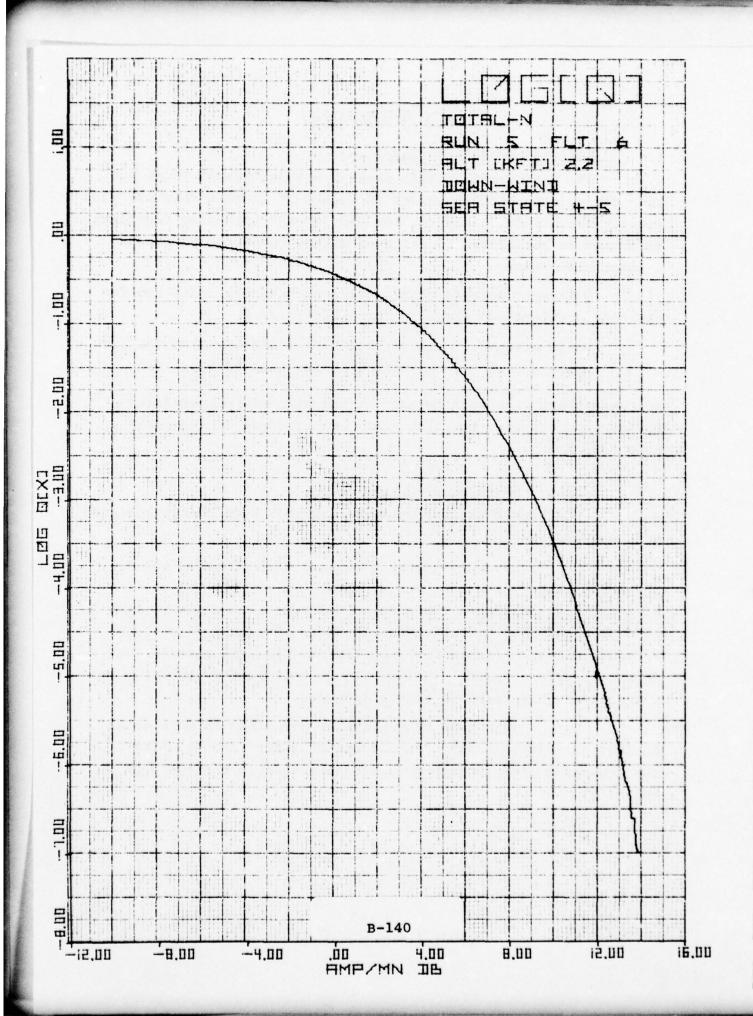
These histograms are defined mathematically as $TOTAL_{(N)} = \Sigma_{ij} H_{ij}$ where H_{ij} is H_{ij} normalized by the mean of H_{ij} . The histograms are displayed in each of the standard output forms. For each output form the histograms are arranged sequentially by flight and run.

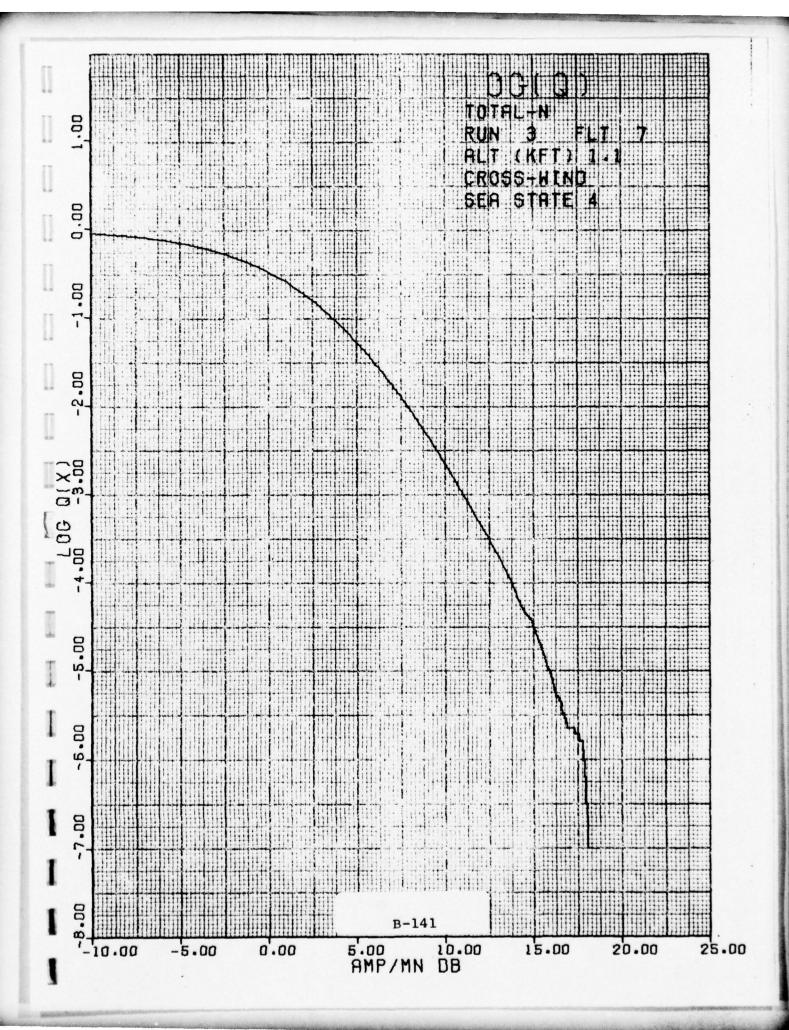
1.8.1 Histograms TOTAL N LOG Q

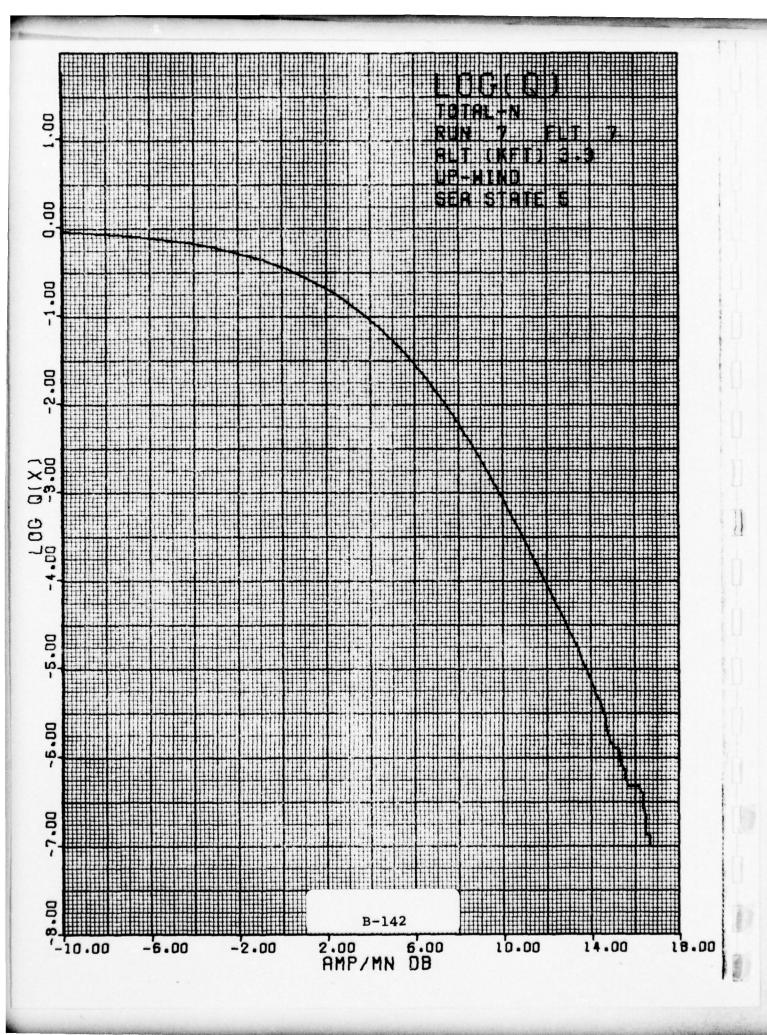
All valid clutter data within each run is included in the histogram.

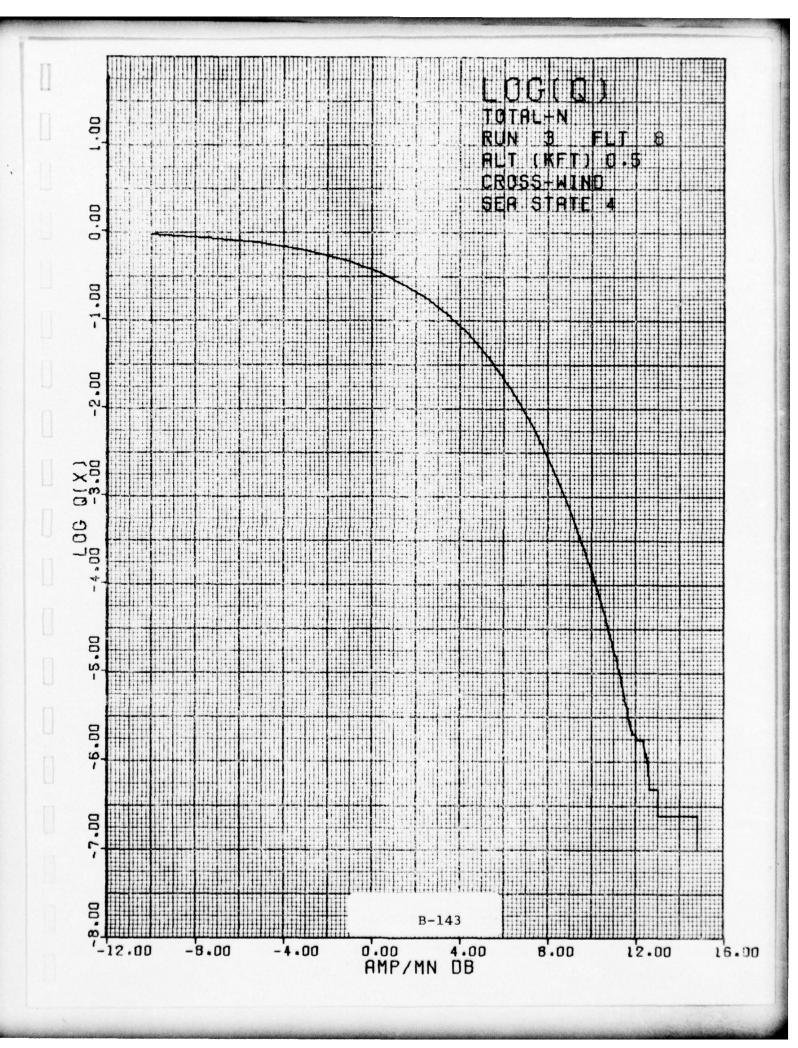
The N indicates that each of the histograms H_{ij} was normalized by its mean before combining to form the total histogram for the run. The vertical axis is the logarithm base 10 of 1 minus the cumulative probability, i.e., $LOG_{10}(1-P_{(x)})$. Various points on the tail of the distribution are clearly read from this type of plot. The horizontal axis is the clutter power per cell in dB referenced to the data mean.

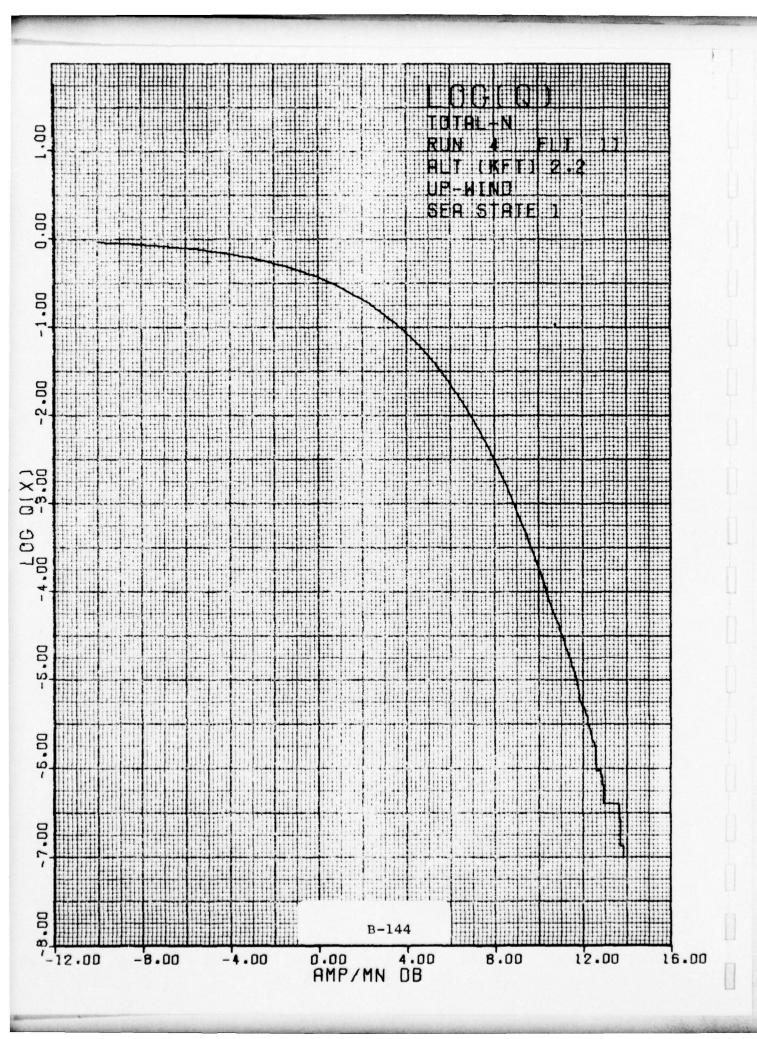
This type of outputs is described in more detail in Section 9 (Volume II). Procedures utilized in developing the histogram from the raw data are described in Section 8 of Volume II.

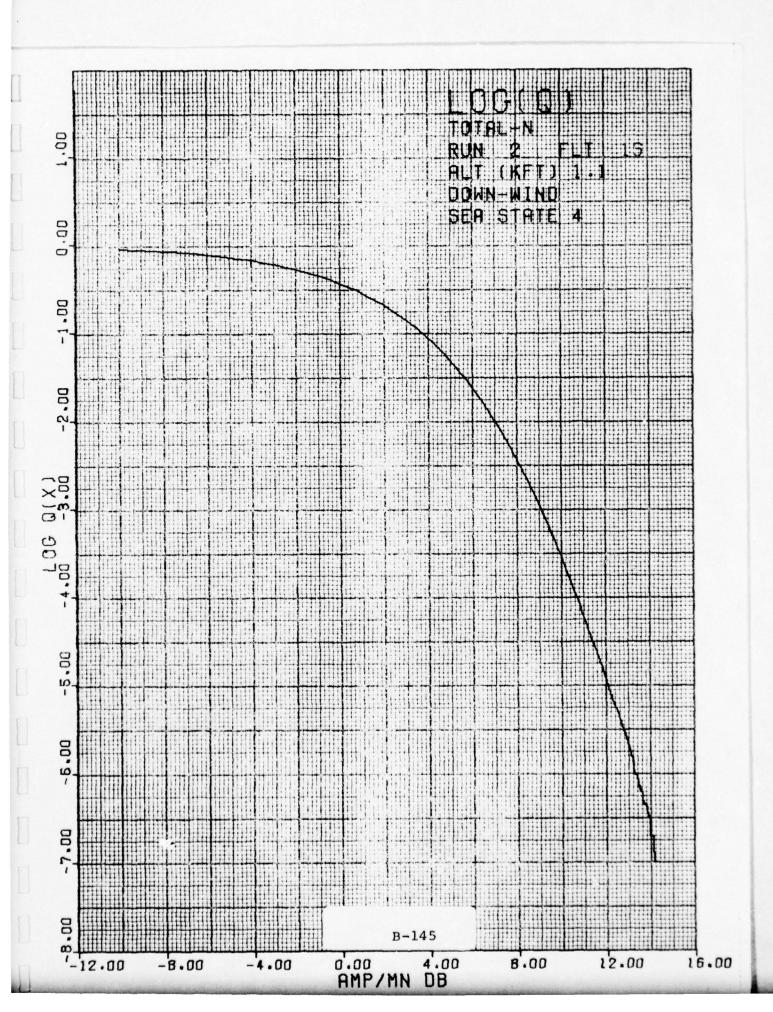


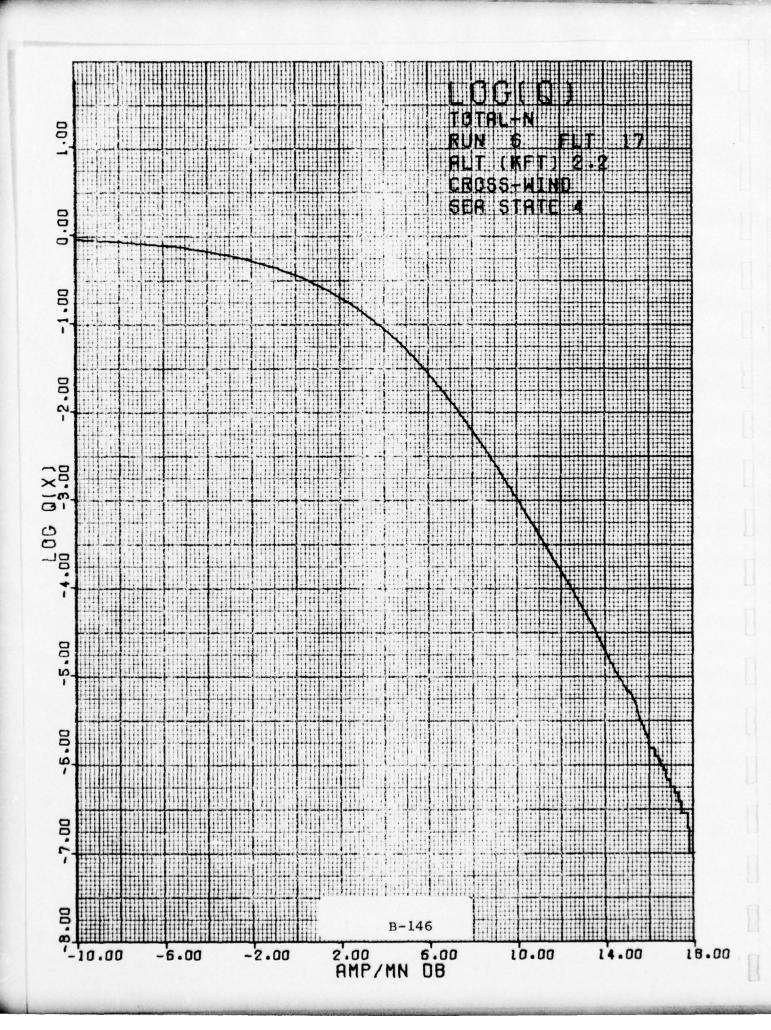


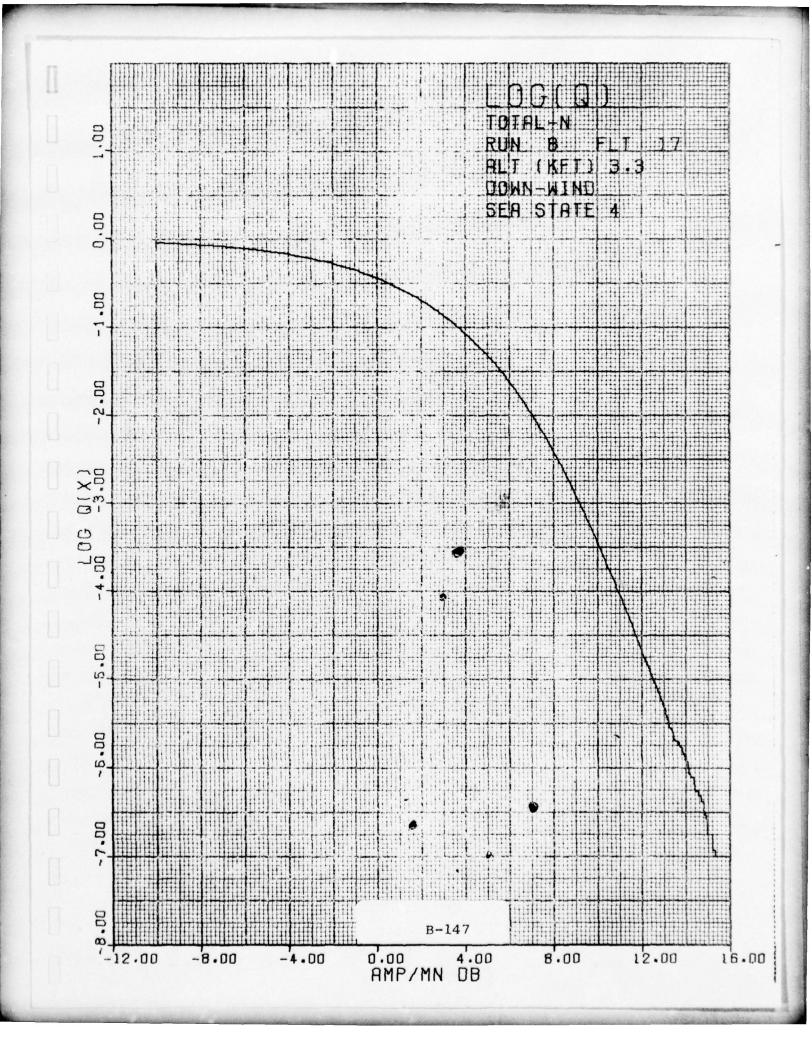


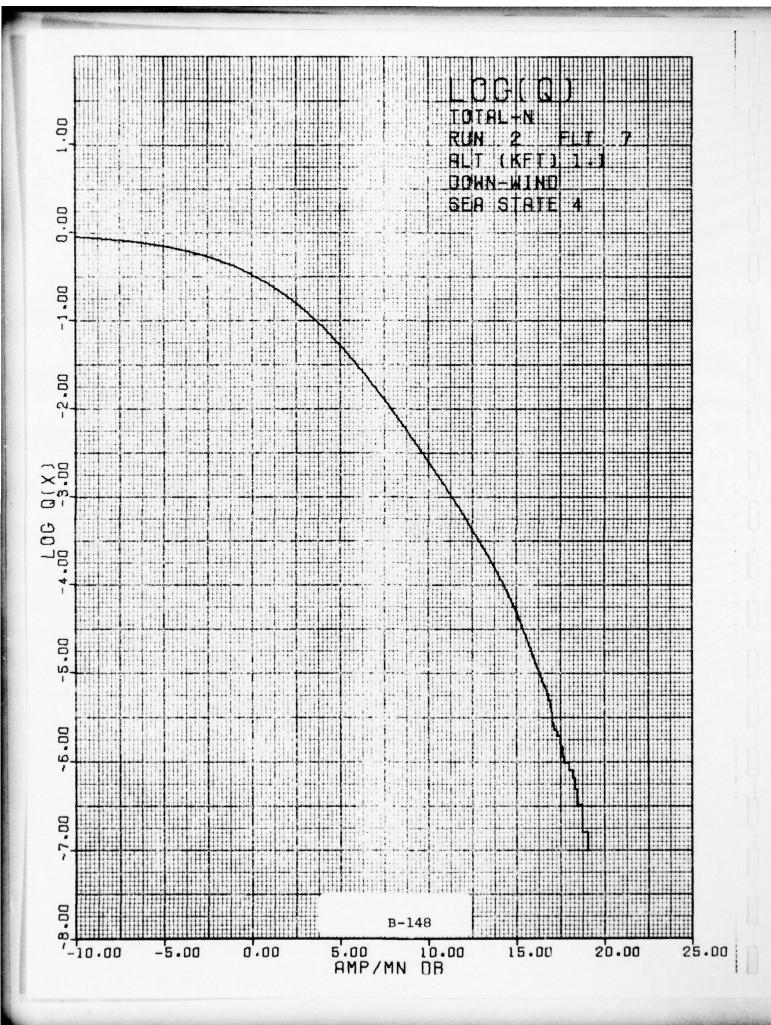


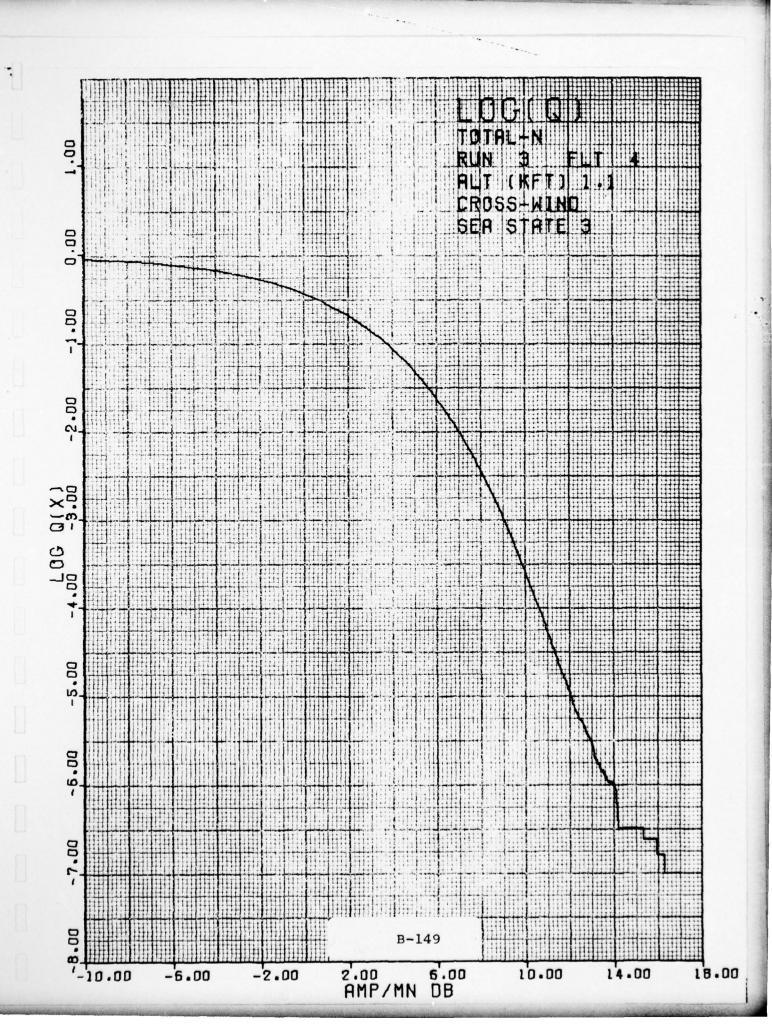












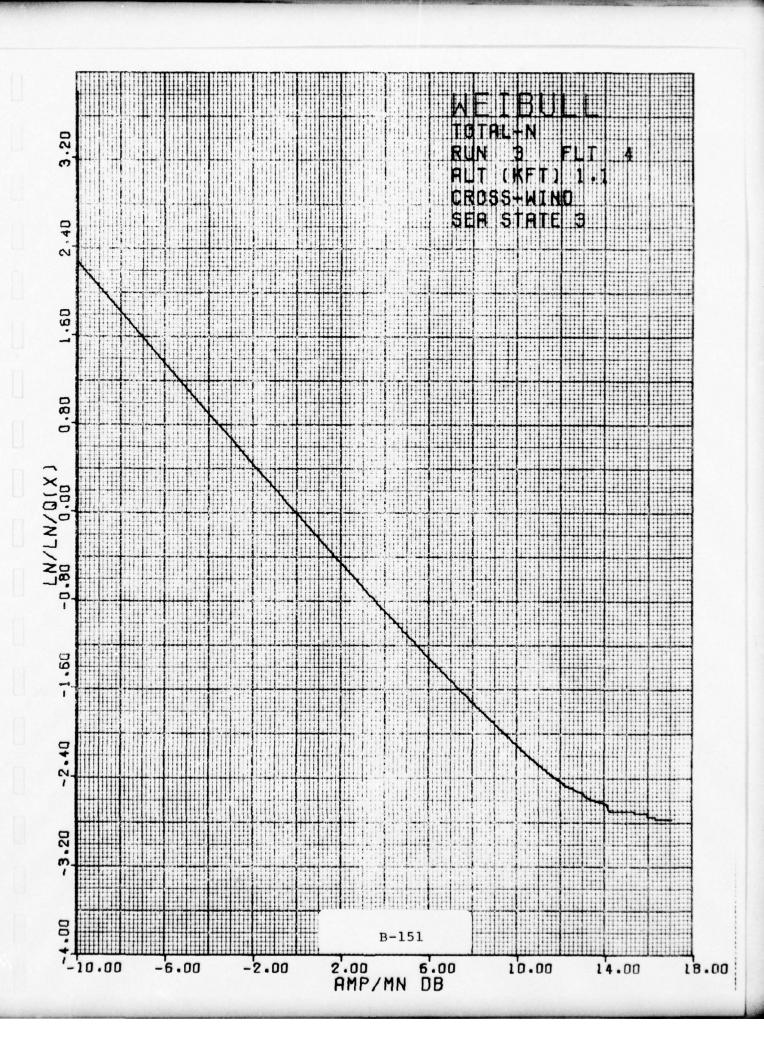
UNCLASSIFIED

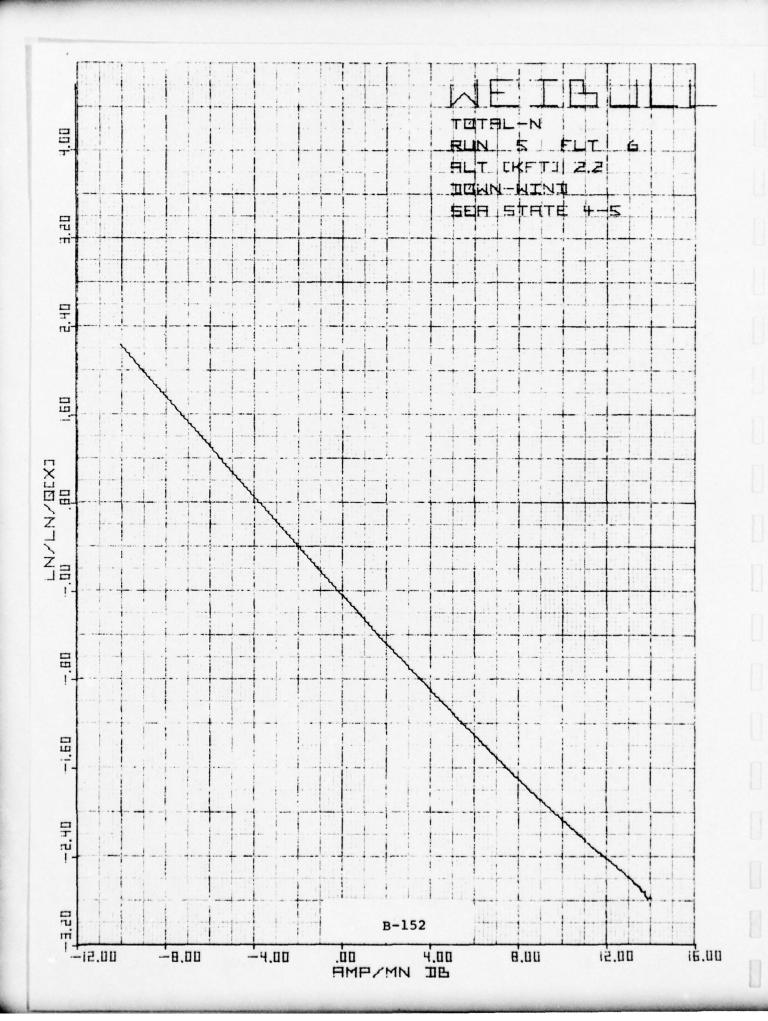
1.8.2 Histograms TOTAL N WEIBULL

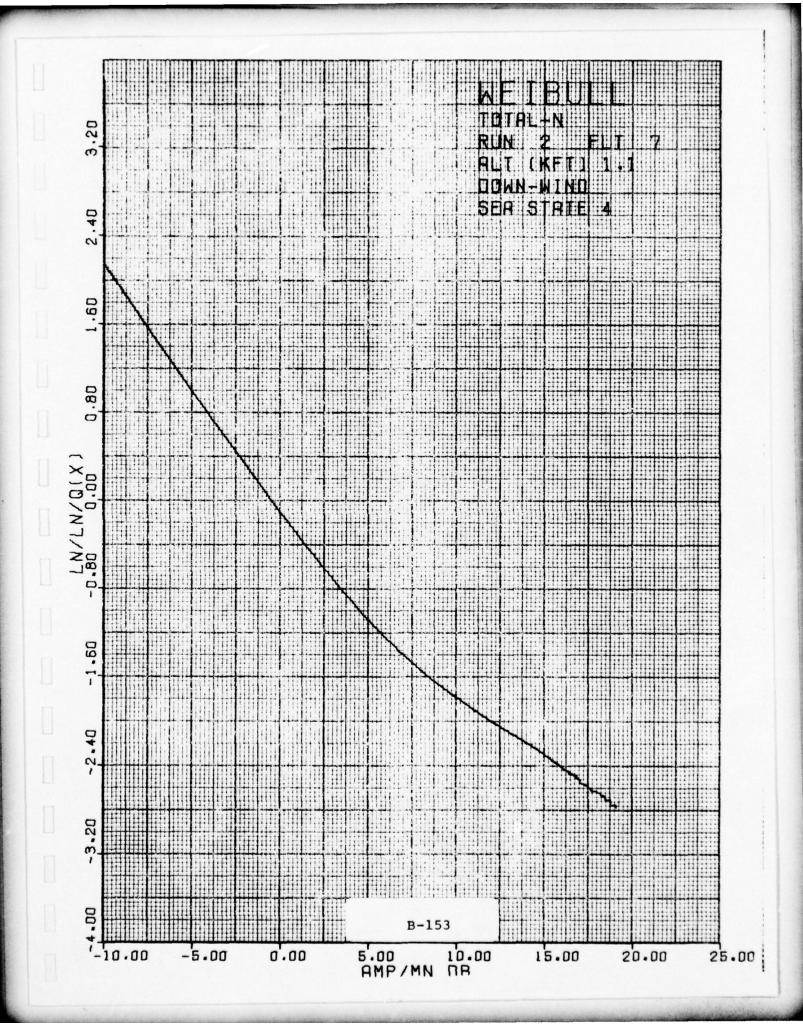
All valid clutter data for each run is included.

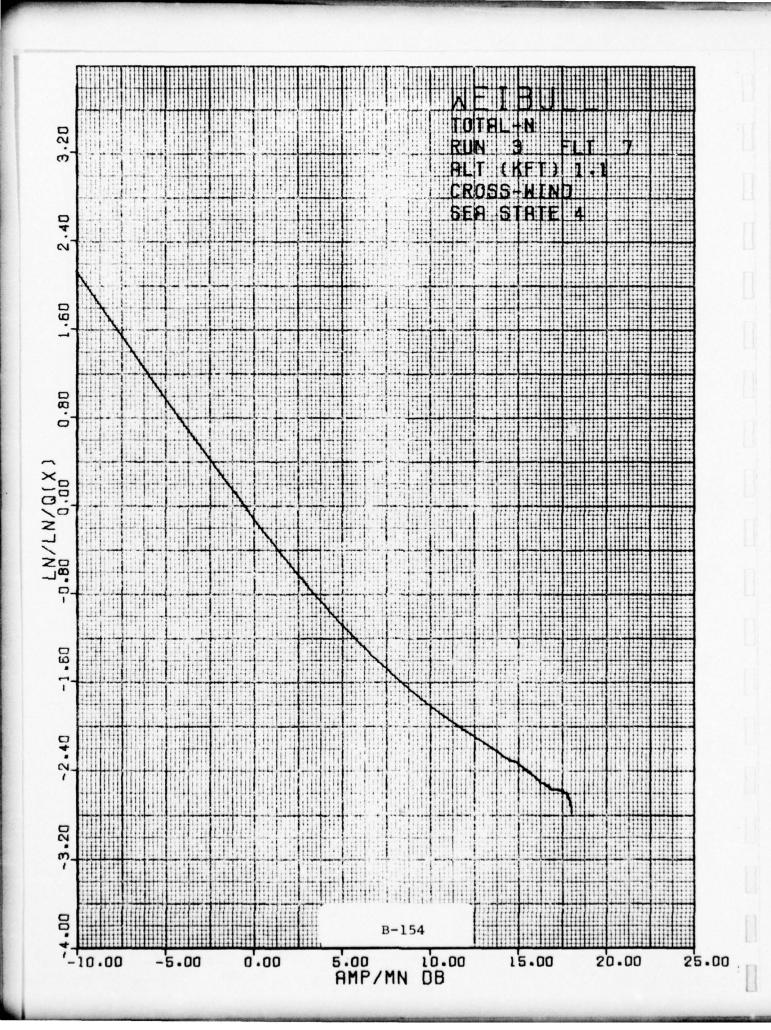
The suffix (N) after TOTAL indicates each histogram was normalized by its mean before combining into the total histogram for the run. The vertical axis of Weibull plots is $\ln \left(\ln \left(\frac{1}{1-P\left(x\right)}\right)\right) \text{ where P(x) is the cumulative probability density function. The horizontal axis is the clutter power per cell in dB referenced to the data mean.}$

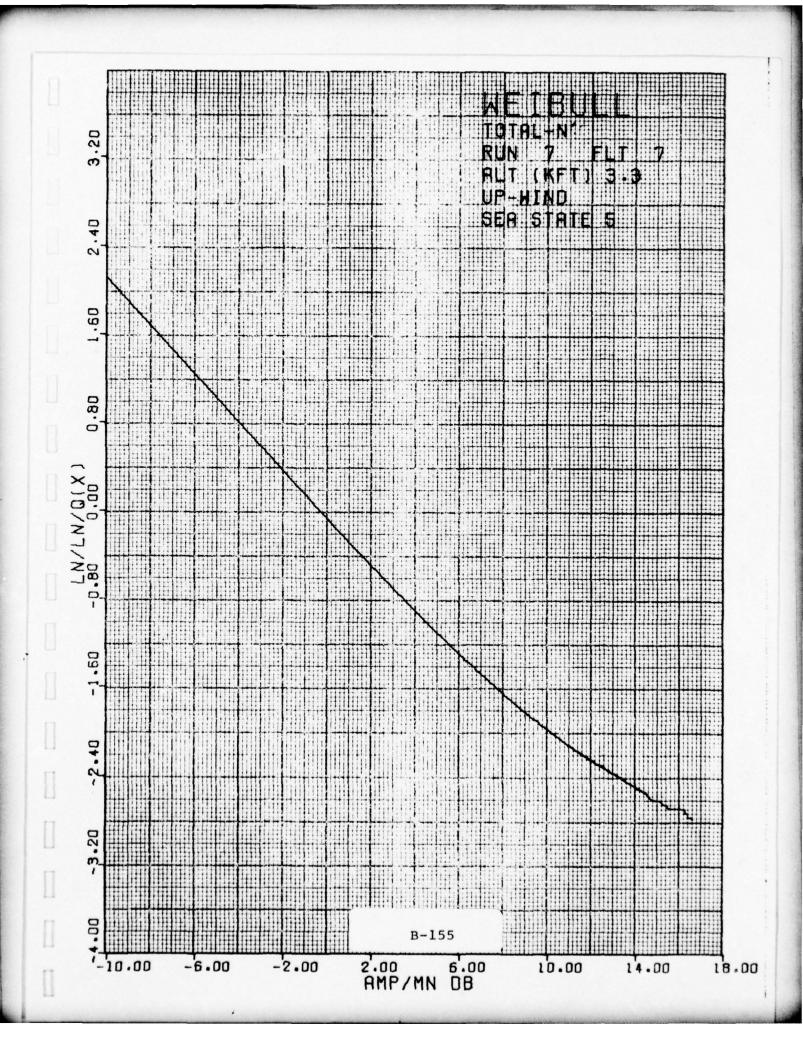
This type of output is described in more detail in Section 9 (Volume II). Procedures utilized in developing the histogram from the raw data are described in Section 8 of Volume II.

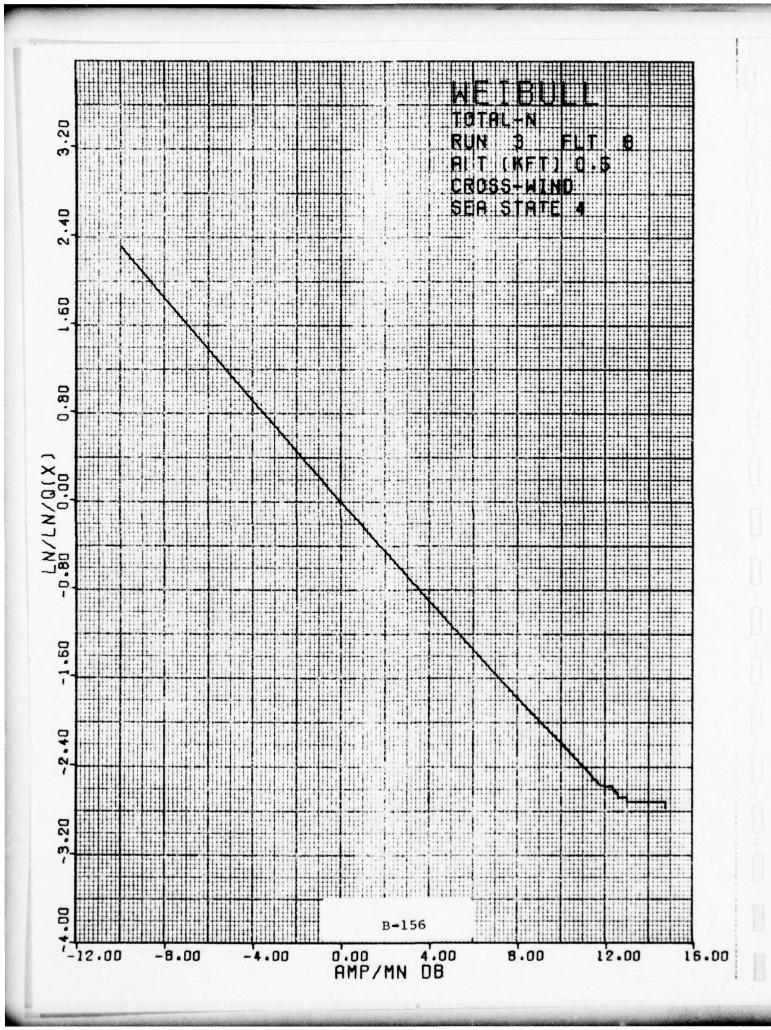


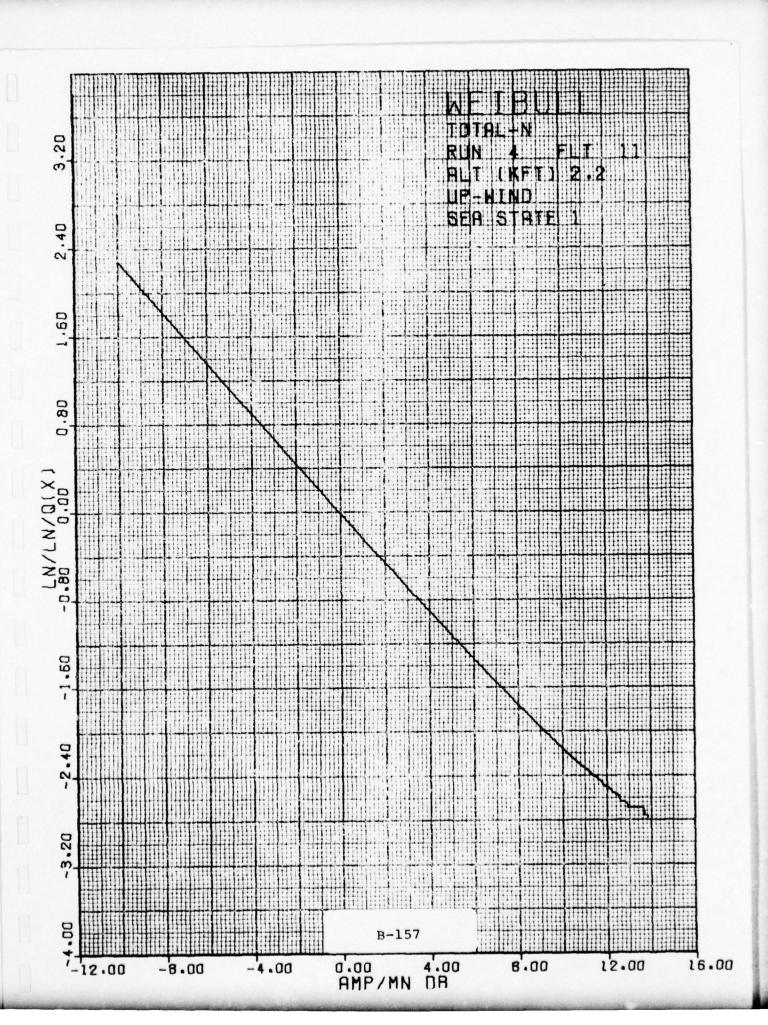


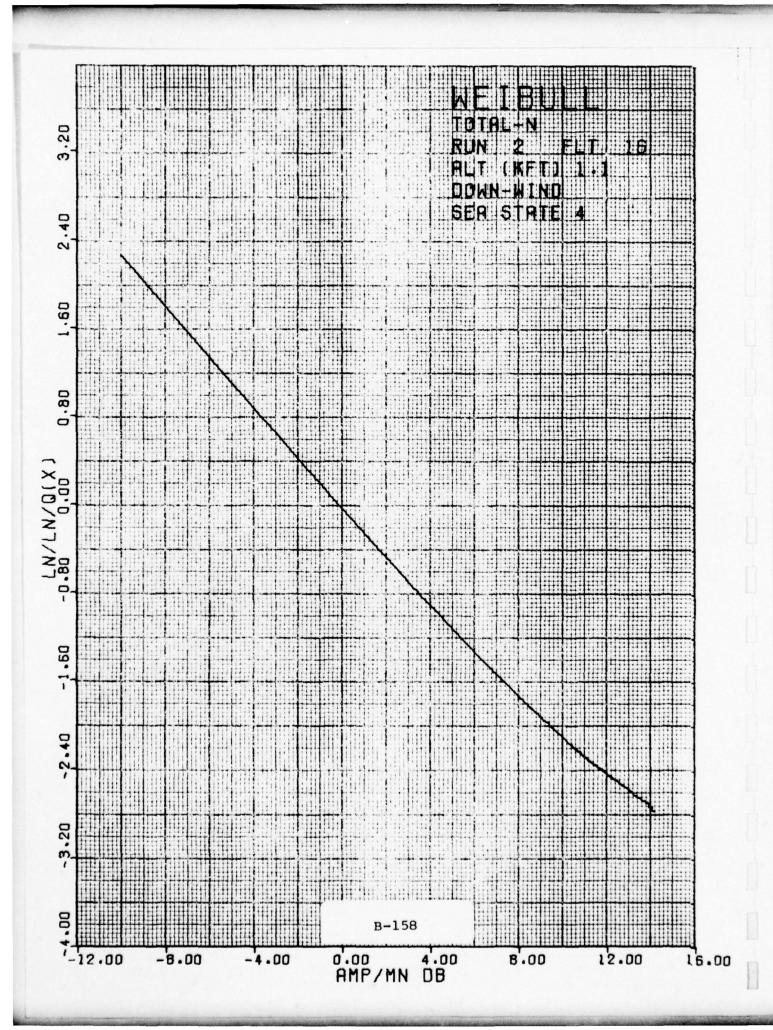


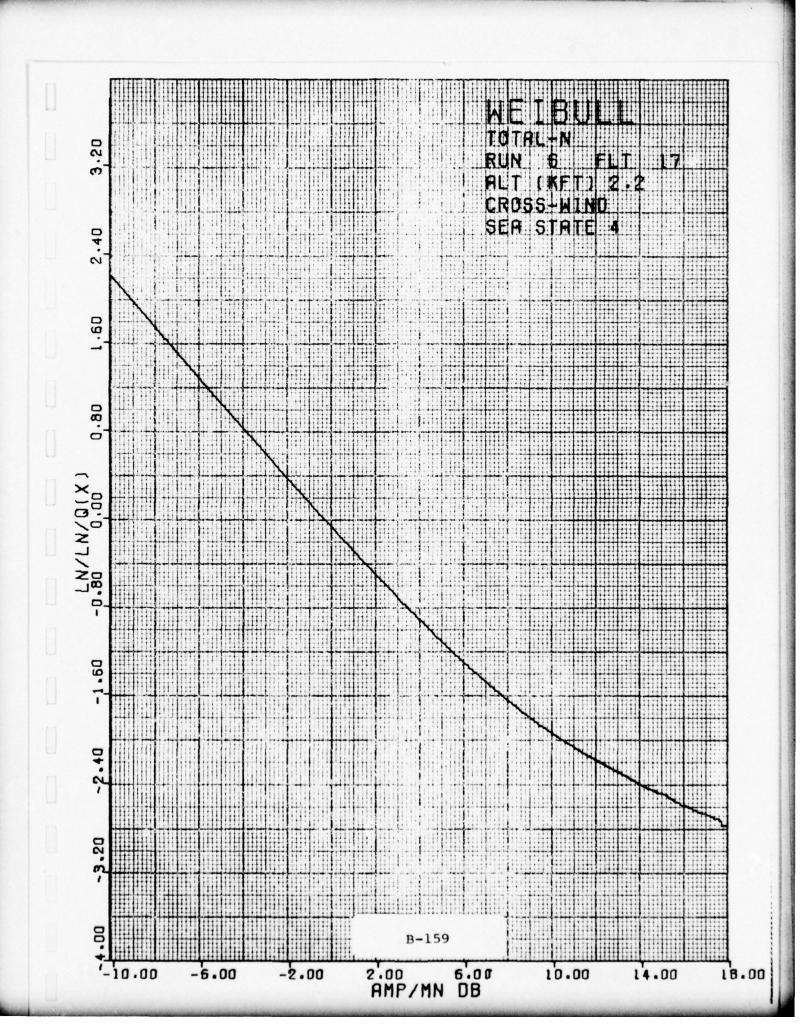


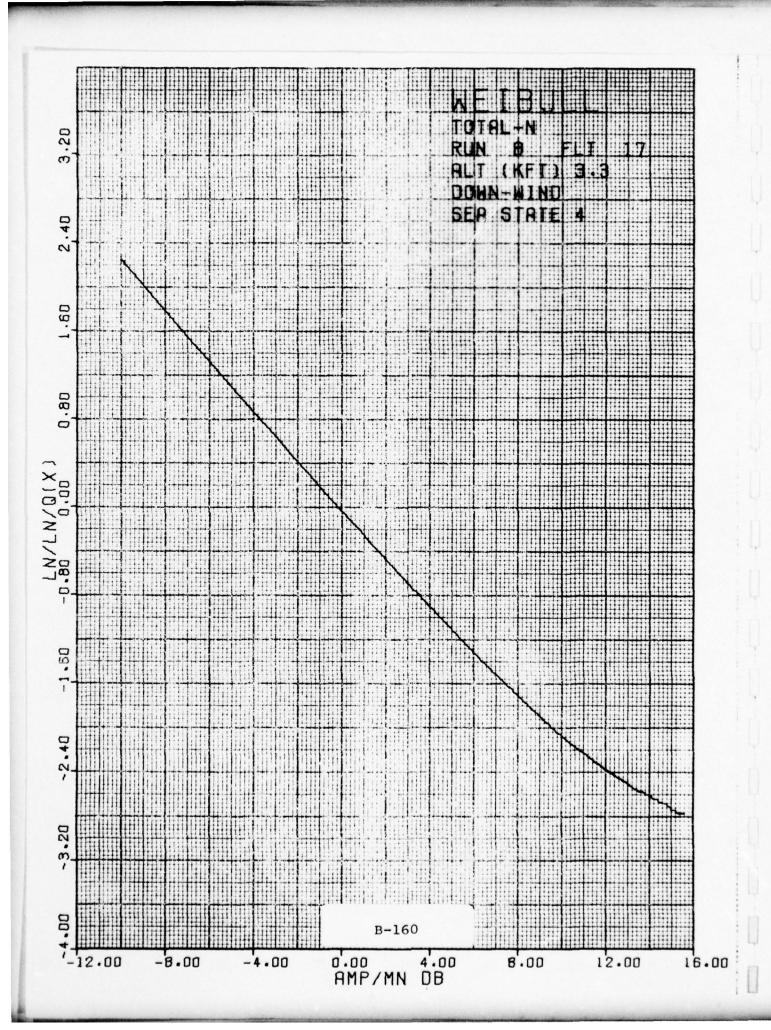












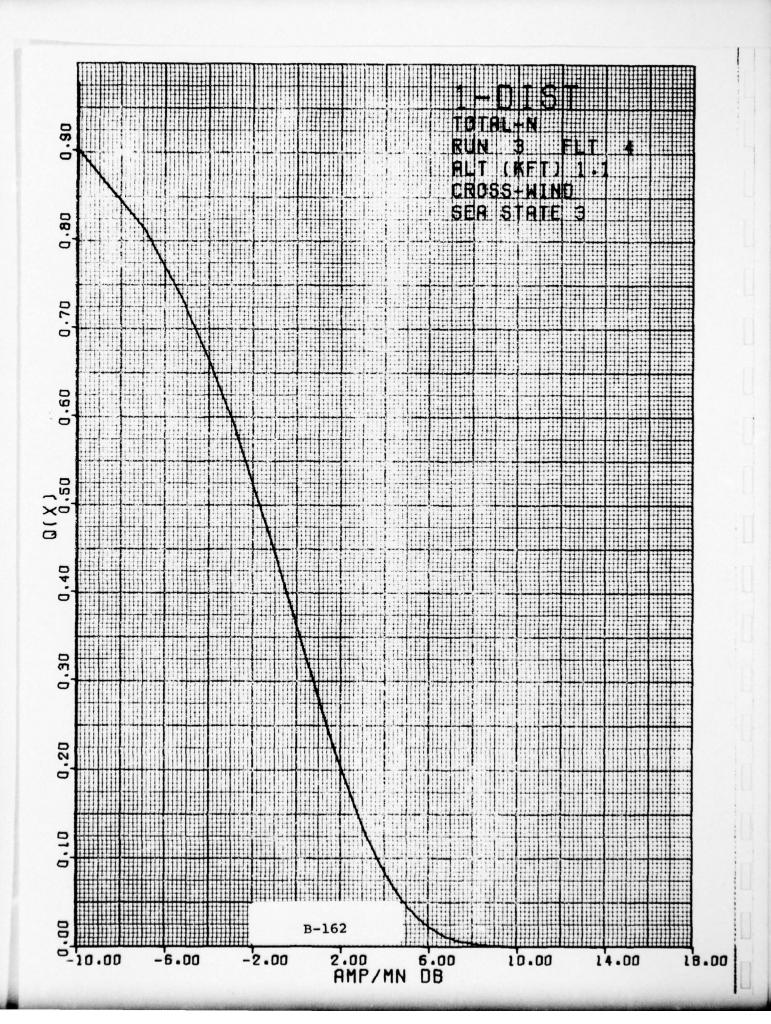
UNCLASSIFIED

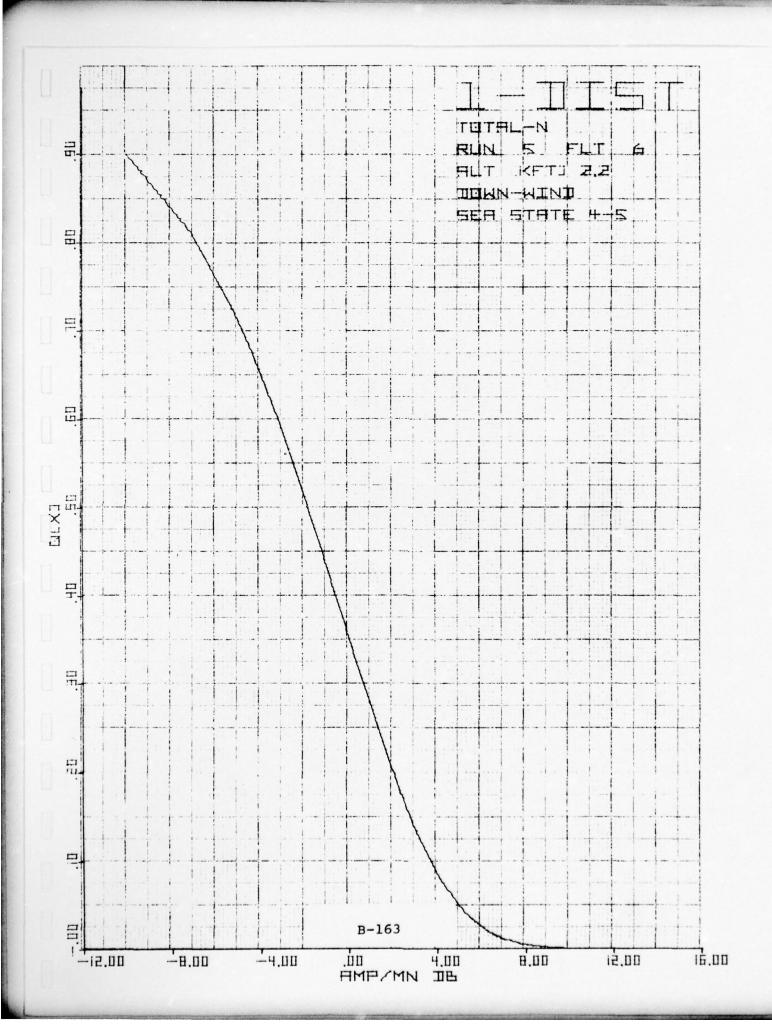
1.8.3 Histograms TOTAL N Q = 1-DIST

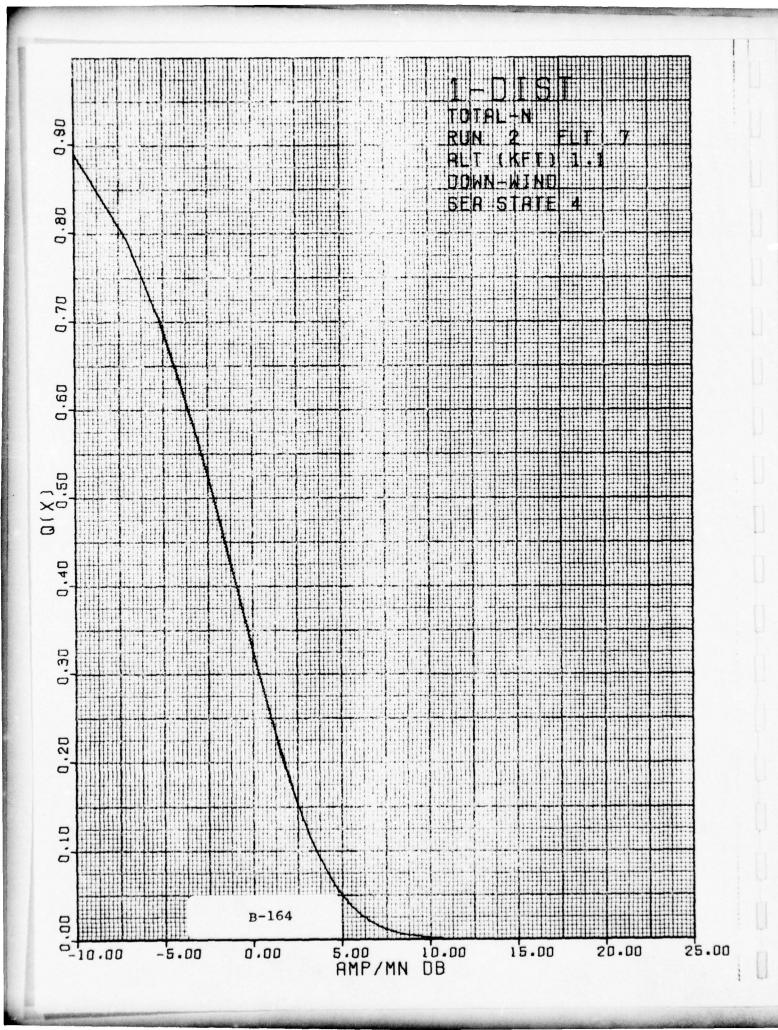
All valid clutter dta for each run is included.

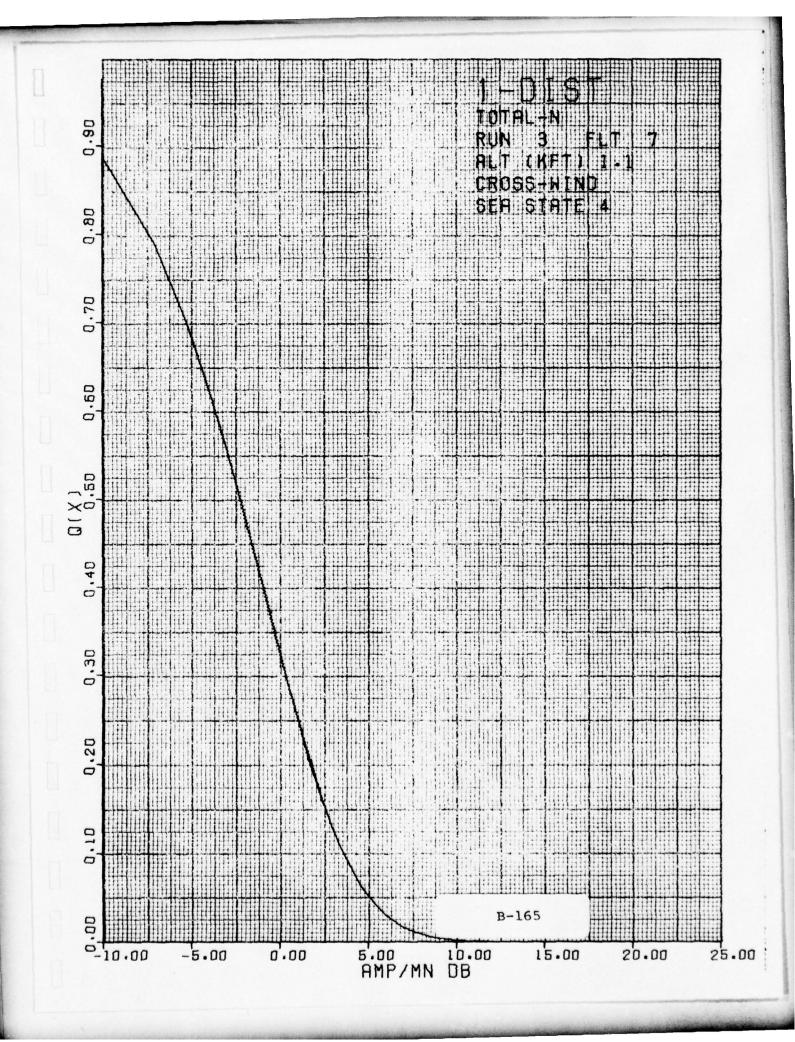
The suffix (N) after TOTAL indicates each histogram was normalized by its mean before combining into the total histogram for the run. The vertical axis is Q or one minus the cumulative distribution. The horizontal axis is the clutter power per cell in dB referenced to the data mean.

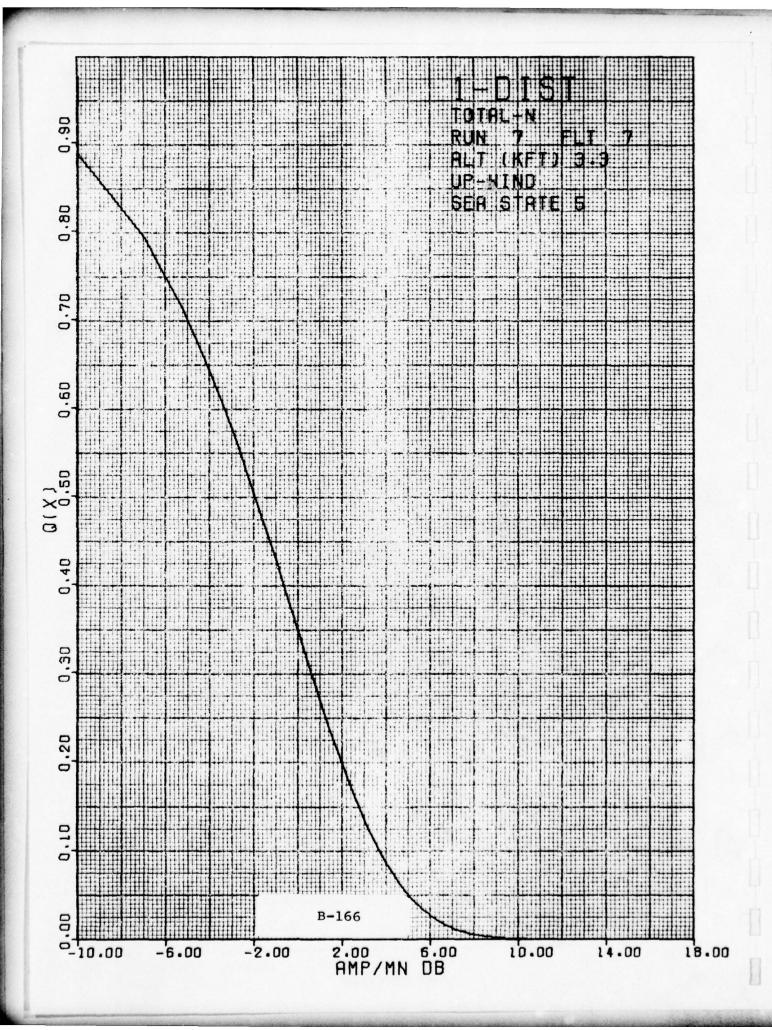
This type of output is described in more detail in Section 9 (Volume II). Procedures utilized in developing the histogram from the raw data are described in Section 8 of Volume II.

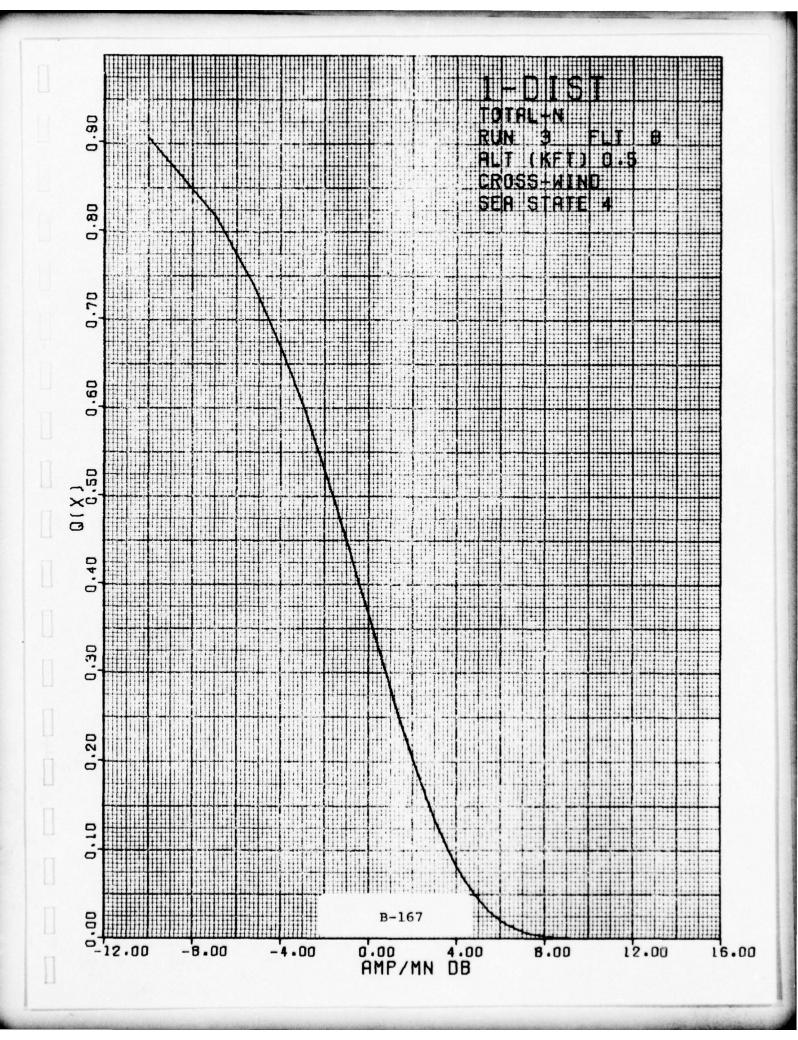


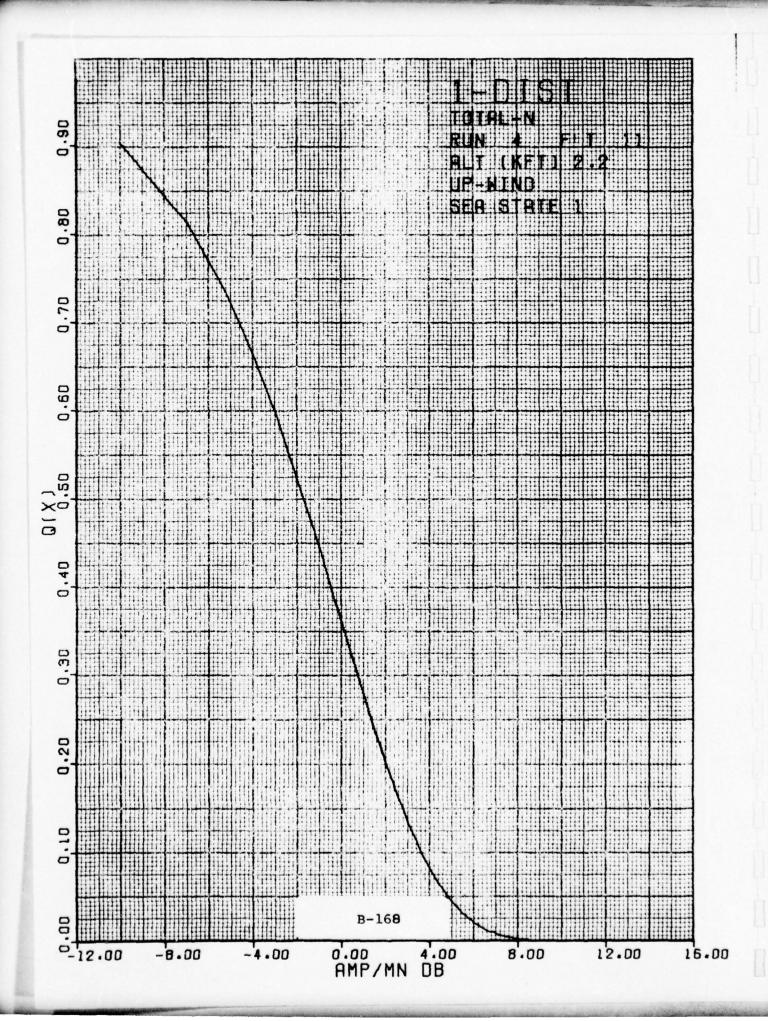


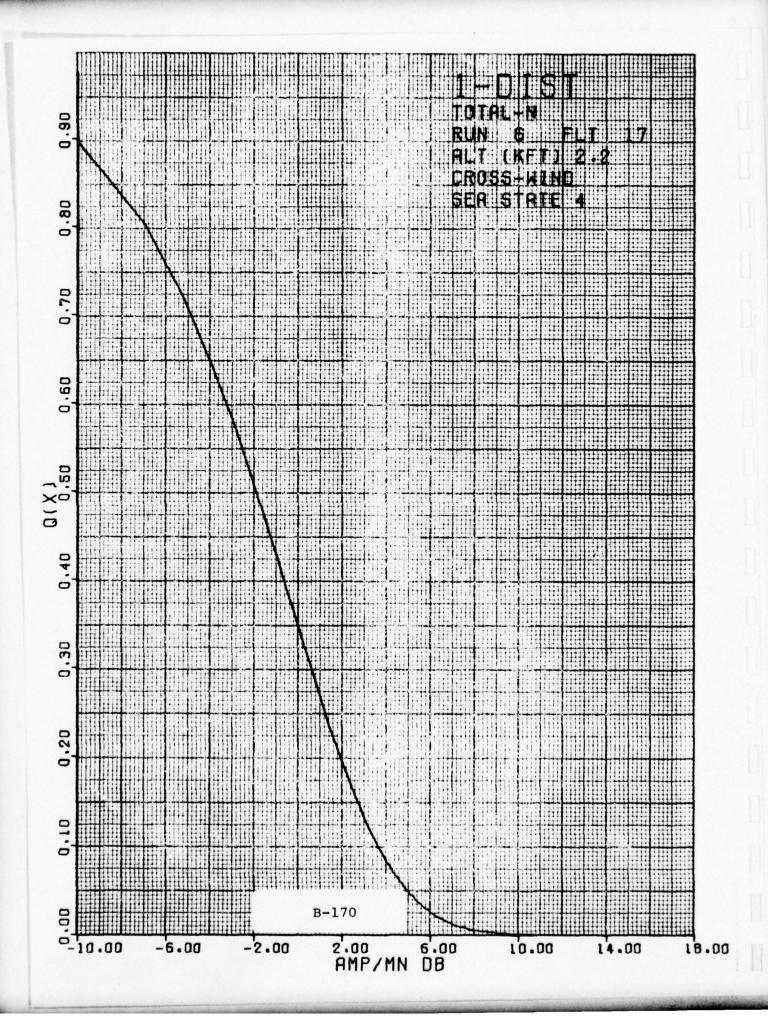


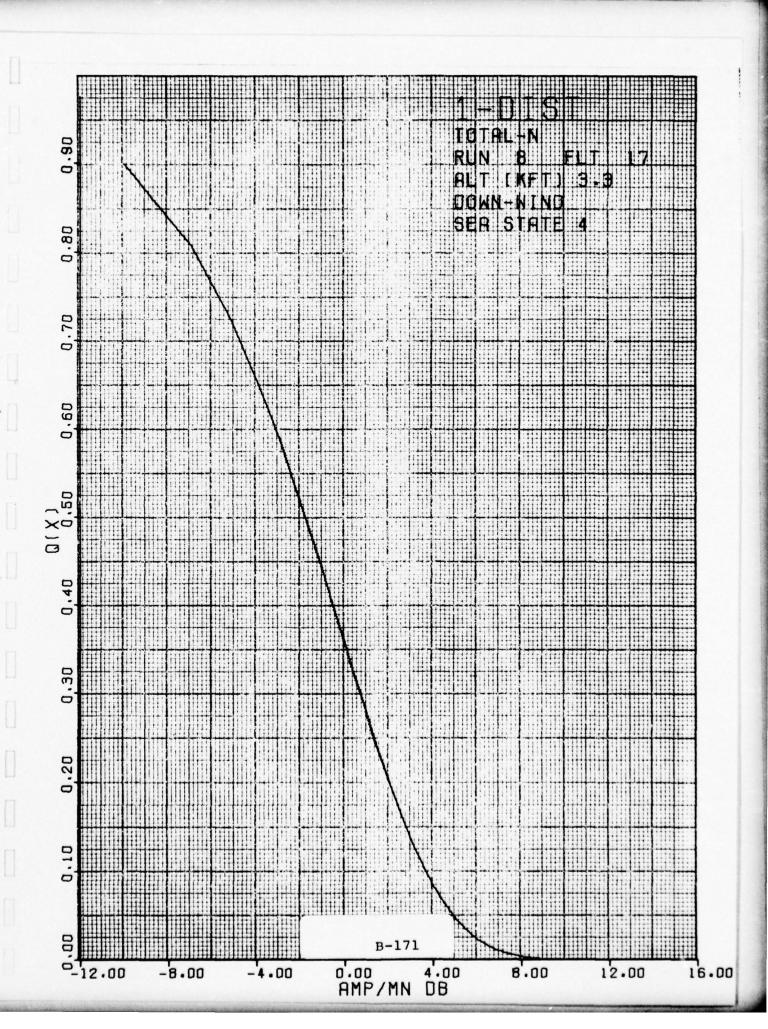












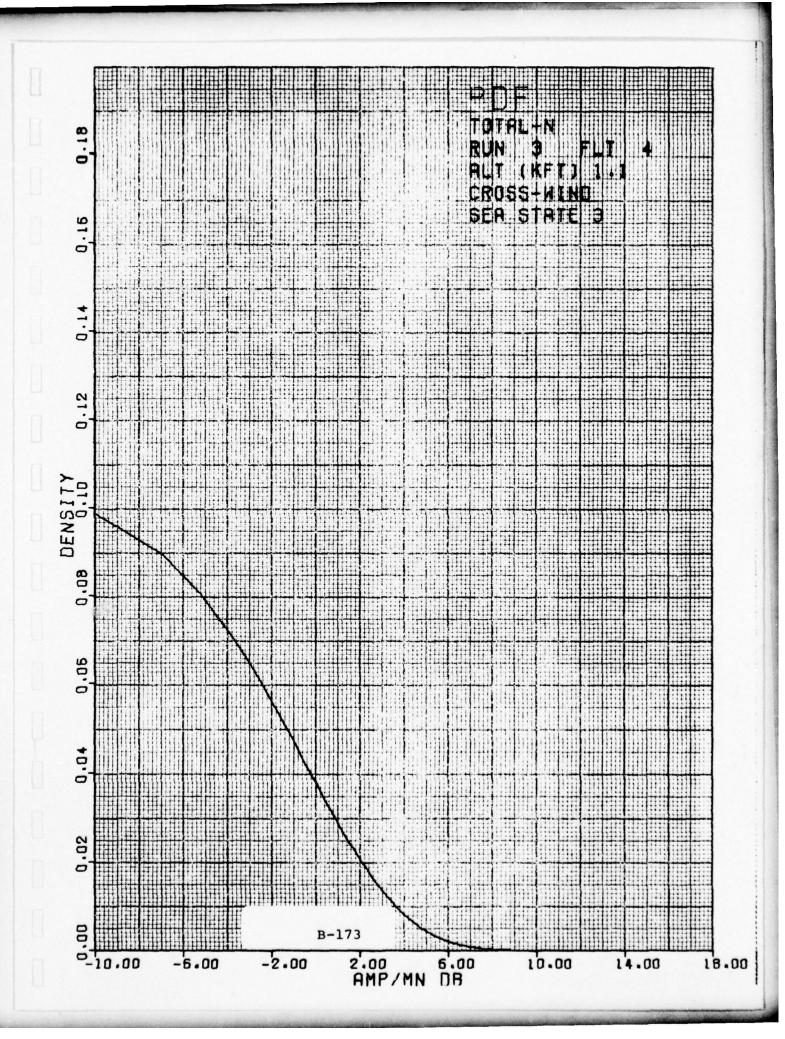
UNCLASSIFIED

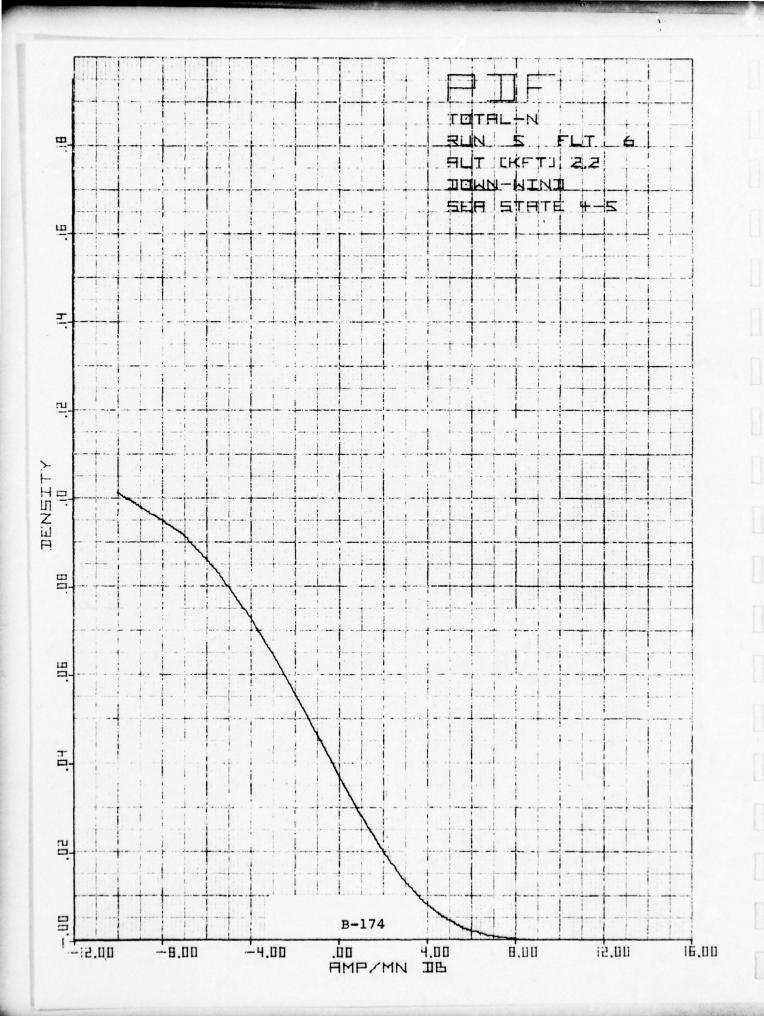
1.8.4 Histograms TOTAL N PDF

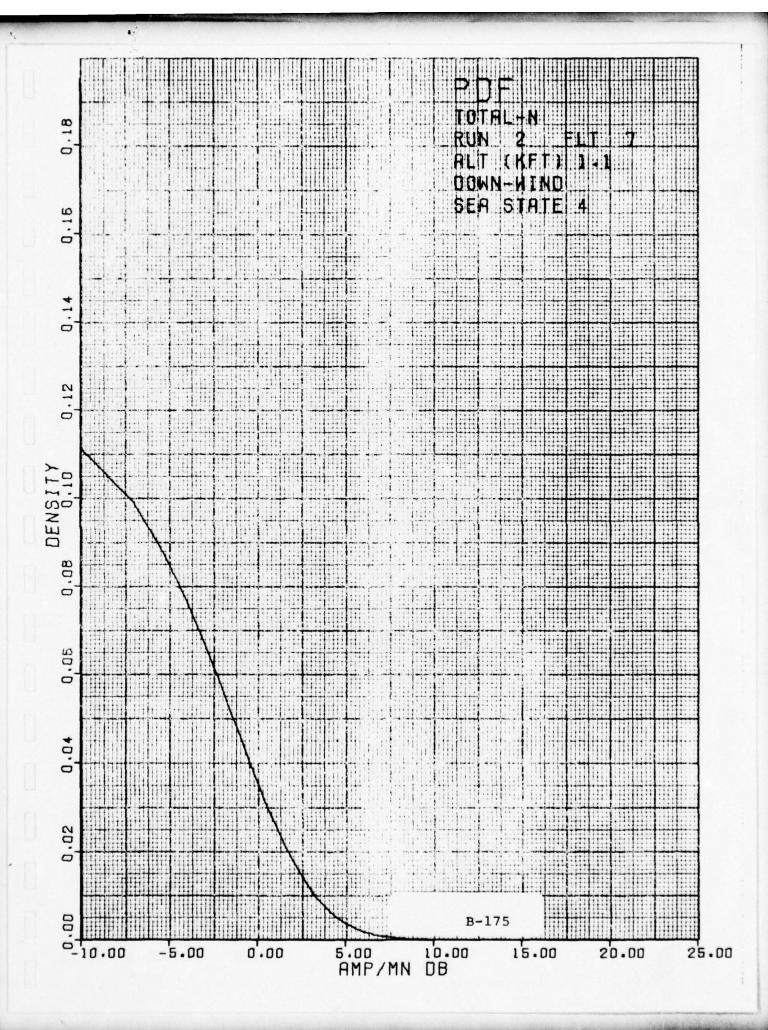
All valid clutter data for each run is included.

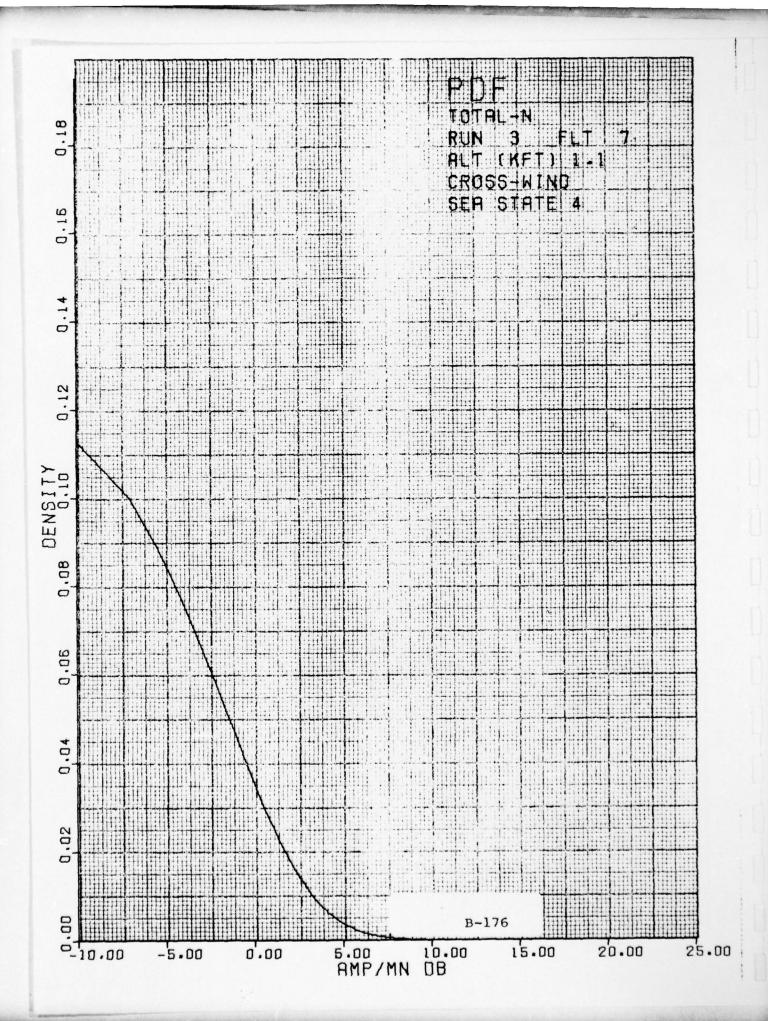
The suffix (N) after TOTAL indicates each histogram was normalized by its mean before combining into the total histogram for the run. The vertical axis is the raw histogram data or probability density. The horizontal axis is the clutter power per cell in dB referenced to the data mean.

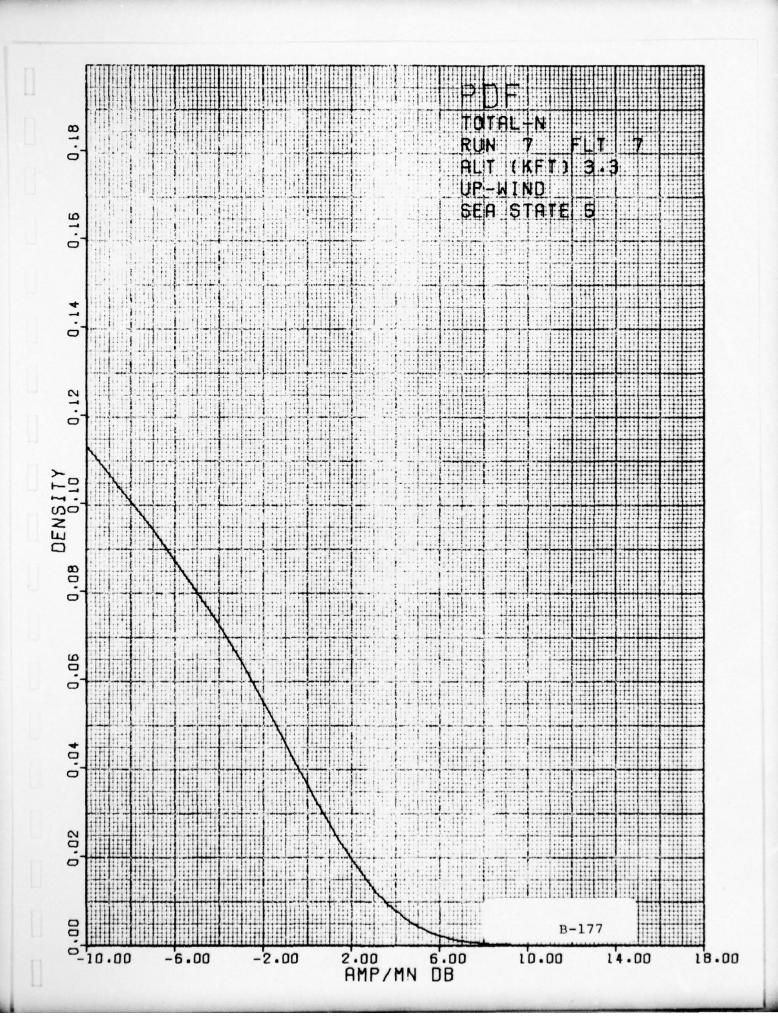
This type of output is described in more detail in Section 9 (Volume II). Procedures utilized in developing the histogram from the raw data are described in Section 8 Volume II.

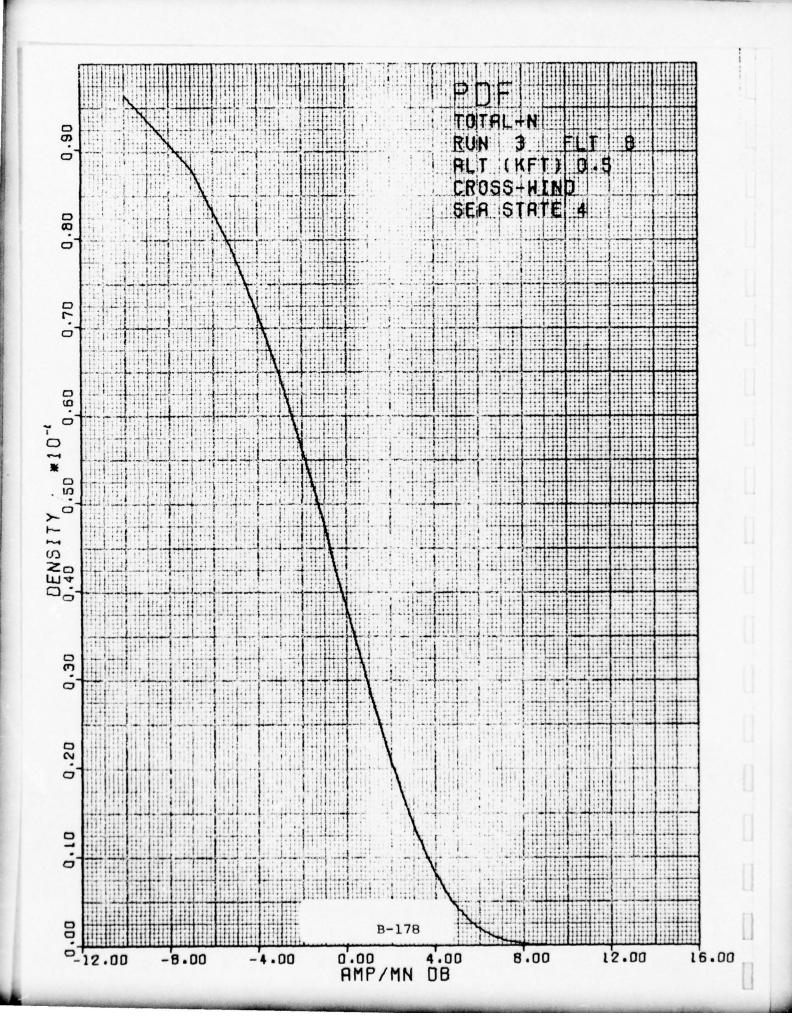


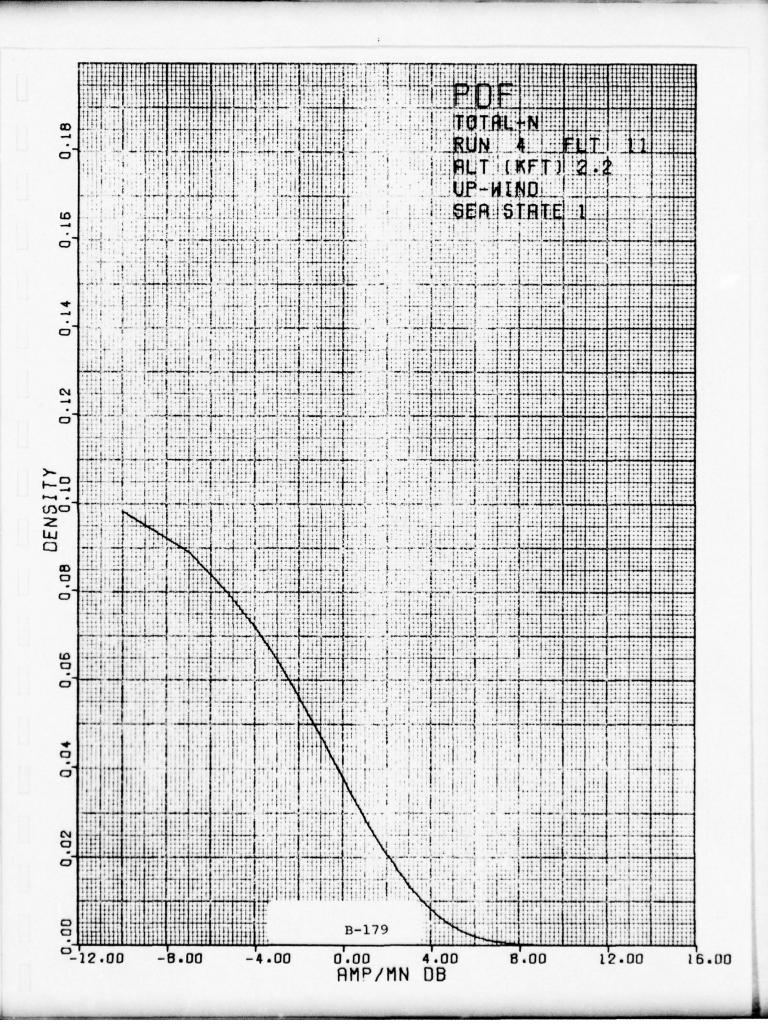


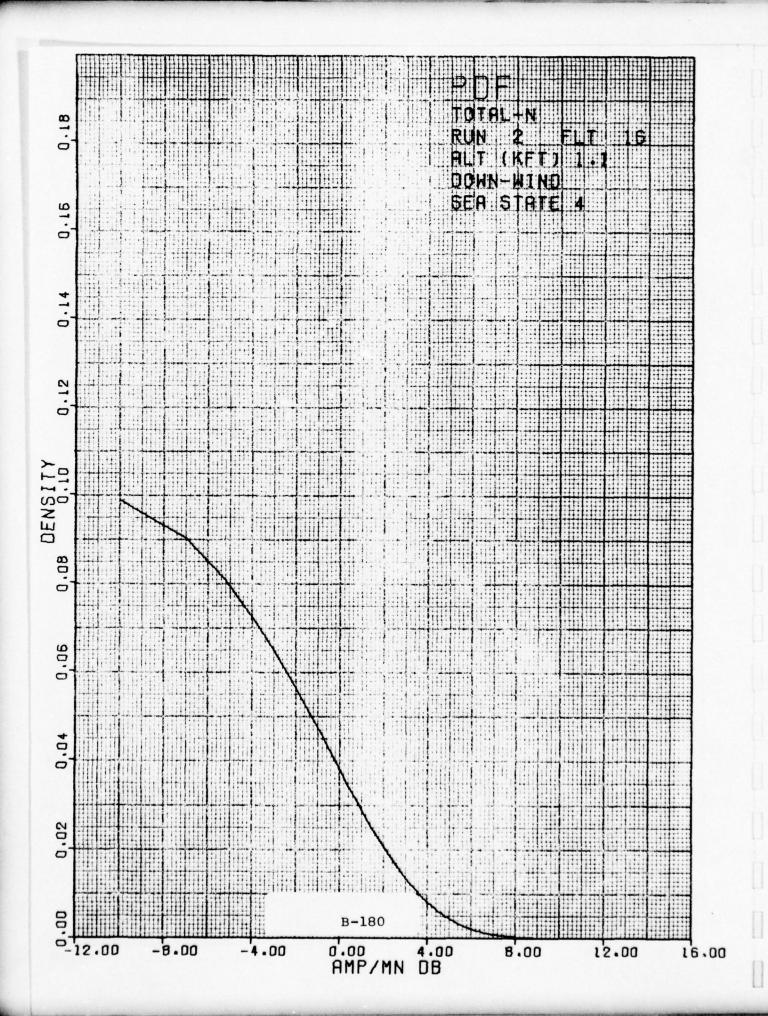


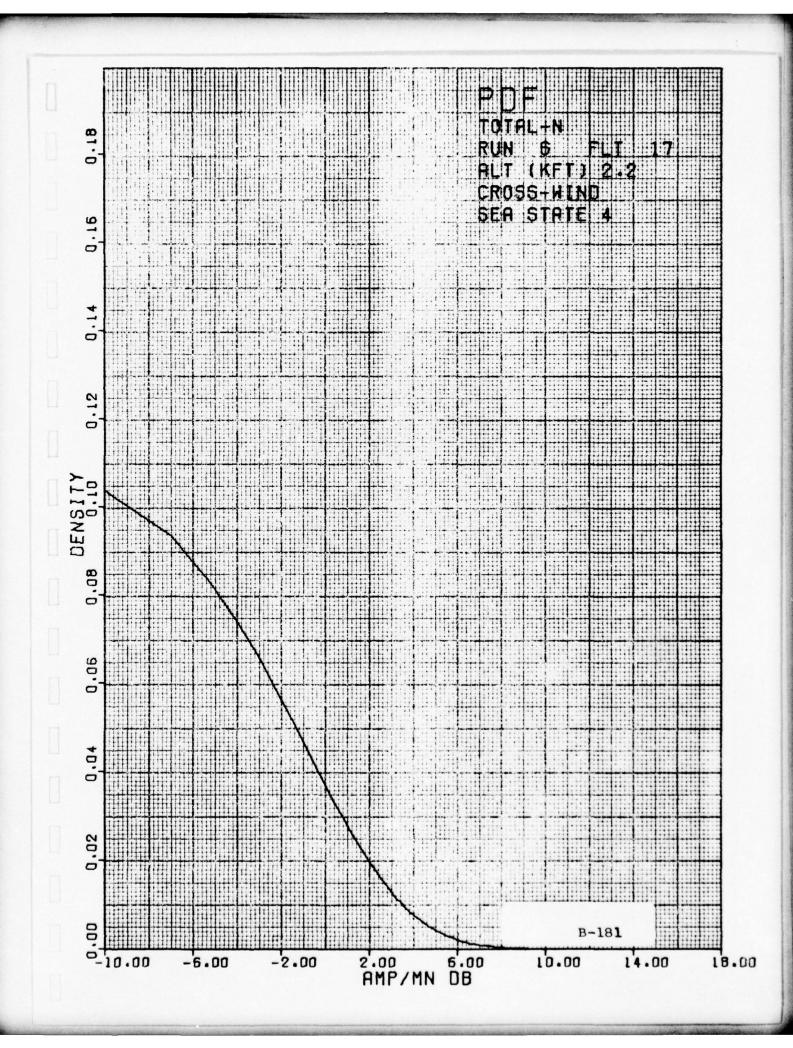


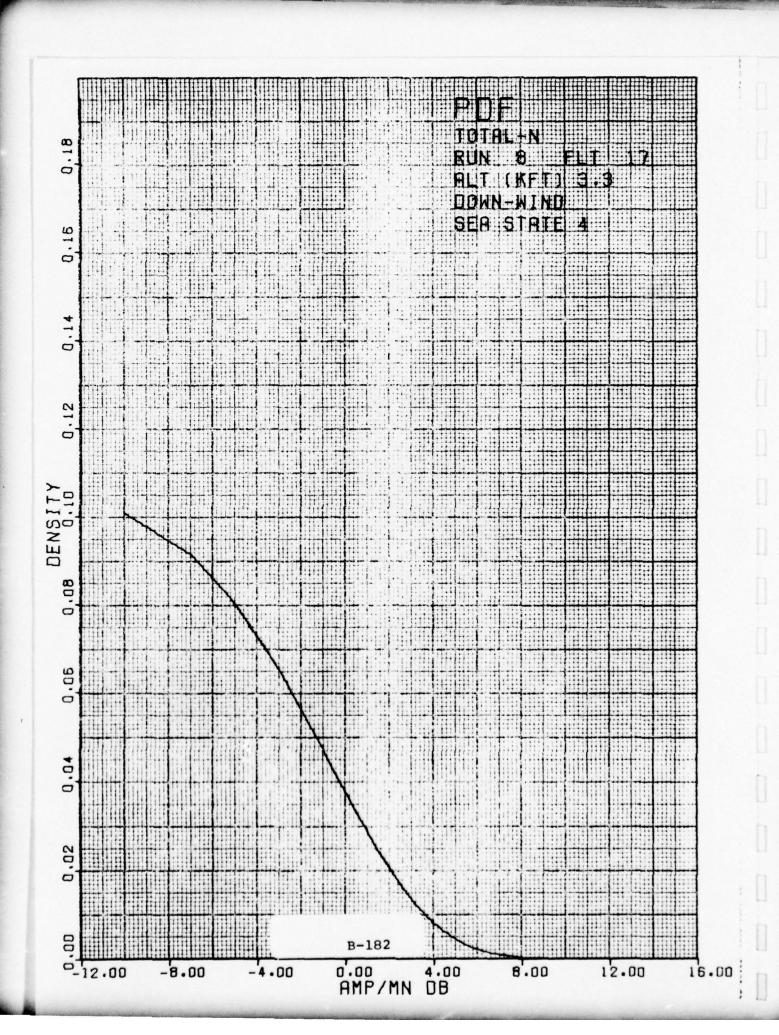










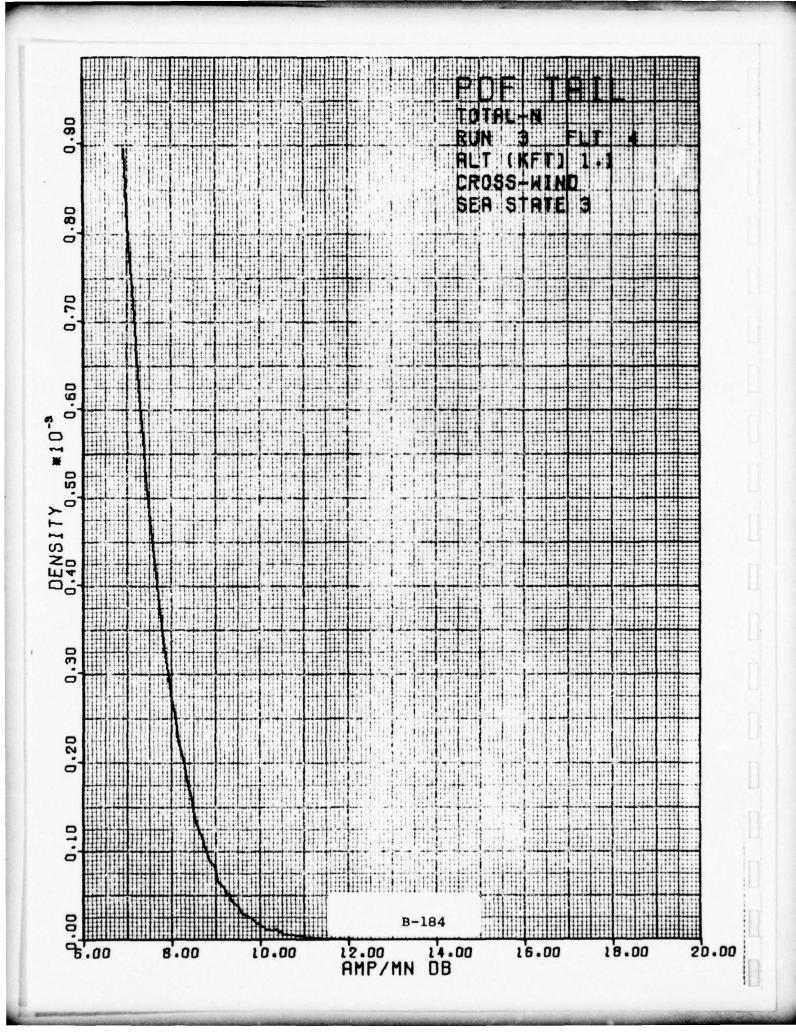


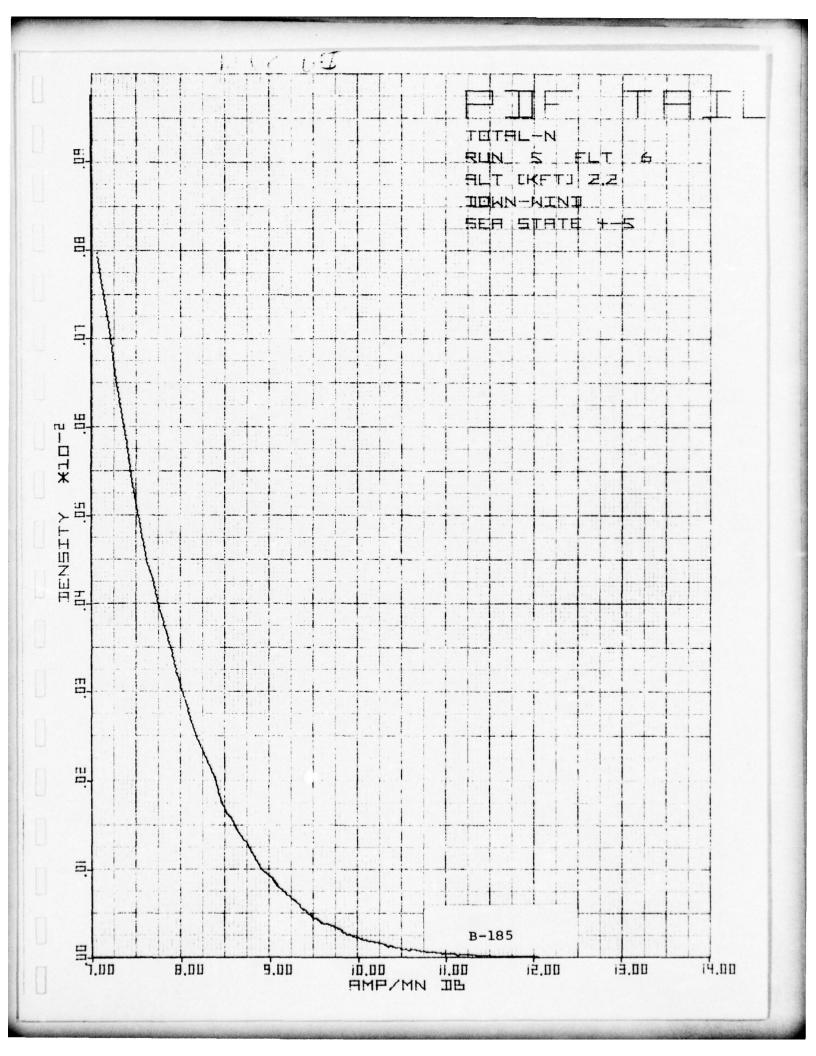
1.8.5 Histograms TOTAL N PDF TAIL

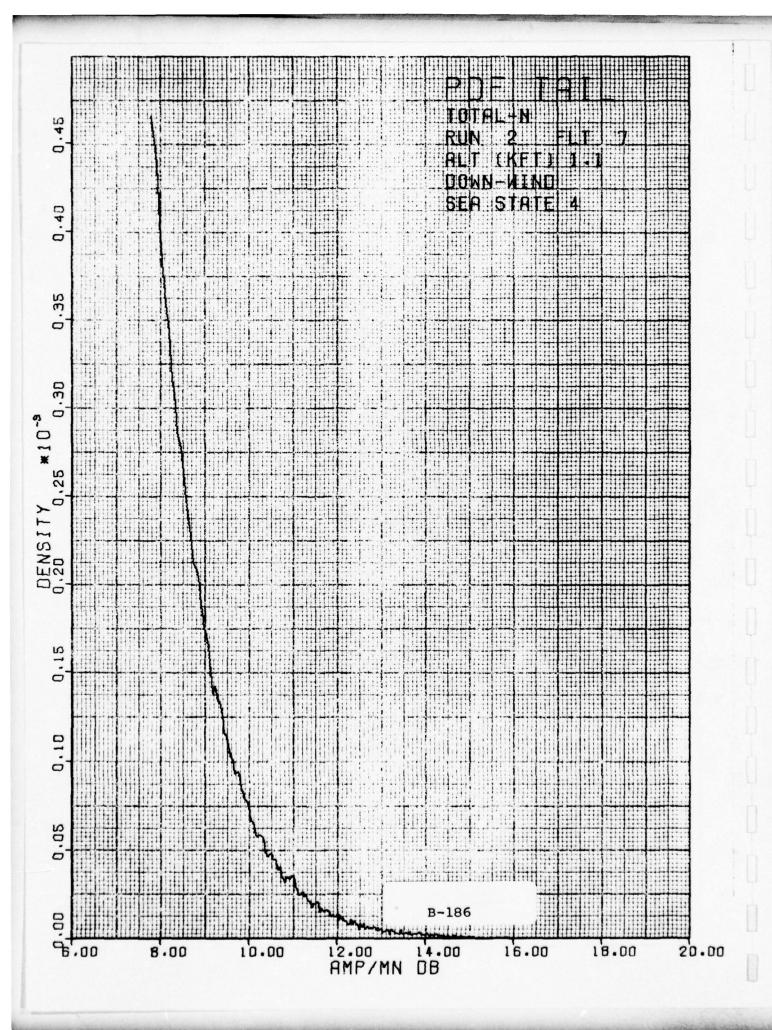
All valid clutter data for each run is included.

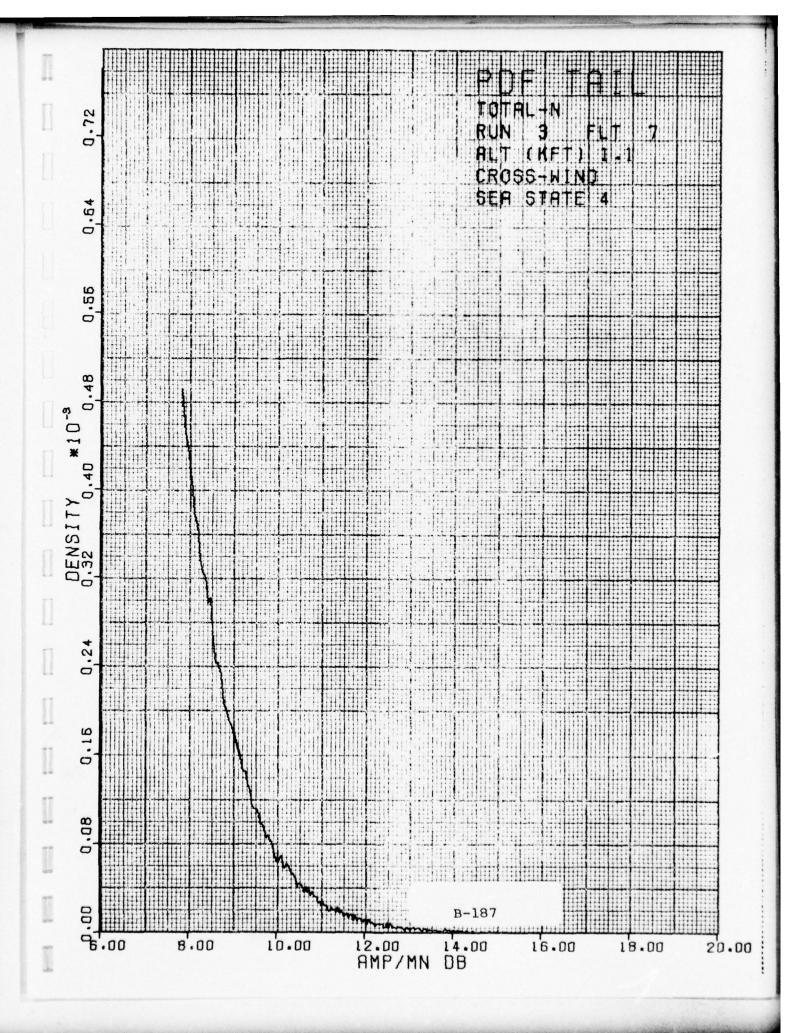
The suffix (N) after TOTAL indicates each histogram was normalized by its mean before combining into the total histogram for the run. The vertical axis is probability density. Only the tail is displayed to give dynamic range. The horizontal axis is the clutter power per cell in dB referenced to the data mean.

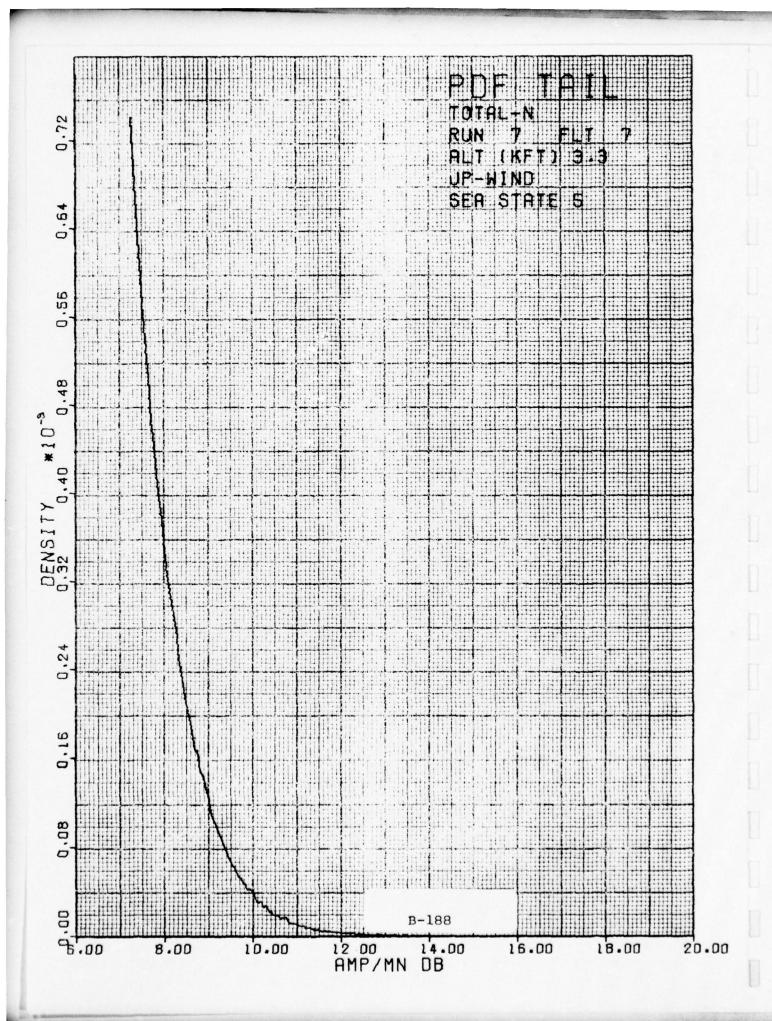
This type of output is described in more detail in Section 9 (Volume II). Procedures utilized in developing the histogram from the raw data are described in Section 8 Volume II.

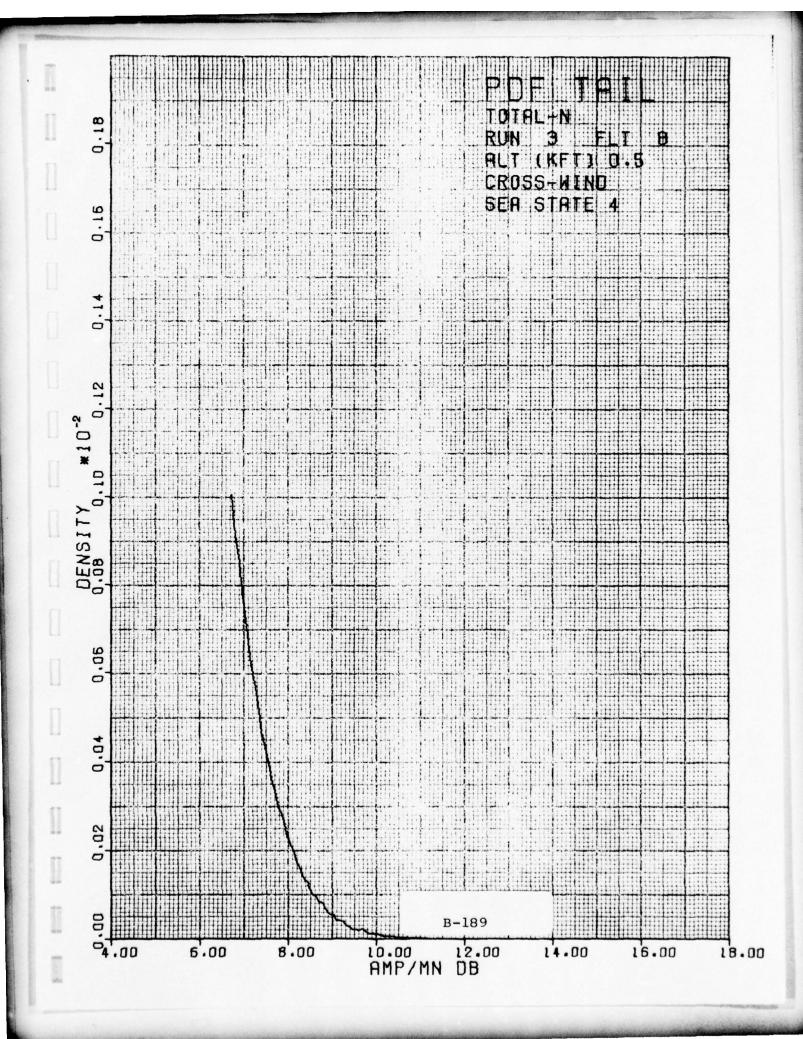


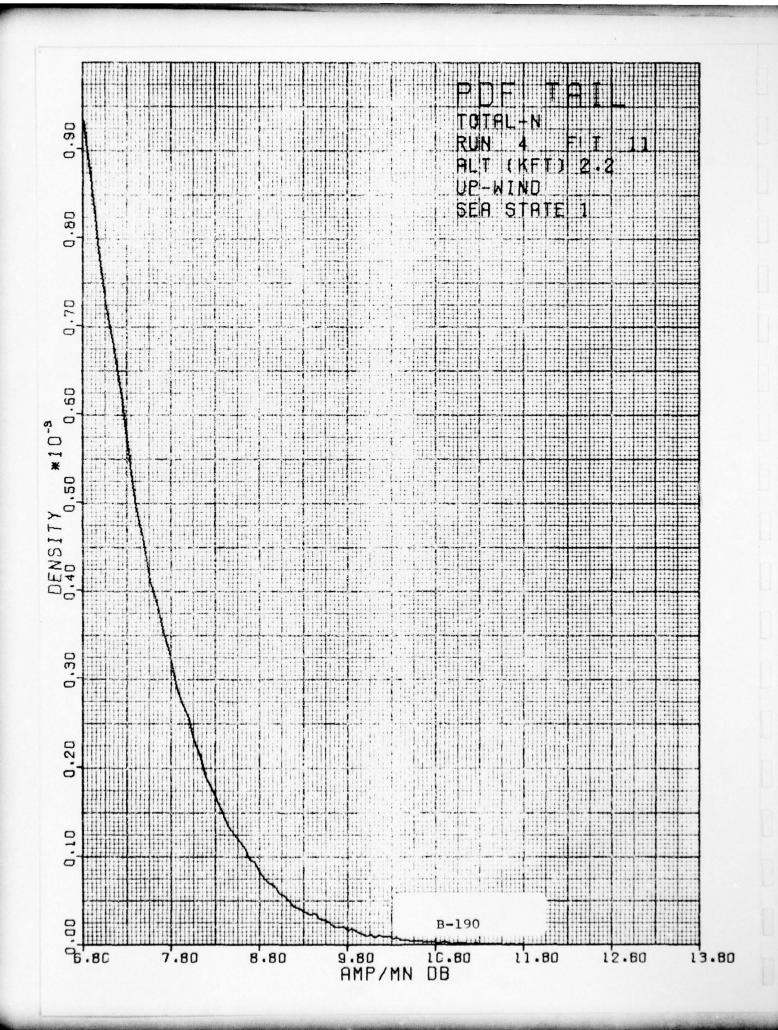


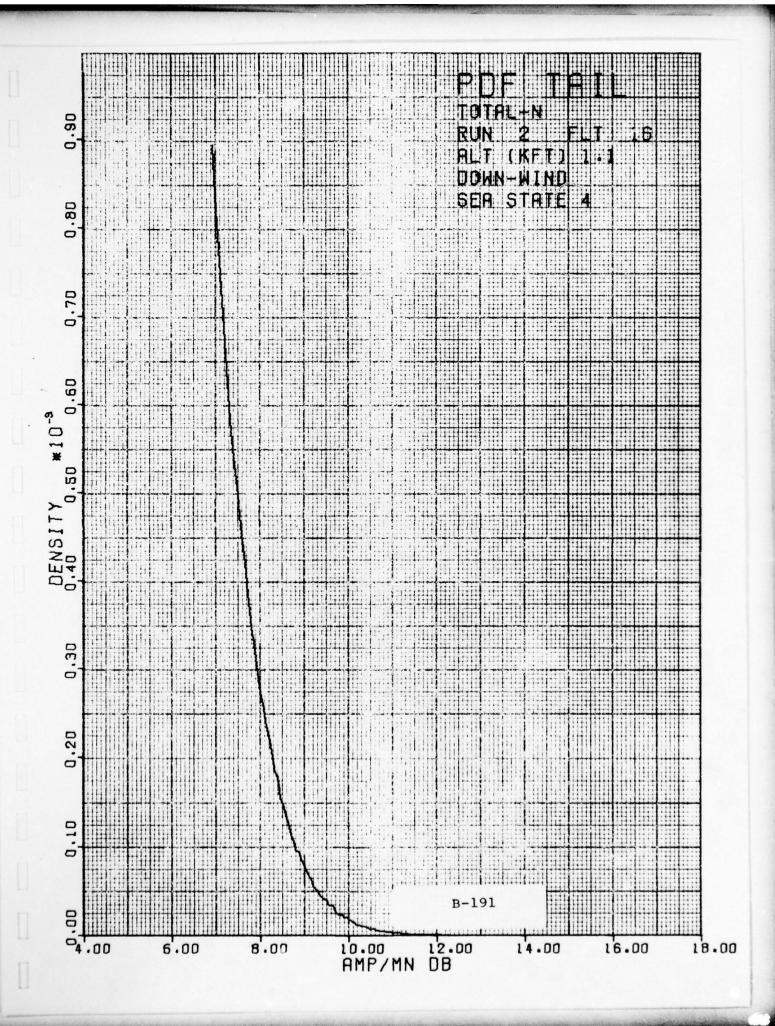


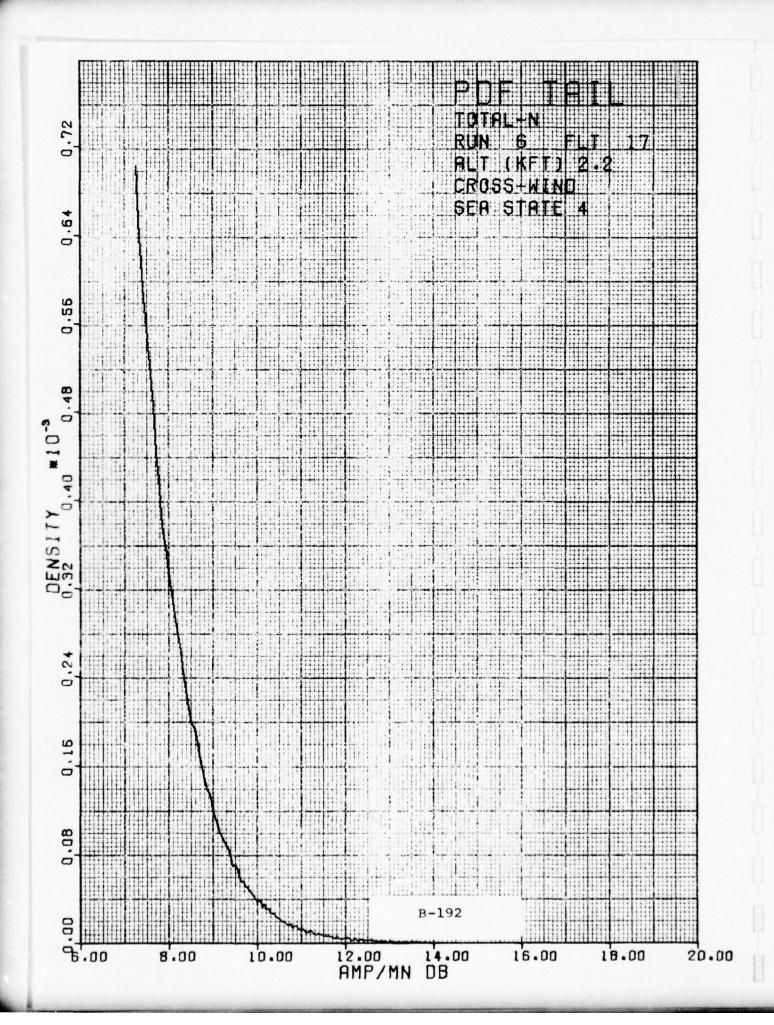


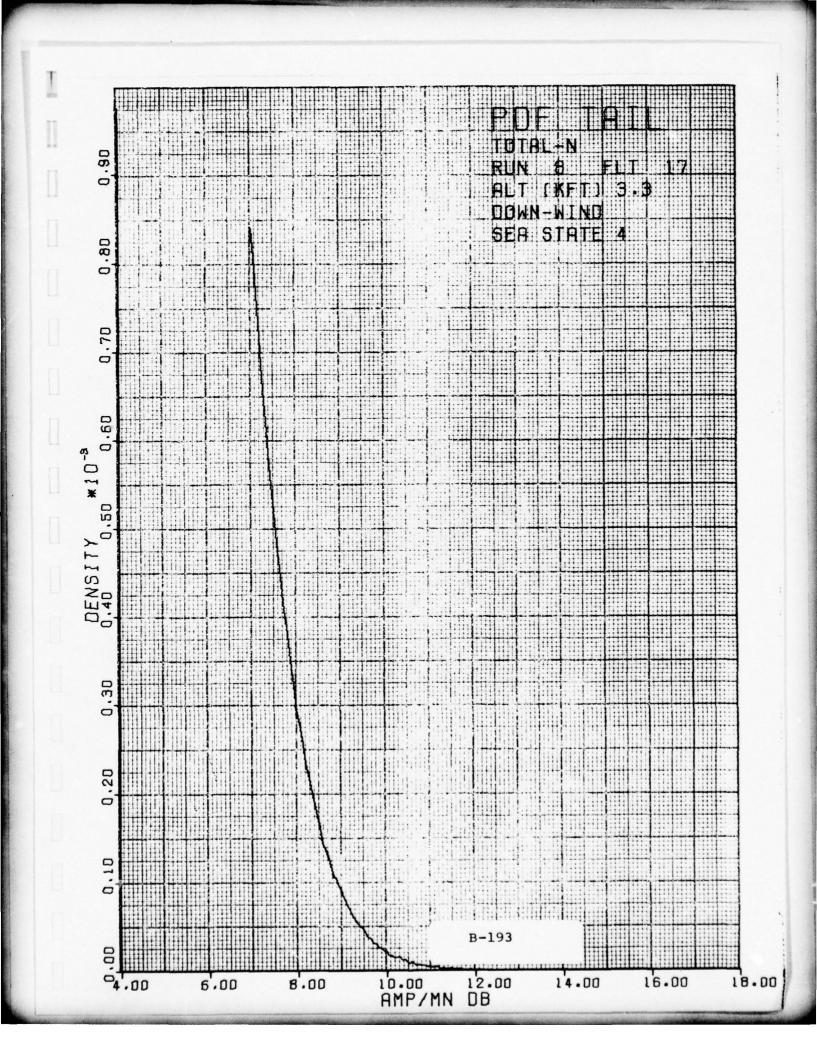












APPENDIX C ENVIRONMENTAL CONDITIONS

Determination of wind and sea conditions was done as part of the flight test program and was a General Dunamics responsibility. The following material was excerpted from their flight test report and is included here for completeness and for the convenience of the reader.

Sea and wind conditions and the resultant sea state were recorded for each flight as summarized in Table C-1. Surface contacts noted were also recorded (Table C-2).

More complete weather data over a period of hours before most flights was also recorded and is repeated from the General Dynamics flight test report as Table C-3 through C-17.

UNCLASSIFIED

TABLE C-1
SEA CONDITIONS FOR TAGSEA CLUTTER FLIGHTS

3E 2/5 whay white caps. Moderate 300 177 6 6 20 310 4 caps. 4E 2/9 Small answers with semic and and the caps. With earlier caps. 230 4 4 114 310 Moderate 5E 2/12 Confused sea with moderate 210 131 4 6 22 250 Moderate 6E 2/12 Large amount of white caps. 300 220 6 8 24 4 4 6E 2/12 Large amount of white caps. 300 220 6 8 24 6 4 7E 2/12 Large amount of white caps. 300 220 6 8 24 6 7 7 6 9 7 7 9 7 7 6 9 7 10 9 7 10 9 10 9 10 9 1 1 1 1 1 1 1 1 1	Flight No. E :: East Coast W :: West Coast	Date of Flight (1976)	General Description of Sen	Wave Direction (Deg True - From)	Wave Length (Ft)	Wave Period (Sec)	Wave Height Crest to Trough (Ft)	Wind Velocity Wind (KTS) Direction (Deg Teac-From)	Sea State (Hydrographic) and Description
2/9 Small answer of white capa. 2.90 9.0 4 4 1.14 3.20 small answer of white caps. Haze and run in the set vertelity. 2/12 Confused sea with moderate 210 131 4 6 22 240 and run in test vertelity. 2/12 I arrye amount of white caps. 300 2.20 6 8 24 300 100 and run in test vertelity. 2/12 Same as 6 except more 278 241 6 10 30 310 and run in test vertelity. 2/13 Same as 6 except more 278 241 6 10 30 310 and run in test vertelity. 2/14 Same as 3 except more 355 155 6 7 1 18 350 and run in test vertelity and confusion 210 250 15 2 1 3 20 250 15 2 25 255 255 255 255 255 255 255 255	3E	2/2	Many white caps. Moderate waves with wind shearing.	300	177	s	9	20	4 Rough
2/12 Confused sea with moderate 210 131 4 6 23 240 amount of white caps, Haze and rain in test vicinity. 2/12 I Large amount of white caps, 1300 220 6 8 24 500 form strenking, and apray ing. Large watch, and apray ing. Large watch and pray ing. Large watch caps are captured of sea surface. 2/12 Same as 6 except more 278 241 6 10 30 310	4E	2/9	Small amount of white caps, Small waves with some uniformity.	280	93	4	4	= \	3 Moderate
2/12 Large amount of white caps. Ing. Large amount of white caps. Ing. Large waves with breaking crests. 300 22 6 8 8 24 300 2/12 Same as 6 except more confusion of sea surface. 278 241 6 10 30 2/13 Same as 3 except more of except more as 3 . 355 164 7 6 17 210 2/13 Same as 3 except more of except more of except more as 3 . 355 164 7 6 17 210 2/14 Same as 3 except more of onlusion of except more onlusion of except more on whal. 360 16 7 18 350 3/9 No white caps or form. 360 16 3 1/2 3 45 3/10 Same as 10. 290 19 2 1 3 285 3/12 Same as 12. 280 42 3 2 9 286 3/22 Same as 3 except loss 300 143 6 6 15 285 3/23 Same as 16. 325 132 6 6 15 285 <td>5E</td> <td>2/11</td> <td>Confused sea with moderate amount of white caps. Haze and rain in test vicinity.</td> <td>210</td> <td>131</td> <td>4</td> <td>ဖ</td> <td></td> <td>4 Rough</td>	5E	2/11	Confused sea with moderate amount of white caps. Haze and rain in test vicinity.	210	131	4	ဖ		4 Rough
2/12 Same as 6 except more 278 241 6 10 30 310 2/13 Same as 3. 220 164 7 6 17 210 2/14 Same as 3 except more 355 155 6 7 18 350 2/14 Same as 3 except more 355 166 7 18 350 3/2 No white caps or foam. 360 16 3 1/2 3 3/10 Same as 10. 290 19 2 1 3 285 3/12 No white caps or foam. 310 31 2 1 3 285 3/12 No white caps or foam. 310 31 2 3 10 290 Simil waves with some captillary motion. 285 35 3 3 10 285 3/22 Same as 12. 285 35 3 3 10 285 3/23 Same as 3 except loss 300 143 6 6 15 285 3/23 Same as 16. 325 132 6 6 15 285	6 E	2/12	large amount of white caps, foam streaking, and spray- ing. Large waves with breaking crests.	300	220	9	œ		5 Very Rough
2/13 Same as 3. 220 164 7 6 17 210 2/14 Same as 3 except more of the confusion of whal shearting and confusion of whal shearting and confusion. 355 155 6 7 18 350 3/2 No white caps or foun. 360 16 3 1/2 3 45 3/10 Same as 10. 290 19 2 1 3 285 3/12 No white caps or foun. 310 31 2 1 3 285 3/12 No white caps or foun. 310 31 2 1 3 285 3/12 Same as 12. 280 42 3 2 9 286 3/22 Same as 12. 285 35 3 10 295 3/23 Same as 16. 325 132 6 6 15 285	7E	2/12	Same as 6 except more confusion of sea surface.	278	241	9	10		5 Very Rough
2/14 Same as 3 except more wind shearing and confusion of seen surface. 356 155 6 7 18 350 3/9 No white caps or foam. 360 16 3 1/2 3 45 3/10 Same as 10. 290 19 2 1 3 285 3/12 Same as 12. 280 42 3 10 290 3/12 Same as 12. 280 42 3 2 9 285 3/23 Same as 3 except loss 300 143 6 6 15 285 3/23 Same as 16. 325 132 6 6 15 285	8E	2/13	6	220	164	7	9		4 Rough
3/9 No white caps or foam, light and	9E	2/14	Same as 3 except more wind shearing and confusion of hen surface.	355	155	9	2		4 Rough
3/10 Same as 10. 290 19 2 1 3 285 3/12 No white caps or foam. 310 31 2 3 10 290 Sund liney notion. 280 42 3 2 9 285 3/17 Same as 12. 285 35 3 10. 295 3/22 Same as 3 except loss 300 143 6 6 15 285 3/23 Same as 16. 325 132 6 6 6 15 285	10W	3/6	No white caps or foam, Ripples with little or no wind,	360	16	3	1/2		1 Smooth
3/12 No white cappe or foam. 310 31 2 3 10 Sume as 12. 280 42 3 2 9 245 3/22 Same as 12. 285 35 3 3 10 285 3/23 Same as 16. 325 132 6 6 15 285	11W	3/10	(290	19	2	1		1 Smooth
3/17 Same as 12. 280 42 3 2 9 2H5 3/22 Same as 12. 285 35 3 3 10 · 295 3/23 Same as 16. 325 132 6 6 15 285	12W	3/12	No white caps or form, Small saives with somo capillary motion,	310	31	7	၈		2 Slight
3/22 Same as 3 except loss 300 143 6 6 15 285 3/23 Same as 16. 325 132 6 6 15 285	13W	3/17	7	280	42	8	2		2 Slight
3/23 Same as 16. 325 132 6 6 15 285	15W	3/22		285	35	n	8		2 Slight
3/23 Same as 16. 325 132 6 6 15	16W	3/23	Same as 3 except loss wind shearing.	300	143	9	9		4 Rough
The state of the s	17W	3/23		325	132	9	9		4 Rough

TABLE C-2 SUMMARY OF SEA SURFACE CONTACTS

FLIGHT NO.*	Date	Runs With Pictures of Sea Surface Objects	Frame Nos.	Location of Sea Surface Objects	Approx. Time T = Start of Run**
		2.2 kft cross wind	25	None within radar range gate coverage.	
3E	2/5/76	3.3 kft up wind	44	None within radar range gate coverage.	
		3.3 kft down wind	23	None within radar range gate coverage.	
			1	Ship approx in range gates 10, 11, 12, & 13	T + 7 sec.
6E	2/12/76	2.2 kft down wind	5	None within radar range gate coverage	
			15	Ship approx in range gates 14, 15, & 16.	T + 1 min: 45 sec.
		2.2 kft up wind	59	Ship appprox in range gates 14, 15, & 16.	T + 6 min: 53 sec.
	7E 2/12/76 2.2 kft cross wind		8	None within radar range gate coverage	
/E	2/12/16	2.2 KIT Cross Wind	9	None within radar range gate coverage	
	3/10/76	1.1 kft cross wind	64	Ship approx, in range gates 3 and 4.	T + 7 min: 28 sec.
11W	3/10/70	1.7 Kit cross wind	65	Ship approx: in range gates 1 and 2.	T + 7 min: 35 sec.
12W	3/12/76	2.2 kft down wind	54	None within radar range gate coverage	
	Coast	NTAINING PICTURES DBJECTS ARE LISTED.	COF	ACT IRIG TIME CAN BE RRELATING FRAME NU N TO CAMERA FRAME I MAGNETIC TAPE RECO	MBERS FROM EACH

TABLE C-3
TAGSEA WEATHER DATA SHEET

East Coast	Swell Height (Ft)	3.2	Calm	1.6	1.6	1.6	Calm	Calm	Calm
- 1	Swell Period (Sec)	5	. 4	5	5	ي.	1	1	1
LOCATION:	Swell Direction (Deg. True- From)	280	Calm	250	280	270	Calm	Calm	Calm
TEST I	eveW bniW IdeieH (17)	1.6	Calm						
	aveW bniW Period (592)	2	10	10	10	10	10	10	10
	Past Weather								
	Present Weather								
	VilidiziV (zəliM)	10	10	10	10	10	10	10	10
	Wind Velocity (Knots)	7	4	2	4	4	80	10	14
	Wind Direction (Deg. True- From)	260	240	10	180	110	170	180	240
2-4-76	(Cloud Cover (Eights of Sky)	4/8	4/8	1/8	5/8	5/8	1/8	2/8	2/8
DATE: 2	əmiT (TMƏ) (sıuoH)	00	03	90	60	12	15	18	21

C-4 UNCLASSIFIED

14giaH Ilaw2	6.5	6.5	6.5	6.5	8.2	ž	3.2	1.6
Swell Period (Sec)	က	က	വ	က	က	. V/N	ည	က
Swell Direction (Deg. True- From)	310	290	300	300	330	N/N	310	310
Wind Wave Height (F1)	3.2	3.2	3.2	4.9	4.9	N/N	1.6	1.6
Wind Wave Period (Sec)	က	2	2	വ	ည	N/A	c	ည
Past Neather								
Present neather								
yzilidisiV (zəliM)	10	10	10	2	5	N/N	10	10
Wind Velocity (Knots)	32	23	30	31	20	N/A	80	9
Mind Direction (Deg. True- From)	260	280	280	280	340	N/A	310	300
(Cloud Cover (Eights of Sky)	3/8	8/0	2/8	2/8	4/8	N/N	5/8	8/9
Time (TMD) (sruoH)	00	03	90	60	12	15	18	21
	(GMT) (Hours) (Hours) (Hours) (Hours) (Hours) (Houge, True- From) (Miles) (Knors) (Kno	(Cloud Cover (Eights of Sky) (Cloud Cover (Eights of Sky) Wind Direction Wind Velocity (Knots) Wind Velocity (Knots) Westher Persent Westher (Sec) Wind Wave (Sec)	00 (GMT) (Hours) (Cloud Cover (Hours) (Cloud Cover (Deg. True-From) 28 (Knots) Wind Velocity (Knots) Wind Velocity (Knots) Wind Velocity (Knots) Westher (Knots) Westher (Sec) 32 Wind Wave (Sec) (Pt) 33 Swell Direction (Pt) 53 Swell Period 54 Crue-From) 55 Swell Period 56 Coc) 57 Swell Period 58 Coc) 59 Swell Period 50 Swell Height	28	2/8 2/8 2/8 2/8 2/8 2/8 2/8 2/8 2/8 2/8	10 10 10 10 10 10 10 10	12 13 10 10 10 10 10 10 10	7

East Coast	Swell Height (17)	1.6	1.6	3.2	6.5	9.8	3.2	3.2	3.2
	Swell Period (Sec.)	വ	വ	ເລ	5	5.	5	5	2
LOCATION:	Swell Direction (Deg. True- From)	40	10	390	340	10	10	300	290
TEST	Wind Wave Height (F1)	Calm	Calm	1.6	3.2	6.5	1.6	1.6	1.6
SHEET	Wind Wave Period (Sec)	. 10	10	5	2	5	3	9	ည
TABLE C-5 TAGSEA WEATHER DATA SHEET	Past Neather								
TABLE WEATHE	Present Weather		Snow	Snow					
TAGSEA	Visibility (zəliM)	. ເວ	. 03	0.1	5	5	10	10	10
	Wind Velocity (Knots)	10	16	25	16	18	14	18	16
	noitection (Deg. True- (mor4	80	10	280	330	330	320	300	280
2-7-76	(Cloud Cover (Eights of Sky)	8/1	8/8	8/8	8/9	8/1	8/1	4/8	2/8
DATE: 2	miT (TMD) (sruoH)	00	03	90	00	12	16	18	21

UNCLASSIFIED

Swell Height (Ft)	4.9	4.9	4.9	1.6	1.6	1.6	3.2	4.9
Swell Period (Sec)	2	2	5	5	5	. 5	5	5
Swell Direction (Deg. True- From)	340	330	330	350	270	220	210	260
evsW bniW 3dpieH (17)	3.2	3.2	3.2	1.6	Calm	Calm	1.6	3.2
Wind Wave Period (Sec)	വ	5	5	5	10	10	5	5
rasq radrasW						Snow	Snow	
Fresent nedtseW						Rain		Rafn
Visibility (Ralim)	2	5	5	10	10	0.5	5	2
Wind Velocity (Knots)	20	16	15	14	8	12	20	14
noitzeation Wind Direction -eur T. (Deg. True- (mor-T	320	320	320	280	220	190	170	200
(Cloud Cover (Eights of Sky)	8/9	7/8	2/8	1/8	4/8	8/8	8/9	8/8
amiT (TMD) (sruoH)	00	03	90	60	12	15	18	21
	(GMT) (Hours) (Cloud Cover (Eights of Sky) Wind Direction From) Wind Velocity (Miles) Westher Present Westher Present Westher (Knots) (Sec)	(Cloud Cover (Eights of Sky) (Cloud Cover (Eights of Sky) Wind Direction (Deg. True-From) Westher Westher Westher (Knots) (Miles) Westher Westher (Knots) (Miles) Westher (Knots) (Miles) (Knots) (Knots) (Knots) (Knots) (Knots) (Knots) (Knots) (Knots) (Knots) (Keriod (Keri	(Cloud Cover (Eights of Sky) (Cloud Cover (Eights of Sky) (Cloud Cover (Eights of Sky) (Deg. True-From) (Miles) (Acsent Weather (Acsent Weather (Acsent Weather (Acsent Weather (Acsent Meight (Acsent Height (Acsent Miles) (Acse	26 (GMT) 27 (Hours) 28 (Eights of Sky) 29 (Cloud Cover (Eights of Sky) 20 (Eights of Sky) 320 (Hous) 40 (Mind Direction From) 41 (Mind Sky) 42 (Minds) 43 (Sec) 44 (Sec) 53 (Sec) 54 (Mind Wave (Sec) 75 (Sec) 76 (Sec) 77 (Sec) 78 (Sec) 79 (Sec) 70 (Sec) 70 (Sec) 71 (Sec) 72 (Sec) 73 (Sec) 74 (Sec) 75 (Sec) 76 (Sec) 77 (Sec) 78 (Sec) 79 (Sec) 70 (Sec) 70 (Sec) 70 (Sec) 71 (Sec) 71 (Sec) 72 (Sec) 73 (Sec) 74 (Sec) 75 (Sec)	1/8 320 33 34 6 (Gent) 1/8 320 320	17	Column C	(GMT)

TABLE C-6

TABLE C-7 TAGSEA WEATHER DATA SHEET

		-							
Const	Swell Height (F1)	3.2	1.6	1.6	1.6	1.6	1.6	3.2	3.2
East	Swell Period (Sec)	7	9	7	. 6	. 2	. 9	. 2	5
LOCATION:	Swell Direction (Deg. True- (mon ¹	270	270	280	290	290	320	270	270
TEST	evsW. bniV/ JdpieH (17)	1.6	Calm	Calm	Calm	Calm	Calm	1.6	3.2
	aveW briW Period (5eC)	ည	0	0	0	0	0	2	5
	izs9 nediseW								
	fresent redisesW								
	ViilidiziV (کتاناش)	ດ	10	10	10	10	5	. 5	5
	Wind Velocity (Knots)	80	14	11	11	10	20	14	20
1	Wind Direction Gog. True- (mor4	220	270	320	290	320	240	320	10
2-9-76	(Cloud Cover (Eights of Sky)	8/8	8/0	3/8	8/0	2/8	7/8.	3/8	4/8
DATE: 2	amiT (TMƏ) (znuoH)	00	03	90	60	12	15	18	21

C-8 UNCLASSIFIED

JAgiaH IIaw2 (14)	3.2	3.2	3.2	1.6	1.6	1.6	1.6	1.6
Swell Period (592)	5	9	5	5	ល	. ເວ	5	5
Swell Direction (Deg. True-	35	1	36	36	30	33	31	29
avsW bniW JugeH (F1)	3.2	1.6	1.6	Calm	Calm	Calm	Calm	Calm
Wind Wave Period (Sec)	5	5	ည	0	0	0	0	0
Past Weather								
Present Weather								
ytilidisiV (zəliM)	5	5	5	10	10	10	10	10
Wind Velocity (Knots)	19	20	. 16	12	11	11	10	14
Mind Direction (Deg. True- from)	10	320	340	320	300	320	330	20
(Cloud Cover (Eights of Sky)	4/8	4/8	1/8	1/8	8/0	8/0	8/0	1/8
	00	03	90	60	12	15	18	21
	(GMT) (Hours) (Cloud Cover (Eights of Sky) Wind Direction (Deg. True- From) Wind Velocity (Knots) Wind Velocity (Knots) Wind Velocity (Knots) (Knots) Wind Velocity (Knots) (K	(Cloud Cover (Eights of Sky) Wind Direction Wind Velocity (Knots) Wind Velocity (Miles) Present Weather Pest Weather Weather (Sec)	4 4 (Cloud Cover (Eights of Sky) 20 10 Wind Direction Wind Velocity (Knots) Westher Westher Westher Westher Westher Westher To Period To Period To CSec)	1/8 320 (Cloud Cover (Eights of Sky) Wind Direction (Deg True- From) Wind Velocity (Knots) Wind Velocity (Knots) Wind Velocity (Knots) Or Usibility Perent Westher Westher Or Or Period (Sec)	1/8 320 (Cloud Cover (Eights of Sky)) 1/8 320 10 Wind Direction (Deg. True-From) 320 32 11 Wind Velocity (Knots) 12 12 20 13 Present Weather 12 31 32 31 31 32 31 31 31 31 31 31 31 31 31 31 31 31 31	9/8 32 (Elghts of Sky) 3 4/8 4/8 (Elghts of Sky) 3 20 10 Wind Direction From) 3 20 20 10 Wind Velocity (Knots) 3 20 20 10 Wind Velocity (Knots) 1 2 2 2 1	0/8 320 11 12 20 19 Wind Wave (Cloud Cover Wind Direction (Cloud Cover Wind Direction (Eights of Sky) 220 320 320 10 Wind Velocity (Knots) 220 33 320 320 320 320 320 320 320 320	9/8 320 0 0 0 0 0 0 0 0 0 0 0 0 0 0 0 0 0 0

UNCLASSIFIED

(17)

4.9 3.2 4.9 4.9 4.9 East Coast Swell Height (2ec) Swell Period 2 2 2 2 D S S 2 TEST LOCATION: From) 200 250 240 250 200 Swell Direction (Deg. True-220 220 Calm (17) 3.2 1.6 1,6 2 2 2 Height 6. 8 Wind Wave TAGSEA WEATHER DATA SHEET (2ec) Period 2 ß S 0 2 S S 2 eveW briW Weather TABLE C-9 Izsq Weather Present (Niles) 10 10 10 5 N N 2 Visibility 20 20 25 27 23 20 (Knots) Wind Velocity Wind Direction (Deg. True-(mor1 200 210 200 210 190 180 170 8/8 1/8 4/8 8/8 8/8 2/8 1/8 2-11-76 (Cloud Cover (Eights of Sky) (Hours) DATE: 60 15 18 21 8 03 90 (CWI) 9mi T

C-10 UNCLASSIFIED

		TEST 1 OC
TABLE C-10	TAGSEA WEATHER DATA SHEET	

									,
Const	JugiaH Haw2	4.9	4.9	4.9	4.9	4.9	4.9	6.5	6.5
N. East	Swell Period (Sec)	വ	ខ	വ	ເດ	വ	ອ	2	က
TEST LOCATION: East Coast	Swell Direction (Deg. True- (mor4	220	260	250	260	. 560	260	290	320
TEST	evsW bniW Meight (14)	4.9	4.9	4.9	4.9	4.9	4.9	4.9	4.9
SHEET	aveW bniW Period (592)	co	က	D.	. 2	ប	D.	D.	ည
מספבת הבתוובה בתוך אחבר	1269 Weather								
	Present nadisaW								
	Visibility (Rijes)	2	87		10	م.	ខ	10	10
	Wind Velocity (Knots)	20	25	18	20	25	24	30	24
1	Nind Direction (Deg. True- From)	220	260	300	260	260	300	330	310
2-12-76	(Cloud Cover	8/8	8/8	2/8	1.8	3/8	2/8	2/8	2/8
DATE:	əmiT (TMƏ) (sruoH)	00	03	90	60	12	15	18	21

TABLE C-11 TAGSEA WEATHER DATA SHEET

Coast	JAgiaH Ilaw2 (F1)	4.9	3.2	3.2	3.2	4.9	N/A	N/A	6.5
N: East	Swell Period (Sec)	5	5	5	2	5	N/A	N/A	5
TEST LOCATION: Fast Coast	Swell Direction (Deg. True- From)	300	280	280	280	210	N/A	N/A	200
TEST	evsW bniW 14pieH (14)	3.2	Calm	Calm	1.6	3.2	N/A	N/A	1.6
	avsW bniW boina9 (5e2)	5		0	2	2	V/N	N/A	5
	Past Weather								
	fnesen¶ nedfseW								
	yillidiziV (zəliM)	10	10	10	5	2	N/A	N/A	5
	Wind Velocity (Knots)	18	80	8	20	22	N/N	N/A	19
1	Wind Direction (Deg. True- From)	270	290	290	180	210	N/A	N/A	210
3-13-76	(Cloud Cover (Eights of Sky)	2/8	1/8	1/8	2/8	1/8	N/A	N/A	8/8
DATE:	SmiT (TMD) (PluoH)	00	03	90	60	12	15	18	21

TABLE C-12 TAGSEA WEATHER DATA SHEET

				-					
East Coast	14gisH Ilsw2 (17)	6.5	3.2	3.2	3.2	1.6	1.6	N/A	6.5
- 1	Swell Period (Sec)	5	. 2	ည	5	വ	. 2	N/A	5
TEST LOCATION:	Swell Direction (Deg. True- From)	25	25	, 25	27	33	33	N/A	33
TEST	eveW bniW IdgieH (17)	3.2	3.2	3.2	1.6	1.6	1.6	N/A	3.2
2116	eveW bniW boin99 (SeC)	S	æ	8	5	5	2	N/A	ဌ
	resq Neather								
	Present Weather								
	y₁ilidiziV (zeliM)	73	10	10	2	. 2	. 2	N/A	10
	Wind Velocity (Knots)	18	17	12	10	18	20	N/A	22
1	noitoeniU briW -Su'T เอO) (ต่อาา	250	270	270	350	350	360	N/A	250
2-14-76	(Cloud Cover	8/8	1/8	1/8	8/8	8/8	8/8	N/A	8/9
DATE: 2	Time (GMT) (Salours)	00	03	90	60	12	15	18	21

TABLE C-13 TAGSEA WEATHER DATA SHEET TEST LOCATION: West Coast	JApiaH Ilaw2 (17)	2	8	23	83		
	Swell Period (Sec)	5	4.5	4.5	4.5		
	Swell Direction (Deg. True- From)	290	290	290	290	*	
	eveW bniW IdeieH (17)	1	1	1	1		
	eveW bniW boin99 (592)	2	2	2	82		
	1259 Weather						
	Present Weather						
	VilidisiV (ReliM)					ı	
	Wind Velocity (Knots)	5	5	S	വ		
	Wind Direction (Deg. True- From)	235	285	295	285	•	
	(Cloud Cover (Eights of Sky)						7
	əmiT (TS9) (niM — zhuoH)	9:55	10;25	10:43	11;26		

UNCLASSIFIED

				,				
Swell Height (Ft)	82	2	8	2	2	23	2	
Swell Perica (Sec)	11	11	111	11	11	. 11	. 11	
noitzeriO llew2 Lous True- (mor3								
evsW bniW 7dpieH (73)	е е	8	3	8	တ	အ	3	
evsW britw Period (Sec)	5.5	5.5	5.5	5.5	5.5	5.5	5.5	
rseq nadrsaW								
Present veather								
VilidisiV (səliM)				25	•			
Wind Velocity (Knots)	9	9	9	9	9	12	15	
Mind Direction -eu:T .eeO) From)	290	290	290	290	285	285	. 285	
(Cloud Cover -{Eights of Sky)							•	
əmiT (T29) (niM — anuoH)	10:38	10:45	11:00	11:15	11;30	12:00	12:30	
	(PST) (Hours — Min) (Cloud Cover (Eights of Sky) Wind Direction (Deg. True- Wind Velocity (Knots) (Miles) Present Westher Westher (Sec) (Petiod (Sec) (Petiod	(PST) (Mourt – Minn) (Cloud Cover – Minn) (Eights of Sky) Wind Direction (Choed – True– Wind Velocity (Miles) Wind Wave Wind Wave Petrod (Petrod (Petrod	100 (PST) 101 (PST) 102 (PST) 103 (Mours — Min) 103 (Cloud Cover of Eights of Sky) 104 (Eights of Sky) 105 (Cloud Cover of Eights) 106 (Cloud Cover of Eights) 107 (Cloud Wave of Eights) 108 (Cloud Wave of Eights) 109 (Cloud Mave of Eights) 110 (Sec) 111 (Sec) 112 (Sec) 113 (Sec) 114 (Sec) 115 (Sec) 116 (Sec) 116 (Sec) 117 (Sec) 118 (Sec) 118 (Sec) 119 (Sec)	1.00 (1.00 (PsT) (PsT) (Hours – Min) (1.00 (1.00 (PsT) (Hours – Min) (Cloud Cover (Eights of Sky) (Mind Velocity (Miles) (Mile	1.10 (1914) (1.10 (1914) (1.10 (1914) (1.10 (1914) (1.10 (1914) (1.10 (1914) (1.10 (1914) (1.10 (1914) (1.10 (1914) (1.10 (1914) (1.10 (1914) (1.10 (1914) (1.10 (1914) (1.10 (1914) (1.10 (1914) (1.10 (1914) (1.10 (1914) (1.10 (1914)	1.1 1.1	1.10 1.10	2.3

C-15 UNCLASSIFIED

TABLE C-15 TAGSEA WEATHER DATA SHEET TEST LOCATION: West Coast	Swell Height (17)	2	2	2	8	2	2	
	Swell Period (Sec)	11	11	11	11	11	11	
	Swell Direction (Deg. True- From)	285	285	285	285	285	285	
	evsW bniW IdgieH (17)	1	1	1	0.5	0.5	0.5	
	eveW bniW boine (SeC)	4	4	4	4	4	4	
	Past Weather							
	Present Neather							
	VilidisiV (səliM)	. 01	10	10	10	10	10	
	Wind Velocity (Knots)	9	, Q	3	9	. 9	3	
	Wind Direction (Deg. True- From)	305	285	285	285	295	295	
	(Cloud Cover (Eights of Sky)							
DATE: 3	əmiT (T29) (niM — anoH)	10:00	10:15	10:45	11:00	11:15	12:00	

UNCLASSIFIED

Swell Height (Ft) TEST LOCATION: West Coast 00 8 œ (Sec) Swell Period 14 14 14 -SunT (Deg. True-From) 270 Swell Direction (14) Height 9veW britw 4 4 4 (2ec) TAGSEA WEATHER DATA SHEET Period 2 വ 2 eveW brit TABLE C-16 Weather Past Weather Present (Niles) Visibility (Knots) 10 10 10 Wind Velocity (Deg. True-From) 295 Wind Direction DATE: 3-22-76 (Cloud Cover (Eights of Sky) 10:05 00:6 emiT (T29) (niM — £1100H) 9:50

2

(F1) Swell Height

~

TEST LOCATION: West Coast (Sec) Swell Period 14 14 Swell Direction (Deg. True-(mor7 N/A N/A Height (Ft) Wind Wave 9 9 (Sec) TAGSEA WEATHER DATA SHEET Period 9 9 Wind Wave Weather TABLE C-17 Iseq Weather Present (Miles) Visibility Wind Velocity (Knots) 10 10 Mind Direction (Deg. True-(mor1 285 3-23-76 (Cloud Cover (Eights of Sky) 12:50 6:45 DATE: (niM - muoH) Time (PST)

APPENDIX D DATA ANALYSIS SOFTWARE

This appendix describes the software used in TAGSEA data analysis. Functionally the tasks performed by the software are described in Section 8 (Vol. II).

Software structure for histograms and hit processing are documented here. Software for average analysis is included with that for histograms since this was the way the software was structured as some commonality exists. Histogram software is divided into two parts, initial and post processing, again based on the way the software was written.

1.1 Histogram and Mean Data Analysis Software

Several programs are used to perform histogram and mean analysis. The interrelationship of the program is shown in Figure D-1.

A description of each of the programs follows.

1.1.1 HISTOGRAM PROGRAM (TAGHIST)

The computer program TAGHIST was written primarily to generate histograms and histogram statistics for the clutter data. The basic tasks of the program were as follows:

- a) Read and decode a data reduction tape
- b) Form summation of time histograms and normalized histograms for forming range gate and total histograms
- c) Extract pertinent statistical parameters for the time histogram (timehist), range gate histograms and the total histograms
- d) Print out statistical parameters and certain histograms

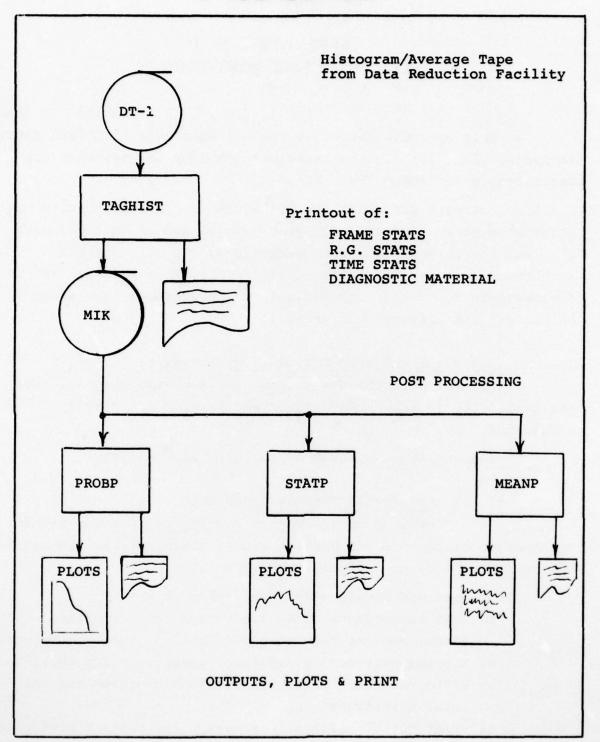


Figure D-1 Relationship of Histogram/Mean Programs

- e) Write data tape in CDC format for further data analysis of histogram results
- f) Extract average power per frame from data tape and write on tape in CDC format

The program has the following general annotated block diagram:

Program begins by clearing histogram arrays and read-in pertinent arrays.

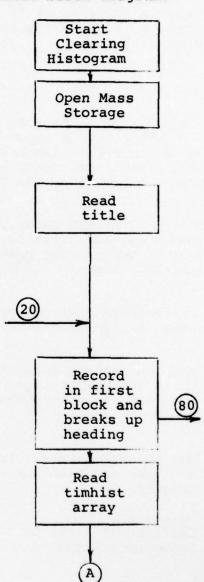
It now sets up for random access storage of the time histograms (timhist) arrays for each frame, zeros are written into timhist arrays,

The program now reads from the data tape the title and writes this information on tapes receiving histogram data and statistics

20 is the return point for the next timhist after the previous timhist per frame and the necessary data has been extracted and recorded.

Reads in the first block and extracts range gate, histogram frame number and altitude from the first word in record. An end of data causes the program to jump to 80.

Reads from mass storage a new timhist array.



When new block contains a change in range gate (r.g.) tag, the program jumps to 60 to output range gate sum histograms (R.G. hists) and statistics.

The program normalizes per logic control given at input and either normalizes the time histograms, R.G. hists, and total histograms (Tothist) or only the Tothist.

The program now reads from the data tape and extracts one word giving the average power for the previous frame.

The average power is printed out onto the lineprinter.

The program now extracts 600 words. These are the averages over 600 FFT frames contained in the previous histogram.

The 600 FFT averages are now put on MIK TAPE and also put out on line printer.

The timhist array of the previous frame is written to mass storage.

32 words are now extracted. These are the average power for the 32 doppler cells over 600 FFT frames in the previous histogram frame record.

T New R.G. Tag (60) (30) Put out range hist data and statistics Normalizes histograms Power per frame Print out power Read 600 Words Write 600 average ON TAPE out and line printer Timhist to mass storage 32 words extracted - average power

UNCLASSIFIED 32 DOP cell The 32 doppler cell averages are printed on the line printer. averages printed out 32 DOP cell The 32 doppler cell averages are written on MIK TAPE. averages on tape out There are logic switches which allow selected histograms to be out Logic out on line printer and out on MIK TAPE (20) (80) When the end of information is Print out encountered in a new block of data, Range Sum the program branches to this point Histo. Stats, Time frame sum, to put out last range sum histograms data and statistics. and total sum The time frame sum histograms and the total sum histogram with statistics are also printed. Read time frame The program now reads from mass storage the time frame histogram histogram data. The array of frame averages are Write array -out written.

on tape.

The information requested by control cards are written out

1.1.2 Probability Plots (PROBP)

Probability plots are generated from a data tape that is written by the histogram program (TAGHIST).

Write TO tape

STOP

- out

The probability density, distribution and mean value for each range gate are read sequentially from the data tape. After the data for each range gate is read, two running sums are accumulated. The first is a sum of normalized range gate histograms, normalized range gate by range gate, and the second is just a sum of the range gate histograms. When the data for the last range gate is processed, the probability density and distribution of the total histogram is read. This data is generated in the histogram program and is already normalized histogram frame by histogram frame.

"TOTAL-N" type plots are generated from this histogram normalized data. The accumulated range gate "normalized" data is then processed to produce "TOTAL-A" type plots and the accumulated "Un"-normalized range gate data is processed to produce "TOTAL" type plots.

1.1.3 Statistics Plots and Processing (STATP)

Statistics plots and the associated processing is done from a data tape written by the TAGHIST program.

The necessary statistics are read from the data tape for each frame and each range gate and are stored. The stored data is scanned to eliminate frames and range gates with incomplete sets of statistics.

Plots are generated of the statistics-vs-frame number and statistics-vs-range gate. The mean is removed from each data set and a normalized set of plots is also generated.

Statistics of the mean are computed for the data set where the mean was computed in each histogram frame. Statistics are also computed for the mean normalized median, 10^{-1} , 10^{-2} , 10^{-3} and 10^{-4} probability levels. These "statistics" of the statistics are then output to the printer.

1.1.4 Average Plots (MEANR)

Average plots are generated from a data tape that is written by the histogram program. The histogram program reformats this data so it is compatible with the CDC computer system.

Data is read from the data tape a range gate at a time. One hundred FFT frames are averaged at a time to produce an output data point. At the completion of a range gate, the next set of range gate data is read.

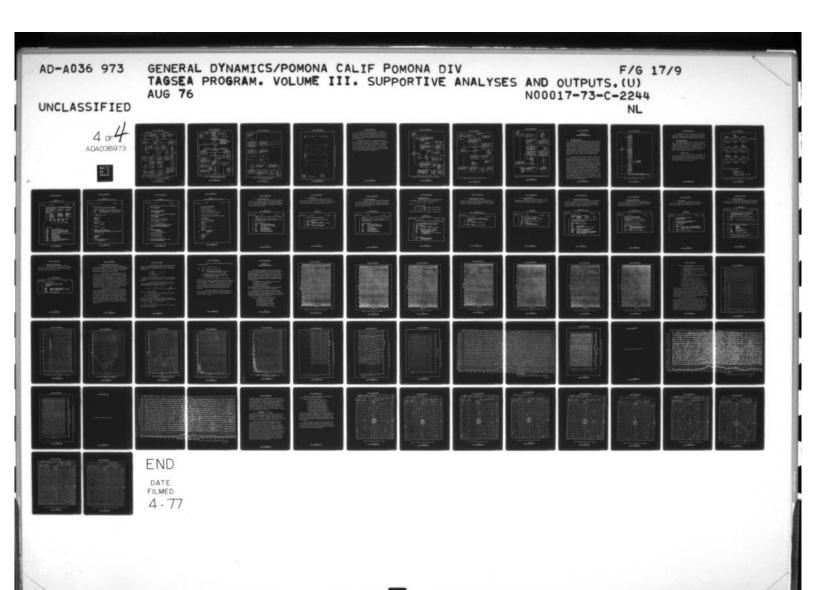
The average range gate data is plotted a range gate at a time. Each range gate is offset from the preceeding range gate by 2dB so the average plots will not overlap.

1.2 Hit Software Flow Charts

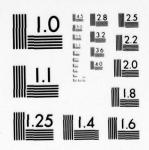
Overall software flow for hit processing is summarized in Figure D-2. The DT-1 hit tape received from the Data Reduction Facility is sorted from sequential range gate to sequential time by use of mass storage devices (i.e., computer disk storage). The sorted hit tape is used for all subsequent software flow.

The three main paths indicated summarize software flow for Hit Map, Hit Counts vs. Time and Conditional Probability Map Processing. A data processing program and plot program are shown within each path. Various summary printouts are generated for use as diagnostic tools at each step in processing. In addition, optional printouts and special dump options are built into the software for special analysis.

Detailed flow charts for Hit Map processing in Figures D-3 and D-4 describe input/output operations, processing algorithms and plot steps. Typical hit map printout is presented in Figure D-5. Hits in each 100 ft. X 100 ft. cell are listed along with sums over range, time and a total.



4 of 4 ADA036973



MICROCOPY RESOLUTION TEST CHART NATIONAL BUREAU OF STANDARDS 1963-A

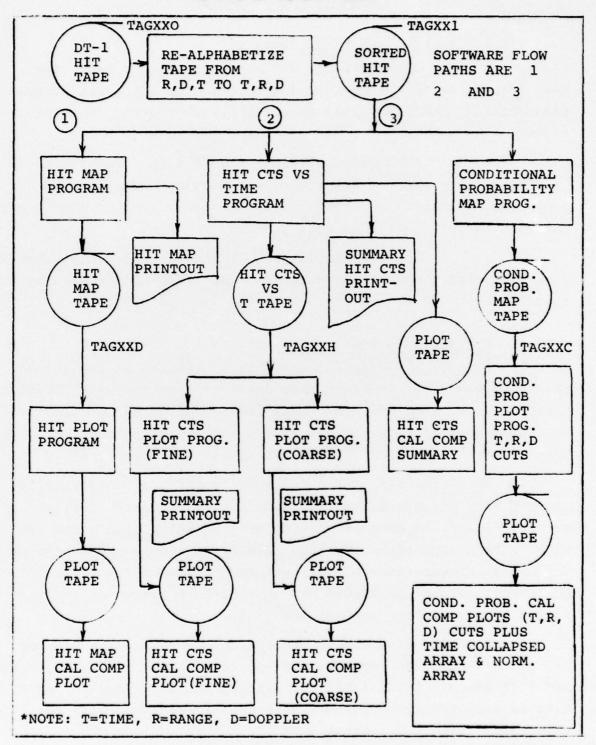


Figure D-2 DT-1 Hit Data Processing Overall Software Flow Chart

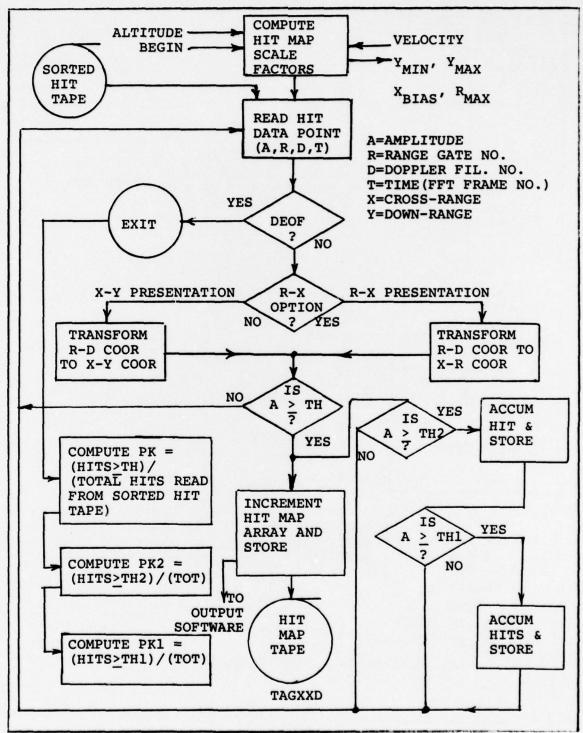


Figure D-3 Hit Data Processing for Hit Map and Large Hit Detection

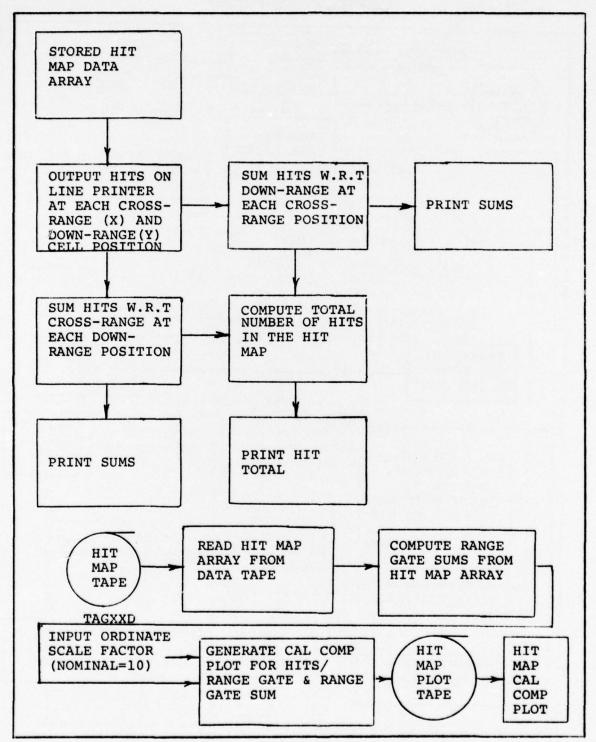


Figure D-4 Hiť Map Output Software Line Printer Outputs & Plots

NOS		10	21	36	32		•	•		•	30	28	38	60480
	16	2	4	e	7	•		•		•	4	1	7	3695
	•	•	•	•	•	•	•	•	•	•	٠	•	•	
	•		•		•	•	•		•	•		•	•	
	•	•	•	•		•	•	•		•	•	•		
	•	•	•	•	•	•		•	•	•	•	•	•	•
NGE		•	•					•		•			•	•
DOWNRANGE	В	2	8	8	7	•	•	•	•		7	9	2	3801
	2	e	1	e	7	•	•	•		•	-	2	e	3690
	1	1	2	9	4	•	•	•	•	•	e	2	1	3780
CROSS RANGE, FEET		100	200	300	400	•	•	•	•		125800	125900	126000	

Figure D-5 Hit Map Line Printer Output

Hit Counts vs. Time data processing is indicated in Figure D-6. Plot program flow is detailed in Figure D-7. Hit Counts in each FFT time frame and range gate are written to an output tape. The plot program contains processing software sufficient for plotting fine and coarse Hit Counts vs. Time from the same data tape.

Processing for generation of Conditional Probability
Maps is detailed in Figure D-8. Data processing for construction
of the Conditional Probability Cube is defined in the left half
of the flow chart. Plot processing is indicated on the right
half of the flow charts. Options are built in for plotting
cuts by time, range and doppler on all cuts. The time collapsed
array and normalization array are standard output for any choice
of cuts through the Conditional Probability Cube.

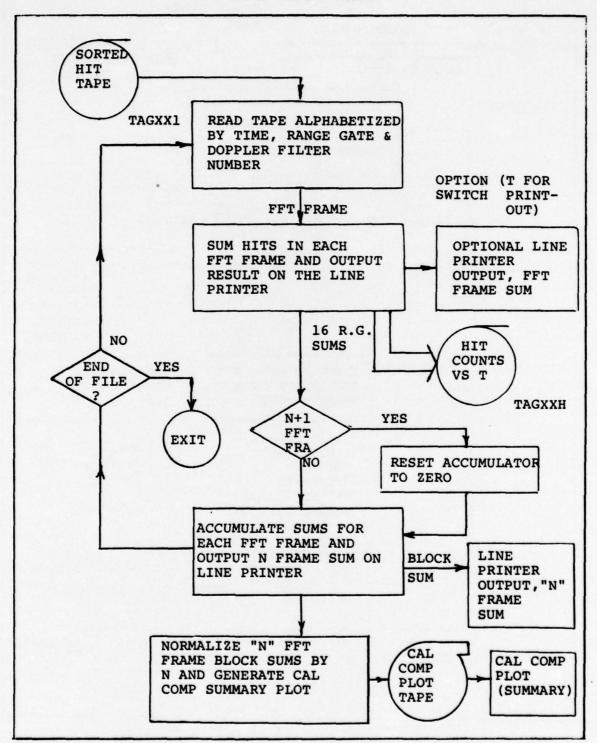


Figure D-6 Hit Counts Versus Time Data Processing

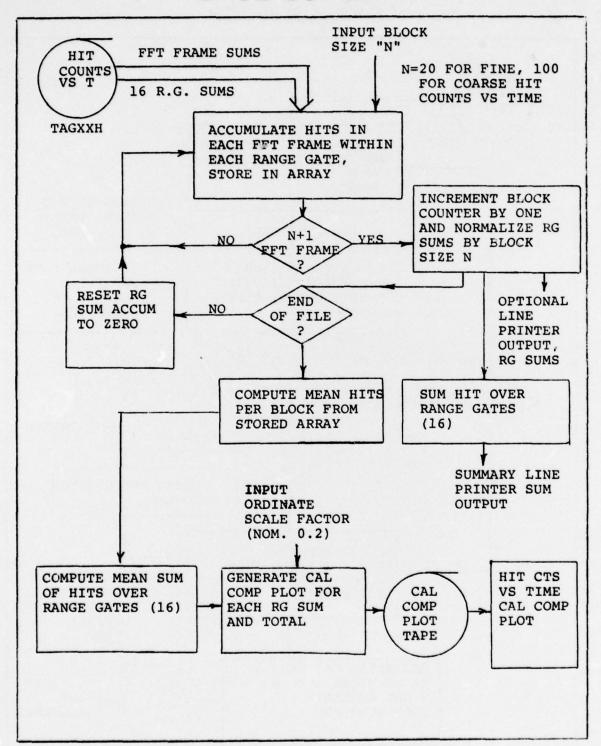


Figure D-7 Hit Counts vs Time Plot Program

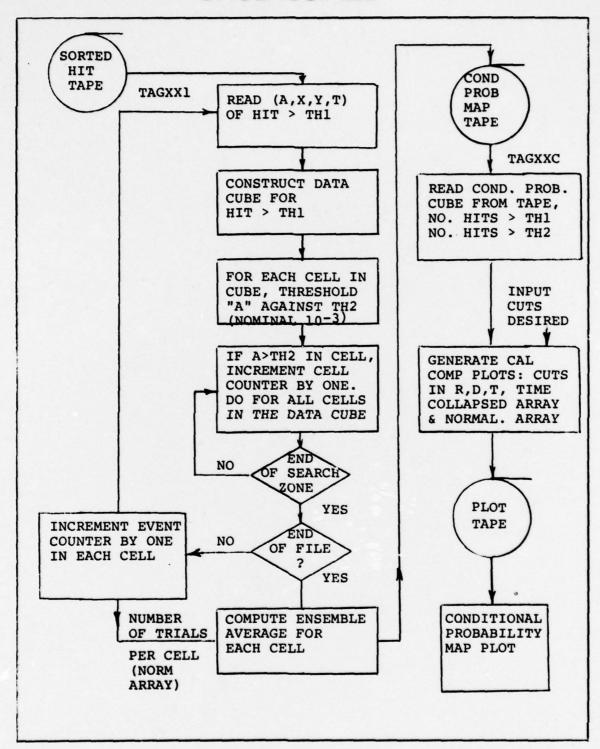


Figure D-8 Software Processing for Conditional Probability Maps

APPENDIX E SIMULATION SOFTWARE

1.1 Simulation Structure

The simulation of the TAGSEA system, clutter model, and analog data reduction was designed to provide accurate results while minimizing the amount of complex calculations required. Considerable effort was devoted to improving efficiency since literally millions of numbers need to be generated to simulate a run. The simulation was specifically designed to model the TAGSEA system only. Ideas and sections of previously existing clutter simulations were utilized, however, and the simulation was configured in such a manner that generalization and/or modification to another system could be accomplished quite easily.

A flow chart of the simulation is shown in Figure E-1. The program starts by reading a set of inputs which define the geometry and various system parameters. Then various system parameters which can be considered "stationary" over a short period of time are generated and placed in arrays. The clutter model is then used to provide values with the correct amplitude and distribution. These values are then passed through a model of data reduction analog processing which modifies the data on the basis of the best estimate of the clutter-independent parameters. These clutter values are then written to two tapes which are equivalent to the digital tapes normally provided by the data reduction facility. After the values have been written to the tape a decision is made to stop of not. If the run continues a further decision is made as to whether to update the "stationary" parameters or not. At the end of the run the tapes are sorted to the correct order and passed on for processing by the standard TAGSEA software.

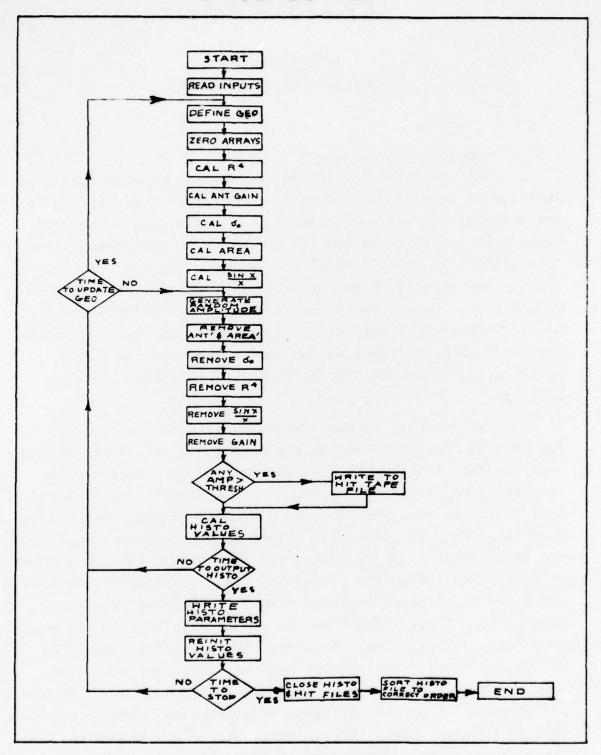


Figure E-1 TAGSEA Simulation Flow Chart

The transfer function block diagram for the simulator is shown in Figure E-2. Shown in this diagram are the effects modeled in the simulation and the neames of the subroutines (discussed in the next section) where the modeling takes place.

1.2 Detailed Description

The following subsections contain the detailed code and description of the TAGSEA simulation. A listing of the main program is provided. This listing contains a definition of the program inputs and outputs and a key variable dictionary. It also defines the overall structure. A description of each subroutine is also included, giving the inputs, outputs, and modeling assumptions used in each routine.

1.2.1 Program Listing

Table E-1 (in four parts) is a reproduction of the simulation program printout including comment cards. It is the basic function of this program to implement the flow chart previously described and to call up the subroutines which are the subject of the succeeding subsections.

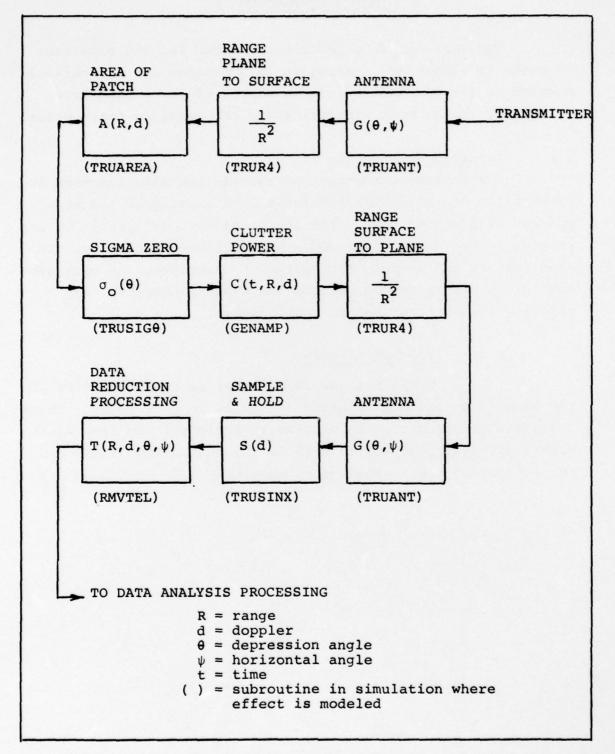


Figure E-2 TAGSEA Simulation Transfer Function Diagram

TABLE E-1 TAGSEA SIMULATION PROGRAM

```
76/0
PROGRAM TAGSIM 74/74 OPT-1
                                                                                   FTN 4.0+420
                 PRCGRAM TAGSIMIINPUT.OUTPUT.HIT.HISTO.TAPE11.M605 .TAPE98
                     *TAPES=INPUT, TAPE6=OUTPUT. TAPE10=HIT, TAPE12=HISTO: TAPE99=M605)
                                                                XPOS (32+16) +
                  DIMENSION
                                   CELLA (32,16)
                                                                                             YPOS (32.16)
                  DIMENSION NCELLAB (32.16)
                                                          HISTARY (1660) .
                  COMMON INCEX (901) .
                                                                                      STOR (110.16)
                                                          FRMPWR (600, 16) .
                             TOTPO# (16) .
                                                                                      UOPAVG (32, 16)
                  EQUIVALENCE (CELLAB, NCELLAB)
                  INTEGER HITTHR
                  REAL LAM
                                                          PLVEL /440./.
                                                                                      PLALTD/0.0/
                  DATA
                             PLALT/1100./*
                . .
                             PLVEL0/0.0/.
                                                          TPLALTD/1000:0/.
                                                                                       TPLVELD/1000.0/
                                                         WDDIR/90.0/.
DHANGE/100.0/.
                             WDVEL/0.0/.
                                                                                       LAM/0.1/
                 3
                             PRF/19300.0/
                                                                                      UDOP/109.0/
                             RANGE/4500.0/.
                                                          DOPOFF/4000.0/.
                                                                                       TOF/1.0/
                             CTGEO/1000.0/.
                                                          OTHISTO/5.0/ .
                                                                                      SHFREQ/14100.0/
                             HITTHR/100/
                  NAMELIST /IN/
                                                                                      PRE
                             PLALT.
                                            PL VEL .
                                                          PLALTD.
                                                                        PL VELD.
                 2
                                           "DVEL"
                                                                        DOPOFF.
                                                          WUDIA.
                             TPLVELU.
                                           DDOP.
                             CRANGE.
                                                          RANGE.
                                                                                      TOF
                                                                      HITTHR
                                                          SHEHEQ.
                             CTEEO.
                                           CTHISTO.
         C
         C
                                    PHOGRAM TO SIMULATE TAGSEA DATA GENERATION
          C
                  PROGRAM INFUTS
                                    ALTITUDE OF PLANE (FT)
VELOCITY OF PLANE (FT/SEC)
RATE OF CHANGE OF PLANE ALTITUDE (FT/SEC)
HATE OF CHANGE OF PLANE VELOCITY (FT/SEC)
PERIOD OF PLANE ALTITUDE VARIATION (SEC)
PERIOD OF PLANE VELOCITY VARIATION (SEC)
                  PLALT
                  PLVEL
          C
                  PLALTO
                  PLVELD
                  TPLALTO
                  TPLVELD
          C
                                    WIND VELOCITY (FT/SEC)
WIND DIRECTION (GLÜCKWISE FROM PLANE VELOCITY) (DEG)
WAVELENGTH (FT)
THANSMITTER PRF (HZ)
                  WOVEL
                  WDDIR
                  LAN
                  PRF
                                    HANGE GATE WIDTH (FT)
                  DRANGE
          CCC
                  DDOP
                                    FFT CELL WIDTH (HZ)
MINIMUM GATED RANGE (FT)
IF DOPPLER OFFSET (HZ)
TIME OF FLIGHT (SEC)
TIME INCREMENT TO DPDATE REDMETRY (SEC)
TIME INCREMENT TO WRITE HISTOGRAM RECORDS (SEC)
SAMPLE AND HOLD FREQUENCY (HZ)
HIT THRESHOLD
                  RANGE
          C
                  DOPOFF
                  TOF
                  DTGEO
          C
                  DTHISTO
                  SHEKEU
                  HITTHR
```

TABLE E-1 TAGSEA SIMULATION PROGRAM (cont'd)

```
PROGRAM TAGSIM
                         74/74 OPT=1
                                                                                FTN 4.6+420
                                                                                                          76/1
         C
                 PROGRAM CUTPUTS
                 FILE HISTO
                                   HISTOGRAM RECORDS FOR TAGSEA PROCESSING
                 FILE HIT
                                   SORTED HIT RECORDS FOR TAGSEA PROCESSING
                 MAJOR INTERNAL VARIABLES
                                34. 16 ARRAY USED TO STORE SEWI-STATIONARY EFFECTS
34. 16 ARRAY CONTAINING TOTAL AND PROCESSED CLUTTER RETURNS TOTAL PLANE VELOCITY
         CC
                 CELLA
                 CELLAB
                 VEL
                                   NURMALIZING GAIN EQUIVALENT TO CALIBRATION SIGNAL
                 INITILIZATION CONSTANTS AND INITIAL VALUES
                 PI=4.04ATAN (1.0)
                 T=0.0
                 TWOPI=2.0*PI
                 TLAST=0.0
         C
                 INITIALIZE FILES
                 REWIND 16
                 CALL UPENMS (11. INDEX. 801.0)
                 REWIND 12
                                   READ INPUTS
                 READ(5, IN)
                 WRITE (6. IN)
         CC
                                   DEFINE GEOMETRY
                 CONTINUE
                 VELP=PLALT+PLALTD*SIN(TWOPI*T/TPLALTD)
VELP=PLVEL+PLVELD*SIN(TWOPI*T/TPLVELD)
VELSQ=VELP*VELP*WDVEL*WDVEL-2.0*VELP*WDVEL*COS((180.-WDDIR)/TWOPI)
                 VEL =SURT (VELSO)
                                   CLEAR ARRAYS
         C
                 DO 10 1=1.16
DO 10 J=1.32
CELLA(J.I)=1.0
                 CONTINUE
          10
                 GNN OR = 1 . 0
         c
                 FIND AREA OF EACH PATCH
AND X AND Y POSITION FOR LATER USE:
AND MODIFY CELL ARRAY BY
```

TABLE E-1 TAGSEA SIMULATION PROGRAM (cont'd)

OGRAM TAG	SIM 74,74 OPT=1 FTN 4.0+420
С	
	CALL TRUAREA (CELLA . XPOS . YPOS . ALT . RANGE . VEL . LAM . DUOP . URANGE . ANNO
c	CO. 1 2
C	FIND RAMA FOR EACH RING AND MODIFY CELL ARRAY BY
č	/HOOA
č	The state of the s
C	
	CALL TRURS (CELLA , RANGE , DRANGE , GNNOR)
C	FIND ANTENNA GAIN FOR EACH PATCH
C	MUDIFY CELL ARRAY BY OGAIN 002
č	The second secon
	CALL TRUANT (CELLA, XPOS, YPOS, ALT, PLVEL, WOVEL, WODIN, VEL, GNNOR)
C	
C C	CALCULATE SIGNA ZERO AS A FUNCTION
C	CF GRAZING ANGLE
,	WUDIFY CELL ARRAY BY *SIGO
CCC	-41ā0
	CALL TRUSIGO (CELLA. ALT. RANGE. DRANGE. GNNOR)
C	CALCULATE SIN X/ X FOR THE AMPLED SPECTIUM
C	PODIFY CELL ARRAY BY
C	*S1NX/X
C	
	CALL TRUSINX(CELLA, PRF, DDOP, DOPOFF)
C	AT THIS POINT THE CELL ARRAY HAS ALL THE
c	SEMI-STATICNARY PARAMETERS ACCOUNTED FOR
C	NEXT IS THE GENERATION OF THE RANDOM PARAMETERS
C	AND THE REMOVEL OF TELE ESTIMATES OF TERMS
C 300	CONTINUE
C	
c	GENERATE RANDOM AMPLITUDES
C	PLACE INTO CELLAB ARRAY CELLAB=CELLA+RANDOM
č	CETETOSOEL PRANTINGON
c	CALL GENAMP (CELLA, CELLAB, XPOS, YPOS, T. VEL)
C	SINULATE TELE MAY PROCESSING
CCC	SINCE THIS IS DONE REPEATATALY
Č	IT WILL BE DONE IN ONE PASS
c	
C	CALL RAVIEL (CELLAR. ALT. DOPOFF. GNNOR)
ç	
C	DATA IS NOW IN A FORM SUITABLE FOR OUTPUT TO TAPES
C	SIMULAR TO TELE TAPES FROM BAY CHECK THE DATA AND WRITE THE TAPES
	CHECK THE DATA AND WRITE THE TAPES

TABLE E-1 TAGSEA SIMULATION PROGRAM (cont'd)

ROGRAM 1	AGSIM 74/74 OPT-1 FTN 4.6-420
c	
C	FIRST QUANTIZE TO 1024 AMPLITUDES
	CALL NORM (CELLAB . NCELLAB . MAX . MIN)
C	WRITE SORTED HIT TAPE
C	CALL WATHIT (GELLAR, MITTHR, MAX, MIN)
c	CALCULATE AND WRITE HISTO TAPE
Č	
c	CALL WRTHIST (GELLABODTHISTOOMAX.MINOALTOFRAME)
00000	PROCESSING FOR THIS DWELL IS NOW FINISHED
C	CHECK FOR END OF RUN AND LOOP BACK TO START ANOTHER UNELL
C	
	IF(T.GT.TOF) GU TO 15 T=T+128./SFFREU
C	CHECK IF TIME TO UPDATE GEOMETRY
С	IF(T-TLAST.LT.UTGEO) GO TO 300 TLAST=T GO TO 200
C	END OF FLIGHT
C	5 CONTINUE
C	CLOSE HISTC AND HIT FILES
Č	The state of the s
	ENCFILE 10 ENCFILE 10
C	HISTO TAPE MUST BE SORTED TO RANGE-TIME FROM
C C C	TIME, RANGE
	CALL SORTHIS(FRAME)
c	ENDFILE 12
	ENOFILE 12
C	END OF RUN
-7 - 7 - 8	STOP 1
	ĒNO

1.2.2 True Area Subroutine

The true area subroutine of Table E-2 responds to the call up TRUAREA of Table E-1. The area is computed using a trapezoidal approximation of the surface range-doppler cell. All four corner locations are computed and the center found by averaging the corners.

TABLE E-2
TRUE AREA SUBROUTINE

UBROUT	INE TR	UAREA 74/T	4 0PT=1	FTN 4	.6+420	76/
	c	SURROUTINE 5 ANNOR)	TRUAREA (CELLA» POS»	YPOS.ALT.MANGE.VEL.LA	M.DDOP.DRANG	e.
	č	-476 6118	IDDITTANE EVANS THE TO	WE AREA OF THE GROUND		
	Č			OSITION OF THE PENTER		
	č	CELES MESA	Trans the a man to	Partition of the Penter	OF THE CECE	
	č	MODIFIES E	ELLA BY OAPEA			
	c					
	č					
	c	MONIFIED #	ARAMETERS			
	Č	CELLA	32.16 RPOUND CELL	ARRAY		
	C	XPOS	32.16 x POSITION	OF CENTER OF CEIL		
	C	YPAS	37.16 POSITION O	F CENTER UF CELL		
	C	GNNOR	NORMALIZING MAIN	FOR TELE PROCESSING		
	C					
	C		INPUTS PEQUIPED			-
	C	ALT	ALTITUDE OF BLANE			
	C	RANGE	MINIMUM RANGE REC			
	C	VE!	TOTAL VELOCITY (FT	/SEC)		
	C	LAW	WAVELENGHIFTS			
	C	DOOP	DELTA DOPPLE BETW			
	C	DRANGE	DELTA RANGE RETWE	EN CELLS (TT)		
	C					

1.2.3 R⁴ Subroutine

As with the previous subsection and those to follow, the R^4 subroutine (shown in Table E-3) is called up by the program of Table E-1. It is the function of this particular program to compute the R^4 term to the center of each cell.

TABLE E-3
R4 SUBROUTINE

SUBMOUTINE TE	PURA 74/	14 OPT=1	FTN 4.6+420	76/
	SURROUTIN	E TRURA (CELLA, MAÑGE, DRANGE	, onnur(
C				
C		THIS SURROUTIEN FINDS	ROOM FAR EACH CELL	
C	TO THE CE	NTER OF THE CELL		
C				
C	MONIFIED	MARAMERERS	The second street was a second	
C	CELLA	WORKING GRUUND CELL ARE	PAY	
Č	GNAIOR	NORMALIZING GAIN FOR PE	EMOVING TELE CONSTANTS	
				-
Č	INDUTS RE	GUIRED		
c	RANGE	RANGE TO EUGF OF FIRST	CFILIÉTI	
· - · · · · · · · · · · · · · · · · · ·	DRANGE			
c	•	DEC. A MANOR METHERN OF		
č				

1.2.2 True Area Subroutine

The true area subroutine of Table E-2 responds to the call up TRUAREA of Table E-1. The area is computed using a trapezoidal approximation of the surface range-doppler cell. All four corner locations are computed and the center found by averaging the corners.

TABLE E-2
TRUE AREA SUBROUTINE

	# ANNOR) THIS SU CELLS ALS MONIFIES	
	MONIFIES MONIFIES MONIFIED CELLA XPOS YPOS	SELLA BY AREA WARAMETERS 32.16 GROUND CELL ARRAY 32.16 X POSITION OF CENTER OF CELL
	MONIFIES MONIFIES MONIFIED CELLA XPOS YPOS	SELLA BY AREA WARAMETERS 32.16 GROUND CELL ARRAY 32.16 X POSITION OF CENTER OF CELL
	MONIFIES MONIFIED CELLA XPOS YPOS	MARAMETERS 32.16 GROUND CELL ARRAY 32.16 X POSITION OF CENTER OF CELL
0000000000	MONIFIFD CELLA XPOS YPOS	WARAMETERS 32.16 GROUND CELL ARRAY 32.16 x POSITION OF CENTER OF CELL
	CELLA XPOS YPOS	32.16 GROUND CELL ARRAY 32.16 x POSITION OF CENTER OF CELL
000000	CELLA XPOS YPOS	32.16 GROUND CELL ARRAY 32.16 x POSITION OF CENTER OF CELL
00000	CELLA XPOS YPOS	32.16 GROUND CELL ARRAY 32.16 x POSITION OF CENTER OF CELL
0 0 0	YPOS	32.16 x POST-TON OF CENTER OF CELL
000	YPAS	
C		37.16 PPOSITION OF CENTER OF CELL
Č	GNAIDE	
C	GITAGON	NORMALIZING MAIN FOR TELE PROCESSING
A STATE OF THE STA		INPUTS REQUIRED
č	ALT	ALTITUDE OF BLANE (FT)
č	RANGE	MINIMUM RANGE RECEIVED (FT)
c	VE!	TOTAL VELOCITY (FT/SEC)
č	LAW	WAVELENGHIPT
Č	DOOP	DELTA HOPPLE RETWEEN CELLS(H)
C	DRANGE	DELTA RANGE RETWEEN CELLS (TT)
C		

1.2.4 Antenna Subroutine

Antenna gain is found to the center of each patch using an analytic formula for the antenna gain

$$\label{eq:Gamma_def} \mathsf{G} \ \left(\theta,\psi\right)_{\mathrm{dB}} = 11 \ - \ \mathsf{K}_{\mathrm{AZ}}(\psi^2) \ - \ \mathsf{K}_{\mathrm{EL}}(\theta^2)$$

where,

11 = peak gain in dB $K_{AZ} = 4.61 \times 10^{-3} \frac{dB}{deg^2}$ azimuth rolloff constant $K_{EL} = 4.70 \times 10^{-3} \frac{dB}{deg^2}$ elevation rolloff constant

Gain is assumed constant over the patch. (See Table E-4).

TABLE E-4 ANTENNA SUBROUTINE

URROUTI	NE TR	UANT 74/14	OPT-1	FTN 4,6+420 76
			TRUANT (CELLA . XÃOS , YPOS, ALT. PLY	EL. WOVEL, WODIR. VEL, GNNOR
		, ,		
	2		THIS SUBROUTINE CALCULATES TH	F ANTENNA RATH
	-		ER OF EACH PATCH	IE WALEGAR GATA
	-		ACCOUNT THE CRAB ANGLE CAUSEY A	V THE MANA
		INCES INIA	ACCOUNT THE CHAR WHOLE CHOSES H	IT THE WIND
		MONIFIED RA	DAMPPOR	
	0			
***	C	CELLA	WORKING ARMAY & GAIN NORMALIZING GAIN USED FOR TEL	P BIN BONGUAL
	c	GNNOR	NUMMETISING WEIN RED LOS IST	E BAY KEMOVAL
	C	INDUTS REQU	TRED	
	č	XPOS	32.16 ARRAY OF X CENTERS OF P	ATCHES (FT)
	C	YPAS	37.16 ARRAY OF Y CENTERS OF P	ATCHES (FT)
	c	ALT		
**************************************	C	01	VELOCIET OF THE ATABLANE (ET Je	103
	č	WDVEL	WIND VELOCITY (FT/SEC)	
	C	WDVEL	WIND DIRECTION (DEG) CLOCKWISE	FROM PLANE VELOCITY
	-e-		VECTOR	
	C	VEL	TOTAL VELOCITY (FT/SEC)	
	C			
	C			
	C			
	C	INTERNAL SO		
	C	KAT	AZMUTH ANTENNA ROOLOFF COEP	
	C	KEL	ELEVATION ANT ROOL OFF COEP	
	. C	DANG	ANT DEPRESSION ANGLE	

1.2.5 Mean Backscatter Subroutine

Mean backscatter, $\sigma_{_{\hbox{\scriptsize O}}}$, is calculated as a function of altitude, range and doppler cell position for each surface cell using the program constants which were inputted to the overall program (see Table E-5).

TABLE E-5
MEAN BACKSCATTER SUBROUTINE

SURROUTINE TR	US 190 74/24 OP7#1 PTN 4.6+420 76.
	SURROUTINE TRUSTED (CELLA . ALT . RANGE . DRANGE; ONNOR)
ç	THIS SUBRUUTINE CALCULATER SIGNA ZERO AS & FUNCTION OF
	BANGE GATE
č	whose sale
Č	MONIFIED MARAMETERS
CCC	CELLA 32.16 WORKING PARAMETER CELLS
Č	INTERNAL CONSTANTS
C	SIGO 16 ARRAY OF GIGMA ZERO CONSTANTS
C	

1.2.6 Sin x/x Subroutine

Calculation of the transfer function of the sample-and-hold implementation over the 16 range gate arrays is performed by the subroutine listed in Table E-6.

TABLE E-6 SIN x/x SUBROUTINE

SUBROUT	NE TRI	JSTNX 74/	74 OPTH	FTN 4.6+420	76/
		SUBROUTIN	E TRUSINX (CELLA, BRF, DDOP, DOPOFE	,	
	č	-	BUTINE ADDS IN THE EFFECTS OF S	J. APARATION	
F	č	11173 3004	ON THE GENERATED SPECTRUM	N OLEWALTON	
	c	MONIFIED	RARAMETERS		
	C		32.16 WORKING CELL ARRAY	TŃX/X	
	C	INPUTS RE	NUIRED SYSTEM PRP(H)		
	C	DOPOFF	DOPPLER BETWEEN FFT CELLS ZERO DOPPLER OFFSET IN FFT	H ý)	

1.2.7 Gain Normalizing Subroutine

In the data reduction processing of the collected clutter data, the gains for the 16 range gates and 32 doppler cells are normalized to restrict the dynamic range required in further processing. The gain normalizing subroutine of Table E-7 performs the same function for the simulation.

TABLE E-7
GAIN NORMALIZING SUBROUTINE

BROUTINE PA	144 14714	OPT41		N 4.6+420	76/
	SURROUTINE	RMVTEL (CELLAD, ILT.DO	POFF , GNNURS		
	DIMENSION C	ELLAB (32,16)			
	DIMENSION			TELR4(16)	
	3 .	TELSNXM(32) . TELSNXP(32)	TELGAIN(16)		
Ę					
Č		TINE SIMULATES TELE RRAYS USED IN THE TE		STEM FACTORS	
č	0060 04	mars este in the te	Ce on.		
č	DONE IN ONE	PASS TO IMPHOVE SPE	20	The second secon	-
C					
ç	MONIFIED NA	32.16 ARRAY OF AMP	1.1711550		
č	OFFERD	SELIO MUNE, UL MU	Linces		
č	INPUTS				
	ALT	ALTITUDE OF BLANE	77 1		
C	DOPOFF	DOPPLER OFFSET (HZ)			
С	GNNOR	GAIN TO NORMALIZIZ	E TELE SIGNALS TO	APPROX 1	
		THE CONTRACT			
č	TEL ARAN	INED CONSTANTS	PNNA AND ASEA -PE	2000	
	TELSIGO	16 ARRAY OF SIGMA		EC13	
č	TEL R4	16 ARRAY OF GOOD E			
c	TEI SNXM	32 ARRAY OF SINX/		TIVE DOPPLERS	
C	TEL SNXP	32 ARRAY OF STNX/			
C .	TEL GAIN	16 ARRAY OF MAINS		INT FOR	
C		PROCESSING DIFFERE	NCES		

1.2.8 Integer Array Subroutine

Clutter power over the array of cells in essentially continuous (analog) form is normalized and arrayed into 1024 bins corresponding to the like bins of the actual clutter data histograms (see Table E-8).

TABLE E-8
INTEGER ARRAY SUBROUTINE

SUBROUTINE N	DRW 74/2	4 OPT-1	FTN 4.6-420 76/
		NORM (CELLAB. NCFLLAB. MAX.) CELLAB (32,16) • NČELLAB (32,	
	THIS SUBRE	UTINE CHANGES A REAL POWER R ARRAY	R ARMAŞ ENTO
	A.LOWS PRE	VISION FOR A GATH CHANGE	AT THE SAME TIME
Ċ	FINDS THE	MIN AND THE MAX IN THE ARI	RAY
Č	TRUNCATES 1	THE AMPLITUDES TO WITHIN 6	7 70 1623
č	MONIFIED MA	ARAMFTERS	
č	NCFLLAR	32,16 INTEGED POWER ARE	
C	MAY	MAXIMUM AMPLITUDE IN TH	HE AMRAY
C	MIN	MINIMUM AMPLITUDE IN TH	HE ATRAY
č	INTERNAL BO	ONSTANTS	
c		GAIN MODIFICATION ALLO	VED TOO SEAP

1.2.9 Hit Subroutine

Using the inputted threshold, the hit subroutine of Table E-9 sorts the simulated clutter returns and write all hits greater than the threshold onto a hit tape.

TABLE E-9 HIT SUBROUTINE

UBROUTI	NE WRT	HTT 74/	A OPTH1	FTN 4.6+420	76,
		DIMENSTON	K MRTHIT(CELLABONITTHROMAXOMINT CELLAB(32,16) GELLABONITTHR		
	Č				
-	C	THIS SUBRE	OUTINE WRITES LANGE AMPLITUDE M WIT TAPE FOR FURTHER PROCESSING	ETURNS TO	
	C		TAGSEA SOFTWAME		
	č	MODIFIED #	HARAMETERS		W.A. 14
	C	NONE			
	C ·	INPUTS REE	DUIRED		
	č	CELLAB	LARGEST AMPLITUDE IN THE AM		
	C	MIN	SMALLEST AMPLITUEE IN THE A	RRAY IREPORE TRUNCTATO	N)
	C	INTERNAL !			
	C	IFOAME	INTERNAL FFT FRAM COUNT		

1.2.10 Histogram Subroutine

Histogram tapes corresponding to those generated from actual data and using the same format (except for rangetime inversion), are generated by the subroutine of Table E-10.

TABLE E-10 HISTOGRAM SUBROUTINE

- 4414421	74/74 OPT=1 FTN 4,6-420			
SURR	OUTINE WRTHIST (CELLAB DTHISTO, MAX MAN', ALT FRAME)			
C				
	THIS SUBROUTINE GENERATES ARRAYS AND PRAAMETERS REQUIRED			
C POI	FOR HISTOGRAM RECORD TAGES OUTPUTS TAPES IN THE ORDER TIME, RANGE, DOPPLER			
C				
	IRED SNPUTS			
C CELL	AB 32,16 INTEGER ARRAY CONTAINING AMPLITEDES			
C OUTPL	UTS			
C				
C TAPE	11 RANDOM ACESS FILE CONTAING HISTOGRAM STATISTICS			
C HIST	TARY IS MADE UP OF THE FOLLOWING SCOCKE			
C HIST	TARY IS MADE UP OF THE FOLLOWING BLOCKS			
C WORD	PARAMETER			
C 1	PARAMETER RANGE GATE			
C WORD	PARAMETER RANGE GATE FRAME COUNT			
C 1 C 2 C 3 C 4 TO	PARAMETER RANGE GATE FRAME COUNT ALTITUDE AMPLITUDE MICTOGRAM			
C 1 C 2 C 3 C 4 TO C 1097	PARAMETER RANGE GATE FRAME COUNT ALTITUDE AMPLITUDE MICTOGRAM			
C WORD C 1 C 2 C 3 C 4 TO C 1098 C 1098	PARAMETER RANGE GATE FRAME COUNT ALTITUDE AMPLITUDE MICTOGRAM AVERAGE POWER FOR THE FRAME			
C WORD C 1 C 2 C 3 C 4 TO C 1098 C 1098	PARAMETER RANGE GATE FRAME COUNT ALTITUDE AMPLITUDE MICTOGRAM AVERAGE POWER FOR THE FRAME TO POWER IN EACH FFT			
C WORD C 1 C 2 C 3 C 4 TO C 1097 C 1098 C 1029 C 1629	PARAMETER RANGE GATE FRAME COUNT ALTITUDE AMPLITUDE MICTOGRAM AVERAGE POWER FOR THE FRAME TO POWER IN EACH FFT TO AVERAGE POWER PER DOPPLER CETT			
C WORD C 1 C 2 C 3 C 4 TO C 1097 C 1098 C 1079 C 1629 C 1660 C 1660	PARAMETER RANGE GATE FRAME COUNT ALTITUDE AMPLITUDE MICTOGRAM AVERAGE POWER FOR THE FRAME O TO AVERAGE POWER PER DOPPLER CEIL			
C WORD C 1 C 2 C 3 C 4 TO C 1098 C 1029 C 1629 C 1620 C 1640 C	PARAMETER RANGE GATE FRAME COUNT ALTITUDE AMPLITUDE MICTOGRAM AVERAGE POWER FOR THE FRAME O TO POWER IN EACH FFT O AVERAGE POWER PER DOPPLER CETT			

1.2.11 Range-Time Sort Subroutine

The range-time sort subroutine listed in Table E-11 is required because the simulation writes records in the order of time, range gate. Normal processing expects to see the records in the order range, time.

TABLE E-11
RANGE-TIME SORT SUBROUTINE

SUBROUT	INE 301	ithis talk	4 OPT-1 PTN 4.6-420 76/
		SURROUTINE	SORTHIS (FRAME)
•	ç	THIS POLITE	NE SORTS THE HIGTOGRAM RECORDS FROM
	CCC	TIME . RANGE . I	NGE TO
	C	INPUTS	•
	C	INDEX	INDEX OF MASE STORAGE LOCATIONS
	Č	TAPE11	RANDOM ACESS STORAGE FILE CONTAINING THE RECORDS
	Č	FRAME	RANDOM ACESS STORAGE FILE CONTAINING THE RECORDS NUMBER OF MISTO FRAMES WRITTEN
	C		
	c-	OUTPUTS	THE RESERVE OF THE PROPERTY OF
		TAPELZ	RESORTED HISTOGRAM TAPE

1.2.12 Amplitude Generator Subroutine

This subroutine, unlike those described in the previous subsections, makes use of previous written programs and thus the listing will not be included here. The description which follows is intended to provide information for a more complete understanding of the overall program.

This subroutine is designed to model the probability density function (pdf) of the clutter process as well as certain statistics of the map means. The process is modeled on the product of two processes: $\mathbf{X}_{\mathbf{M}}$ and $\mathbf{X}_{\mathbf{Q}}$. $\mathbf{X}_{\mathbf{M}}$ is a slowly varying process with a time constant of a few seconds while $\mathbf{X}_{\mathbf{Q}}$ is independent from one FFT look to the next (and from clutter cell to clutter cell). It is assumed that the pdf and autocorrelation of $\mathbf{X}_{\mathbf{M}}$ and the cdf of $\mathbf{X}_{\mathbf{Q}}$ has been established to model specific clutter data. For example, in the simulation output presented in the report, a 2.2KFT altitude look at the ocean in SS4-5 with vertical polarization was employed.

The simulation made extensive use of a previously developed uniform random number generator (URV) which gives a range of numbers from 0 to 1. First, \mathbf{X}_Q was generated by comparing the output of URV to the amplitude that \mathbf{X}_Q must have so that the cdf evaluated at \mathbf{X}_Q will equal the number from URV. Gaussian random numbers were then generated by using a transformation on URV outputs. From the existing data a Gaussian pdf appears reasonable for \mathbf{X}_M as does an exponential fit to its autocorrelation function. The process can then be simulated as the output of a low pass filter excited by "white" Gaussian noise.

To illustrate the method used to obtain Gaussian numbers from a uniform number generator, we first construct a Rayleigh (voltage) random variable and then pick a random phase from 0 to 2π :

T is Gaussian with zero mean and unit variance. The parameter \mathbf{x} is simply used as a calling argument to the systems URV number generator.

We now examine the required analog filter to yield an exponentail autocorrelation function. If $R(\tau)$ is the autocorrelation function desired, we note that

$$F \left\{ R(\tau) \right\} = F \left\{ e^{-\frac{\tau}{T_C}} u(\tau) + e^{\frac{\tau}{T_C}} u(-\tau) \right\} = \frac{\frac{2}{T_C}}{(\frac{1}{T_C})^2 + w^2} = S(u)$$

where: F = Fourier Transform

 T_{c} = the time constant on the autocorrelation function

S(u) = Power density spectrum

 $u(\tau) = unit step function$

We also note that white noise passing through a filter of the form $H(ja) = 1/(jwt_C + 1)$ will result in the same spectral slope. The impulse response of H(ja) has the form:

$$I(t) = e^{-\frac{t}{T_c}} \text{ for } t \ge 0$$

This means the autocorrelation function and the low pass filter time constants are identical.

The filter required was modeled with the following difference equation:

$$X_{m}(t+1) = A X_{m}(t) + B X_{N}(t+1) + C$$

where: $X_{M}(t+1) = New mean value from filter$

 X_N (t+1) = New Gaussian random variable with mean of 1.00 and standard deviation of σ_{XN}

A = A constant related to the filter bandwidth

B = A constant picked to keep the variance of X_{M} at a constant level (= σ^{2}_{XM})

C = A constant to provide $X_{M}(t+1)$ with a proper mean

Parameter "A" was developed by using the impulse invariant digital filter approach, so if the simulation sample time is Δt , then the value of A becomes: $A=e^{-\Delta t/tc}$. It can be further shown if $B=(1-A^2)^{1/2}$ and C=1-A-B, the X_M will be Gaussian with a mean of 1.00, a standard deviation of the driving function σ_{XN} and will have an exponential autocorrelation function with time constant T_C .

In the model, the value of X_M so obtained was used for every cell in the FFT, while the value of X_Q was allowed to vary from cell to cell. The resulting amplitude from each cell is "X" where $X = X_M X_Q$.

APPENDIX F SIMULATION OUTPUTS

This appendix presents the results of the simulation described in the previous appendix. Throughout this appendix, the simulation output data is compared to one of two datagathering missions (run 5 flight 6 and run 4 flight 6) both of which are high sea state (SS-4 or SS-5) with a 2200 foot aircraft altitude with vertical polarization. Essentially, four different types of simulation output are provided and compared to the flight data:

- 1) Various functions of the PDF of the overall data
- 2) Map mean PDF and autocorrelation
- 3) Hit counts and hit maps
- 4) Conditional probability maps

(For explanations of the terminology used throughout this section, the reader is referred to Volume II, Section 9).

Beginning with the first type of simulation output, several measures of the density function are used to provide the detail necessary for interpretation of the PDF. The following figures are presented to obtain the derived clarity as well as to provide for a comparison to actual data:

Figure F-1 Simulation-Log Density of TOTAL

F-2 Simulation-Log Q of TOTAL(A)

F-3 Simulation-Log Q of TOTAL(N)

F-4 Simulation-Log Q of TOTAL

F-5 Run 5 Flight 6-Log Q of TOTAL

F-6 Simulation-Weibull of TOTAL

F-7 Run 5 Flight 6-Weibull of TOTAL

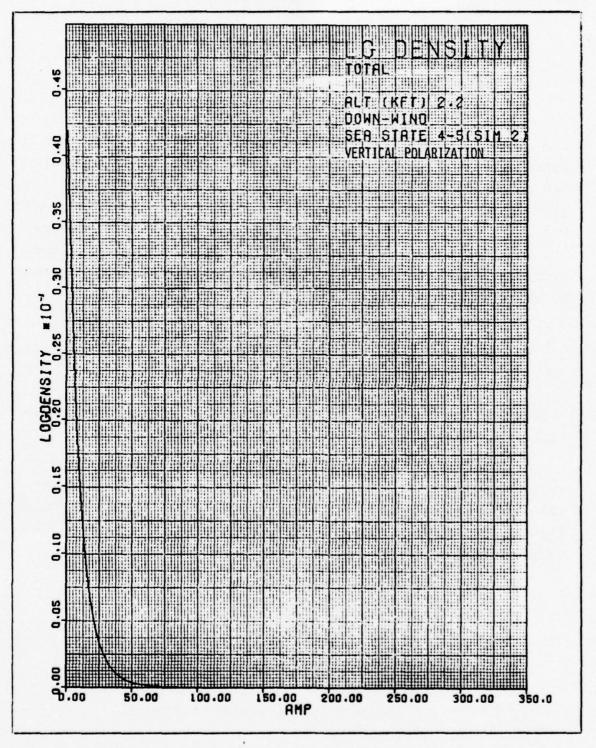


Figure F-1 Simulation-Log Density of TOTAL

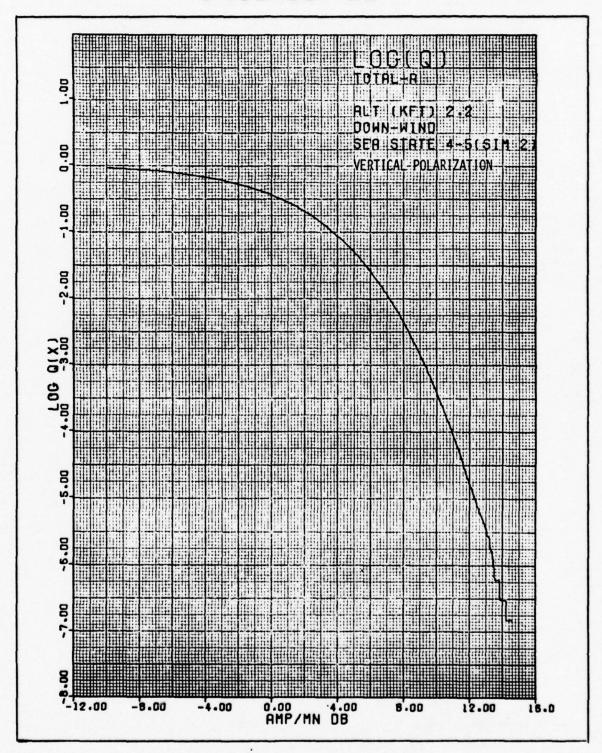


Figure F-2 Simulation-Log Q of TOTAL(A)

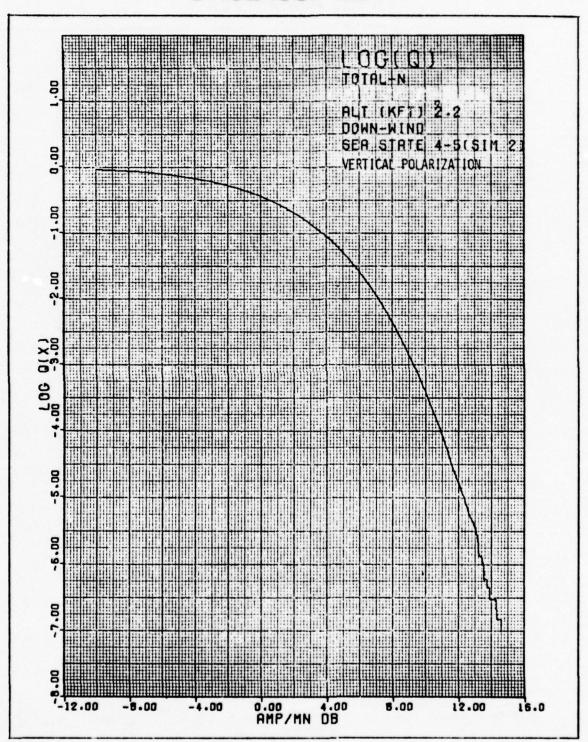


Figure F-3 Simulation-Log Q of TOTAL(N)

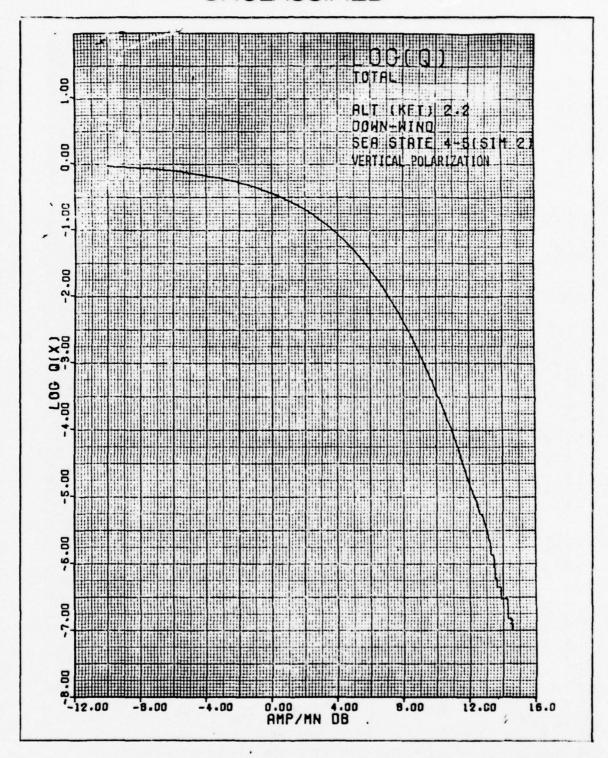


Figure F-4 Simulation-Log Q of TOTAL

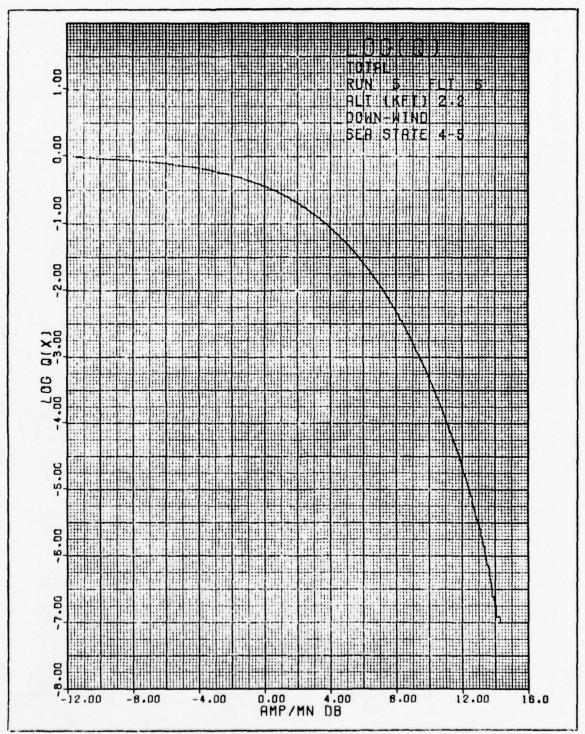


Figure F-5 Run 5 Flight 6-Log Q of TOTAL

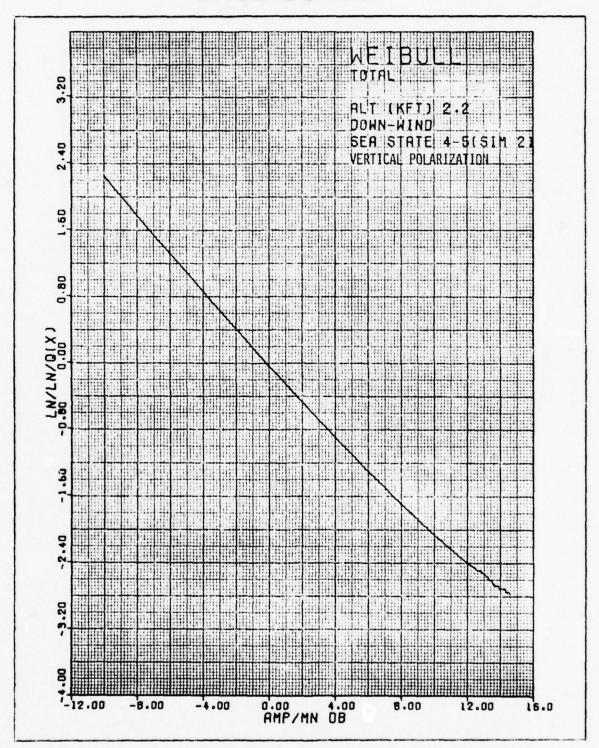


Figure F-6 Simulation-Weibull of TOTAL

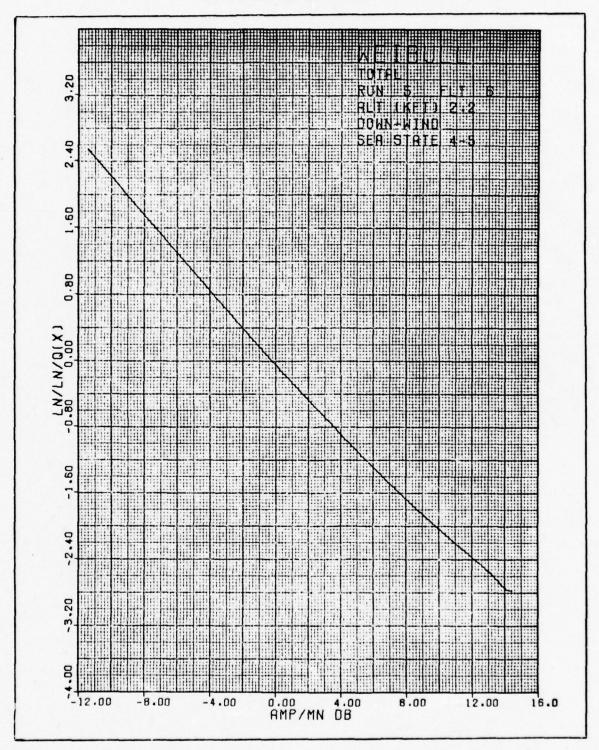


Figure F-7 Run 5' Flight 6-Weibull of TOTAL

- Figure F-8 Simulated Probability Density Function of the Map Mean
 - F-9 Mean Analysis Histogram, Run 5 Flight 6
 - F-10 Simulated Autocorrelation Function of the Map Mean
 - F-11 Autocorrelation Function of the Map Mean, Run 5 Flight 6
 - F-12 Mean Analysis-Simulated Power Spectral Density
 - F-13 Mean Analysis-Power Spectral Density, Run 5 Flight 6
 - F-14 Simulation Mean vs. FFT Number
 - F-15 Mean vs. FFT Number, Run 4 Flight 16
 - F-16 Simulator Hit Counts vs. Time (Coarse)
 - F-17 Hit Counts vs. Time (coarse), Run 4 Flight 16
 - F-18 Simulation Nit Count vs. Time (Fine)
 - F-19 Hit Counts vs. Time (Fine), Run 4 Flight 16
 - F-20 Simulation Hit Map vs. Ground Position
- F-21 Hit Map vs. Ground Position, Run 4 Flight 16 Comparing the Log Q plots between the simulated and real data,

it is seen that less than a 0.2dB difference exists between the two thus indicating that the random variables generated represent a close correspondance to the observed data. It should be emphasized that no information of the time varying characteristics of the process involved is contained in the PDF plots. For this, we must turn to an autocorrelation function.

In the mean analysis that was done, the 32 X 16 radar map was developed for each FFT look and the mean value of the resulting 512 points was obtained. This map mean varies with time and one can describe the variation first by a PDF of the map mean and secondly, by a time autocorrelation function of the observed mean. For simulation purposes, a Gaussian fit to the PDF was made, while an exponential fit to the autocorrelation function seemed appropriate. As explained in Section 10 of Volume II, the only characteristic of the mean PDF that was

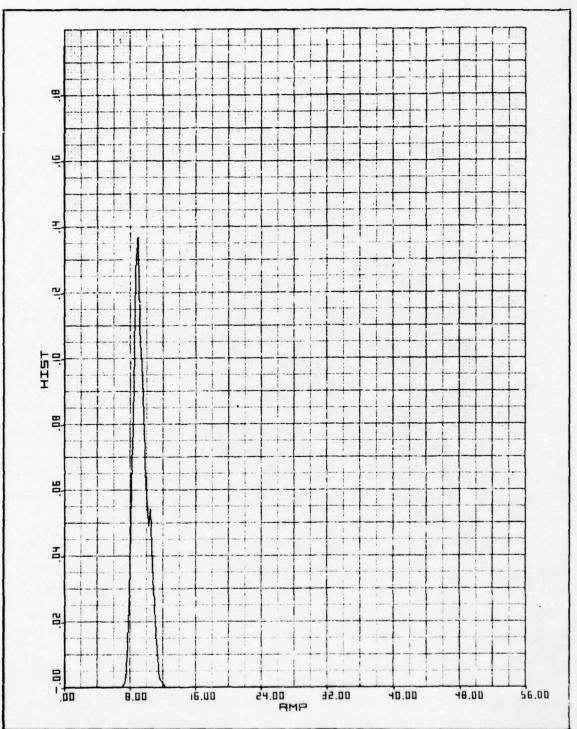


Figure F-8 Simulated Probability Density Function of the Map Mean

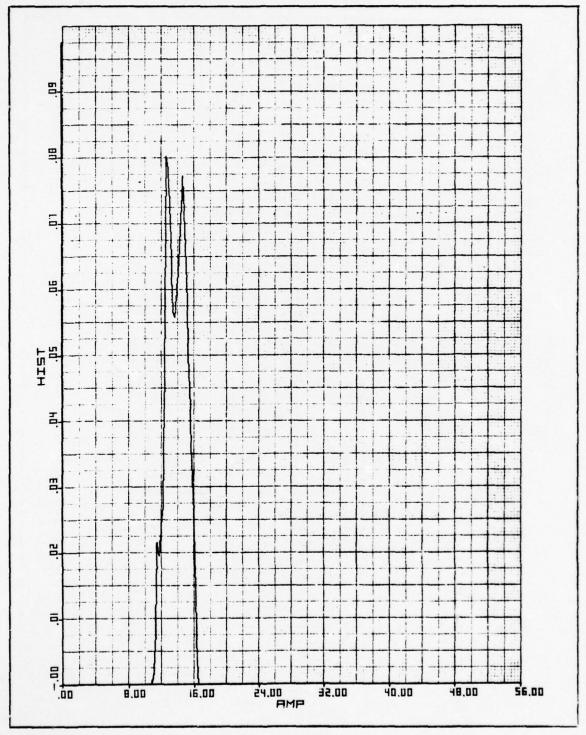


Figure F-9 Mean Analysis Histogram, Run 5 Flight 6

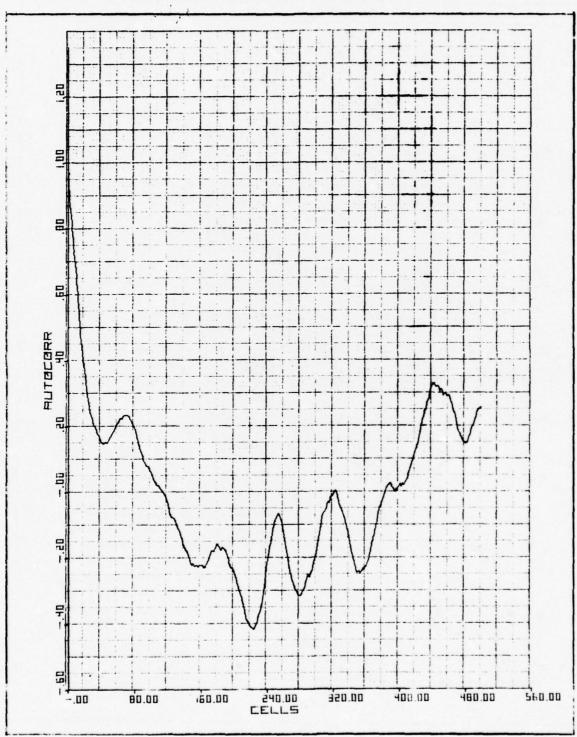


Figure F-10 Simulated Autocorrelation Function of the Map Mean

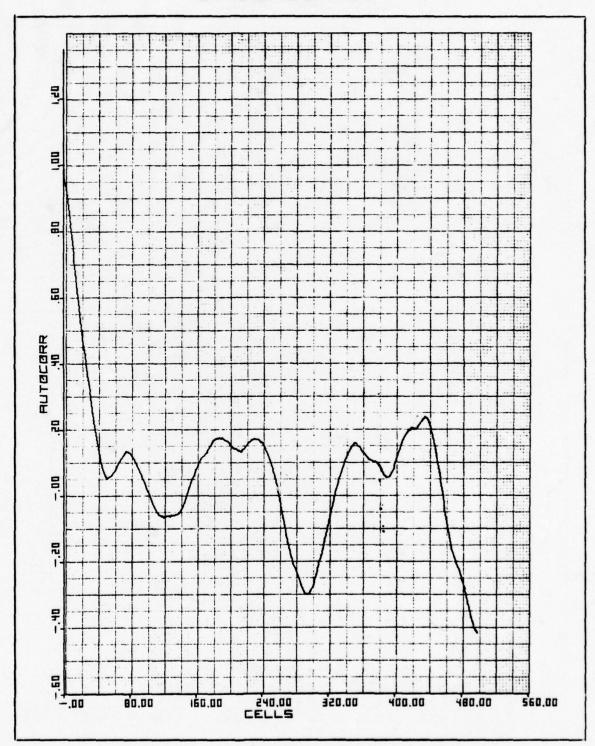


Figure F-11 Autocorrelation Function of the Map Mean, Run 5 Flight 6

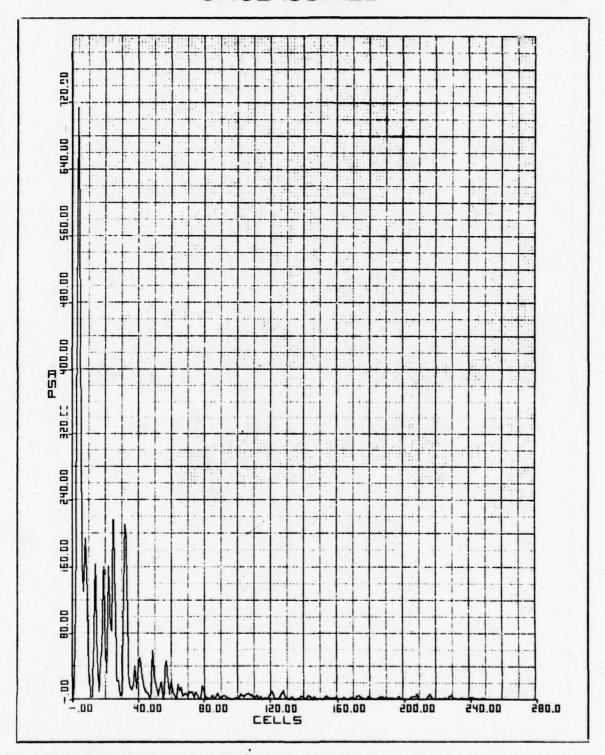


Figure F-12 Mean Analysis-Simulated Power Spectral Density

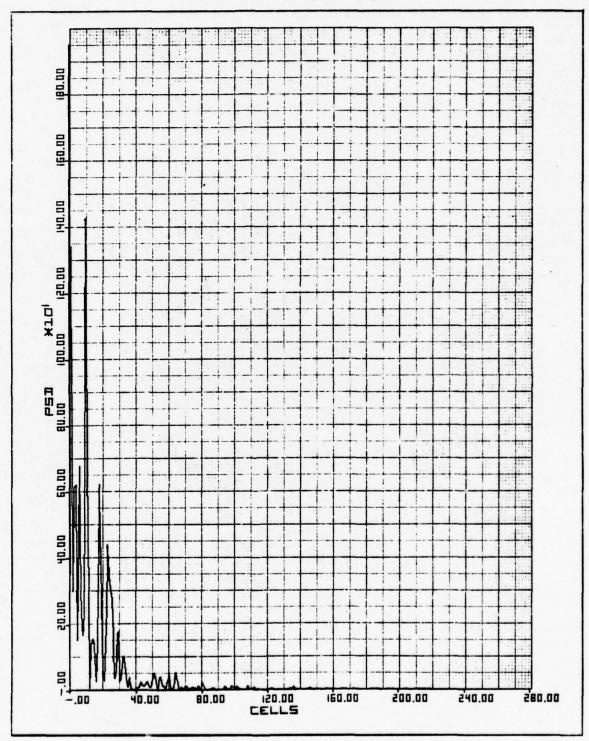


Figure F-13 Mean Analysis - Power Spectral Density, Run 5 Flight 6

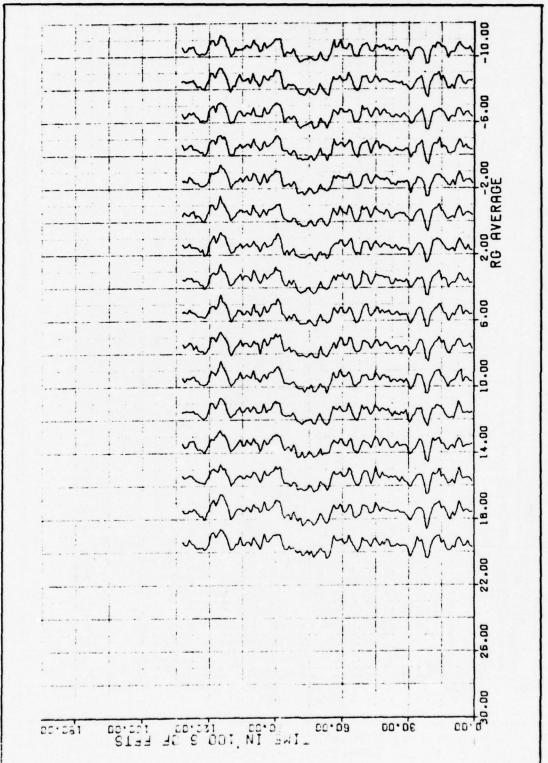


Figure F-14 Simulation Mean vs FFT Number

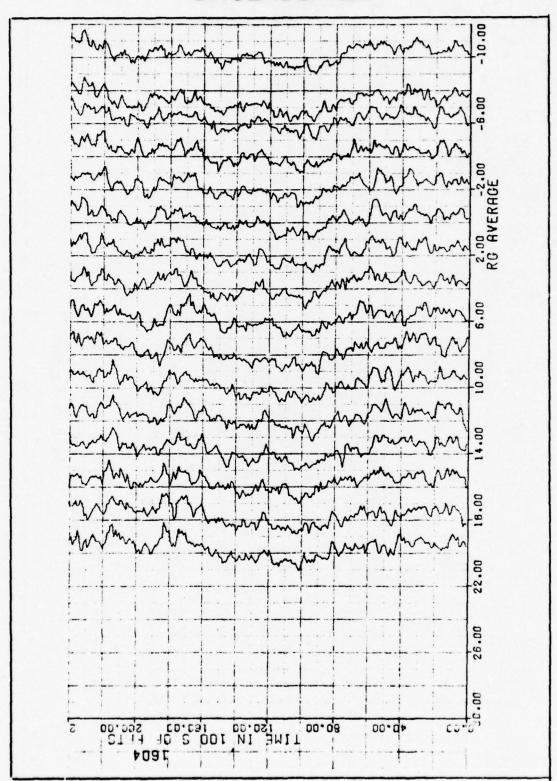


Figure F-15 Mean vs FFT Number, Run 4 Flight 16

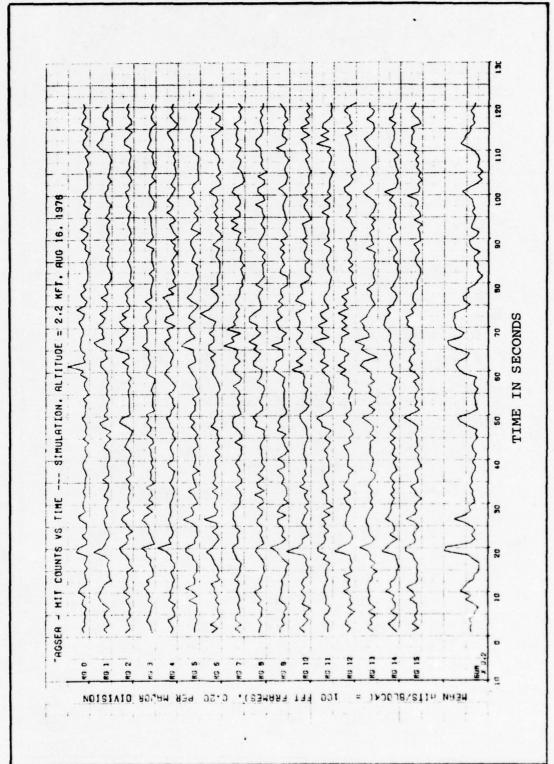
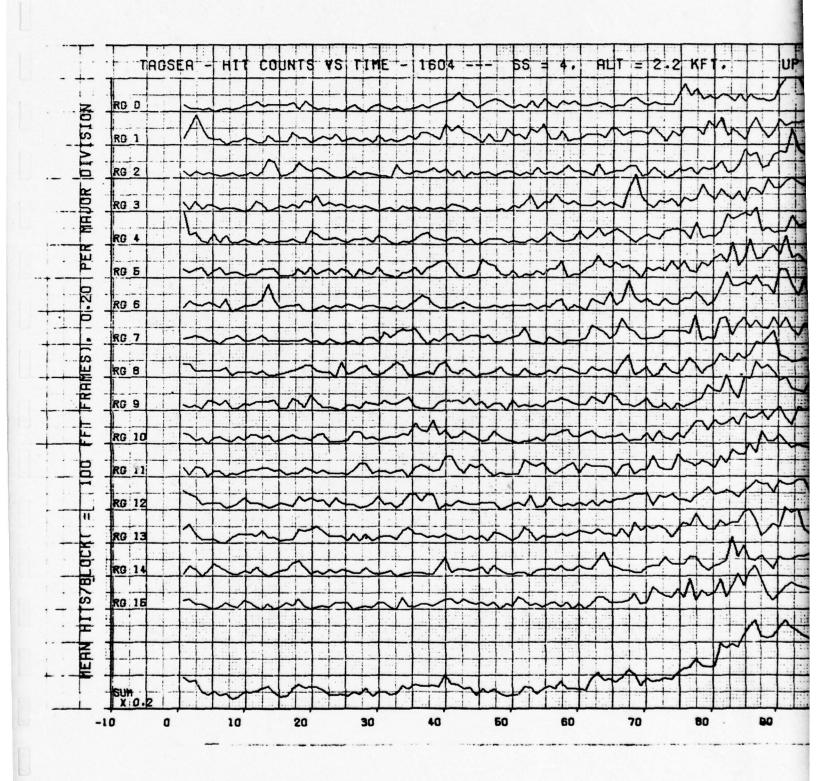


Figure F-16 Simulation Hit Counts vs Time (Coarse)

UNCLASSIFIED



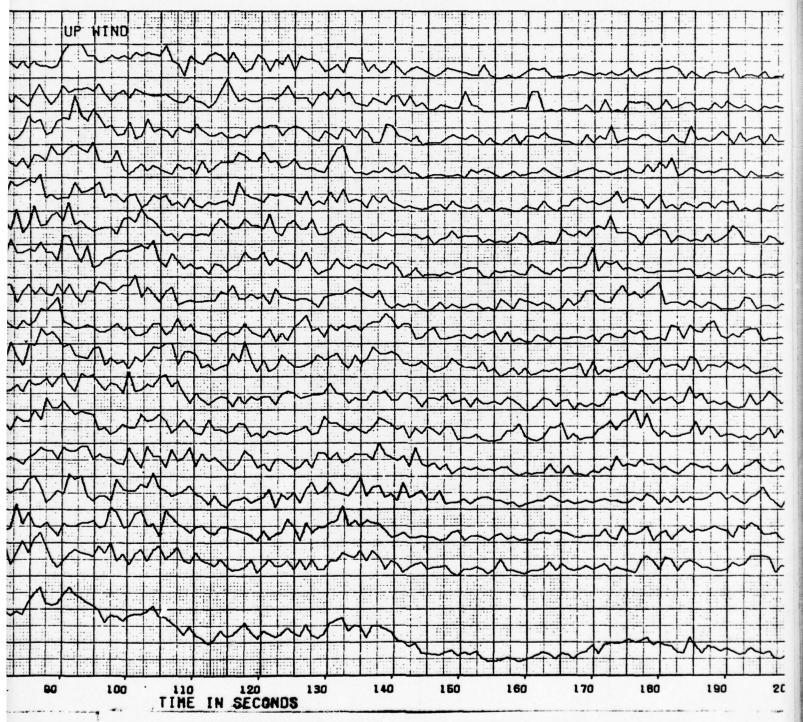


Figure F-17 Hit Counts vs Time (Coarse), Run 4 Flight 16 F-19/F-20

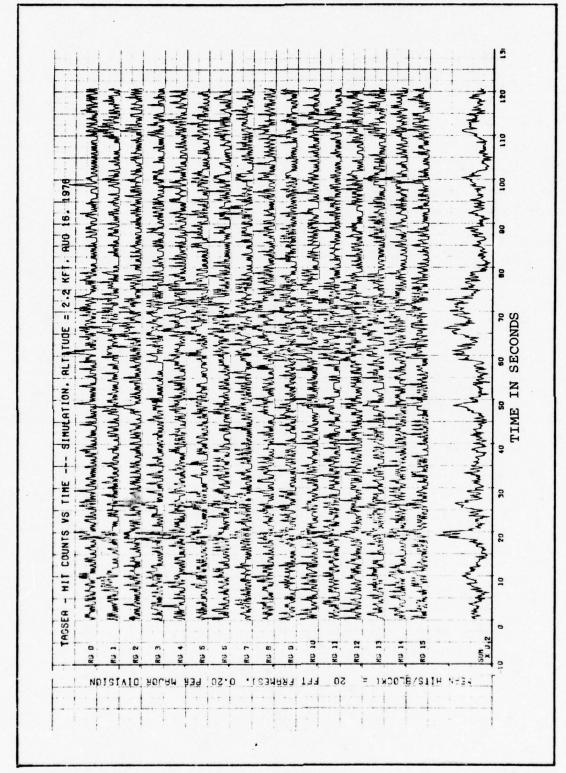


Figure F-18 Simulation Hit Counts vs Time (Fine)

This page intentionally left blank.

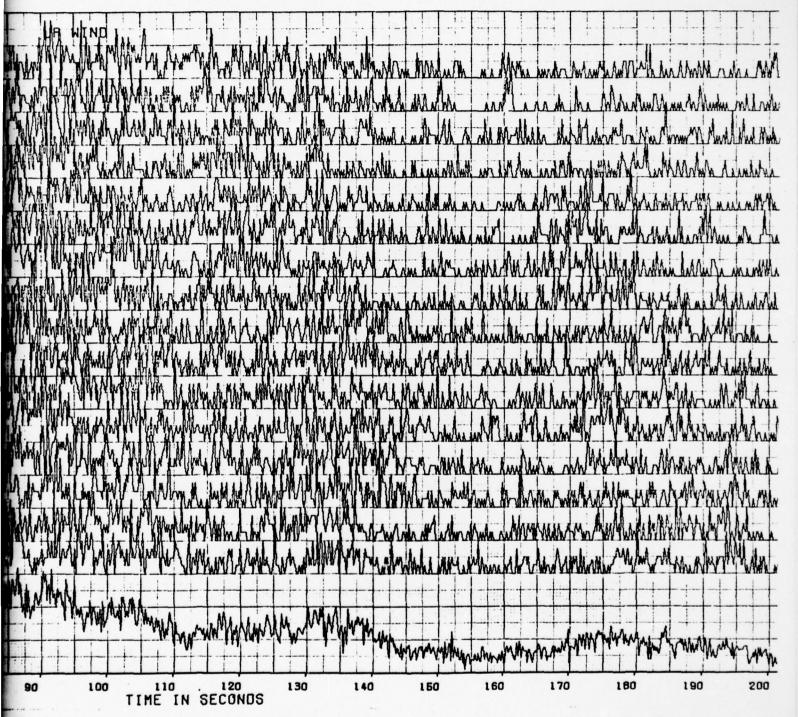


Figure F-19 Hit Counts vs Time (Fine), Run 4 Flight 16

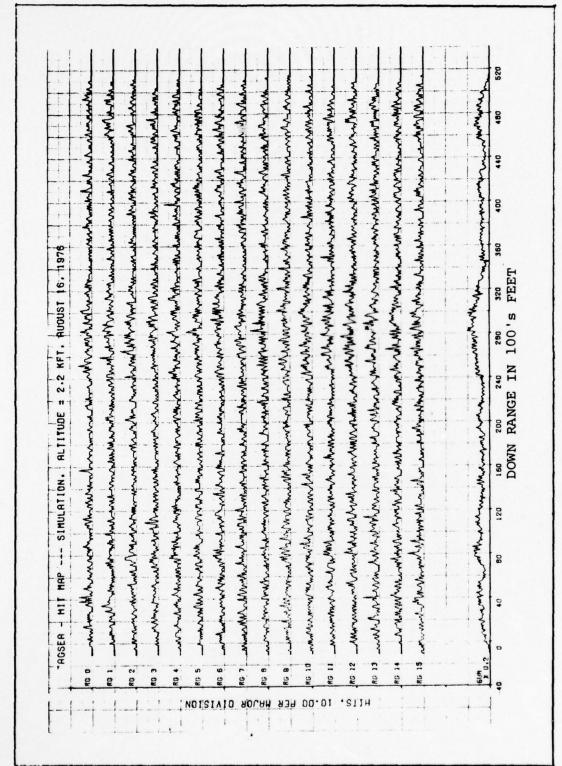
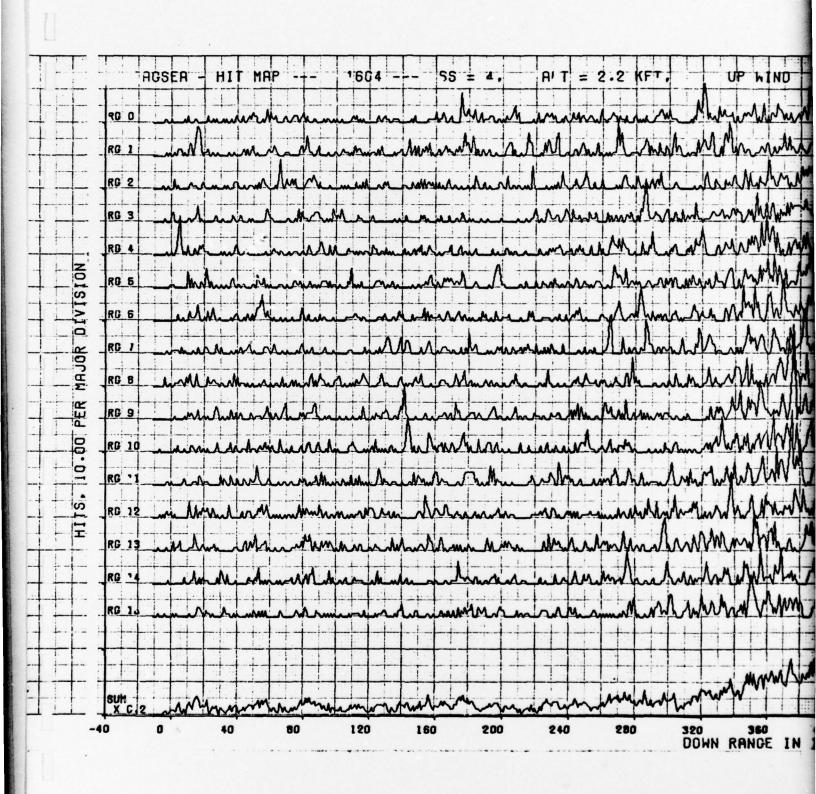


Figure F-20 Simulation Hit Map vs Ground Position

This page intentionally left blank.



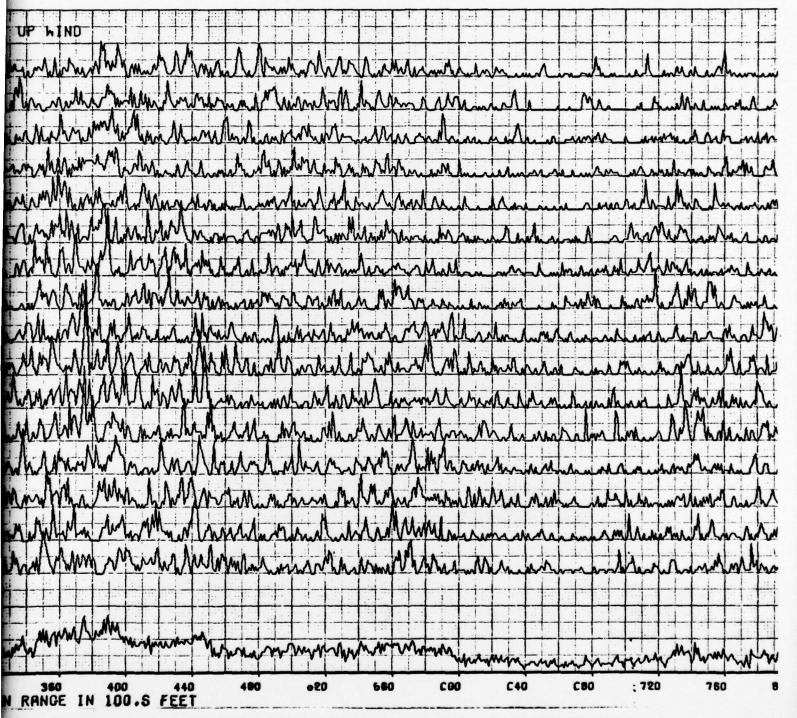


Figure F-21 Hit Map vs Ground Position, Run 4 Flight 16
F-27/F-28

maintained was the ratio of the standard deviation to the mean. This can be observed from Figures F-8 and F-9. An analysis of the autocorrelation of the mean indicates approximately the same time constant for the simulation data and the actual data. Below the region $R(\tau) \le .4$, the autocorrelation function is unreliable due to sample noise. Figure F-10 illustrates a time constant of 291 FFTs (29.1 cells on the graph) which, at the rate of lll FFTs/second, results in a "fresh" sample of the mean every At seconds when At is given as:

At =
$$(\pi)$$
 $\frac{291 \text{ FFTs}}{111 \text{ FFTs/s}}$ = 8.25 seconds

The autocorrelation was developed by examining 10240 FFTs which yields only 11 good samples of the mean. Figure F-11 is the comparable plot for run 605. The power spectral densities of the means (i.e., the Fourier Transform of the time autocorrelation functions) are also provided in Figures F-12 and F-13.

Moving on to the third type of output, we examine a comparison of the mean of 100 FFTs (3200 numbers) for the simulated and real data (Figures F-14 and F-15). It can be observed that both have roughly the same spectral constant and amplitude variation, but the actual data decorrelates somewhat farther from range gate to range gate. Comparing the mean of the range gate versus time to the slope of the coarse hit counts versus time plots for the simulated data and then for the actual data (Figures F-16 and F-17), we can note a correlation in both. A finer grain hit counts versus time plot is also provided (Figures F-18 and F-19), and again very similar trends can be observed. The hit map versus surface position plots (Figures F-20 and F-21) both show less correlation to the mean versus time plots then to the hit count plots.

Finally, the conditional probability map comparisons are presented in the following 10 graphs:

Figure F-22 Simulation-Relative Time 0

F-23 Run 5 Flight 6 - Relative Time 0

F-24 Simulation-Relative Range 0

F-25 Run 5 Flight 6-Relative Range 0

F-26 Simulation-Relative Doppler 0

F-27 Run 5 Flight 6-Relative Doppler 0

F-28 Simulation-Time Collapsed Array

F-29 Run 5 Flight 6-Time Collapsed Array

F-30 Simulation-Normalization Array

F-31 Run 5 Flight 6 - Normalization Array

Scanning through all these figures, we note a strong similarity between the simulated and observed data. No exact measure of simulation vs. actual runs is possible but the texture of the pairs of plots shows that the simulation yielded results which matched the form and shape of the conditional probability maps almost exactly.

Thus the overall simulation outputs have shown that the data gathering, reduction, analysis and the simulation itself are all verified. It shows further that the clutter model used is indeed a good model to use for simulation which is a pertinent point for use in future missile system work.

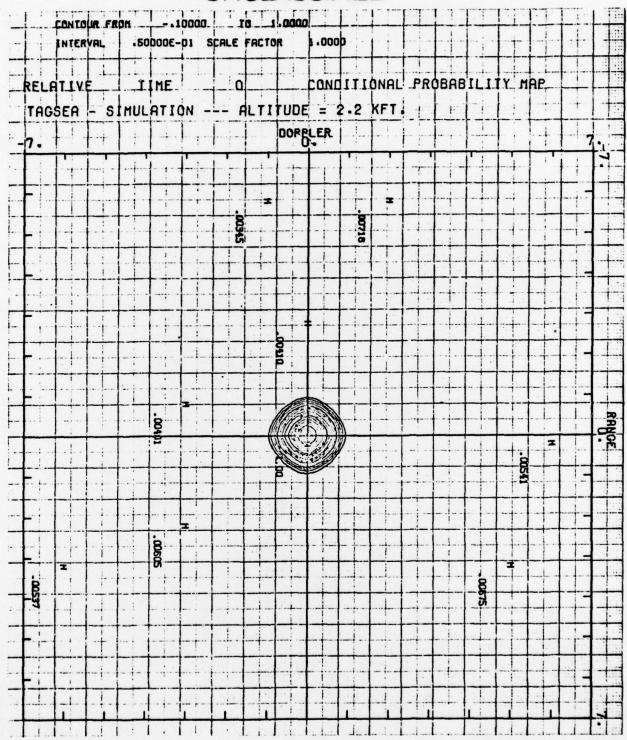


Figure F-22 Simulation-Relative Time 0

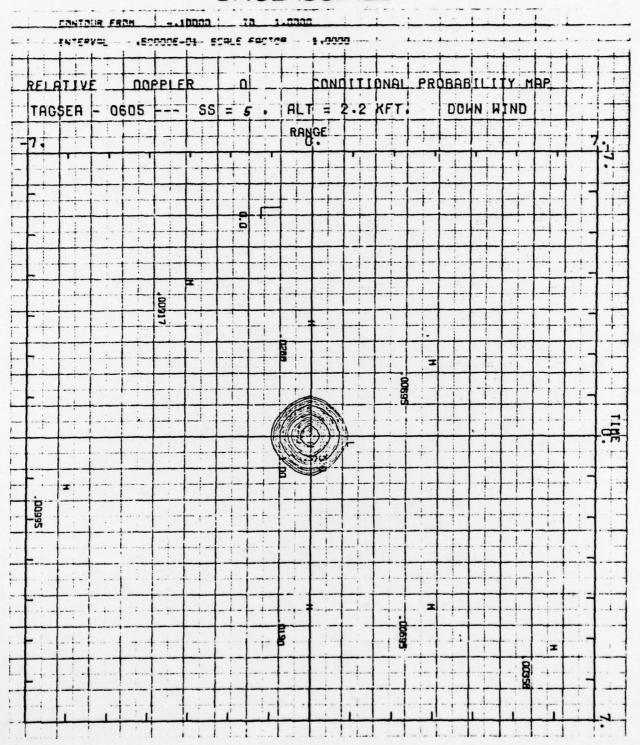


Figure F-23 Run 5 Flight 6-Relative Time 0

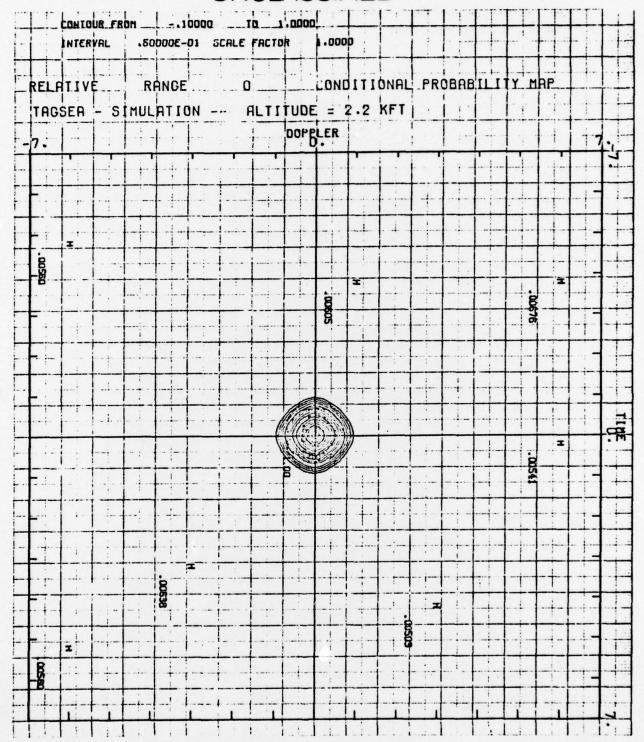


Figure F-24 Simulation-Relative Range 0

RELATIVE RANGE O									CON	dП	PRCBABILITY MAP											
TAG	SEA	- 0	605		s	s	= :	5		ALT	=	2.2	KFT		00	M	M	IND	上	-		
7.	-	F	-			-	-	-	م .	OPE	LER	+	-		1			+		+-	+	7.
				1					1			1							1			12
	-	++	+	+	++	+	-	-	+	- i-	-	++	+-	++	+-	H	_	+	+	+	+	
F i	-									-								1	1			
			T		1							-	1-1-		- -			-				_
	+	++	++	++	+	\dashv	+		-	-		+	+	1	+ +	+	-	+	+	+		-
						1	1			-								4	1			+-
		-		-	++	+	+	-	-	+		++	++-	++-		+-		+	+			1-
-					11														1			1
	1	-	++	H	++	+	+		-	\perp		+			-	H	-	+	+	-	-	++
e J.,		-		Ti		+			200	-		1-1-						1				1
			1-		1-1		-					Ι.					_				_ i] !
-	-	1	+	1	+	+			-!-		-	-	+	+-			-	+	+	+-	- - -	1
		t				1			(1)		17	1					1		1			10
			-	-	+ :	-	+	1-1	1/3	1		1					-			=		1
-	1	-		1		1			B	-									126		1.	1
				+	+	+	-		- -	+	-	-	-	-	-	-	-	-	+-	-		-
	+		1	1	1+	+	+				+	1-:-	1-1-	-					1	+		1 +
		į. I.,	1.			1			1.								-	-4.	1			11
-	-+-	-	-	++	++	+		++				+	-			-	-	+	-	-	-	1-
							1		-										1			1+
	2				1-1	-	-	-		: 1	-					++	+	+	-	-	-	
00349				1	11	1			0610				Li						T			1:
6				-	-	-	+	-	-								-	<u> </u>	+-			-
-		- :		-	1-1	-	-			1		-					-	+	-			
	_	-!-			1	-		1											2		!	
	1		H			7	+		1		1	1	1	\dashv		-	-	-	20797		-	

Figure F-25 Run 5 Flight 6-Relative Range 0

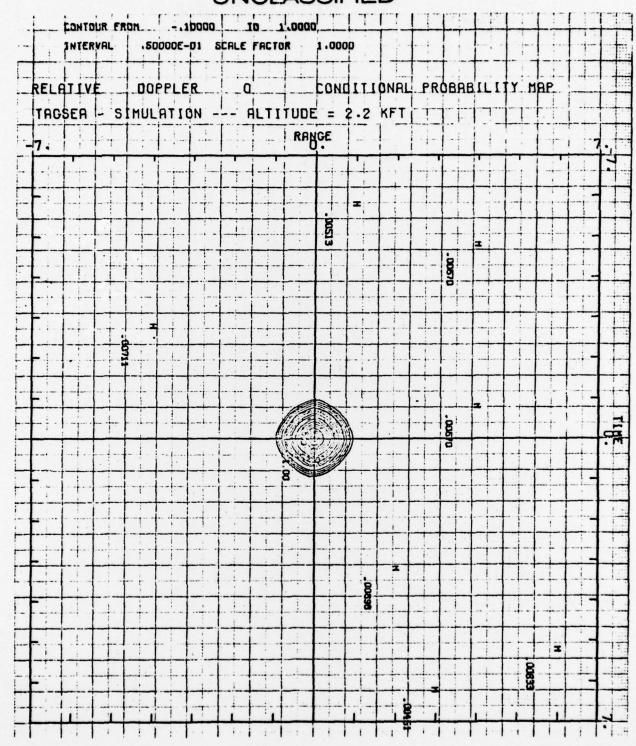


Figure F-26 Simulation-Relative Doppler 0

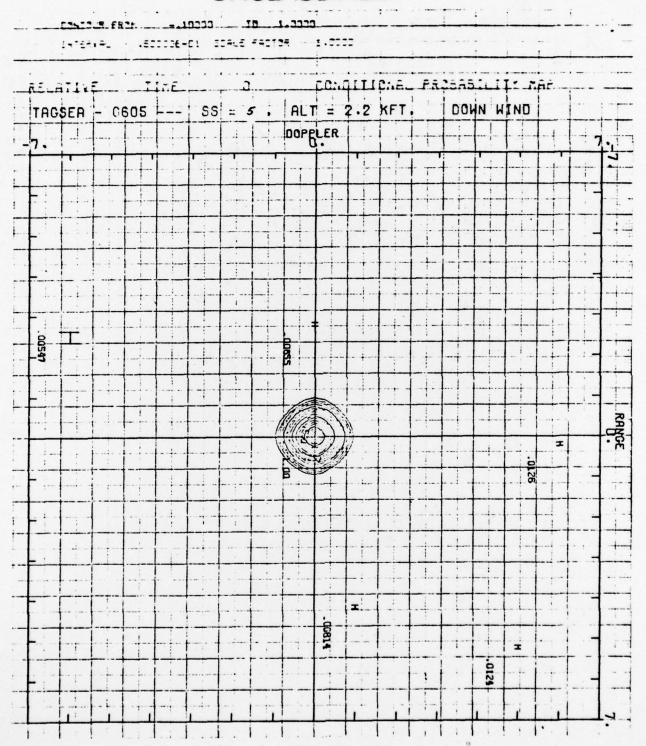


Figure F-27 Run 5 Flight 6-Relative Doppler 0

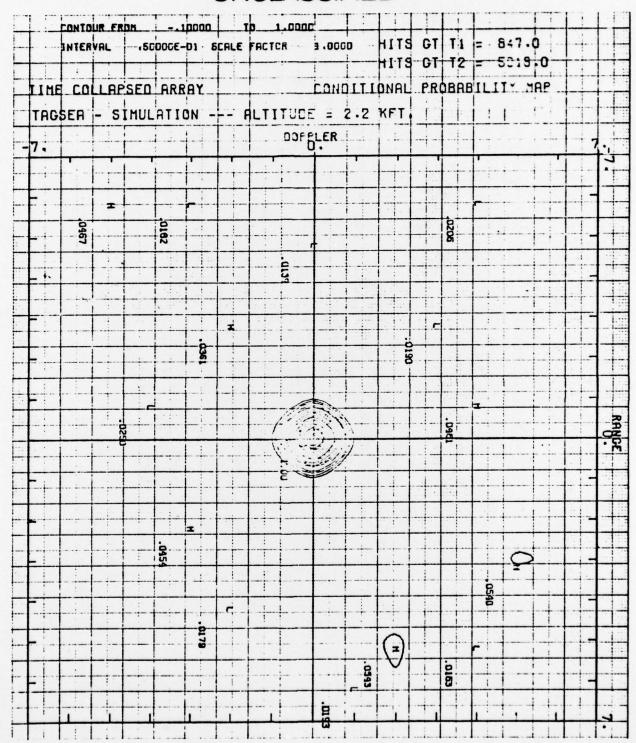


Figure F-28 Simulation-Time Collapsed Array

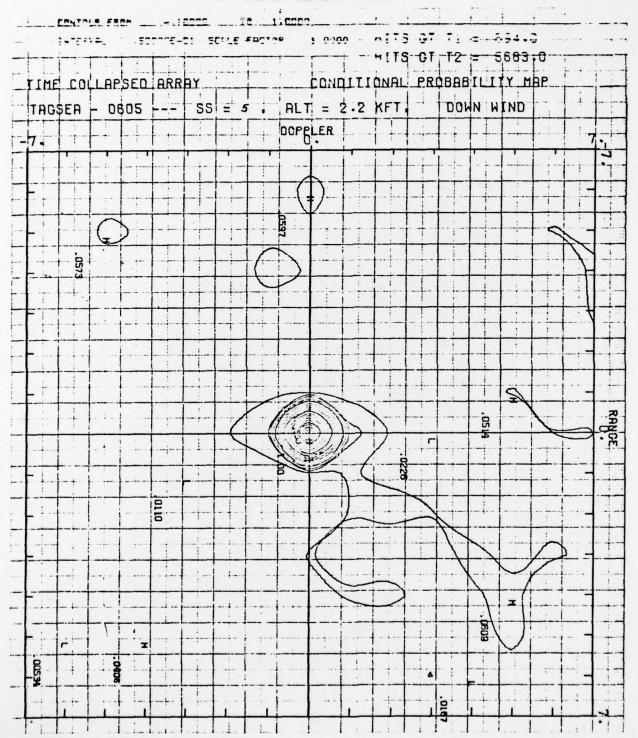


Figure F-29 Run 5 Flight 6-Time Collapsed Array

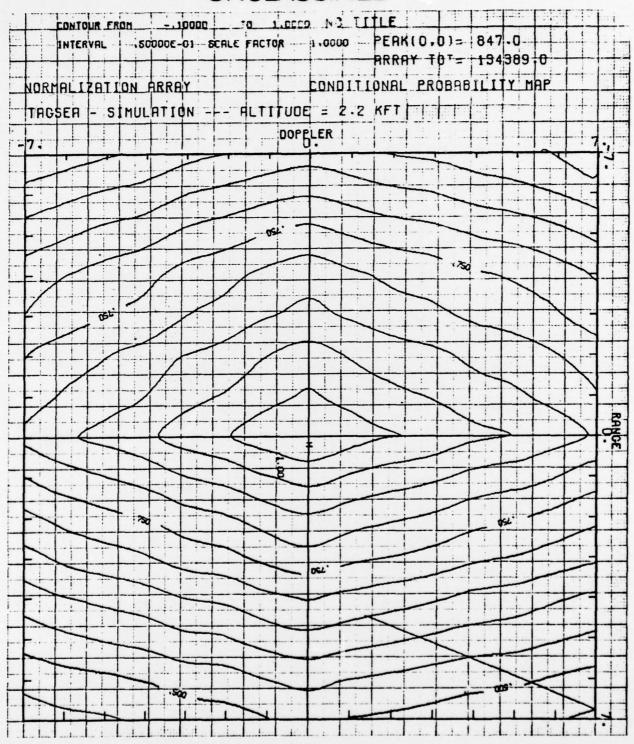


Figure F-30 Simulation-Normalization Array

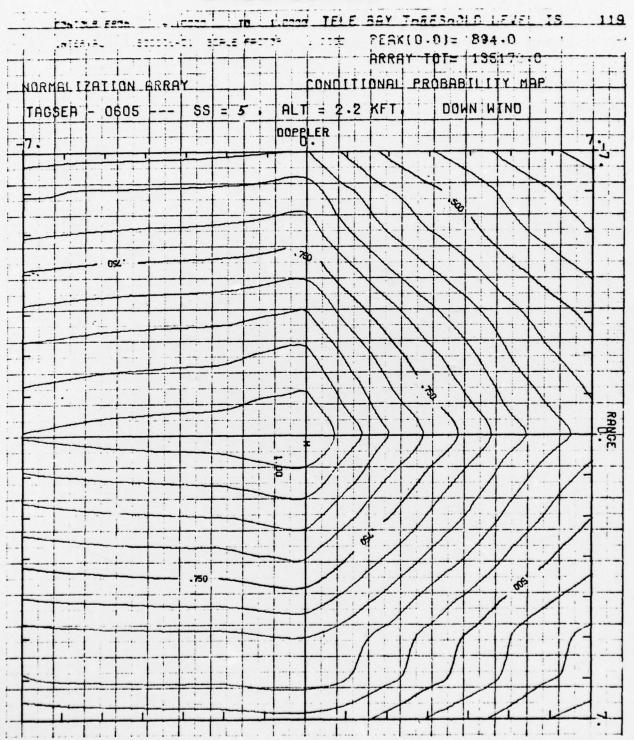


Figure F-31 Run 5 Flight 6-Normalization Array